



# RESEARCH

2008-47

## Corrosion Protection Performance of Epoxy-Coated Reinforcing Bars

Take the  steps...

Research... Knowledge... Innovative Solutions!

Transportation Research

## Technical Report Documentation Page

|  |  |  |           |
|--|--|--|-----------|
| 1. Report No.<br>MN/RC 2008-47   | 2.   | 3. Recipients Accession No.  |           |
| 4. Title and Subtitle<br>Corrosion Protection Performance of Epoxy-Coated Reinforcing Bars   |  | 5. Report Date<br>September 2008   |           |
| 7. Author(s)<br>José A. Pincheira, Antón A. Aramayo, Kyu Sun Kim, and Dante Fratta   |  | 6.   |           |
| 9. Performing Organization Name and Address<br>Department of Civil and Environmental Engineering<br>University of Wisconsin-Madison<br>1415 Engineering Drive<br>Madison, Wisconsin 53706  |  | 8. Performing Organization Report No.  |           |
| 12. Sponsoring Organization Name and Address<br>Minnesota Department of Transportation<br>395 John Ireland Boulevard<br>Saint Paul, Minnesota 55155  |  | 10. Project/Task/Work Unit No.   |           |
|  |  | 11. Contract (C) or Grant (G) No.<br><br>(c) 89264   |           |
| 15. Supplementary Notes<br><a href="http://www.lrrb.org/PDF/200847.pdf">http://www.lrrb.org/PDF/200847.pdf</a>   |  | 13. Type of Report and Period Covered<br>Final Report  |           |
|  |  | 14. Sponsoring Agency Code   |           |
| 16. Abstract (Limit: 200 words)<br><br><p>The main purpose of this investigation was to conduct an in-depth study to determine the level of corrosion protection offered by epoxy-coated bars in four bridge decks in the Minneapolis/St. Paul, MN metropolitan area. The bridges studied were built between 1973 and 1978 and all decks had a top mat built with epoxy-coated bars. The bottom mat was epoxy-coated in only one deck whereas black steel was used for the bottom mat in the other bridges. These bridges had been assessed in 1996 and thus, the present study is a follow up investigation to obtain data and assess the field performance of epoxy-coated bars over a period of approximately 30 years. The investigation included field inspection and surveys of the decks, as well as laboratory tests of concrete core and bar samples. After 30 years of service, the overall condition of the epoxy-coated bars is good to very good, with no or modest levels of corrosion activity. In only one bridge, corrosion activity appears to be moderate to severe. The majority of corroded bars were found near joints or at crack locations. The amount of delamination in all decks is very low.</p> |  |  |           |
| 17. Document Analysis/Descriptors<br>chloride ion content, concrete bridge decks, delamination, diffusion, half-cell potential, electrochemical impedance spectroscopy, corrosion, epoxy-coated bars, ground penetrating radar   |  | 18. Availability Statement<br>No restrictions. Document available from:<br>National Technical Information Services,<br>Springfield, Virginia 22161 |           |
| 19. Security Class (this report)<br>Unclassified   | 20. Security Class (this page)<br>Unclassified | 21. No. of Pages<br>224  | 22. Price |

# **Corrosion Protection Performance of Epoxy-Coated Reinforcing Bars**

## **Final Report**

*Prepared by:*

José A. Pincheira  
Antón A. Aramayo  
Kyu Sun Kim  
Dante Fratta

Department of Civil and Environmental Engineering  
University of Wisconsin-Madison

**September 2008**

*Published by:*

Minnesota Department of Transportation  
Research Services Section  
395 John Ireland Boulevard, Mail Stop 330  
St. Paul, Minnesota 55118

This report represents the results of research conducted by the authors and does not necessarily represent the views or policies of the Minnesota Department of Transportation and/or the Center for Transportation Studies. This report does not contain a standard or specified technique.

The authors and the Minnesota Department of Transportation and/or Center for Transportation Studies do not endorse products or manufacturers. Trade or manufacturers' names appear herein solely because they are considered essential to this report.

## **ACKNOWLEDGEMENTS**

This project was supported with funds provided by the Minnesota Department of Transportation (Mn/DOT). This support is gratefully acknowledged. The University of Wisconsin-Madison research team recognizes the ideas, field support, and enthusiasm from the Mn/DOT team. The Mn/DOT officials participating in the project included Paul Rowekamp, Mark Spafford, Bernard Izevbekhai, Gary Peterson, Jack Pirkel, Marc Loken, Phillip Erickson, Ronald Mulvaney, and the field crew during the September/October 2006 field visits.

Thanks are also extended to the Midwest Regional University Transportation Center (MRUTC) who provided additional support through matching funds to this project.

## TABLE OF CONTENTS

|   |           |
|---|-----------|
| CHAPTER 1. INTRODUCTION .....                                       | <b>1</b>  |
| 1.1 INTRODUCTION .....  | 1         |
| 1.2 OBJECTIVE.....  | 1         |
| 1.3 SCOPE .....   | 2         |
| CHAPTER 2. BACKGROUND AND LITERATURE REVIEW .....                   | <b>3</b>  |
| 2.1 INTRODUCTION .....  | 3         |
| 2.2 CORROSION PROCESS .....   | 3         |
| 2.2.1 General.....  | 3         |
| 2.2.2 Macro and micro corrosion cells.....                          | 4         |
| 2.2.3 Chloride threshold level.....                                 | 5         |
| 2.2.4 Corrosion propagation .....                                   | 6         |
| 2.3 CARBONATION.....  | 7         |
| 2.4 EPOXY-COATED REBARS (ECR) REVIEW.....                           | 8         |
| 2.4.1 Performance evaluation .....                                  | 9         |
| 2.4.2 Certification program.....                                    | 9         |
| 2.5 METHODS FOR EVALUATING BRIDGE DECKS .....                       | 10        |
| 2.5.1 Chain-drag survey.....  | 10        |
| 2.5.2 Half-cell potential .....                                     | 10        |
| 2.5.3 Impedance Spectroscopy Measurements .....                     | 11        |
| 2.5.4 Ground Penetrating Radar Measurements .....                   | 14        |
| 2.6 METHODS FOR EVALUATING CONCRETE .....                           | 15        |
| 2.6.1 Chloride ion intrusion – AASHTO T259/260 .....                | 15        |
| 2.6.2 Carbonation depth - RILEM.....                                | 16        |
| 2.7 METHODS FOR EVALUATING EPOXY-COATED REBARS .....                | 17        |
| 2.7.1 Specification for epoxy-coated steel bars – ASTM A775-06..... | 17        |
| 2.7.2 Coating hardness NACE TM-0174.....                            | 17        |
| 2.7.3 Coating adhesion NACE TM-0185 .....                           | 17        |
| CHAPTER 3. DESCRIPTION OF INSPECTED BRIDGES.....                    | <b>18</b> |
| 3.1 INTRODUCTION .....  | 18        |
| 3.2 DESCRIPTION OF BRIDGES .....                                    | 18        |
| 3.2.1 Bridge 19015, US 52 over Southview Blvd.....                  | 20        |
| 3.2.2 Bridge 27062, Old Shakopee Rd. over Cedar Ave. ....           | 21        |
| 3.2.3 Bridge 27812, North Dowling Ave. over I-94.....               | 22        |
| 3.2.4 Bridge 27815, West Broadway Ave. over I-94.....               | 23        |
| 3.3 PREVIOUS STUDY .....  | 24        |
| 3.3.1 Bridge 19015.....   | 24        |
| 3.3.2 Bridge 27062.....   | 25        |
| 3.3.3 Bridge 27812.....   | 25        |
| 3.3.4 Bridge 27815.....   | 26        |
| CHAPTER 4. FIELD PROCEDURES .....                                   | <b>28</b> |
| 4.1 INTRODUCTION .....  | 28        |

|  |  |           |
|--|--|-----------|
| 4.2  | BRIDGE SITE INSPECTION .....                 | 28        |
| 4.2.1  | Visual inspection.....                       | 28        |
| 4.2.2  | Chain-drag survey.....                       | 29        |
| 4.3  | HALF-CELL POTENTIAL MEASUREMENTS .....       | 29        |
| 4.4  | CORING SELECTION .....                       | 30        |
| 4.5  | DEPTH OF COVER .....                         | 31        |
| <br>   |  |           |
| CHAPTER 5. LABORATORY PROCEDURES .....                     |  | <b>32</b> |
| 5.1  | INTRODUCTION .....                           | 32        |
| 5.2  | CORE EXAMINATION .....                       | 32        |
| 5.3  | CHLORIDE ION ANALYSIS.....                   | 32        |
| 5.3.1  | Sample retrieval .....                       | 32        |
| 5.3.2  | Equipment and chemicals .....                | 34        |
| 5.3.3  | Sample decomposition .....                   | 34        |
| 5.3.4  | Potentiometric titration .....               | 34        |
| 5.3.5  | Data collection .....                        | 36        |
| 5.4  | CARBONATION DEPTH MEASUREMENT .....          | 37        |
| 5.5  | EPOXY-COATED REBAR EVALUATION.....           | 38        |
| 5.5.1  | Evaluation of coating hardness .....         | 39        |
| 5.5.2  | Evaluation of coating adherence.....         | 40        |
| 5.5.3  | Measurement of coating thickness.....        | 41        |
| 5.5.4  | Evaluation of corrosion condition.....       | 42        |
| <br>   |  |           |
| CHAPTER 6. FIELD EVALUATION - RESULTS AND DISCUSSION ..... |  | <b>43</b> |
| 6.1  | INTRODUCTION .....                           | 43        |
| 6.2  | BRIDGE 19015 .....                           | 43        |
| 6.2.1  | Visual inspection.....                       | 43        |
| 6.2.2  | Chain-drag survey.....                       | 44        |
| 6.2.3  | Half-cell potential survey.....              | 44        |
| 6.2.4  | Electrochemical impedance spectroscopy ..... | 49        |
| 6.2.5  | Ground penetrating radar measurements .....  | 54        |
| 6.3  | BRIDGE 27062 .....                           | 58        |
| 6.3.1  | Visual inspection.....                       | 58        |
| 6.3.2  | Chain-drag survey.....                       | 59        |
| 6.3.3  | Half-cell potential survey.....              | 59        |
| 6.3.4  | Electrochemical impedance spectroscopy ..... | 63        |
| 6.3.5  | Ground penetrating radar measurements .....  | 65        |
| 6.4  | BRIDGE 27812 .....                           | 69        |
| 6.4.1  | Visual inspection.....                       | 69        |
| 6.4.2  | Chain-drag survey.....                       | 70        |
| 6.4.3  | Half-cell potential survey.....              | 71        |
| 6.4.4  | Electrochemical impedance spectroscopy ..... | 75        |
| 6.4.5  | Ground penetrating radar measurements .....  | 78        |
| 6.5  | BRIDGE 27815 .....                           | 82        |
| 6.5.1  | Visual inspection.....                       | 82        |
| 6.5.2  | Chain-drag survey.....                       | 84        |

|       |   |    |
|-------|---|----|
| 6.5.3 | Half-cell potential survey.....             | 84 |
| 6.5.4 | Electrochemical impedance spectroscopy..... | 87 |
| 6.5.5 | Ground penetrating radar .....              | 89 |
| 6.6   | CORE SELECTION.....                         | 92 |
| 6.7   | REBAR COVER DEPTH.....                      | 94 |
| 6.8   | SUMMARY OF FIELD RESULTS .....              | 94 |
| 6.8.1 | Cracks, spalls and patches.....             | 94 |
| 6.8.2 | Chain-drag survey.....                      | 95 |
| 6.8.3 | Half-cell potential readings.....           | 96 |
| 6.8.4 | Electrochemical impedance spectroscopy..... | 96 |
| 6.8.5 | Ground penetrating radar .....              | 96 |

**CHAPTER 7. LABORATORY EVALUATION - TEST RESULTS AND DISCUSSION ..... 98**

|       |                                |     |
|-------|--------------------------------|-----|
| 7.1   | INTRODUCTION.....              | 98  |
| 7.2   | CHLORIDE ION CONTENT.....      | 98  |
| 7.3   | CHLORIDE CONTENT PROFILES..... | 98  |
| 7.3.1 | Uncracked cores.....           | 98  |
| 7.3.2 | Cracked cores.....             | 99  |
| 7.4   | BRIDGE 19015 .....             | 100 |
| 7.4.1 | Chloride ion content.....      | 100 |
| 7.4.2 | Diffusion coefficient .....    | 102 |
| 7.4.3 | Carbonation depth.....         | 105 |
| 7.4.4 | Epoxy coating hardness .....   | 105 |
| 7.4.5 | Epoxy coating adherence .....  | 106 |
| 7.4.6 | Epoxy coating thickness.....   | 106 |
| 7.4.7 | Corrosion condition.....       | 107 |
| 7.5   | BRIDGE 27062 .....             | 107 |
| 7.5.1 | Chloride ion content.....      | 107 |
| 7.5.2 | Diffusion coefficient .....    | 110 |
| 7.5.3 | Carbonation depth.....         | 111 |
| 7.5.4 | Epoxy coating hardness .....   | 111 |
| 7.5.5 | Epoxy coating adherence .....  | 111 |
| 7.5.6 | Epoxy coating thickness.....   | 112 |
| 7.5.7 | Corrosion condition.....       | 112 |
| 7.6   | BRIDGE 27812 .....             | 113 |
| 7.6.1 | Chloride ion content.....      | 113 |
| 7.6.2 | Diffusion coefficient .....    | 117 |
| 7.6.3 | Carbonation depth.....         | 117 |
| 7.6.4 | Epoxy coating hardness .....   | 118 |
| 7.6.5 | Epoxy coating adherence .....  | 118 |
| 7.6.6 | Epoxy coating thickness.....   | 119 |
| 7.6.7 | Corrosion condition.....       | 119 |
| 7.7   | BRIDGE 27815 .....             | 120 |
| 7.7.1 | Chloride ion content.....      | 120 |
| 7.7.2 | Diffusion coefficient .....    | 125 |

|                  |   |            |
|------------------|---|------------|
| 7.7.3            | Carbonation depth.....  | 125        |
| 7.7.4            | Epoxy coating hardness .....  | 126        |
| 7.7.5            | Epoxy coating adherence .....   | 126        |
| 7.7.6            | Epoxy coating thickness .....   | 127        |
| 7.7.7            | Corrosion condition .....   | 127        |
| 7.8              | SUMMARY OF LABORATORY RESULTS .....   | 128        |
| 7.8.1            | Visual inspection of cores.....   | 128        |
| 7.8.2            | Chloride content values.....  | 128        |
| 7.8.3            | Coating hardness.....   | 131        |
| 7.8.4            | Coating adherence.....  | 132        |
| 7.8.5            | Coating thickness.....  | 133        |
| 7.8.6            | Relationship between chloride ion content and bar corrosion condition.....                                    | 133        |
| <br>             |   |            |
| CHAPTER 8.       | COMPARISON OF BRIDGE DECK CONDITION BETWEEN<br>1996 AND 2006.....   | <b>135</b> |
| 8.1              | INTRODUCTION .....  | 135        |
| 8.2              | FIELD INSPECTION .....  | 135        |
| 8.3              | CHLORIDE ION CONTENT.....   | 136        |
| 8.4              | EPOXY COATING EVALUATION.....   | 141        |
| 8.4.1            | Coating deterioration .....   | 141        |
| 8.4.2            | Bar corrosion condition.....  | 143        |
| 8.5              | ESTIMATING THE CORROSION CONDITION OF ECR IN BRIDGE DECKS.....  | 144        |
| 8.5.1            | Estimation of chloride ion depth profiles.....  | 144        |
| 8.5.2            | Estimation of the chloride content at the bar level corresponding to a given<br>corrosion activity level..... | 145        |
| <br>             |   |            |
| CHAPTER 9.       | SUMMARY AND CONCLUSIONS .....   | <b>154</b> |
| 9.1              | SUMMARY .....   | 154        |
| 9.2              | MAIN FINDINGS .....   | 154        |
| 9.2.1            | ECR performance.....  | 154        |
| 9.2.2            | Chloride ion content.....   | 154        |
| 9.2.3            | Observations from field inspections and surveys .....   | 155        |
| 9.3              | CONCLUSIONS .....   | 155        |
| 9.4              | RECOMMENDATIONS .....   | 156        |
| 9.5              | FINAL REMARKS.....  | 156        |
| <br>             |   |            |
| REFERENCES ..... |   | 158        |

APPENDIX A: DETAILED CORE DESCRIPTION

APPENDIX B: DIFFUSION COEFFICIENT CALCULATION



## LIST OF TABLES

|  |     |
|--|-----|
| <b>Table 3.1</b> Bridges studied.....  | 18  |
| <b>Table 3.2</b> Main characteristics of bridges studied.....                                | 18  |
| <b>Table 3.3</b> Bar size and type in both mats .....  | 24  |
| <b>Table 3.4</b> WJE's 1996 study results on bridge 19015.....                               | 25  |
| <b>Table 3.5</b> WJE's 1996 study results on bridge 27062.....                               | 25  |
| <b>Table 3.6</b> WJE's 1996 study results on bridge 27812.....                               | 26  |
| <b>Table 3.7</b> WJE's 1996 study results on bridge 27815.....                               | 27  |
| <b>Table 4.1</b> Bridges visits.....   | 28  |
| <b>Table 4.2</b> Cores extracted per bridge .....  | 31  |
| <b>Table 5.1</b> Measured concrete densities .....   | 37  |
| <b>Table 5.2</b> Epoxy coated bars extracted per bridge .....                                | 39  |
| <b>Table 5.3</b> Coating adhesion rating description.....                                    | 41  |
| <b>Table 5.4</b> Description of bar corrosion rating .....                                   | 42  |
| <b>Table 6.1</b> Summary of coordinates by core selected.....                                | 93  |
| <b>Table 6.2</b> Average measured bar cover depth.....                                       | 94  |
| <b>Table 6.3</b> Crack density.....  | 95  |
| <b>Table 6.4</b> Delaminated areas identified by chain-drag.....                             | 95  |
| <b>Table 7.1</b> Number of samples tested for chloride ion content .....                     | 98  |
| <b>Table 7.2</b> Chloride ion content in bridge 19015 cores .....                            | 101 |
| <b>Table 7.3</b> Diffusion coefficient in bridge 19015 cores.....                            | 102 |
| <b>Table 7.4</b> Measured carbonation depth in bridge 19015 cores .....                      | 105 |
| <b>Table 7.5</b> Measured coating hardness of bars extracted from bridge 19015 cores .....   | 105 |
| <b>Table 7.6</b> Coating adhesion of bars extracted from bridge 19015 cores.....             | 106 |
| <b>Table 7.7</b> Measured coating thickness of bars extracted from bridge 19015 cores .....  | 106 |
| <b>Table 7.8</b> Bar corrosion condition in bars extracted from bridge 19015 cores.....      | 107 |
| <b>Table 7.9</b> Chloride ion content in bridge 27062 cores .....                            | 108 |
| <b>Table 7.10</b> Diffusion coefficient in bridge 27062 cores.....                           | 110 |
| <b>Table 7.11</b> Measured carbonation depth in bridge 27062 cores .....                     | 111 |
| <b>Table 7.12</b> Measured coating hardness in bars extracted from bridge 27062 cores .....  | 111 |
| <b>Table 7.13</b> Coating adherence in bars extracted from bridge 27062 cores .....          | 112 |
| <b>Table 7.14</b> Measured coating thickness in bars extracted from bridge 27062 cores ..... | 112 |
| <b>Table 7.15</b> Corrosion condition in bars extracted from bridge 27062 cores.....         | 113 |
| <b>Table 7.16</b> Chloride ion content in bridge 27812 cores .....                           | 114 |
| <b>Table 7.17</b> Diffusion coefficient in bridge 27812 cores.....                           | 117 |
| <b>Table 7.18</b> Measured carbonation depth in bridge 27812 cores .....                     | 117 |
| <b>Table 7.19</b> Measured coating hardness in bars extracted from bridge 27812 cores .....  | 118 |
| <b>Table 7.20</b> Coating adherence in bars extracted from bridge 27812 cores .....          | 119 |
| <b>Table 7.21</b> Measured coating thickness in bars extracted from bridge 27812 cores ..... | 119 |
| <b>Table 7.22</b> Corrosion condition in bars extracted from bridge 27812 cores.....         | 120 |
| <b>Table 7.23</b> Chloride ion content in bridge 27815 cores .....                           | 121 |
| <b>Table 7.24</b> Diffusion coefficient in bridge 27815 cores.....                           | 125 |
| <b>Table 7.25</b> Measured carbonation depth in bridge 27815 cores .....                     | 125 |
| <b>Table 7.26</b> Measured coating hardness in bars extracted from bridge 27815 cores .....  | 126 |
| <b>Table 7.27</b> Coating adherence in bars extracted from bridge 27815 cores .....          | 126 |

|  |     |
|--|-----|
| <b>Table 7.28</b> Measured coating thickness in bars extracted from bridge 27815 cores ..... | 127 |
| <b>Table 7.29</b> Corrosion condition in bars extracted from bridge 27815 cores.....         | 127 |
| <b>Table 7.30</b> Cores by probability of corrosion .....                                    | 128 |
| <b>Table 7.31</b> Average chloride ion content per bridge for non-delaminated cores.....     | 128 |
| <b>Table 7.32</b> Hardness test results per bridge.....                                      | 132 |
| <b>Table 7.33</b> Adherence test results per bridge .....                                    | 133 |
| <b>Table 8.1</b> Comparison of delaminated areas in 1996 and 2006 .....                      | 135 |
| <b>Table 8.2</b> Comparison of chloride ion content test results 1996-2006.....              | 136 |
| <b>Table 8.3</b> Comparison of average chloride ion content 1996-2006 .....                  | 137 |
| <b>Table 8.4</b> Comparison of average chloride ion content .....                            | 140 |
| <b>Table 8.5</b> Comparison of adherence test results 1996-2006 .....                        | 142 |
| <b>Table 8.6</b> Conversion of corrosion condition between both studies .....                | 143 |
| <b>Table 8.7</b> Comparison of the bar corrosion condition in 1996 and 2006.....             | 143 |
| <b>Table 8.8</b> Parameters used to calculate the chloride ion profiles.....                 | 145 |

## LIST OF FIGURES

|  |    |
|--|----|
| <b>Figure 2.1</b> Example of corroded epoxy-coated bars (extracted from bridge 19015 in 2006, core DCS2). The bar on the right has the epoxy coating severely disbonded.....   | 4  |
| <b>Figure 2.2</b> Corrosion by macrocell and microcell.....  | 5  |
| <b>Figure 2.3</b> Example of concrete carbonation (clear surface) in a vertical crack [46]. .....  | 8  |
| <b>Figure 2.4</b> Half-cell potential measurements .....   | 11 |
| <b>Figure 2.5</b> Electrical impedance spectroscopy schematic setup and equivalent circuit.....  | 12 |
| <b>Figure 2.6</b> Electrical impedance spectroscopy setup and data acquisition system. ....  | 13 |
| <b>Figure 2.7</b> Ideal electrochemical impedance spectroscopy response for an epoxy coated rebar (case A) and a black rebar (case B).....   | 13 |
| <b>Figure 2.8</b> Ground Penetrating Radar System used in the imaging of the bridge decks.....   | 15 |
| <b>Figure 3.1</b> Location and aerial pictures of bridges studied in the Minneapolis/St. Paul metropolitan area (Images: Google maps). .....   | 19 |
| <b>Figure 3.2</b> Plan view (above) and cross section (below), bridge 19015 .....  | 20 |
| <b>Figure 3.3</b> Plan view (above) and cross section (below), bridge 27062 .....  | 21 |
| <b>Figure 3.4</b> Plan view (above) and cross section (below), bridge 27812 .....  | 22 |
| <b>Figure 3.5</b> Plan view (above) and cross section (below), bridge 27815 .....  | 23 |
| <b>Figure 4.1</b> Chain-drag survey.....   | 29 |
| <b>Figure 4.2</b> Connection to epoxy-coated bars.....   | 30 |
| <b>Figure 5.1</b> Concrete powder sample extraction by drilling.....   | 33 |
| <b>Figure 5.2</b> Typical sample location for chloride ion analysis in cores without cracks .....  | 33 |
| <b>Figure 5.3</b> Beaker-electrode-buret assembly during a chloride ion analysis titration:<br>1) magnetic stirring device, 2) 25mL buret, 3) Orion electrode, 4) multivoltmeter and<br>5) computer to record and plot results.....          | 35 |
| <b>Figure 5.4</b> Typical titration curve.....   | 36 |
| <b>Figure 5.5</b> Determination of carbonation depth using phenolphthalein solution.....   | 38 |
| <b>Figure 5.6</b> Rilem CPC-18 different carbonation depth $d_k$ development: a) Constant $d_k$ ,<br>b) Variable $d_k$ , c) Constant $d_k$ with singularities .....  | 38 |
| <b>Figure 5.7</b> Pencil hardness test.....  | 40 |
| <b>Figure 5.8</b> Dry knife adhesion test.....   | 40 |
| <b>Figure 6.1</b> Spalled area in bridge 19015 .....   | 43 |
| <b>Figure 6.2</b> Crack layout, spalled and delaminated areas on bridge 19015.....   | 44 |
| <b>Figure 6.3</b> Half-cell potential grid used in bridge 19015. ....  | 45 |
| <b>Figure 6.4</b> Half-cell potential readings along grid line A, B, C, D1, and D2 in bridge 19015. ...  | 46 |
| <b>Figure 6.5</b> Half-cell potential readings along grid line 1 to 5 in bridge 19015.....   | 47 |
| <b>Figure 6.6</b> Contour map of HCP along longitudinal survey lines, bridge 19015.....  | 48 |
| <b>Figure 6.7</b> Contour map of HCP along transverse survey lines, bridge 19015.....  | 48 |
| <b>Figure 6.8</b> Impedance spectroscopy grid used in bridge 19015.....  | 50 |
| <b>Figure 6.9</b> Typical impedance spectroscopy results from bridge 19015 (Line B):<br>(a) Cole-Cole plot and (b) amplitude and phase versus frequency. ....  | 51 |
| <b>Figure 6.10</b> Electrical impedance spectroscopy along longitudinal line A. (a) Impedance magnitude at four frequencies and (b) Contour plot of impedance amplitude versus frequency and measurement position along the survey line..... | 52 |

|  |    |
|--|----|
| <b>Figure 6.11</b> Electrical impedance spectroscopy along longitudinal line 4. (a) Impedance magnitude at four frequencies and (b) Contour plot of impedance amplitude versus frequency and measurement position along the survey line.....                   | 53 |
| <b>Figure 6.12</b> Location of ground penetrating radar (GPR) survey. ....   | 55 |
| <b>Figure 6.13</b> Ground penetrating radar (GPR) survey lines along the shoulder and left most lane on the southbound Bridge 19015. ....  | 56 |
| <b>Figure 6.14</b> Distribution of (a) electromagnetic wave velocity and (b) calculated volumetric water content on Bridge 19015. ....   | 57 |
| <b>Figure 6.15</b> Distribution of rebar depths in Bridge 19015 as estimated from GPR measurements. ....   | 57 |
| <b>Figure 6.16</b> Detailed view of transverse cracking on the deck of bridge 27062.....   | 58 |
| <b>Figure 6.17</b> Evidence of efflorescence and rust staining on the underside of the deck of bridge 27062.....   | 59 |
| <b>Figure 6.18</b> Crack layout, spalled and/or delaminated areas on bridge 27062 .....  | 59 |
| <b>Figure 6.19</b> Half-cell potential grid used in bridge 27062. ....   | 60 |
| <b>Figure 6.20</b> Half-cell potential readings along grid line A, B, C and D in bridge 27062.....   | 61 |
| <b>Figure 6.21</b> Half-cell potential readings along grid line 1 to 5 in bridge 27062.....  | 61 |
| <b>Figure 6.22</b> Half-cell potential readings along grid line 6 to 10 in bridge 27062.....   | 62 |
| <b>Figure 6.23</b> Contour map of HCP readings in the longitudinal survey lines, bridge 27062.....   | 62 |
| <b>Figure 6.24</b> Contour map of HCP readings in the transverse survey lines, bridge 27062.....   | 62 |
| <b>Figure 6.25</b> Electrical impedance spectroscopy along longitudinal line A bridge 27062.<br>(a) Impedance magnitude at four frequencies and (b) Contour plot of impedance amplitude versus frequency and measurement position along the survey line. ....  | 63 |
| <b>Figure 6.26</b> Electrical impedance spectroscopy along longitudinal line C, bridge 27062.<br>(a) Impedance magnitude at four frequencies and (b) Contour plot of impedance amplitude versus frequency and measurement position along the survey line. .... | 64 |
| <b>Figure 6.27</b> GPR results along survey lines in bridge 27062.....   | 66 |
| <b>Figure 6.28</b> Bridge 27062 (a) Mapping of crack, patches and delamination areas and (b) Calculated velocity contours (m/ns).....  | 67 |
| <b>Figure 6.29</b> Distribution of (a) electromagnetic wave velocity and (b) volumetric water content on Bridge 27062 as determined by the GPR survey.....   | 68 |
| <b>Figure 6.30</b> Distribution of rebar depths in Bridge 27062 as estimated from GPR measurements. ....   | 68 |
| <b>Figure 6.31</b> Detailed view of transversal cracking on the deck of bridge 27812.....  | 69 |
| <b>Figure 6.32</b> Evidence of efflorescence and rust staining on the underside of the deck of bridge 27812.....   | 70 |
| <b>Figure 6.33</b> Layout of cracks, spalled and delaminated areas on bridge 27812. ....   | 70 |
| <b>Figure 6.34</b> Delaminated area detected in bridge 27812.....  | 71 |
| <b>Figure 6.35</b> Half-cell potential grid used in bridge 27812. ....   | 72 |
| <b>Figure 6.36</b> Half-cell potential readings along grid line A, B, C and D in bridge 27812. ....  | 73 |
| <b>Figure 6.37</b> Half-cell potential readings along grid lines Joint, 1, 2 and 3 in bridge 27812.....  | 74 |
| <b>Figure 6.38</b> Contour map of HCP readings in the longitudinal survey lines, bridge 27812.....   | 75 |
| <b>Figure 6.39</b> Contour map of HCP readings in the transverse survey lines, bridge 27812.....   | 75 |

|  |     |
|--|-----|
| <b>Figure 6.40</b> Electrical impedance spectroscopy versus half-cell potential measurement along line D-D' in Bridge 27812. (a) half-cell potential measurements, (b) four-frequency impedance measurement, and (c) contour plots of impedance magnitude versus frequency and positions along the survey line. .... | 76  |
| <b>Figure 6.41</b> Electrical impedance spectroscopy versus half-cell potential measurement along line Joint line in Bridge 27812. (a) four-frequency impedance measurement and (b) contour plots of impedance magnitude versus frequency and positions along the survey line. ....                                  | 77  |
| <b>Figure 6.42</b> GPR survey lines in east-most part of the eastbound direction of bridge 27812 .....   | 79  |
| <b>Figure 6.43</b> Distribution of (a) electromagnetic wave velocity and (b) calculated volumetric water content. ....   | 81  |
| <b>Figure 6.44</b> Distribution of rebar depths in Bridge 27812 as estimated from GPR measurements. For comparison, the rebar depths obtained from extracted cores are presented in the top figure. ....   | 82  |
| <b>Figure 6.45</b> Crack layout, spalled and/or delaminated areas on bridge 27815 .....  | 83  |
| <b>Figure 6.46</b> Transverse crack in bridge 27815 .....  | 83  |
| <b>Figure 6.47</b> Evidence of efflorescence and rust staining on the underside of the deck of bridge 27815. ....  | 84  |
| <b>Figure 6.48</b> Half-cell potential grid used in bridge 27815. ....   | 85  |
| <b>Figure 6.49</b> Half-cell potential readings along grid line A, B, C and D in bridge 27815. ....  | 86  |
| <b>Figure 6.50</b> Half-cell potential readings along grid line 1 to 5 in bridge 27815. ....   | 86  |
| <b>Figure 6.51</b> Contour map of HCP readings in the longitudinal survey lines, bridge 27815. ....  | 87  |
| <b>Figure 6.52</b> Contour map of HCP readings in the transverse survey lines, bridge 27815. ....  | 87  |
| <b>Figure 6.53</b> Electrical impedance spectroscopy versus half-cell potential measurement along line C-C'. Bridge 27815: (a) half-cell potential measurements, (b) four-frequency impedance measurement, and (c) contour plots of impedance magnitude versus frequency and positions along the survey line. ....   | 88  |
| <b>Figure 6.54</b> GPR survey lines in bridge 27815 and interpretation of the distribution of electromagnetic wave velocity. ....  | 90  |
| <b>Figure 6.55</b> Distribution of (a) electromagnetic wave velocity and (b) volumetric water content (overlapped with crack mapping) on Bridge 27815 as determined by the GPR survey. ....  | 91  |
| <b>Figure 6.56</b> Distribution of rebar depths in Bridge 27815 as estimated from GPR measurements. For comparison, the rebar depths obtained from extracted cores are presented in the top figure. ....   | 91  |
| <b>Figure 7.1</b> Example of chloride content taken from a non-delaminated core at different depths .....  | 99  |
| <b>Figure 7.2</b> Example of chloride content taken from a delaminated core at different depths .....  | 100 |
| <b>Figure 7.3</b> Chloride ion content profile results for Bridge 19015, Cores "A2", "AP", "C2" and "CP" .....   | 103 |
| <b>Figure 7.4</b> Chloride ion content profile results for Bridge 19015, Cores "D2", "DP", "DCS1" and "DCS2" .....   | 104 |
| <b>Figure 7.5</b> Chloride ion content profile results for Bridge 27062, Cores "A1", "B1", "C1" and "D1" .....   | 109 |
| <b>Figure 7.6</b> Chloride ion content profile results for Bridge 27062, Cores "D2" and "D3" .....   | 110 |

|  |     |
|--|-----|
| <b>Figure 7.7</b> Chloride ion content profile results for Bridge 27812, Cores “22”, “23”, “31” and “32” .....   | 115 |
| <b>Figure 7.8</b> Chloride ion content profile results for Bridge 27812, Cores “33”, “J1”, “J2” and “J3” .....   | 116 |
| <b>Figure 7.9</b> Example of chloride ion content at vertical crack and away from crack .....  | 122 |
| <b>Figure 7.10</b> Chloride ion content profile results for Bridge 27815, Cores “11”, “12”, “22” and “32” .....  | 123 |
| <b>Figure 7.11</b> Chloride ion content profile results for Bridge 27815, Cores “41”, “42”, “51” and “52” .....  | 124 |
| <b>Figure 7.12</b> Chloride ion content at 0.5 in. ....  | 129 |
| <b>Figure 7.13</b> Chloride ion content at the upper bar level for cracked and uncracked cores .....   | 130 |
| <b>Figure 7.14</b> Calculated chloride ion diffusion coefficient in concrete for all four bridge decks   | 131 |
| <b>Figure 7.15</b> Example of pencil hardness test .....   | 132 |
| <b>Figure 7.16</b> Relationship between chloride ion content and corrosion condition.....  | 134 |
| <b>Figure 8.1</b> Comparison of average measured chloride ion content at 0.5 in. below the surface in 1996 and in 2006. ....   | 137 |
| <b>Figure 8.2</b> Envelope of chloride ion content profiles in 1996 and 2006.....  | 139 |
| <b>Figure 8.3</b> Relationship between chloride ion content at the bar level and corrosion condition of the bars.....  | 141 |
| <b>Figure 8.4</b> Detail of coating disbondment in core.....   | 142 |
| <b>Figure 8.5</b> Estimated chloride ion content profiles in 2006 for the decks studied.....   | 146 |
| <b>Figure 8.6</b> Regression of chloride ion content and corrosion condition .....   | 147 |
| <b>Figure 8.7</b> Estimated chloride ion content profiles in 2006 and bar corrosion threshold levels for the bridges studied.....  | 148 |
| <b>Figure 8.8</b> Example of chloride ion content profiles predicted for year 2016. ....   | 151 |
| <b>Figure 8.9</b> Effect of a surface crack in year 5 (and sealed in year 6) on the chloride ion concentration distribution. (a) non-cracked bridge deck chloride ion distribution and (b) cracked bridge deck chloride ion distribution. .... | 153 |

## EXECUTIVE SUMMARY

The deterioration of reinforced concrete structures is a major problem facing the transportation infrastructure. In bridge decks, the primary cause of this deterioration is the corrosion of steel reinforcing bars due to chloride ion intrusion. The two main sources of chlorides are seawater in coastal areas and large amounts of salt-based deicing chemicals used during the winter months in the northern parts of the country.

The main purpose of this investigation was to conduct an in-depth study to determine the level of corrosion protection offered by epoxy-coated bars in four bridge decks in the Minneapolis/St. Paul, MN metropolitan area. The bridges were built between 1973 and 1978 and in 2008 are approximately 30 to 35 years old. All decks had the top mat built with epoxy-coated bars. The bottom mat reinforcing steel was epoxy-coated in only one bridge deck (bridge 19015). Black steel was used for the bottom mat in the other three bridges (bridges 27062, 27812 and 27815). In 1989, however, the Minnesota Department of Transportation (Mn/DOT) changed its policies to include epoxy coating on the top and bottom mats of deck bars.

A previous study conducted in 1996 showed that some epoxy-coated bars had corroded at crack locations and that the level of corrosion was sufficient to cause delamination of the deck in some areas. It was noted, however, that bars adjacent to heavily corroded bars were sometimes corrosion free, even though they were exposed to the same levels of chloride ion concentrations. The present study is a follow up investigation to assess the corrosion performance of the bars in the same four bridge decks to obtain data over a period of approximately 30 years. Evaluation of the performance of the epoxy-coated bars included field inspection and surveys conducted on all four bridge decks, as well as laboratory tests of concrete core and bar samples. This report includes the results of the data collected during the inspection and surveys conducted in the field and the results of the laboratory tests.

The field study included several methods to assess the existing condition of the decks, the corrosion state of the epoxy-coated bars, as well as the overall health of the bars. The methods used in the field in all four bridge decks were the following:

- Visual Inspection
- Chain Drag
- Half-Cell Potential (HCP)
- Electrochemical Impedance Spectroscopy (EIS)
- Ground Penetrating Radar (GPR)

Field survey results were complemented with targeted core extraction and evaluation of the condition of concrete and of the bars removed with the cores. The laboratory measurements included the following:

- Chloride ion content
- Carbonation depth
- Concrete density
- Diffusion coefficient
- Epoxy-coating hardness, adhesion and thickness
- Bar corrosion condition

Observations from the site visit showed that the bridge decks are in good condition. After approximately 30 years of service, the decks showed light cracking and few delaminated areas (some of which have already been patched), and only one deck (bridge 19015) had an open spalled area. Overall delaminated and spalled areas represented a small fraction of the total bridge deck area (less than 1.1 % of the total surveyed areas).

Results from half-cell potential and electrochemical impedance spectroscopy readings obtained in the field indicated that the overall condition of epoxy-coated bars is good to very good, with no or modest levels of corrosion activity. In only one bridge (bridge 19015), corrosion activity appears to be severe in some areas, mainly around the joints over the bridge piers. This result is attributed mainly to the high level of chloride ion content and a small cover depth of the bars (2 to 2.5 in.)

The data obtained in this and the 1996 study show that the epoxy-coated bars in these bridge decks are likely to show corrosion when the bar level chloride ion content is 5.3 lb/cy. or greater. Only a few bars (three bars in this study and one bar in the 1996 study) showed corrosion at a chloride ion content level comparable to that of black bars (i.e., 1.2 lb/cy). The majority of corroded bars were found near joints or crack locations.

Two of the decks studied (bridges 27812 and 27815) had 2.5 in. low slump, high density overlays. While the data gathered in this study indicates that other mechanisms may control the chloride ion ingress in bridge decks, the lower chloride ion content measured near the surface, the lower diffusion coefficient and the smaller amount of delamination observed in these decks suggest that low slump, high density concrete overlays can improve the performance and extend the service life of bridge decks.

The results showed no evidence that the use of black bars for the bottom mat influences the corrosion activity in the epoxy-coated bars of the top mat. However, rust staining and efflorescence was observed only on the underside of decks with a bottom mat of black bars. Thus, the current Mn/DOT practice of using epoxy-coated bars for both the top and bottom mats should enhance the overall health of the bridge deck and should be continued.

The bridge decks studied here were all built in the 1970s. The procedures for coating fabrication and application, as well as storage and handling of the bars in the field have improved significantly in the last 30 years through tighter specifications and plant certification programs. As a result, the quality of the epoxy coating and, therefore, the performance of the bars used today are expected to be as good or better than that observed in this study.



## **CHAPTER 1. INTRODUCTION**

### **1.1 INTRODUCTION**

The deterioration of reinforced concrete structures is a major problem for maintenance engineers. The cost of repairing or replacing deteriorated structures (estimated to be more than \$20 billion and to be increasing at \$500 million a year) has become a major liability for highway agencies [1]. The primary cause of this deterioration is the corrosion of steel reinforcing bars due to chlorides. The two main sources of chlorides are seawater and large amounts of salt-based deicing chemicals used during the winter months in the northern parts of the country.

Several measures have been developed and implemented to prevent the chloride-induced corrosion of steel reinforcing bars and the resulting deterioration. Some of the early measures used included lowering the water-cement ratio of the concrete to reduce permeability and increasing the concrete cover over the steel reinforcing bars. Concrete permeability can also be reduced by the use of admixtures. While these measures generally do not stop corrosion from eventually initiating, they do increase the service life of reinforced concrete structures by slowing the corrosion process.

Epoxy-coated reinforcing steel (ECR) was introduced in the mid 1970s as a means to minimize concrete deterioration caused by corrosion of the reinforcing steel and to extend the useful life of highway structures. The epoxy coating is a barrier system intended to prevent moisture and chlorides from reaching the surface of the reinforcing steel and reacting with the steel.

Doubts have been raised concerning the performance of epoxy-coated reinforcement due to failures in high chloride environments (i.e. a marine environment) within three years. Although many bridge decks constructed with epoxy-coated reinforcing steel exhibit no evidence of deterioration after more than twenty years, there is evidence that epoxy-coated rebars may still corrode over the life time of the structure.

The Federal Highway Administration (FHWA) recommended that states evaluate the performance of ECR in existing bridge decks. As a result, several states initiated investigations and prepared reports documenting their findings and results.

### **1.2 OBJECTIVE**

The main purpose of this report is to assess the corrosion performance of epoxy-coated reinforcing bars in four bridge decks located in the Minneapolis-St Paul metropolitan area in Minnesota, over a period of time of approximately 30 years. This research project provides an opportunity to assess the in-situ performance of epoxy-coated bars over an extended period of time under actual operation conditions. The results of this investigation provides the necessary data to allow bridge maintenance engineers to estimate the performance of bridge decks with epoxy-coated bars over time, and to develop and improve appropriate bridge deck health and to update ongoing rehabilitation programs.

### **1.3 SCOPE**

The report includes field and laboratory measurements to assess the corrosion condition of bridge deck and epoxy-coated reinforcing bars in four Minnesota bridges. Field studies include chain-drag surveys to identify and map delaminated areas. They will also include half-cell potential (HCP) measurements to determine the level of corrosion activity in the rebars, electrochemical spectroscopy measurements to evaluate the in-situ quality of epoxy cover or rebars, and ground penetrating radar (GPR) testing to evaluate internal deterioration and estimate rebar depths. Laboratory tests include determination of chloride content at the surface, at the bar level, carbonation depth, and epoxy-coated rebar evaluation in samples retrieved from the decks at selected locations. Field and laboratory data are analyzed and cross-correlated to assess the corrosion performance of the bars. In addition, the data obtained in the present study is compared to those obtained in a previous study on the same bridge decks to evaluate the progression of corrosion in the bars. Other characteristics, influence of the cover depth, presence of low slump high density concrete overlays, and the presence of chloride ions on the performance of the epoxy-coated reinforcing steel are also examined.

## CHAPTER 2. BACKGROUND AND LITERATURE REVIEW

### 2.1 INTRODUCTION

In this chapter, the main characteristics of the corrosion process, epoxy-coated rebars and concrete evaluation are presented. Also, the most commonly used methods for evaluating concrete treated with deicing salt and epoxy-coated bars exposed to chloride ions are described, including the standard test methods used in this study. A summary of previous experiences are also presented.

### 2.2 CORROSION PROCESS

#### 2.2.1 *General*

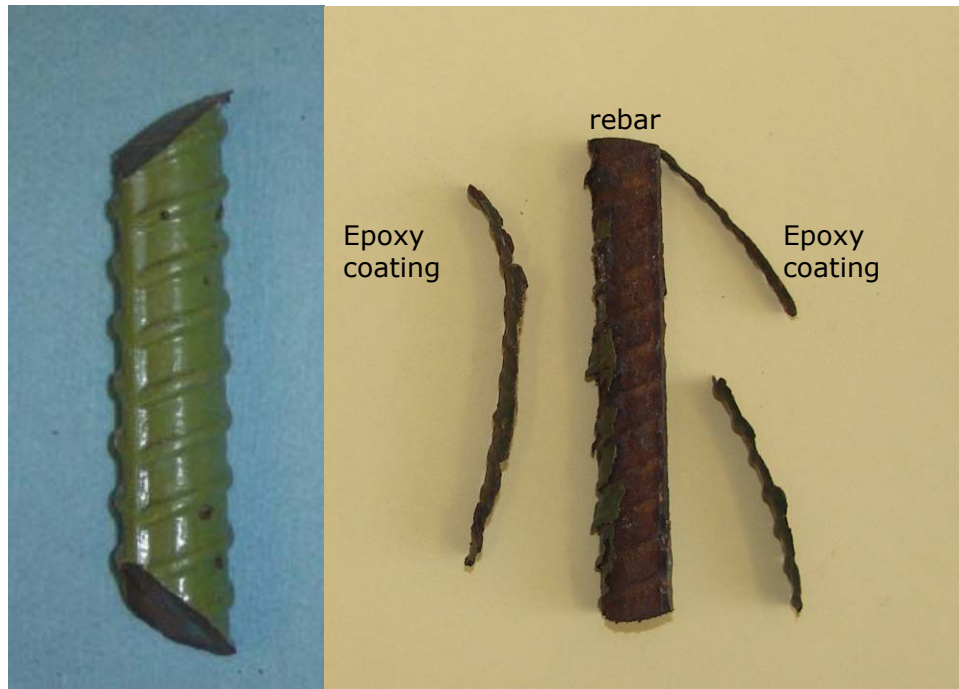
The corrosion process of reinforcement in bridge decks results from an electrochemical process [2,3]. There has to be a current flow, which results from a potential difference between a cathode and an anode in the reinforced concrete element. In most cases, the top mat of steel in a bridge deck acts as the cathode and the bottom mat acts as the anode. At the anode site, the iron atoms lose the electrons that move into the surrounding concrete as positively charged ferrous ions ( $\text{Fe}^{2+}$ ). Free electrons ( $e^-$ ) flow through the rebar to the cathodic site where they react with dissolved oxygen and water to produce hydroxyl ions ( $\text{OH}^-$ ). To maintain the electrical neutrality, the hydroxyl ions diffuse through concrete pores toward the anode site where they react with the ferrous ions to form iron oxide or rust. The volume of the rust increases the original volume of the steel. The volumetric ratio of the rust to steel depends on the form of corrosion product. Generally, the ratio ranges from 2.2 for  $\text{Fe}_3\text{O}_4$  to 6.4 for  $\text{Fe}(\text{OH})_3\cdot 3\text{H}_2\text{O}$  [4].

The amount of corrosion present and the rate at which the steel corrodes depend on various factors. Wet and dry cycles accelerate the corrosion process and, thus, make the environment an important factor [3]. It has been found that the corrosion rate is highest during the spring season and lowest during the winter [3, 5]. These rates can vary by a factor of about four or five times during the year [3].

A rebar is embedded in moist concrete. The concrete pores contain various dissolved ions which serve as electrolytes. Once the presence of carbonation or the presence of chloride ions is above the critical concentration, the rebar corrosion will most likely take place, provided that oxygen is also present. Under these conditions, one region of rebar will act as an anode and another region will act as a cathode. Since both anode and cathode may exist on the same rebar, there is an electrical connection between the two.

Exposure of reinforced concrete to chloride ions is the primary cause of premature corrosion of steel reinforcement. The intrusion of chloride ions, present in deicing salts and seawater, into reinforced concrete can cause steel corrosion if oxygen and moisture are also available to sustain the reaction. Chlorides dissolved in water can permeate through concrete and reach the steel reinforcement. Although the use of high performance concrete reduces the risk of corrosion, the increasing use of deicing salt and the increasing concentration of carbon dioxide has made rebar corrosion one of the primary causes of the deterioration of highway concrete structures. Figure 2.1 shows an example of two epoxy coated rebars, one with no corrosion (left) and the other with

corrosion (right). The bar on the right had severe coating disbondment but it had no section loss. This represents the worst case of all of the bars removed in this study (see Section 8.4.2).

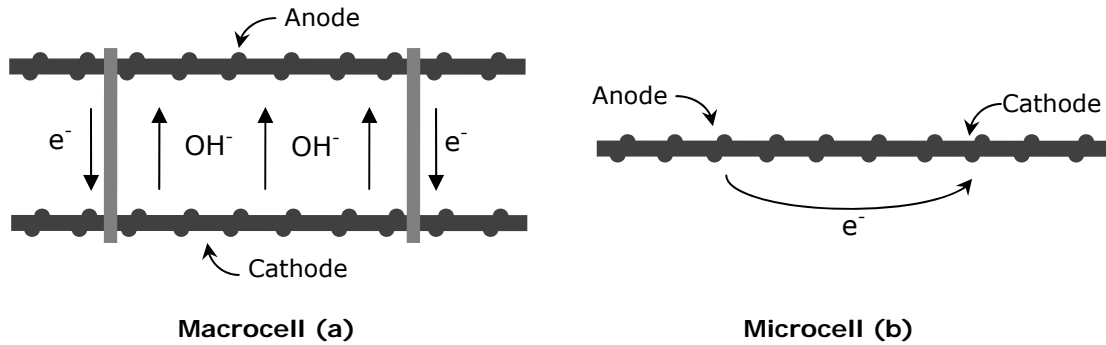


**Figure 2.1** Example of corroded epoxy-coated bars (extracted from bridge 19015 in 2006, core DCS2). The bar on the right has the epoxy coating severely disbonded.

Decks without epoxy-coated rebars normally conduct current throughout the reinforcement quite well because the reinforcing steel is in direct contact with the surrounding concrete. This acts to significantly increase the corrosion of the reinforcement and reduce the life span of a bridge deck. The use of epoxy-coated rebars in bridge decks could decrease this type of continuity, but defects in the epoxy coating (holidays) and careless material handling during construction allow contact between the reinforcing bars and concrete [3].

### 2.2.2 Macro and micro corrosion cells

The distribution of chloride ions in a concrete bridge deck is not uniform. The chlorides typically enter the concrete from the top surface. The top mat of reinforcing steel is then exposed to higher concentrations of chlorides. The chloride ions shift the potential of the top mat reinforcing steel to a more negative (anodic) value. Since the potential of the bottom mat has a more positive (cathodic) value, the resulting difference in potentials sets up a galvanic type of corrosion cell called a macrocell, see Figure 2.2 (a). The concrete serves as the electrolyte. Wire ties, metal chair supports, and steel bars serve as metallic conductors. An electric circuit is established. Likewise, the concentration of chlorides is not uniform along the length of the steel bars at the top mat due to the heterogeneity of the concrete and uneven deicer application. These differences in chloride concentrations establish anodes and cathodes on individual steel bars in the top mat and result in the formation of microcells, see Figure 2.2 (b).



**Figure 2.2** Corrosion by macrocell and microcell.

### 2.2.3 Chloride threshold level

Most researches determine the total chloride (acid-soluble) ion content at the rebar level. This value, called threshold, is used to determine the level of chloride ion content necessary to initiate corrosion in the reinforcement. A common threshold value documented in the literature is 1.2 lb/yd<sup>3</sup> (0.71 kg/m<sup>3</sup>) [6,7] for unprotected reinforcement or black bars. This is based on 6.5 sacks of cement per cubic yard of concrete (equivalent to 5.4 ft<sup>3</sup>), Cady and Weyers [8]. However, many investigations have concluded different threshold values for ECRs, as follows:

- Munjal [9] referred to FHWA laboratory results that indicated values between 1.5 to 2.0 lb/cy.
- Sagüés et al. [10] suggest a range of the corrosive threshold for ECR from 1.2 to 3.6 lb/cy.
- A field study of bridge decks in Pennsylvania revealed moderate corrosion associated with as little chloride content as 0.1 lb/cy [11].
- Berke [12] reported experimental results of severe corrosion occurring at values between 0.2 and 26 lb/cy.
- Sohanchpurwala et al. [13], documented a lower threshold value of 1.2 lb/cy
- Fanous et al. [2], proposed a threshold range between 3.6 and 7.5 lb/cy.
- Weyers and Cady [14] noted the value 1.2 lb/cy.
- Al-Qadi, Peterson, and Weyers [15] reported values in the range of 0.3-4.7 lb/cy.
- Hagen [16] referred to a threshold range of 1.1-1.6 lb/cy.
- Fraczek [17] gave the range of 1.0-1.4 lb/cy.
- Others [18] suggested values in the range of 1.01 to 1.52 lb/cy.

The use of ECR is expected to delay the time required to initiate corrosion, or prevent it, and, as a result, the chloride ion content threshold should be higher than that for a black steel bars. However, others believe that the actual chloride threshold for epoxy-coated reinforcing bar varies on a project-by-project basis due to design, workmanship, concrete, and the quality of the epoxy coating. Thus, there is not a consensus about a specific higher threshold value for ECRs.

#### 2.2.4 Corrosion propagation

The rate of corrosion is dependent on the availability of water, oxygen, and chloride ions; the ratio of steel surface area at the anode to that at the cathode; the electrical resistivity of the concrete; and the temperature. The availability of oxygen is a function of its rate of diffusion through the concrete, which is affected by how water saturates the concrete. When totally submerged, the diffusion rate is slowed because the oxygen must diffuse through the pore water. When the concrete is dry, the oxygen can freely move through the pores. Alternating wet-dry cycles accelerates the corrosion process.

Corrosion rate ( $\mu\text{A}/\text{cm}^2$ ), measured in terms of corrosion current density, indicate how fast corrosion is occurring at the time of measurement. Corrosion rate can change over time depending on a number of factors, and are useful for determining local corrosion conditions and for comparing areas of the bridge deck. The following guidelines are generally used for black reinforcing bars:

- Less than  $0.1 \mu\text{A}/\text{cm}^2$ : very low corrosion.
- Between  $0.1$  to  $0.5 \mu\text{A}/\text{cm}^2$ : low to moderate corrosion.
- Between  $0.5$  to  $1.0 \mu\text{A}/\text{cm}^2$ : moderate to high corrosion.
- Greater than  $1.0 \mu\text{A}/\text{cm}^2$ : very high corrosion.

There is no equivalent classification for ECRs; instead, the corrosion propagation for these bars is commonly expressed in years necessary to have generalized corrosion of the bar.

- For Weyers et al. [7], the expected corrosion propagation time for ECRs is between 6 and 10 years. For bare steel they found a propagation time of 3-4.5 years, therefore, the extension in propagation due the coating can be estimated between 3 to 5.5 additional years beyond that expected for bare steel.
- According to Fanous et al. [2], the time of propagation of ECRs is about 5 years.
- For WJE [21], the time of corrosion propagation is between 3 to 6 years when the deck has ECR only in the top mat, this number increase to 15 years when both mats are made of ECR.
- The software Life-365 (Service Life Prediction Model), use a default time of propagation of 6 years for black steel and 20 years for ECR.

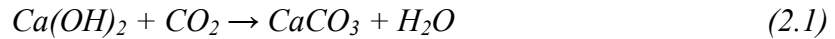
The variability of corrosion propagation lie in its primary rate-controlling factors, these are the availability of oxygen, the electrical resistivity and relative humidity of the concrete, the pH, and temperature. Although the presence of chloride ion is directly responsible for the initiation of corrosion, they appear to play only an indirect role in the rate of corrosion after initiation.

The corrosion process has a great impact on bridge deck deterioration; mainly because the level of corrosion propagation of steel reinforcing bars will determine the increment of steel volume. When corroded, steel occupies a volume three to six times the volume of the original non-corroded steel. This increment in volume induces stresses in the concrete that result in cracks, delaminations, and spalls [22], which accelerates the corrosion process by providing an easy pathway for the water and chlorides to reach the steel.

The point at which delaminations and spalls start to occur is subject to some variability. According to Broomfield [7], “It has been shown that cracking is induced by less than 0.1 mm of steel section loss, but in some cases far less than 0.1 mm has been needed.” Broomfield also stated that once these cracks occur, they allow for even more exposure of the steel to deicing chemicals and the environment. The presence of cracks acts to further increase the corrosion of the reinforcement and can have a noticeable impact on the bridge deck and underlying structure. According to Torres and Sagüés [24], the amount of corrosion needed to crack the concrete is much higher in specimens with localized corrosion (ECR) than specimens with uniform corrosion reported (bare steel).

### 2.3 CARBONATION

Carbonation occurs when carbon dioxide from the air penetrates the concrete and reacts with hydroxides, such as calcium hydroxide, to form carbonates. In the reaction with calcium hydroxide, calcium carbonate is formed:

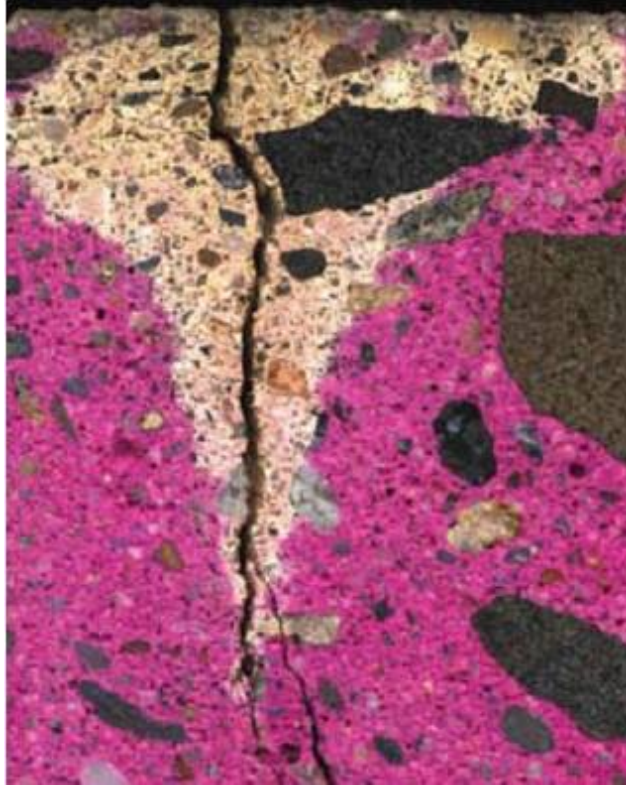


When concrete is carbonated near or at a depth of the embedded reinforcing steel, the concrete next to the steel surface is depassivated. As a result, the reinforcing steel is no longer protected and corrosion may then begin when moisture and oxygen gain access to the steel surface.

Carbonation is generally a slow process. In high-quality concrete, it has been estimated that carbonation will proceed at a rate up to 1.0 mm (0.04 in.) per year. The amount of carbonation is significantly increased in concrete with a high water-to-cement ratio, low cement content, short curing period, low strength, and highly permeable or porous paste [25].

Carbonation is highly dependent on the relative humidity of the concrete. The highest rates of carbonation occur when the relative humidity is maintained between 50% and 75%. Below 25% relative humidity, the degree of carbonation that takes place is considered insignificant. Above 75% relative humidity, moisture in the pores restricts CO<sub>2</sub> penetration.

Figure 2.3 shows an example of concrete carbonation in a vertical crack, the clear (light gray) surface indicates that carbon dioxide has penetrated. The red surface indicated no carbonation. This is explained in more detail in section 5.4.



*Figure 2.3 Example of concrete carbonation (clear surface) in a vertical crack [46].*

## **2.4 EPOXY-COATED REBARS (ECR) REVIEW**

Epoxy-coated reinforcing steel (ECR) was introduced in the mid 1970s as a means to minimize concrete deterioration caused by corrosion of the reinforcing steel and to extend the useful life of highway structures. The epoxy coating is a barrier system intended to prevent moisture and chlorides from reaching the surface of the reinforcing steel and reacting with the steel [3]. It also serves to electrically insulate the steel to minimize the flow of corrosion current [25].

The first bridge with epoxy-coated reinforcement (ECR) was constructed in West Conshohocken in Pennsylvania in 1973. By the early 1980s, the use of ECR in bridge structures became a standard procedure. At the same time, a lack of fundamental or basic research that would examine protective mechanism(s) of epoxy coating against chloride induced corrosion in concrete environment existed in North America [27].

Countries outside of North America represented a slightly different approach relative to the incorporation of ECR into the market place [27]. Studies were initiated to evaluate protective properties of epoxy coating on reinforcing steel.

By 1989, there were 17 coating applicator firms in the United States and Canada, and the market was dominated by one product, Scotchkote 213, manufactured by 3M. The advantage of the 3M product was its good flexibility, which allowed for a production line that could be operated at high speed.



Over the years, until the mid-1980s, bid prices for the supply and installation of ECR in comparison to bare steel dropped significantly. Estimated life-cycle costs for ECR demonstrated that other protection systems including interlayer membrane, latex-modified concrete (LMC) overlay, and low slump dense concrete (LSDC) overlay were more expensive than ECR, used for both top and bottom mats or top mat only [27]. Throughout the economical analysis, one corrosion protection system with a lower life-cycle cost than ECR was recognized, a reinforcement cover depth of 3.5 in.

#### ***2.4.1 Performance evaluation***

Several test methods are used in the performance evaluation of ECR. An overview of currently used laboratory and field evaluation techniques was given by Weyers [29]. In general, test methods are divided into laboratory and field assessment practices. Laboratory test methods include an evaluation of the structural behavior of ECR, mainly the bond strength between the ECR and concrete (pullout test, flexural bending, and bending fatigue) as well as bar flexibility and creep.

However, since the application of the epoxy coating on the reinforcing bar as a corrosion protection method, tests which measure the corrosion protection performance of ECR are of the primary concern. Tests that propose to address this issue can be classified into three major groups: tests on the coating, tests on the coated bar, and tests on coated bar in concrete.

Coating damage has received close attention during the past few years. New standards have been developed to ensure tighter limits on acceptable damage to coating in the future. Current specifications, such as ASTM A775, ASTM D3963, AASHTO M284, and industry recommendations (e.g., Concrete Reinforcing Steel Institute (CRSI) guidelines for inspection and acceptance of epoxy-coated reinforcing bars [19]) set limits on acceptable coating damage and repair.

#### ***2.4.2 Certification program***

In 1991, the CRSI established a program under which steel coating plants can be certified for maintaining a required level of quality [30]. The objective of the program was to ensure the production of ECRs with the latest approved standards and specifications. By encouraging a quality product, public investment in the infrastructure would be protected. Participation in the program was voluntary. In order for a plant to be certified, it must have a written quality control policy statement, keep careful records, and post a quality inspector on every work shift [30]. In general terms, the assessment includes the equipment, technology, and operators involved in the coating process.

The certification program addresses most of the plant's procedures and quality control tests. The issues of concern covered in the plan are the following [30, 31]:

- Abrasive blast cleaning of the steel before coating, including testing for chlorides and copper sulfate contamination.
- The temperature at which the steel is coated.
- The coating thickness
- Handling of the coated steel, including checking for holidays and the bend test.

## **2.5 METHODS FOR EVALUATING BRIDGE DECKS**

### **2.5.1 Chain-drag survey**

The chain drag method is the most common method for detecting delaminations in concrete decks. Listening for the characteristic hollow sound produced by dragging a chain across a delaminated surface, an experienced person can detect a damaged area. However, the chain drag method is not as effective in detecting small delaminated areas, and thus smaller suspect areas are typically found by tapping with a small hammer. The chain drag, as described in ASTM D 4580-86, is useful for initial delamination detection on large, flat surfaces. The advantage of this technique is its speed and low cost; however, the subjectivity of relying on the experienced ear of the operator limits the method to the location of gross surface delaminations where breakdowns have occurred over a large area.

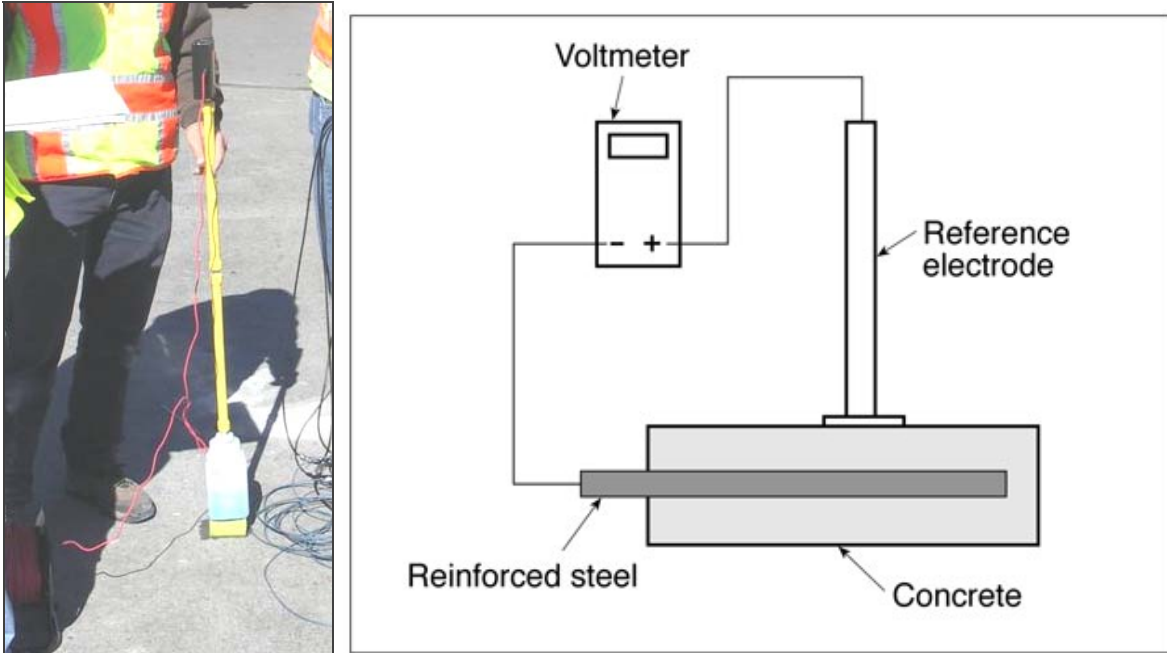
### **2.5.2 Half-cell potential**

Half-cell potential (HCP) measurements are a standard methodology for evaluating the corrosion activity in reinforced concrete elements. Concrete when exposed to chloride ions (deicers or salt water) and carbonation depassivate, generating the electrochemical potential that can drive the corrosion process in rebars. The electrochemical potential is measured as a negative shift in the HCP. One of the main values of HCP measurements is that, when plotted, they provide an indication where the most corroding (anodic) locations are on the deck. Testing and sampling can then be concentrated in those areas. To ensure high quality HCP readings, electrical continuity tests should be performed to verify the degree of electrical continuity between rebars in different locations within a span. The electrical continuity (low resistance) is a critical component for a valid HCP measurement. If there is a high resistance between the two grounding spots, erroneous HCP readings may result. However, in these bridge decks, electrical continuity can be established because at least one mat was uncoated. In practice, this means that the half-cell corrosion potential can only be measured on bridge decks with a top mat of epoxy-coated reinforcing bar and a bottom mat of uncoated reinforcing bar. Bridge decks with both the top and bottom mats of epoxy-coated reinforcing bar may not have any electrical continuity. Therefore, half-cell potentials may not yield meaningful results.

HCP data is conventionally interpreted using the Numeric Magnitude Technique specified in ASTM C876 “Standard Test Method for Half-Cell Potentials of Uncoated Reinforcing Steel in Concrete.” According to the criteria, if potentials over an area are more positive than  $-0.200$  Volt vs. copper-copper sulfate electrode ( $V_{CSE}$ ), there is a greater than 90% probability that no reinforcing steel corrosion is occurring in that area at the time of measurement. If potentials over an area are more negative than  $-0.350$  V, there is a greater than 90% probability that reinforcing steel corrosion is occurring in that area at the time of measurement [50]. If half-cell potentials readings range between  $-0.200$  and  $-0.350$   $V_{CSE}$ , corrosion activity of the reinforcing steel in that area is uncertain.

Because many factors such as concrete resistivity, temperature, carbonation, oxygen content, presence of coating, and degree of water saturation (moisture content) can influence the potential readings, the interpretation of the HCP data in this study was not made using the conventional ASTM criteria discussed above. Instead, the measured potentials were presented in the form of

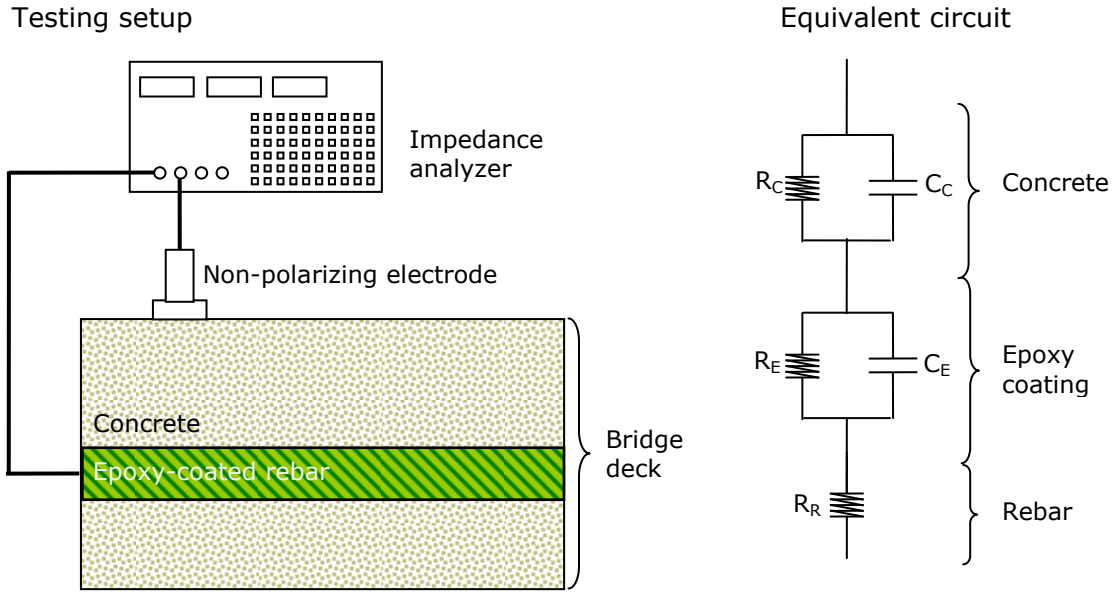
equi-potential contour maps, in which each color corresponds to a certain range of the potential readings obtained. As HCP becomes more negative, the contour map has a darker red color in that area indicating an actively corroding area. As the potential becomes more positive, the corresponding area shows a greener color. Also, the relative variation of potential measurements within a test area and the spacing between the contour lines can indicate areas of active corrosion. Narrower spacing (steeper gradient) of equi-potential contour lines may indicate higher corrosion rates. Based on the potential contour map, areas of the bridge deck in various states of corrosion were selected for subsequent coring. Figure 2.4 shows an illustrative diagram of the test.



*Figure 2.4 Half-cell potential measurements.*

### **2.5.3 Impedance Spectroscopy Measurements**

Impedance spectroscopy is a technique based on the interpretation of equivalent electrical circuits for the evaluation of corrosion and health of corrosion protection layers on metals over a wide frequency range [56, 57, 58]. The analysis of the impedance spectrum allows solving for different electrical circuit elements (i.e., resistors, capacitors, and inductors) and the evaluation of physical and electrochemical processes responsible for corrosion at interfaces [58]. The interpretation is based on developing equivalent circuits representing the different system components (e.g., concrete, epoxy coating, and rebars – Figure 2.5). In this project, electrochemical impedance spectroscopy was used to evaluate the quality of the epoxy coating in the reinforcing rebars. That is, a sound coating with no holidays should yield high values for resistance  $R_E$  and capacitor  $C_E$ .



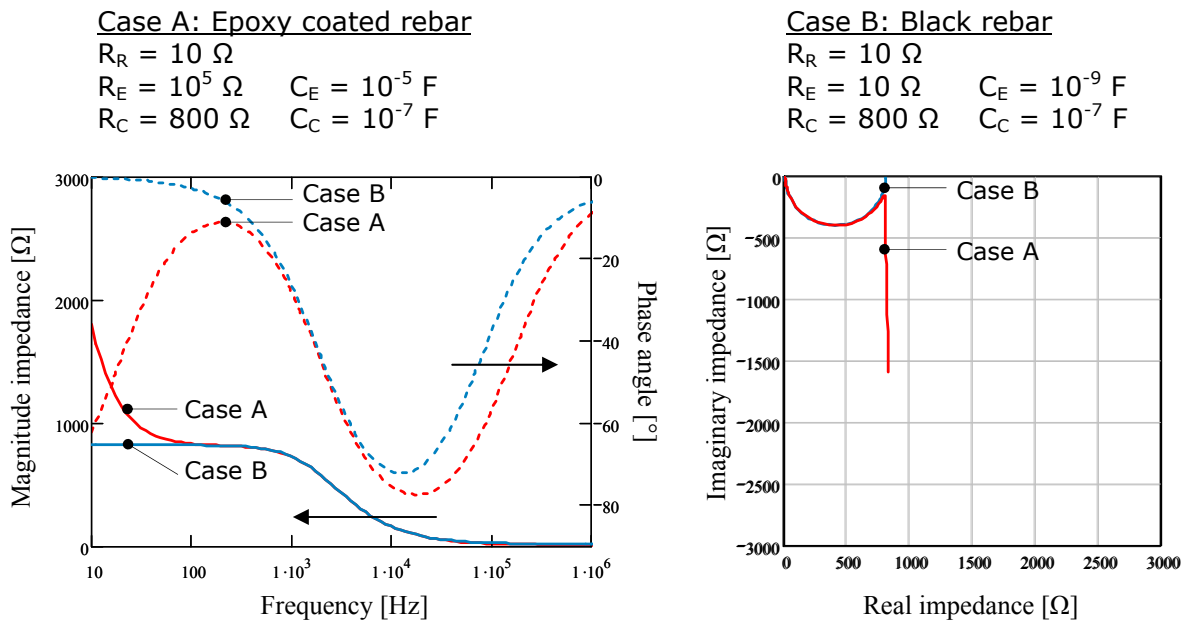
**Figure 2.5** *Electrical impedance spectroscopy schematic setup and equivalent circuit.*

Figure 2.6 shows the instrumentation used in the collection of electrochemical impedance spectroscopy data. The setup includes an HP4192A impedance analyzer, a laptop computer for instrument control and data collection, a Cu-CuSO<sub>4</sub> non-polarizing electrode, and a cable connected to a rebar. Impedance spectroscopy measurements were taken along the same grid used for the half cell readings. However, the speed of data acquisition of the electrochemical impedance spectroscopy is much slower than half cell potential measurements. For this reason, only few lines of electrochemical impedance spectroscopy were completed during field testing.

Typically, impedance spectroscopy data results are presented as real vs. imaginary components and magnitude and phase of the measured impedance spectra as shown in Figure 2.7. These data are then fitted with equivalent electrical circuits in an attempt to determine the capacitive (negative imaginary component of impedance) or resistive behavior (real component of impedance) of epoxy-coated rebars.



**Figure 2.6** Electrical impedance spectroscopy setup and data acquisition system.



**Figure 2.7** Ideal electrochemical impedance spectroscopy response for an epoxy coated rebar (case A) and a black rebar (case B).

#### 2.5.4 Ground Penetrating Radar Measurements

Ground penetrating radar (GPR) is a non-destructive evaluation technique based on sending electromagnetic (EM) pulses motoring reflections from heterogeneities in the concrete (e.g., changes in volumetric water content and presence of metal inclusions – [59-60]). The technique has been gaining acceptance for the evaluation of deterioration and the maintenance prediction of bridge decks [45]. One of the main advantages of GPR is that the system can be mounted on a truck and the survey can be performed without closing the roadway. The technique is commonly used in combination with other techniques including half-cell potential measurements and chain-drag to cross-correlate results and interpretations [45].

The interpretation of the GPR data includes the evaluation of reflection times and the amplitude of reflection signals from a collection of traces obtained at regular space intervals [45, 59, 60]. The velocity of the EM waves in the medium depends on the amount of water (expressed in terms of volumetric water content) and the amplitude of the reflected waves depends on the medium-inclusion reflection coefficient and the attenuation coefficients that depend of the salt concentration in the medium. As the corrosion phenomenon in reinforced concrete is directly related to the presence of water and chloride ion concentration, the GPR signals change to “image” the deterioration process. However, there is no one-to-one relationship between GPR signal signature and corrosion processes. For that reason, researchers use GPR surveys in combination with other testing methodologies and ground truth data [45].

In this study, to further characterize possible deterioration areas and complement other surveys, the UW-Madison team contacted Dr. Mark Loken (Minnesota Department of Transportation - Mn/DOT) and requested his services to run GPR surveys on the fours bridges under evaluation. Dr. Loken collected the GPR survey data on all four bridges using a 1.5 GHz GSSI GPR system (Figure 2.8). The survey lines show a number of hyperbolas that correspond to the reflection signature of the rebars. The location and shape of these hyperbolas permit the evaluation of ELM wave velocity in the concrete and the depth of each steel rebars (curve fitting is used). The mapping of ELM wave velocity and the amplitude of the reflection are indicators of the volumetric water content and salt content in the concrete.

GPR can be used to estimate the volumetric water content of porous media with high resolution. The relative dielectric permittivity  $\kappa$  is calculated using the electromagnetic wave velocity  $V$  in porous medium having low electrical conductivity [60]:

$$\kappa \approx \left( \frac{c}{V} \right)^2 \quad (2.2)$$

where  $c$  is the speed of electromagnetic waves in a vacuum ( $3 \times 10^8$  m/s). In porous media (e.g., concrete), the relative dielectric permittivity is mainly dependent upon the volumetric water content  $\theta_v$ . Changes in water contents affect the value of dielectric the relative dielectric permittivity and the measure EM wave velocity. An empirical correlation suggests the relationship between the dielectric constant and the volumetric water content (Topp et al. 1980).

$$\theta_v = -5.3 \times 10^{-2} + 2.92 \times 10^{-2} \kappa - 5.5 \times 10^{-4} \kappa^2 + 4.3 \times 10^{-6} \kappa^3 \quad (2.3)$$

Contour maps of volumetric water content are constructed by using Equations 2.2 and 2.3 from the GPR travel time profiles.



**Figure 2.8** Ground Penetrating Radar System used in the imaging of the bridge decks.

## 2.6 METHODS FOR EVALUATING CONCRETE

Before starting the field and laboratory measurements, a comprehensive review of the most recent literature on bridge deterioration, bridge corrosion, and epoxy-coated rebar performance was conducted. We aimed to provide a background for this study and so the literature presented herein is specifically focused on the details for each different test. It is important to note that the available research evidence about the long term benefits of bridges reinforced with epoxy-coated rebars is limited. Few field studies have been conducted to assess the long term performance of epoxy coated bars in bridge decks. Almost all studies focus on a single issue (usually corrosion levels) with very few comparative studies. There is very little research evidence available about the impact of epoxy-coated rebars on bridge deck health.

### 2.6.1 Chloride ion intrusion – AASHTO T259/260

The AASTHO T-259 standard describes a test method for the determination of the resistance of concrete specimens to chloride ion penetration. The method can be used to establish the effects of variations in the properties of concrete on the resistance of the concrete to penetration of chloride ions. Possible variations in the concrete outlined in the standard include the cement and aggregate type and content, water-cement ratio, admixtures, treatments, curing conditions, and consolidation.

The standard describes procedures for preparing the concrete test specimens. After concrete treatments are applied, specimens are abraded to simulate wear from vehicular traffic. If the concrete or treatment is to be used on a surface not subjected to traffic wear, abrasion is omitted. Dams are placed around the top edge of the specimens, before beginning 90 days of continuous ponding of a deicing solution. Following ponding, the specimens are wire brushed to remove any salt crystal buildup.

The AASHTO T-260 test method describes procedures used to determine the water-soluble or acid soluble chloride ion content of aggregates, cement, mortar, or concrete. In this test, the chloride ion content can be determined by three distinct methods: potentiometric titration (which was used in this test program), atomic absorption, and specific ion probe-field. All three methods require the use of an ion-selective electrode. In addition, the standard describes the procedure used in the preparation of powdered concrete samples for determination of the chloride ion content, including sample digestion and dilution. Equations for calculating the percent chloride ion and precision statements are also included. A detailed description of the AASHTO T 259 and T 260 test methods is given later in section 5.3 of this report.

### ***2.6.2 Carbonation depth - RILEM***

The procedure described in RILEM Paper CPC-18, “Measurement of hardened concrete carbonation depth”, is a test elaborated by the Recommendations for the Testing and Use of Constructions Materials, RILEM (Réunion Internationale des Laboratoires et Experts des Matériaux, systèmes de construction et ouvrages). This test measures the depth of carbonation as measured by the application of phenolphthalein on concrete specimens exposed to carbon dioxide. The solution is sprayed on exposed surfaces of concrete. The phenolphthalein solution reacts with a non carbonated cement paste leaving a magenta color. Carbonated areas appear with no color. The carbonation depth is determined by measuring the depth from the surface to the non-carbonated, magenta colored region.

According to the standard, the carbonation depth should be measured in different ways depending on how the carbonation develops through the concrete.

- a) Perpendicular distance from top of the sample to a constant and uniform magenta region.
- b) Average of perpendicular distances from top of the sample to an irregular or variable magenta region.
- c) Perpendicular distance from top of the sample to a constant magenta region with a singularity. The singularity is not considered in the measure.

The RILEM CPC-18 paper suggests that carbonation depths should be not measured where large aggregate is present. Instead, the measurement must be placed where the cement paste is predominant. To ensure that the measurement of the carbonation depth is perpendicular from the top of the sample, the use of a measuring tape is sufficient, though in this study a magnifier measuring device was used.



## **2.7 METHODS FOR EVALUATING EPOXY-COATED REBARS**

### **2.7.1 *Specification for epoxy-coated steel bars – ASTM A775-06***

This specification covers deformed and plain steel reinforcing bars with protective epoxy coating applied by the electrostatic spray method. The coating applicator is identified throughout this specification as the manufacturer.

The standard describes test requirements in the use of materials, coating application, coating thickness, coating continuity, coating flexibility and coating adhesion. Also, the permissible amount of damaged coating is specified along with repairing requirements. The inspection procedures, handling, rejection and certification requirement for epoxy-coated rebars are detailed as well. Finally, requirements for organic coatings are specified.

### **2.7.2 *Coating hardness NACE TM-0174***

The standard NACE TM-0174 describes the laboratory methods for the evaluation of protective coatings used as lining materials in immersion service. This standard was prepared by NACE International (The Corrosion Society) to help manufacturers and users of protective coatings and linings in their selection of materials by providing standard test methods for the evaluation of protective coatings and linings for immersion service.

The purpose of this test is to evaluate the performance of protective coatings. The standard provides two test methods for evaluating coatings on any metallic substrate, such as steel, copper, aluminum, etc., so that the factors of both chemical resistance and permeability can be considered. The results obtained give an indication of what would happen on exposure to similar service conditions.

Protective coatings, as referred to in this standard, can be applied in liquid form (solution, dispersion, etc.) or dry form (powders), using spray, dip, roller, brush, trowel, or other appropriate application techniques. These coatings may contain fillers or reinforcement, such as glass cloth or flakes, silica, mica, etc.

### **2.7.3 *Coating adhesion NACE TM-0185***

The standard NACE TM-0185 describes the test used in the evaluation of internal plastic coatings for corrosion. This standard was prepared by NACE International (The Corrosion Society) and recommended practice prescribes the material characteristics, application methods, and handling, shipping, and installation procedures for polyolefin resin coating systems extruded over soft adhesives for the prevention of external corrosion of underground or submerged pipelines. This standard is intended for use by coating applicators, engineers, and pipeline owners as a guide to qualifying coating materials and specifying application parameters.

## CHAPTER 3. DESCRIPTION OF INSPECTED BRIDGES

### 3.1 INTRODUCTION

In this chapter, the main characteristics of the bridge studies are presented. The chapter concludes with a summary of results from the previous study performed on these same bridges in 1996.

### 3.2 DESCRIPTION OF BRIDGES

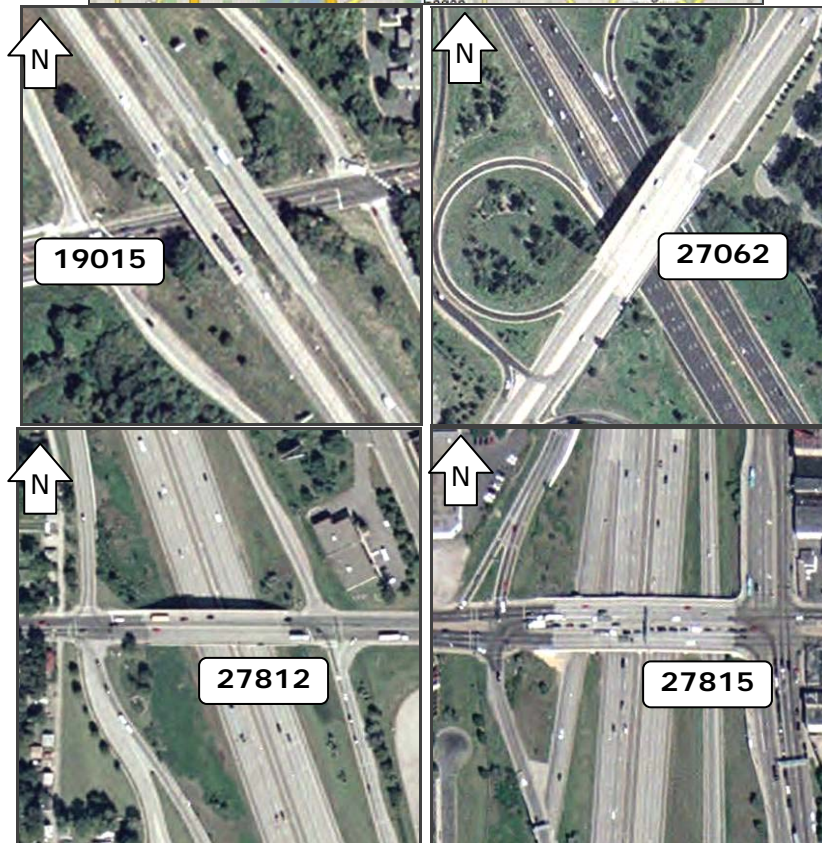
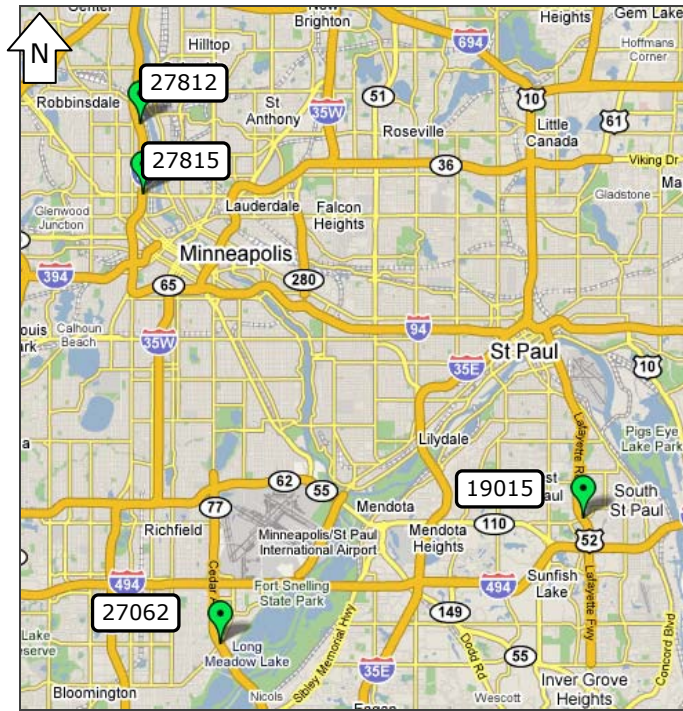
Four bridges built between 1973 and 1978 were inspected in this study. All bridges were located in the Minneapolis-St. Paul metropolitan area as shown in the Table 3.1 and Figure 3.1. The main characteristics of each bridge are summarized in Table 3.2.

*Table 3.1 Bridges studied*

| <b>Bridge</b> | <b>Location</b>                | <b>Year Built</b> |
|---------------|--------------------------------|-------------------|
| 19015         | US 52 over Southview Blvd      | 1973              |
| 27062         | Old Shakopee Rd over Cedar Ave | 1978              |
| 27812         | N Dowling Ave over I-94        | 1977              |
| 27815         | W Broadway Ave over I-94       | 1978              |

*Table 3.2 Main characteristics of bridges studied*

| <b>Bridge</b> | <b>ADT</b>       | <b>Length</b> | <b>Width</b> | <b>Spans</b> | <b>Overlay</b> |
|---------------|------------------|---------------|--------------|--------------|----------------|
| 19015         | 30,500<br>(2004) | 163'-6" ft    | 44'-4" ft    | 3            | No             |
| 27062         | 10,000<br>(2003) | 249'-2" ft    | 114'-4" ft   | 2            | No             |
| 27812         | 25,000<br>(2003) | 291'-8" ft    | 70'-4" ft    | 2            | Yes            |
| 27815         | 22,700<br>(2003) | 360'-3" ft    | 104'-4" ft   | 4            | Yes            |



*Figure 3.1 Location and aerial pictures of bridges studied in the Minneapolis/St. Paul metropolitan area (Images: Google maps).*

### 3.2.1 Bridge 19015, US 52 over Southview Blvd.

Bridge 19015 was built on precast concrete girders and has a concrete deck with all epoxy-coated reinforcement, i.e., both the top and bottom mats are made of epoxy-coated reinforcement. The thickness of the deck is 9 in. in spans 1 and 3, and 7-3/4 in. span 2. The upper bar of the top mat in the longitudinal direction is a #4 bar, while the lower bar in the transverse direction is a #6 bar. In the bottom mat, both bars are #5. A plan view and a cross section of the bridge are shown in Figure 3.2.

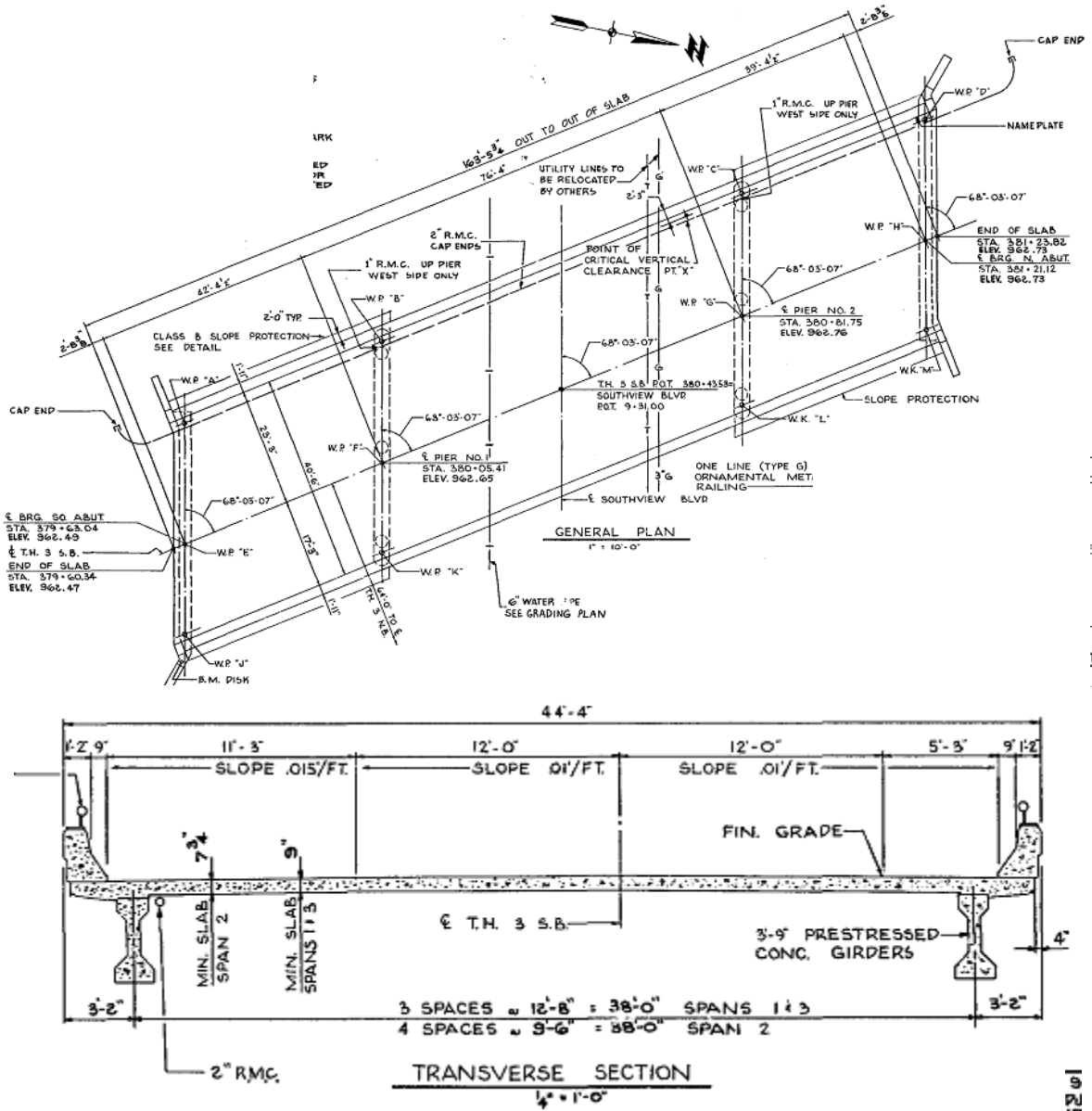


Figure 3.2 Plan view (above) and cross section (below), bridge 19015.

3.2.2 Bridge 27062, Old Shakopee Rd. over Cedar Ave.

This bridge deck in bridge 27062 is supported on steel girders and has a 9 in. thick concrete deck with epoxy-coated reinforcement in the top mat and black steel in the bottom mat. The lower bar of the top mat in the longitudinal direction is a #4 bar, while the upper bar in the transverse direction is a #6 bar. In the bottom mat, bars are #5 and #6 in the longitudinal and transverse direction respectively. The bridge deck does not have a concrete overlay and went through patch work in the summer 2006. A plan view and a cross section of the bridge are shown in Figure 3.3.

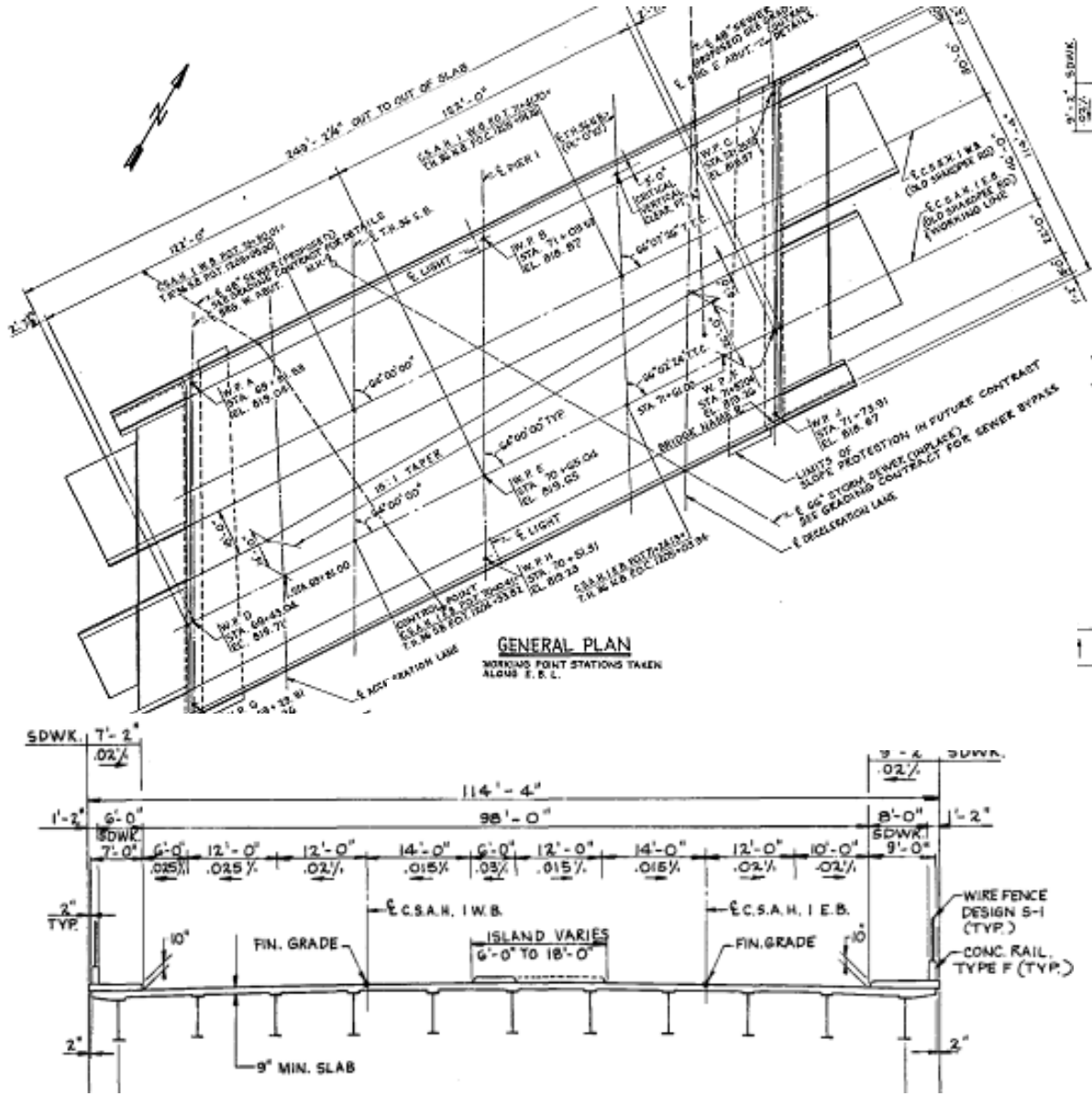


Figure 3.3 Plan view (above) and cross section (below), bridge 27062.

### 3.2.3 Bridge 27812, North Dowling Ave. over I-94

Bridge 27812 is supported on concrete girders and has a 9 in. thick concrete deck with epoxy-coated reinforcement in the top mat and black reinforced concrete in the bottom mat. The lower bar of the top mat in the longitudinal direction is a #4 bar (#6 over piers), while the upper bar in the transverse direction is a #5 bar. In the bottom mat, both the longitudinal and transverse reinforcement are #5 black bars. The bridge was originally constructed with a 2-in, low slump, high density concrete overlay. A plan view and a cross section of the bridge are shown in Figure 3.4.

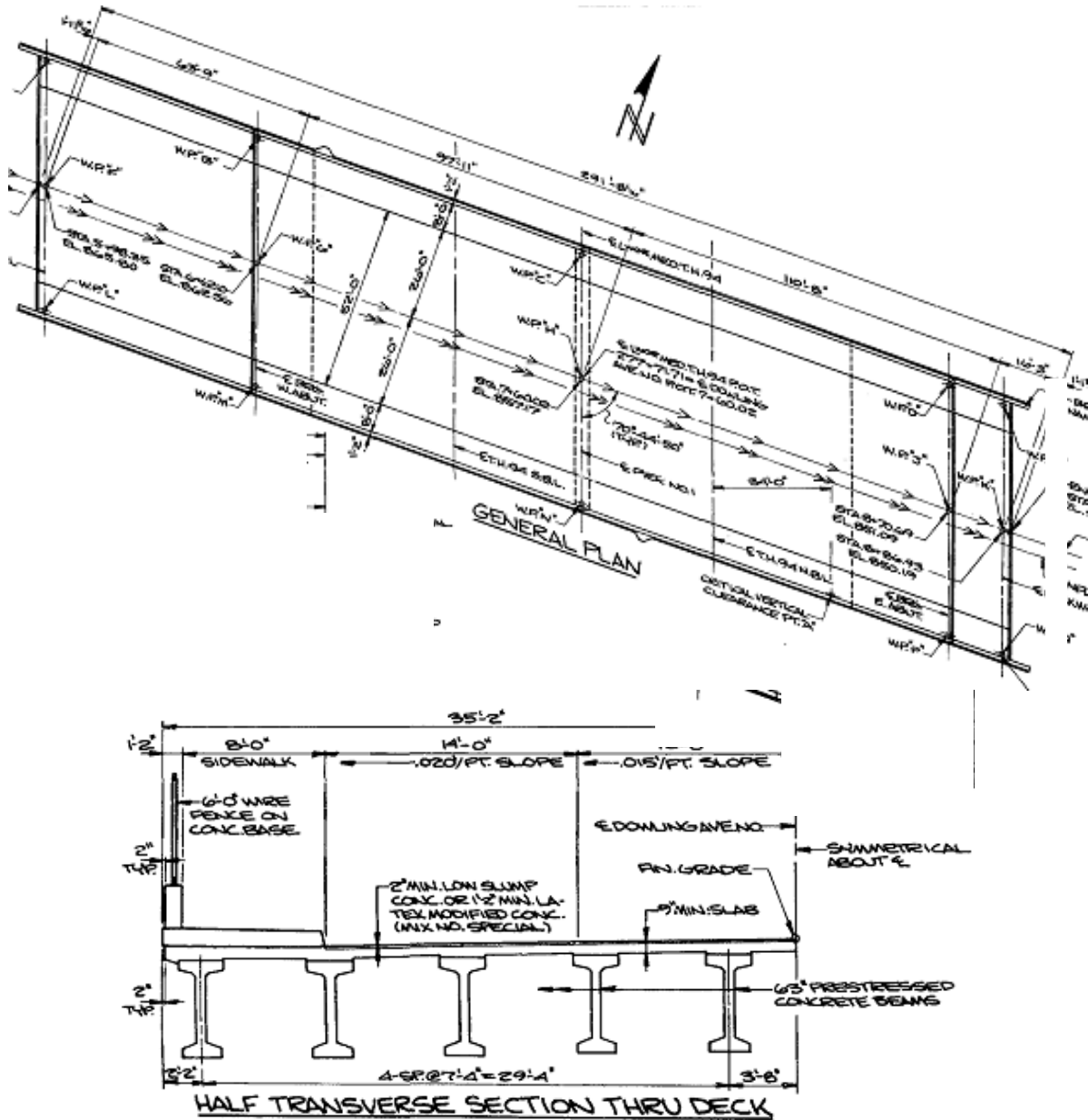


Figure 3.4 Plan view (above) and cross section (below), bridge 27812.

### 3.2.4 Bridge 27815, West Broadway Ave. over I-94

The bridge 27815 is supported on steel girders and has an 8.75 in. thick concrete deck with epoxy-coated reinforcement in the top mat and black reinforcing steel in the bottom mat. The lower bar of the top mat in the longitudinal direction is a #4 bar (#6 over piers), while the upper bars in the transverse direction consist of #5 bars. In the bottom mat, both the longitudinal and transverse reinforcement are #5 black bars. The deck was built with a 2-in, low slump, high density concrete overlay. A plan view and a cross section of the bridge are shown in Figure 3.5.

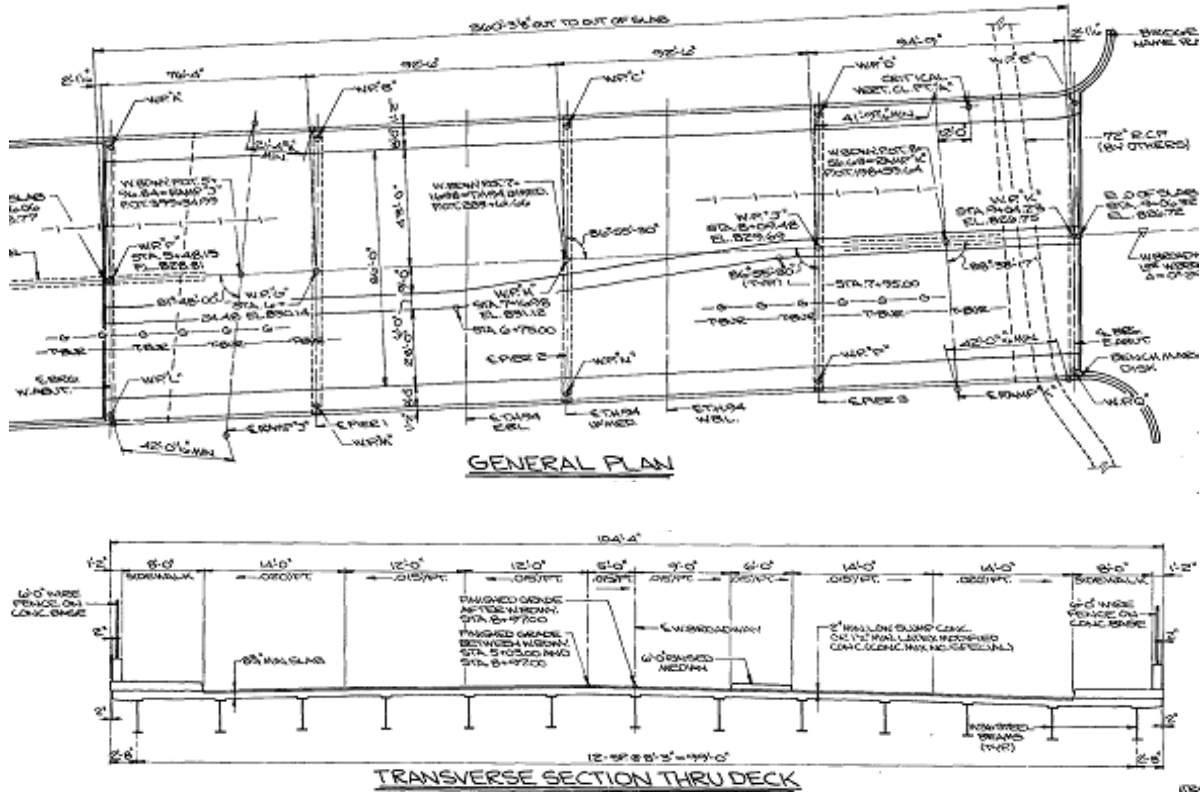


Figure 3.5 Plan view (above) and cross section (below), bridge 27815.

Table 3.3 shows a summary of the bar type and size used in the top and bottom mats of the deck in all four bridges.

**Table 3.3 Bar size and type in both mats**

| Bridge No. | Bar Arrangement   |
|------------|---|
| 19015      | <p>The diagram for Bridge 19015 shows two horizontal mats of epoxy coated bars. The top mat is labeled 'Long. #4' and 'Trans. #6'. The bottom mat is labeled 'Long. #5' and 'Trans. #5'. Both mats consist of three green bars with three green dots representing reinforcement points.</p> |
| 27062      | <p>The diagram for Bridge 27062 shows two horizontal mats. The top mat is labeled 'Long. #4' and 'Trans. #6' and consists of three green bars with three green dots. The bottom mat is labeled 'Long. #6' and 'Trans. #5' and consists of three black bars with three black dots.</p>       |
| 27812      | <p>The diagram for Bridge 27812 shows two horizontal mats. The top mat is labeled 'Long. #4' and 'Trans. #5' and consists of three green bars with three green dots. The bottom mat is labeled 'Long. #5' and 'Trans. #5' and consists of three black bars with three black dots.</p>       |
| 27815      | <p>The diagram for Bridge 27815 shows two horizontal mats. The top mat is labeled 'Long. #4' and 'Trans. #5' and consists of three green bars with three green dots. The bottom mat is labeled 'Long. #5' and 'Trans. #5' and consists of three black bars with three black dots.</p>       |

### 3.3 PREVIOUS STUDY

In June of 1996, the company Wiss, Janney, Elstner Associates, Inc. (WJE) performed an in-depth field investigation into the performance of epoxy-coated reinforcing bar in these same four bridges [32]. In that study, half-cell potential readings were taken on the deck and chloride content was determined by drilling powder samples from 6 random locations on each studied area. Some cores were extracted without retrieving the rebar because the coring process did not sever the bar completely. The exposed bar was then evaluated in-situ regarding its coating adhesion and corrosion level.

Next, a summary of half-cell potential measurements, chloride ion content, corrosion condition and coating adhesion collected in the WJE's 1996 study is shown by bridge.

#### 3.3.1 Bridge 19015

Some short discontinuous transverse cracks were noted over the piers and no delamination was found. Table 3.4 shows the results of the WJE's 1996 core tests performed in-situ and in the laboratory.



**Table 3.4 WJE's 1996 study results on bridge 19015**

| Core | Half-Cell<br>(mV) | Chloride Content |                      | Bar Corrosion              | Coating<br>Adhesion<br>(1 good, 5<br>poor) |
|------|-------------------|------------------|----------------------|----------------------------|--|
|      |                   | 0.5"<br>(lb/cy)  | Bar Level<br>(lb/cy) |                            |  |
| 1    |                   | 20.6             | 0.3                  | Good                       | 5 (Poor)                                   |
| 2    |                   | 5.1              | 0.3                  | Good                       | 5 (Poor)                                   |
| 3    | -300              | 20.7             | 2.3                  | Corrosion (rust<br>stains) | 5 (Poor)                                   |
| 4    | -345              | 13.9             | 0.3                  | Good (rust<br>colored)     | 3 (Good)                                   |
| 5    | -360              | 16.3             | 0.3                  | None (minor rust)          | 5 (Easily<br>peeled)                       |

Note: Chloride content values come by multiplying the percent of chloride ion content by the concrete weight, which is usually taken as 3915 lb/cy for normal structural mass concrete

### 3.3.2 Bridge 27062

Extensive transverse cracking was observed in this bridge and most of them were full depth. Also, two small delaminations were found. Table 3.5 shows the results of the WJE's 1996 core tests performed in-situ and in the laboratory.

**Table 3.5 WJE's 1996 study results on bridge 27062**

| Core | Half-Cell<br>(mV) | Chloride Content |                      | Bar Corrosion                                | Coating<br>Adhesion<br>(1 good, 5<br>poor) |
|------|-------------------|------------------|----------------------|--|--|
|      |                   | 0.5"<br>(lb/cy)  | Bar Level<br>(lb/cy) |  |  |
| 1    | -330              | 16.3             | 0.3                  | Good (millscale-<br>red corrosion<br>stains) | 5 (Poor)                                   |
| 2    | -104              | 18.9             | 0.3                  | Good   | 3 (Good)                                   |
| 3    | -482              | 24.0             | 0.3                  | Corroded                                     | 5 (Poor)                                   |
| 4    | -480              | 21.4             | 0.3                  | Good (discolored)                            | 1 (Good)                                   |
| 5    | -550              | 19.3             | 10.1                 | Heavy corrosion                              | 5 (Poor)                                   |

### 3.3.3 Bridge 27812

The deck of this bridge had some limited random transverse and longitudinal cracking. Corrosion staining areas were present on the underside of the deck. No delaminations were found on the deck, however, some raveling and minor patching had occurred along the transverse expansion joint. Table 3.6 shows the results of core tests performed in-situ and laboratory.

*Table 3.6 WJE's 1996 study results on bridge 27812*

| Core | Half-Cell<br>(mV) | Chloride Content |                      | Bar Corrosion             | Coating<br>Adhesion<br>(1 good, 5<br>poor) |
|------|-------------------|------------------|----------------------|---------------------------|--|
|      |                   | 0.5"<br>(lb/cy)  | Bar Level<br>(lb/cy) |                           |  |
| 1    |                   | 9.7              | 5.5                  | Minor rust                | 5 (Poor)                                   |
| 2    |                   |                  |                      | Good                      | 2 (Good)                                   |
| 3    |                   |                  |                      | Clean                     | 2 (Good)                                   |
| 4    | -69               | 8.9              | 0.3                  | Slight rust               | 2 (Good)                                   |
| 5    | -173              |                  |                      | Good                      | 3 (Good)                                   |
| 6    | -120              |                  |                      | No bar retrieved          |  |
| 7    | -193              |                  |                      | Good                      | 3 (Good)                                   |
| 8    | -620              | 11.8             | 7.2                  | Corrosion base of<br>ribs | 5 (Poor)                                   |
| 9    | -108              | 7.1              | 0.3                  | Good (discolored)         | 3 (Good)                                   |
| 10   | -500              | 9.1              | 5.7                  | Corrosion stains          |  |
| 11   | -500              | 6.0              | 0.5                  | Good                      | 5 (Easily<br>peeled)                       |

### 3.3.4 Bridge 27815

No delaminations were located. Rust staining was also found on the underside of the deck at some crack locations. Table 3.7 shows the results of WJE's 1996 core tests performed in-situ and in the laboratory.

*Table 3.7 WJE's 1996 study results on bridge 27815*

| Core | Half-Cell<br>(mV) | Chloride Content |                      | Bar Corrosion   | Coating<br>Adhesion<br>(1 good, 5<br>poor) |
|------|-------------------|------------------|----------------------|-----------------|--|
|      |                   | 0.5"<br>(lb/cy)  | Bar Level<br>(lb/cy) |                 |  |
| 1    |                   |                  |                      | Heavy corrosion |  |
| 2    |                   | 6.0              | 0.3                  | Good            | 2 (Good)                                   |
| 3    |                   |                  |                      | Good            | 2 (Good)                                   |
| 4    |                   | 3.4              | 0.3                  | Good            | 2 (Good)                                   |
| 5    |                   | 8.1              | 2.4                  | Heavy corrosion | 5 (Poor)                                   |
| 6    | -314              |                  |                      | Good            | 5 (Poor)                                   |
| 7    | -369              |                  |                      | Good            | 3 (Good)                                   |
| 8    | -264              | 4.9              | 0.3                  | Good            | 1 (Good)                                   |
| 9    | -565              | 8.8              | 5.5                  | Corroded        | 5 (Poor)                                   |
| 10   | -481              |                  |                      | Good            | 5 (Poor)                                   |
| 11   |                   |                  |                      | Minor stains    |  |
| 12   | -639              |                  |                      | Clean           | 5 (Poor)                                   |
| 13   | -292              | 4.3              | 0.3                  | Good            | 1 (Good)                                   |

## CHAPTER 4. FIELD PROCEDURES

### 4.1 INTRODUCTION

In this chapter, a complete description of the field methodologies used in this study is presented. The test method and procedures, tools and equipment used are described in detail.

The four bridges described in the previous chapter were visited and visual inspections were performed, including locating and recording all defects found in the deck. Cracking, spalls, suspect areas of delamination, rust stains, and patches were the main concerns documented.

These inspections were followed by five non-destructive surveys:

- Visual Inspection
- Chain Drag
- Half-Cell Potential
- Electrochemical Impedance Spectroscopy (EIS)
- Ground Penetrating Radar (GPR)

The following sections describe in detail the field evaluations.

For operational and traffic reasons, only one traffic direction was selected to conduct the study. During the months of September and October 2006, each bridge was visited one day and MnDOT personnel provided traffic safety and equipment support. Table 4.1 shows the date when each bridge was visited and the direction where the field work was conducted.

*Table 4.1 Bridges visits*

| <b>Bridge</b> | <b>Visited</b> | <b>Bound</b> |
|---------------|----------------|--------------|
| 19015         | 09/25/2006     | Southbound   |
| 27062         | 09/27/2006     | Eastbound    |
| 27812         | 10/26/2006     | Westbound    |
| 27815         | 10/25/2006     | Eastbound    |

### 4.2 BRIDGE SITE INSPECTION

A detailed visual inspection was performed on each bridge deck during the visits. The purpose of this survey was to document the condition of the bridge decks and relate this data with laboratory results. Some of the data collected included: photographs, structure dimensions, surface condition, deck configuration (lanes, shoulders, median, etc), and superstructure type. A set of on-site surveys performed is described in the following sections.

#### *4.2.1 Visual inspection*

A detailed visual examination of the selected deck area was made on each bridge deck. The cracks, spalls, and marked delaminations were photographed and their location was documented

on mapping sheets. The damage level of each deck was calculated to be the ratio of the total damaged surface area (spalled and delaminated areas) to the total surface area that was inspected.

Crack density (ft/ft<sup>2</sup>) of the bridge deck was calculated by dividing the total length of the identified cracks by the total inspected deck surface in each bridge.

#### 4.2.2 Chain-drag survey

This survey was conducted by Mn/DOT personnel and the result of this inspection is a set of measurable suspect delaminated areas. For operational reasons, one delaminated area was further delineated using hammer tapping.

Figure 4.1 shows a Mn/DOT crew member dragging the chain across a deck surface; at the right the figure shows the preliminary evaluation of delaminated area by hollow sound using chain drag (outer yellow square) and the final evaluation of delaminated area (shaded area) by hollow sound using hammer tapping.



*Figure 4.1 Chain-drag survey.*

#### 4.3 HALF-CELL POTENTIAL MEASUREMENTS

In this study, one connection to an epoxy-coated rebar was used per longitudinal or transversal line of readings. The approximate location of the bars was first determined using the reinforcing schedule shown in the construction drawings and then more precisely with the aid of a pachometer (also known as covermeter). Once the bars were located, a 1-1/8 in. hole was drilled through the concrete to the upper mat of reinforcing steel. The indications of the pachometer were often precise enough that, in most cases, only one hole was necessary to find the bar.

The electrical connection to the bars was initially done by drilling a small hole through the coating in the steel reinforcing using a self-tapping screw connected to a lead wire. This approach proved to be time consuming and unreliable. At the suggestion of the Mn/DOT personnel, the connection to the bars was later modified and later accomplished by welding a rod (or electrode) to the bars. This procedure was much faster, very efficient, and much more reliable, and thus it was used for the measurements taken on the subsequent bridges surveyed. Figure 4.2 shows the three-step procedure used to connect the electrode to the bar.



*Figure 4.2 Connection to epoxy-coated bars.*

Measurements using the half cell potential method were done at selected sites defined by one or more orthogonal grids layed out on the deck. The grid layout and size varied for each deck, but it was generally defined as follows. In the longitudinal direction, gridlines were drawn along each and in between the wheel paths. A fourth gridline was drawn on the shoulder. In the transverse direction, gridlines were drawn at random locations, or to coincide with areas of suspect delaminations and/or spalled areas. Details of the grid layout and the measurements obtained with each technique are provided for each bridge deck surveyed in section 6.8.3.

#### **4.4 CORING SELECTION**

To select the location of coring, several sources of information were used. The Half-Cell Potential readings were the main data necessary in selecting the core locations. However, as was explained in section 4.2.1 (Visual inspection), information of the presence of crack, spalls and patches was also considered to select locations. Cores were selected close to delaminated areas, joints, spalls and cracks. In addition to that, a couple of cores were selected in healthy areas of the deck to compare between good and bad condition.

Cores were drilled through the upper reinforcement only and were extracted by Mn/DOT personnel. Later, the cores were sent to UW-Madison to initiate the laboratory analyses. Table 4.2 summarizes the total number of cores extracted in each deck.

*Table 4.2 Cores extracted per bridge*

| <b>Bridge</b> | <b>Cores</b> |
|---------------|--------------|
| 19015         | 8            |
| 27062         | 7            |
| 27812         | 9            |
| 27815         | 10           |
| <b>Total</b>  | <b>34</b>    |

Each core was visually inspected to assess its overall condition by observing the presence of cracks, and delamination at the bar level, as well as the condition of the rebars. In addition, data including rebar cover, bar size, and core depth was measured.

#### **4.5 DEPTH OF COVER**

Along with the half-cell readings, in each electrical connection with the reinforced steel, the depth of concrete cover was measured. Also, the core samples extracted and the interpretation of GPR surveys provided information about the actual concrete cover depth.

## **CHAPTER 5. LABORATORY PROCEDURES**

### **5.1 INTRODUCTION**

This chapter summarizes the findings of the chemical/physical laboratory test program on the core specimens from all four bridges surveyed. The laboratory test program included the physical evaluation of the overall condition of the cores, chloride ion content distribution measurements, carbonation depth measurements, and evaluation of the condition of the epoxy-coated rebars. In addition, chloride ion diffusion coefficients were determined.

### **5.2 CORE EXAMINATION**

Cores were drilled through the upper reinforcement only and were extracted by Mn/DOT personnel. Later, the cores were sent to UW-Madison laboratories where each core was labeled and stored in a sealed plastic bag. The cores were also visually examined, measured and photographed; then, a preliminary analysis was done to identify the presence of cracks, corrosion, delamination, or other relevant defects (see the detailed laboratory visual examination in Appendix A: Detailed Core Description).

Actual cover depth was measured from core samples and compared to that measured in the field by the pachometer. Then, concrete paste samples were extracted and chemically tested to evaluate the chloride ion concentration. Carbonation depth was also measured. The epoxy-coated bars were visually inspected to determine the level of corrosion and then tested for hardness and adherence of the epoxy coating to the bar. A description of the laboratory tests and results follow.

### **5.3 CHLORIDE ION ANALYSIS**

The chloride ion content was measured using the test procedure outlined in the AASHTO-T260 standard (2004) [36]. This standard permits the determination of the water-soluble or acid soluble chloride ion content of aggregates, cement, mortar, or concrete, using the following methods: potentiometric titration, atomic absorption, and specific ion probe-field. In this study the potentiometric titration method was selected for the laboratory testing.

#### ***5.3.1 Sample retrieval***

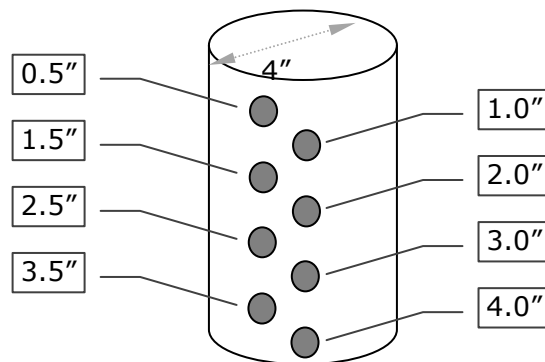
Samples for chloride ion analysis were retrieved from the extracted cores in accordance with the AASHTO-T260 standard [36]. Concrete powder samples were taken at selected depths using a rotary hammer drill with a depth indicator and a drill bit #13 of ½ in. (see Figure 5.1). To confirm the measured chloride ion content, a minimum of two samples were extracted from different perforations at each depth. Approximately six to seven grams of material were retrieved from the hole at each depth using a sampling spoon and placed in a labeled, clean sample container. Although only three grams of material are necessary to perform a single chloride ion analysis, more material (six to seven grams) was retrieved to allow to repeat the test if necessary.





**Figure 5.1** Concrete powder sample extraction by drilling.

The number and location of samples extracted varied depending on the condition of the core. In cores without cracks, powder samples were extracted every 0.5 in (12.6 mm) below the surface up to the bar level (typically at 4 in – 100 mm) as shown in Figure 5.2. In cores with cracks or spalled areas, samples were generally extracted at 0.5 in (12.6 mm) and at the bar level only. However, in some cores with vertical cracks, samples were taken every 0.5 in. increments.



**Figure 5.2** Typical sample location for chloride ion analysis in cores without cracks.

Each sample was passed through a No. 50 sieve. If the sample as collected did not completely pass a No. 50 sieve, additional pulverizing was performed until the entire sample was finer than the No. 50 sieve. All drill bits, spoons, sample containers and other tools were washed with distilled water between sample retrieval to prevent contamination.

### **5.3.2 Equipment and chemicals**

The primary equipment used for the chloride ion analysis consisted of a chloride ion selective electrode and a multimeter capable of measuring mV. The electrode recommended in the T259 standard, a combination chloride electrode, Orion model 96-17, and an Orion model 720-A plus multimeter was used in this study.

The procedure to determine the acid-soluble chloride ion content required several chemical reagents and solutions. Concentrated nitric acid ( $\text{HNO}_3$ ) was used in the initial stages of the procedure to decompose the concrete sample. Later in the procedure, methyl orange indicator was used to verify the acidity of the solution. An ionic strength adjuster and chloride activity standard of a known concentration were used to calibrate the electrode and meter each day before use. Two additional solutions, sodium chloride ( $\text{NaCl}$ ) and silver nitrate ( $\text{AgNO}_3$ ), both of 0.01 normal concentrations as well as an ionic strength adjuster were used in the titration process.

### **5.3.3 Sample decomposition**

A three-gram sample of pulverized concrete material was transferred from its sample container to a clean 100 mL beaker. Ten milliliters of distilled water were added to the beaker containing the sample, which was swirled to bring the concrete powder into suspension. Next, 3 mL of concentrated nitric acid solution was added, and swirled continuously until the material was completely decomposed, which usually took 3-4 minutes. Hot distilled water was stirred into the sample to bring the volume to 50 mL. To ensure that the solution was sufficiently acidic, pH was measured and additional nitric acid was added to the solution with continuous stirring until reaching a pH greater than 10. The beaker was covered with a watch glass and heated to boiling on a hot plate over medium heat (250 to 400°C).

After allowing the sample to boil for one minute, it was removed from the hot plate and filtered through a funnel double-lined with filter paper, Whatman No. 41 over No. 40, into a clean 250mL beaker inside a vacuum chamber. The sample residue left in the original sample beaker was washed into the filter setup with hot distilled water. The filter paper was continuously washed with hot distilled water, until the volume of the filtered solution reached between 125 and 150mL. The sample was then covered with a watch glass and allowed to cool to room temperature.

### **5.3.4 Potentiometric titration**

While the sample was cooling, the electrode was filled with the appropriate filling solution and plugged into the multimeter. The electrode was calibrated by verifying that its slope was within the range of chloride concentrations expected in the actual chloride ion test samples.

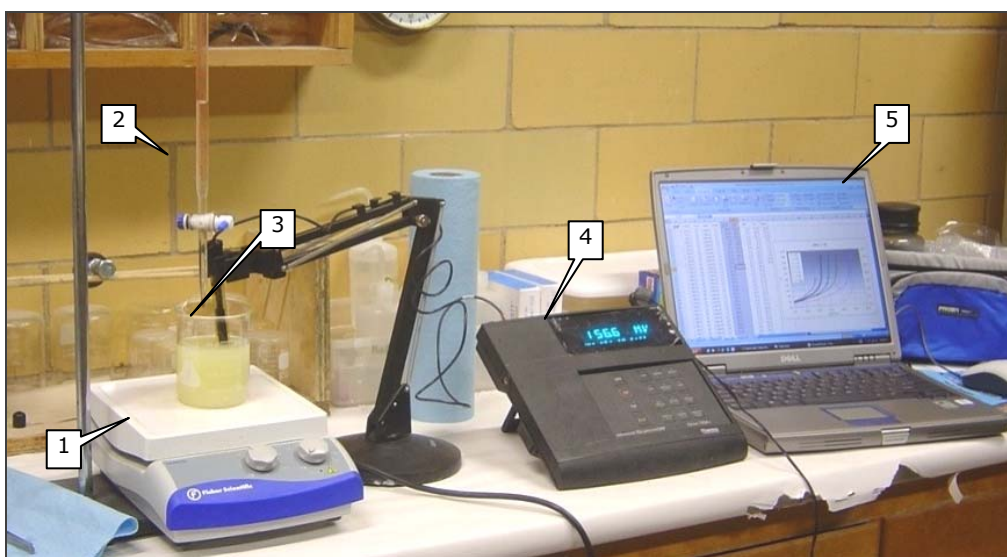
To calibrate the electrode, a standard solution was prepared using the chloride activity standard, ionic strength adjuster and distilled water, and the voltage reading was measured and recorded. Additional chloride activity standard was then added to the solution to increase the chloride concentration. The voltage reading and temperature were then measured and recorded. The

difference between the voltage readings from the two solutions, along with the known concentrations of the solutions, defined the slope of the electrode. The electrode was functioning properly when the slope fell within the range specified by the manufacturer. The temperature of the chloride test solution had to match the temperature of the standard solution to ensure accurate millivolt readings during the actual chloride tests. Finally, the calibrated electrode was submerged in a beaker of distilled water to determine the approximate equivalence point of the electrode.

The test sample was prepared for titration when it reached the temperature of the standard solution used to calibrate the electrode. Four milliliters of 0.01 normal sodium chloride aqueous solution and three milliliters of the ionic strength adjuster were stirred into the test sample. The electrode was immersed in the test sample solution, and the beaker-electrode assembly was placed beneath the spout of a 25 mL calibrated buret containing 0.01 normal silver nitrate aqueous solution. Figure 5.3 shows the beaker-electrode-buret assembly during a chloride ion analysis titration.

With continuous stirring, 0.01 normal silver nitrate aqueous solution was added and the volume recorded to bring the millivoltmeter reading to within 40 mV below the equivalence point determined in distilled water. Then the 0.01 normal silver nitrate aqueous solution was added in 0.20 mL increments with continuous stirring, recording the voltage reading after each addition.

As the equivalence point was approached, equal additions of silver nitrate solution caused larger changes in the voltage reading. Once the equivalence point was reached, the changes in the voltage reading for equal additions of silver nitrate solution again decreased. The AASHTO-T260 standard requires that the titration continue until the voltage reading is at least 40 mV past the equivalence point. In this study, titrations were continued to approximately 50-60 mV beyond the equivalence point.



**Figure 5.3** Beaker-electrode-buret assembly during a chloride ion analysis titration: 1) magnetic stirring device, 2) 25mL buret, 3) Orion electrode, 4) multivoltmeter and 5) computer to record and plot results.

### 5.3.5 Data collection

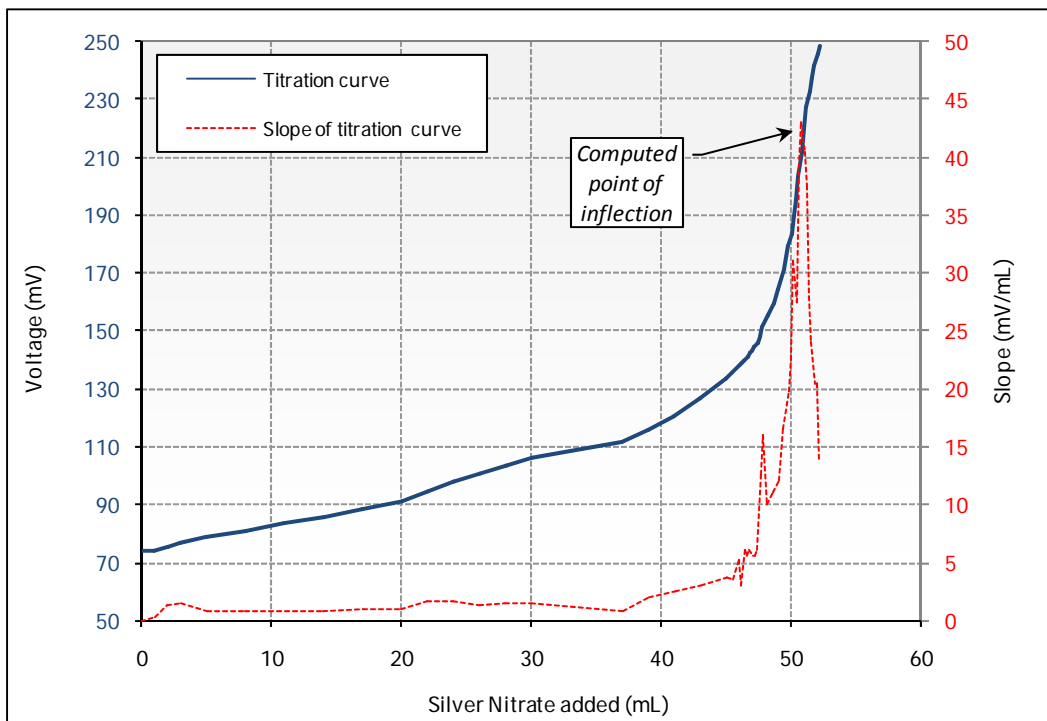
Every addition of silver nitrate aqueous solution and the corresponding voltage reading was recorded and the data were plotted. The endpoint of the titration used to calculate the percent chloride ion was determined by plotting the voltage readings against the volume of silver nitrate solution added. Figure 5.4 shows a typical plot of this curve. The endpoint of the titration corresponded to the point of inflection of the resultant curve. To better identify the point of inflection of each curve, the change in slope was also plotted (shown as a dashed line in Figure 5.4).

The volume of silver nitrate,  $V_1$ , added to reach the inflection point of the titration was used to calculate the percent of ion chloride in each concrete sample using the following equation from AASHTO-T260 standard:

$$\text{Cl}^{-}(\%) = 3.5453 \frac{V_1 N_1 - V_2 N_2}{W} \quad (5.1)$$

Where

- $\text{Cl}^{-}(\%)$  = percent of ion chloride in the sample
- $N_1$  = normality of the  $\text{AgNO}_3$  solution
- $N_2$  = normality of the  $\text{NaCl}$  solution
- $V_1$  = volume added in milliliters of the  $\text{AgNO}_3$  solution
- $V_2$  = volume added in milliliters of the  $\text{NaCl}$  solution
- $W$  = mass in grams of the original concrete sample (*default 3gr*).



**Figure 5.4** Typical titration curve.

The percent chloride ion was then converted into pounds of chloride ion per cubic yard of concrete by the following equation:

$$lbs\ Cl^- / yd^3 = Cl^- \text{ percent} \left( \frac{UW}{100} \right) \quad (5.2)$$

Where            lbs Cl<sup>-</sup>/yd<sup>3</sup>    = ion chloride in pounds per cubic yard  
                      Cl<sup>-</sup>                = percent of ion chloride in the sample  
                      UW                 = density of concrete per cubic yard.

The value of the density of concrete UW was measured from the cores extracted from the decks. Cylindrical samples from the cores were taken and dried for one hour in convection oven at 230°F (110°C). The dimensions of the cylindrical samples were taken with a measuring tape and recorded to the nearest millimeter. The samples were weighed and the value recorded in grams. The measured concrete densities are shown in Table 5.1.

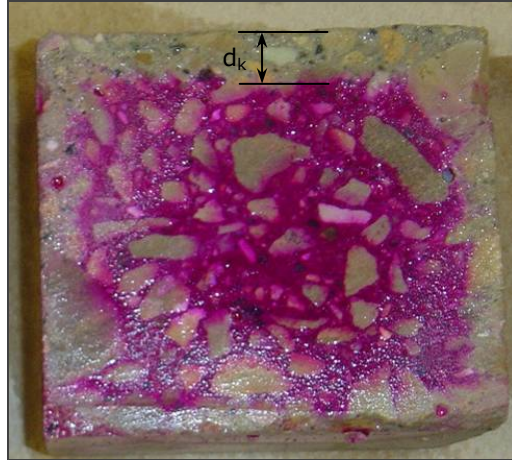
*Table 5.1 Measured concrete densities*

| Bridge | Level   | Dry Mass (g) | Volume (cm <sup>3</sup> ) | Density (lb/yd <sup>3</sup> ) | Density (lb/ft <sup>3</sup> ) |
|--------|---------|--------------|---------------------------|-------------------------------|-------------------------------|
| 19015  | Deck    | 502.2        | 212.6                     | 3977                          | 147.3                         |
| 27062  | Deck    | 1324.0       | 562.1                     | 3967                          | 146.9                         |
| 27812  | Overlay | 881.9        | 376.0                     | 3953                          | 146.4                         |
|        | Deck    | 433.0        | 184.0                     | 3957                          | 146.6                         |
| 27815  | Overlay | 853.6        | 360.9                     | 3984                          | 147.6                         |
|        | Deck    | 810.2        | 347.0                     | 3932                          | 145.6                         |

Note: the values obtained are within 1 and 2% of the standard value of 3915 lb/yd<sup>3</sup>.

#### 5.4 CARBONATION DEPTH MEASUREMENT

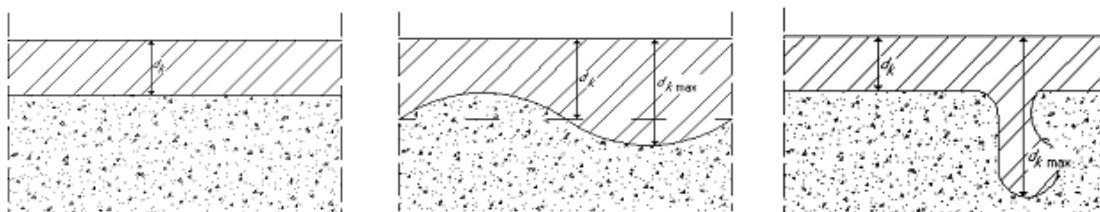
The method used to determine the carbonation depth is based on the recommendations of the RILEM CPC-18 standard (1988) [33]. The test was done by cutting the core using a wet saw to expose its internal surface. The surfaces were then dried with paper towels and a flow of air (less than a minute). A phenolphthalein solution was sprayed on one of the exposed surfaces. The phenolphthalein solution reacts with a non carbonated cement paste leaving a magenta color. Carbonated areas appear with no color. The carbonation depth is determined by measuring the depth from the surface to the non-carbonated, magenta colored region as shown in Figure 5.5 (The sample shown in this figure was chosen for illustration purposes and it does not correspond to any of the cores extracted in this study).



**Figure 5.5** Determination of carbonation depth using phenolphthalein solution.

According to the standard, the carbonation depth  $d_k$  should be measured in different ways depending on how the carbonation develops through the concrete.

- a) Perpendicular distance from top of the sample to a constant and uniform magenta region. Figure 5.6 (a).
- b) Average of perpendicular distances from top of the sample to an irregular or variable magenta region. Figure 5.6 (b).
- c) Perpendicular distance from top of the sample to a constant magenta region with a singularity. The singularity is not considered in the measure. Figure 5.6 (c).



**Figure 5.6** Rilem CPC-18 different carbonation depth  $d_k$  development: a) Constant  $d_k$ , b) Variable  $d_k$ , c) Constant  $d_k$  with singularities.

The RILEM CPC-18 recommendations indicate that carbonation depths  $d_k$  should not be measured where large aggregate is present. Instead, the measurement must be placed where the cement paste is predominant. To ensure that the measurement of  $d_k$  is perpendicular from the top of the sample, the use of measuring tape is sufficient, though in this study a magnifier measuring device was used.

## 5.5 EPOXY-COATED REBAR EVALUATION

A total of 45 epoxy-coated rebars (ECRs) were extracted by cracking the concrete cores with a chisel along the ECR length. In cores where bar corrosion was severe, the bars could be easily removed by hand. Table 5.2 summarizes the total number of ECRs extracted from each deck.

*Table 5.2 Epoxy coated bars extracted per bridge*

| <b>Bridge</b> | <b>ECRs</b> |
|---------------|-------------|
| 19015         | 12          |
| 27062         | 9           |
| 27812         | 14          |
| 27815         | 10          |
| <b>Total</b>  | <b>45</b>   |

The condition of the ECRs was assessed using the following procedures:

- i) visual inspection
- ii) coating hardness evaluation
- iii) coating adherence evaluation
- iv) coating thickness measurement
- v) bar corrosion condition estimation

In addition, the bar traces left in the concrete were examined for presence of corrosion, for the presence of cracks, or any other potential source of water.

A holiday count was not done on the bars extracted in this study because of the difficulty in distinguishing manufacturing- and installation-related holidays from those caused during aging, chlorine attack, coring or bar removal. Furthermore, the number and length of the bars extracted during coring was too small to be considered representative of the holidays or the damage that might have been present during construction. The 1996 WJE [21] study showed an extremely high holiday count, ranging from an average of 22 to 40 holidays per foot [32], a value that is inadmissible today for the manufacturing of epoxy coated bars. The ASTM A775/A775M [36] limits the maximum number of holidays to an average of one per foot over the length of the bar. Clearly, and as acknowledged in the 1996 WJE study, while many of the holidays counted were caused during core and/or bar removal.

### **5.5.1 Evaluation of coating hardness**

The coating hardness of the rebars was measured using the pencil hardness test, described in the NACE TM-0174 standard [34]. The purpose of this test is to evaluate the performance of protective coatings, the procedure consists of poking the coating surface with sharpened mechanical pencil leads of different grades until a marring of the coating is observed. A summary of the test procedure is provided next:

1. Flatten the tip of the exposed lead by pressing against No. 400 carbide abrasive paper and rotating with a gentle motion.
2. With the pencil held in the writing position or at an approximate 45° angle, push the lead forward against the coating (as shown in Figure 5.7).
3. Remove the lead marks with an art gum eraser. Any marring of the coating surface when viewed at an oblique angle in strong light indicates that the pencil lead is harder than the film.

4. Express the hardness of the coating as the next softer grade of pencil to the pencil grade used in the test. Grades of pencil hardness from soft to hard are 5B, 4B, 3B, 2B, B, HB, H, 2H, 3H, 4H, 5H and 6H.
5. After each pencil hardness test, the pencil should be turned to produce a new edge. Three or four tests can be made without redressing the pencil lead.



*Figure 5.7 Pencil hardness test.*

### **5.5.2 Evaluation of coating adherence**

To determine the adhesion of the coating to the bar, the recommended procedure described in the NACE TM-0185 standard [35] was used. In this test, the coating is cut to the base metal using a hobby knife blade. The point of the blade shall be drawn across the film (using multiple cuts if necessary) to cut a single V-shaped groove. Using the sharp side of the blade as a wedge, the coating film should be pried up within the groove as shown in Figure 5.8.. The exposed base should be observed under a magnifier lens to determine adhesion performance. An average of three attempts shall be used to rate the sample.

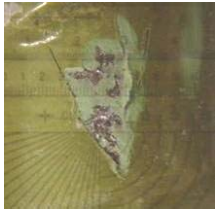





*Figure 5.8 Dry knife adhesion test.*



In this study, the test was conducted at three locations over the bar length. These locations were selected to represent the condition of the bar. The results were qualitatively evaluated using a 4 level rating system as shown in Table 5.3.

*Table 5.3 Coating adhesion rating description*

| <b>Rating</b> | <b>Description</b>   | <b>Example</b>  |
|---------------|--|---|
| 4             | <b>Good adherence:</b> Coating cannot be totally peeled or lifted from the substrate steel.                                  |    |
| 3             | <b>Moderate adherence:</b> Coating can be pried from the substrate steel in small pieces but it cannot be peeled off easily. |    |
| 2             | <b>Poor adherence:</b> Coating can be peeled from the substrate steel easily, without residue.                               |   |
| 1             | <b>No adherence:</b> Coating can be peeled from the substrate steel without the aid of the knife.                            |  |

### **5.5.3 Measurement of coating thickness**

Coating thickness can have a considerable impact on coating performance and the reinforcement quality. The likelihood of a greater number of holidays present and potential damage to the coating during construction increases if the coating is thinner than specified.

Current practice indicates that the epoxy coating thickness is required to meet ASTM A775/A775M-07 standard [36] unless specified otherwise. The ASTM A775 standard requires that the coating thickness be between 7 and 16 mils (0.007-0.016 inches). At the manufacturing plant, the coating thickness is commonly measured with magnetic gauges. In this study, the thickness was measured using a digital caliper with a precision of +/- 0.5 mils.





Epoxy coating thickness was determined by averaging 3 thickness measurements taken at random locations along the length of the bar. Measurements were taken only in bar areas where

no corrosion was observed. If the bar was severely corroded, thickness measurements were not made.

#### 5.5.4 Evaluation of corrosion condition

A visual inspection of the steel underneath the coating was performed in each bar to identify the corrosion condition of the bar. The inspection was made at three locations over the bar length; the same locations where coating adhesion was tested. The condition of the bar was classified into four categories as illustrated in Table 5.4. For bars in good condition, the coating could not be removed. In such cases, the bar was assigned the highest rating, i.e. No. 4, no corrosion observed.

*Table 5.4 Description of bar corrosion rating*

| Rating | Description  | Example   |
|--------|--|---|
| 0      | <b>No corrosion:</b> A black or silver color is observed on surface.                       |   |
| 1      | <b>Light corrosion:</b> A small number of countable spots of rust are observed on surface. |  |
| 2      | <b>Moderate Corrosion:</b> A significant area of corroded steel is observed on surface.    |  |
| 3      | <b>Severe corrosion:</b> Significant deterioration of the surface is observed.             |  |

## CHAPTER 6. FIELD EVALUATION - RESULTS AND DISCUSSION

### 6.1 INTRODUCTION

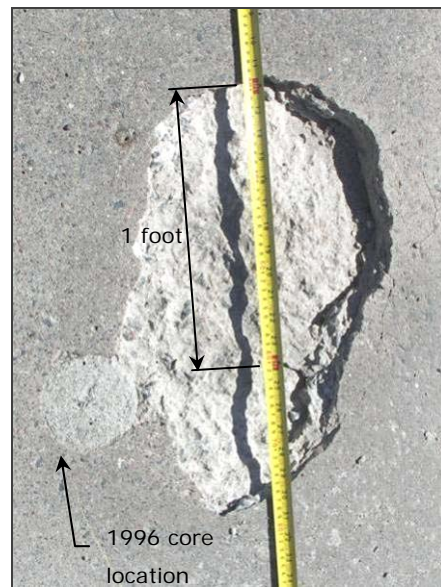
In this chapter, the results of the field surveys conducted on the four bridge decks are presented and discussed. These results are presented separately for each bridge and include the data obtained from visual inspection, the chain drag survey, half-cell potential survey, selection of the core location, cover depth measures, electrochemistry impedance spectroscopy, and ground penetrating radar surveys. Then the data is tabulated and compared among the bridges studied.

### 6.2 BRIDGE 19015

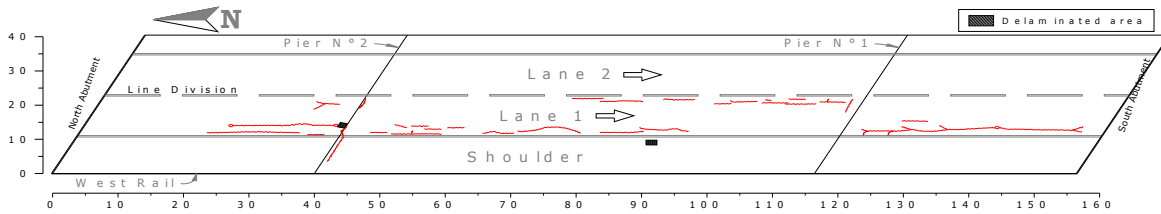
Corrosion activity in this bridge appears to be severe due to the presence of spalled areas and the very negative half-cell potential readings. However, the data show that corrosion of the top bars is constrained to the area around the joints over the bridge piers.

#### 6.2.1 Visual inspection

Visual inspection was performed in the shoulder and the right lane (lane 1). The deck showed light cracking mainly in the longitudinal direction, and few discontinuous cracks in the transverse direction. The total crack length in the area inspected was 220 ft, corresponding to a frequency of 0.062 ft/ft<sup>2</sup>. Crack widths ranged from 0.016 in. (0.4 mm) in the South span, to 0.080 in. (2.0 mm) in the transverse cracks next to the Pier No. 1. The right lane also had an open spalled area of about 1 sq. ft. (0.09 m<sup>2</sup>) next to the joint above Pier No. 2 on the North span of the bridge; this spall is presented in Figure 6.1. Figure 6.2 shows the crack layout of the surveyed deck (right lane and shoulder). There was no evidence of rebar corrosion at the bottom of the deck.



*Figure 6.1 Spalled area in bridge 19015.*



**Figure 6.2** Crack layout, spalled and delaminated areas on bridge 19015.

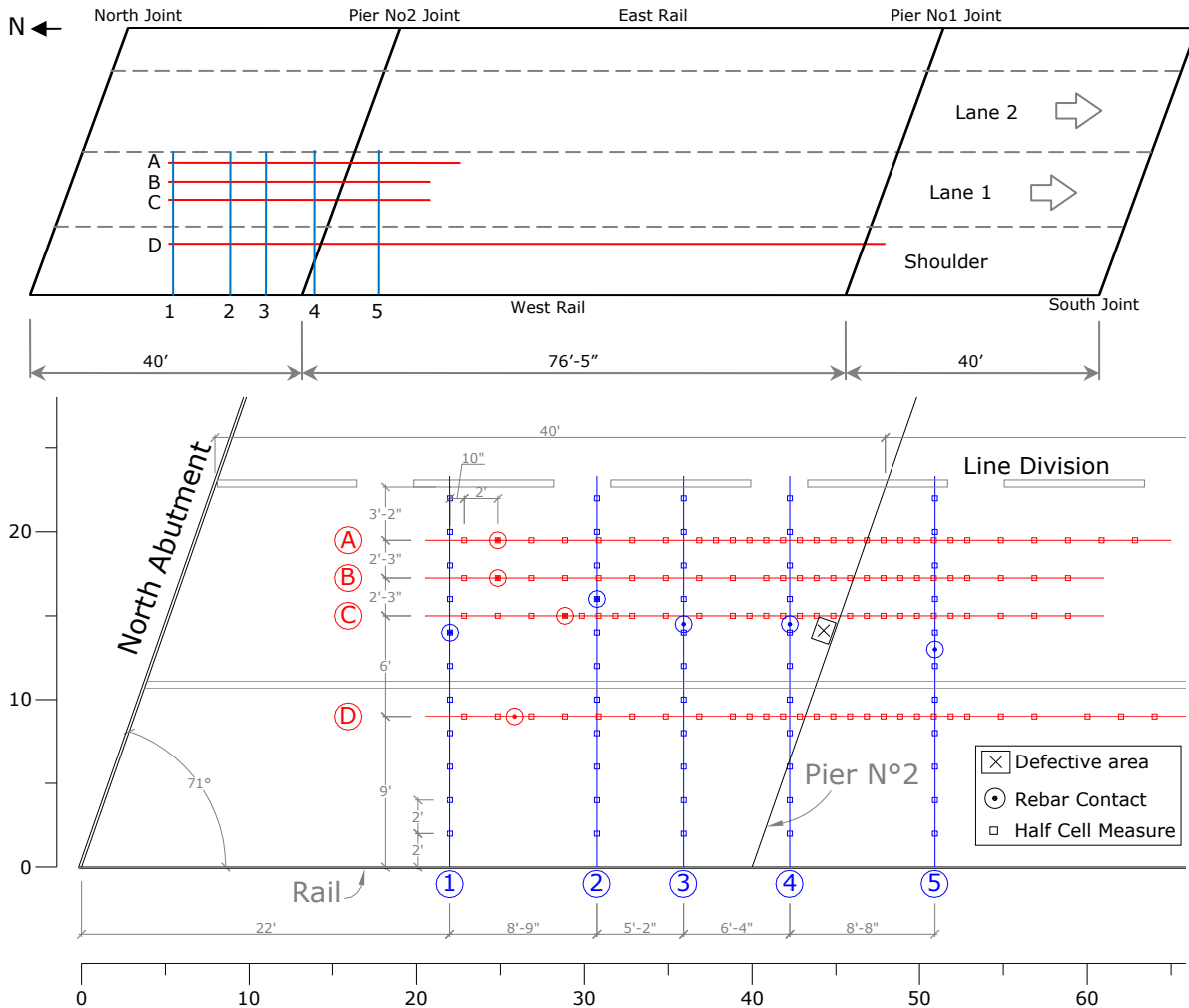
### 6.2.2 Chain-drag survey

This survey was conducted by Mn/DOT personnel and it was performed in the right lane and the shoulder along the whole bridge length. The survey yielded three delaminated areas totaling 39 sq. ft., representing about 1.1% of the inspected area. Most of the delaminated area was adjacent to the joint above Pier No. 2 and the spall shown in Figure 6.1. Additionally, 4 and 6 sq. ft. delaminated areas were found on the right lane (lane 1) and the shoulder respectively. Details of the survey method are presented in section 4.2.2.

### 6.2.3 Half-cell potential survey

Based on visual inspection and the chain drag survey, the first span was chosen for detailed evaluation. This span had an open spalled area and delaminated areas, an indication of potential corrosion activity on the reinforcing rebars.

To conduct the half-cell potential survey, four lines in the longitudinal direction and five lines in the transverse direction were layed out in the first span of the bridge as shown in Figure 6.3. Grid lines A and C in the longitudinal direction were chosen to coincide approximately with the wheel paths of the vehicles. Grid line B was arbitrarily chosen to be in between grid lines A and C. Grid line D was at a distance of approximately 2 ft from the shoulder line (about 8 ft from the bridge's curb). The location of lines 1 through 4 in the transverse direction was chosen to provide confirmation of the potential readings obtained from the measurements in the longitudinal direction. Grid line 5 was chosen as additional line of measurements after half-cell potential readings had indicated a high level of corrosion activity near the joint at Pier No. 2.

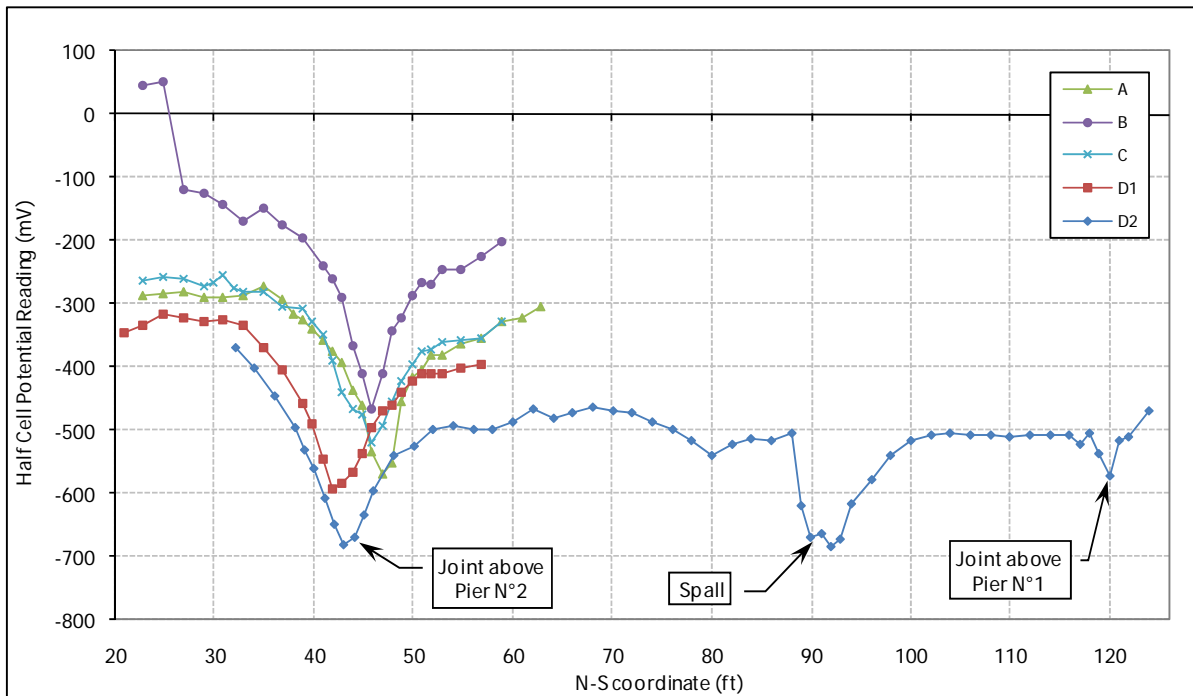


**Figure 6.3** Half-cell potential grid used in bridge 19015.

Along grid line D, two measurements were taken using two different connections to the bar. These readings are shown as D1 and D2 in Figure 6.4. Half-cell potential readings along grid line D on the shoulder showed much lower voltage readings (less than -350 mV) than along any of the other gridlines in the longitudinal direction. In addition, the chain drag deck survey showed areas of delamination on the shoulder. For this reason, half-cell potential measurements were continued into the second span of the bridge up to pier No. 1 as shown in Figure 6.3. As discussed in section 2.5.2, values of half cell potential readings lower than -350 mV indicate 90% probability of corrosion activity in the bars [50]. These absolute values, however, may vary significantly for epoxy-coated reinforcement depending on the concentration of oxygen and chloride, and on the electrical resistance of the concrete. Therefore, more important is the difference in the potential readings along a grid line, where the more negative the potential readings, the higher the level of corrosion activity.

Figure 6.4 shows plots of the voltage readings along grid lines A, B, C, and D. This was done as a confirmation of the unusually low readings (less than -700mV) obtained at some locations.

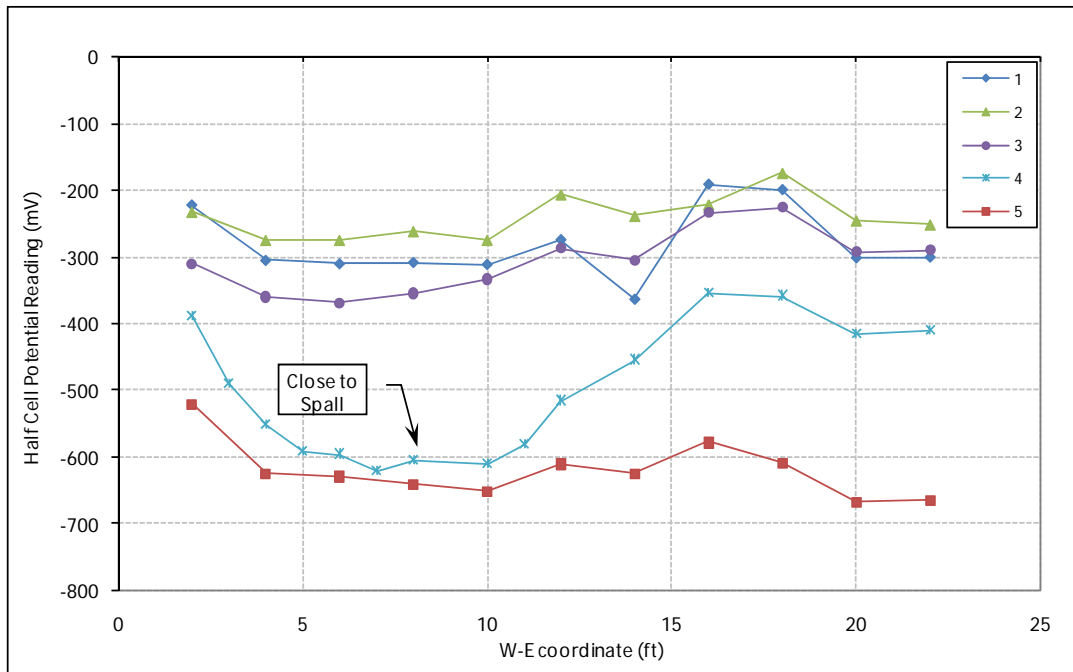
While the two readings (D1 and D2) did not match perfectly, they do show nearly the same values of potential, and more important, nearly same difference in the potential readings.



**Figure 6.4** Half-cell potential readings along grid line A, B, C, D1, and D2 in bridge 19015.

All the readings clearly show a drastic drop in potential readings of -250 mV or more at various locations along the grid lines. Not coincidentally, this drop in voltage occurred at the joints above the piers that allow the ingress of deicing salts to the bars. A similar drop in potential readings can be seen along grid line D2, 90 ft from the north end of the deck. This location coincided with one of the delaminated areas detected during chain drag survey of the deck. The survey lines located in the wheel paths of the vehicles (lines A and C), show readings lower than line B located in between, this situation might be indicating that traffic is producing an effect in the half-cell potential readings.

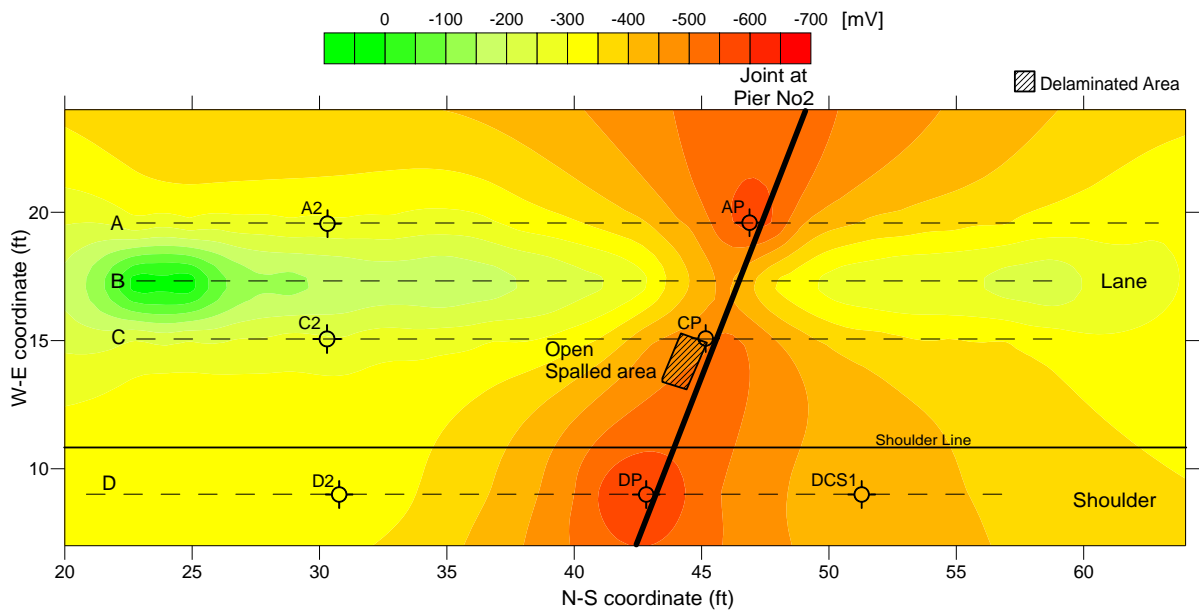
Figure 6.5 shows plots of the voltage readings along transverse grid lines 1, 2, 3, 4 and 5. Lines 1, 2 and 3 showed uniform readings around the -300mV. Lines 4 and 5 show lower half-cell potential readings because of their proximity to the joint over Pier No. 2. In particular, line 4 shows two clear levels among the readings; one around -600mV right on the joint over Pier No. 2 (between 3 and 12 ft in W-E coordinate) and other around -400mV farther that joint (between 12 and 22 ft in W-E coordinate). These measurements confirm the effect of the joint in the half-cell readings.



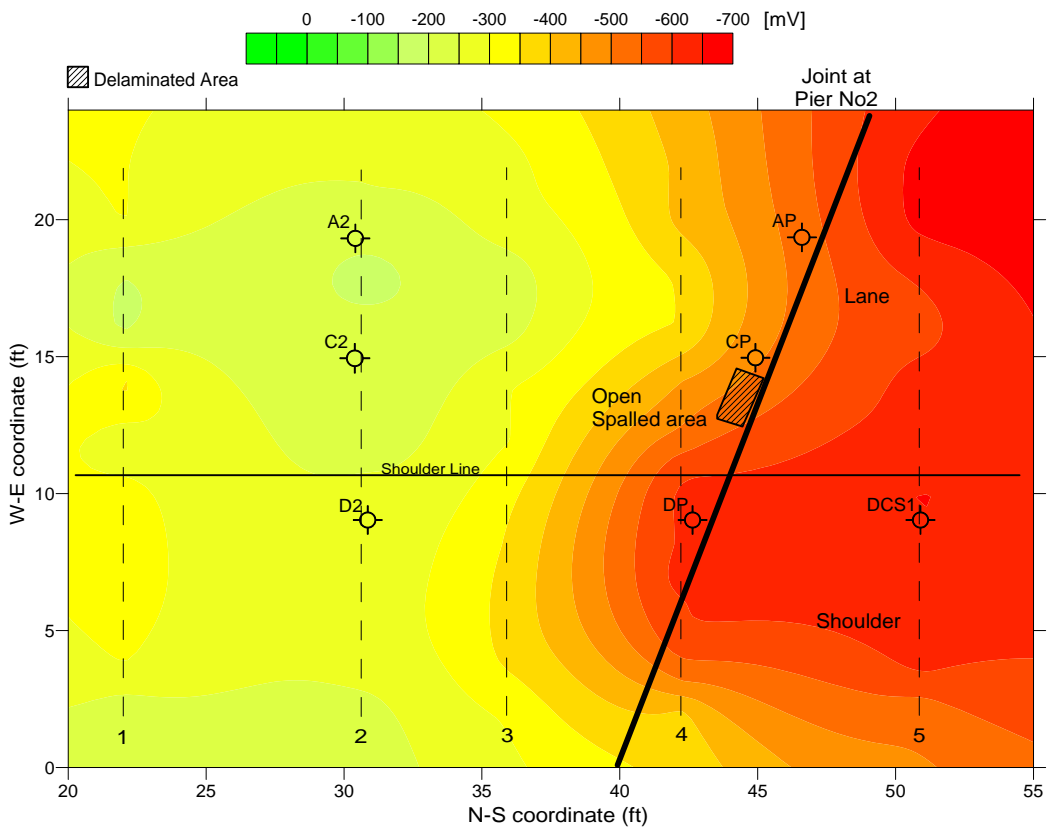
**Figure 6.5** Half-cell potential readings along grid line 1 to 5 in bridge 19015.

To provide a global idea about how the HCP readings are distributed on the deck and to easily identify high and low readings on the deck, the half-cell potential results along the longitudinal and transversal gridlines are presented in the contour plots shown in Figure 6.6 and Figure 6.7. The delaminated areas identified by the chain drag survey are also displayed. Although the two set of gridlines correspond to measurements in different rebars, both indicate that the area along the joint over pier No. 2 show the highest corrosion activity. Both figures show the significant effect of the saw cut at Pier No. 2.

Note that the extrapolation to the right of transverse line 5 in Figure 6.7 can not be considered as a prediction of the condition of the deck because no further cell potential readings were made beyond survey line 5.



**Figure 6.6** Contour map of HCP along longitudinal survey lines, bridge 19015.



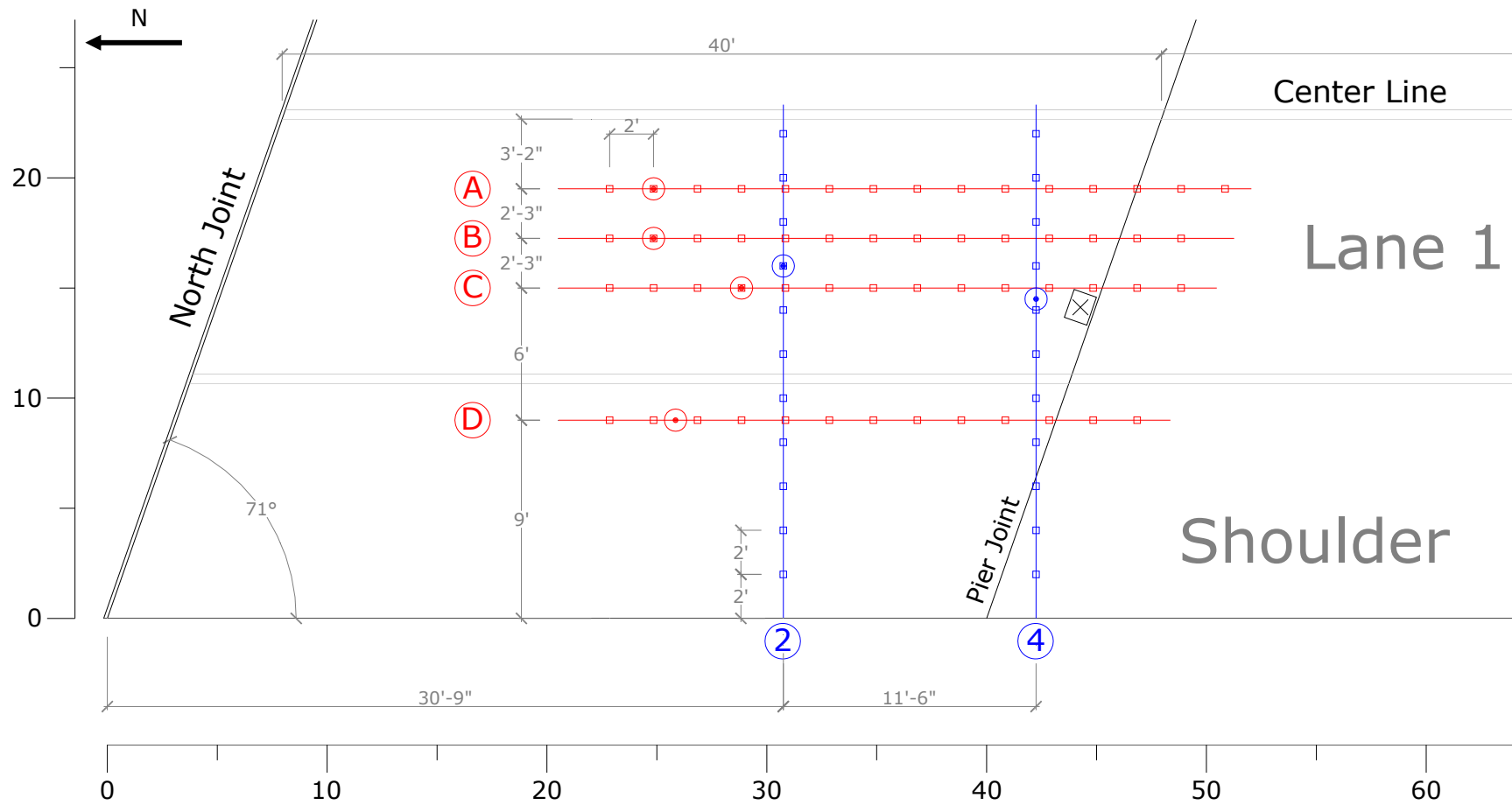
**Figure 6.7** Contour map of HCP along transverse survey lines, bridge 19015.



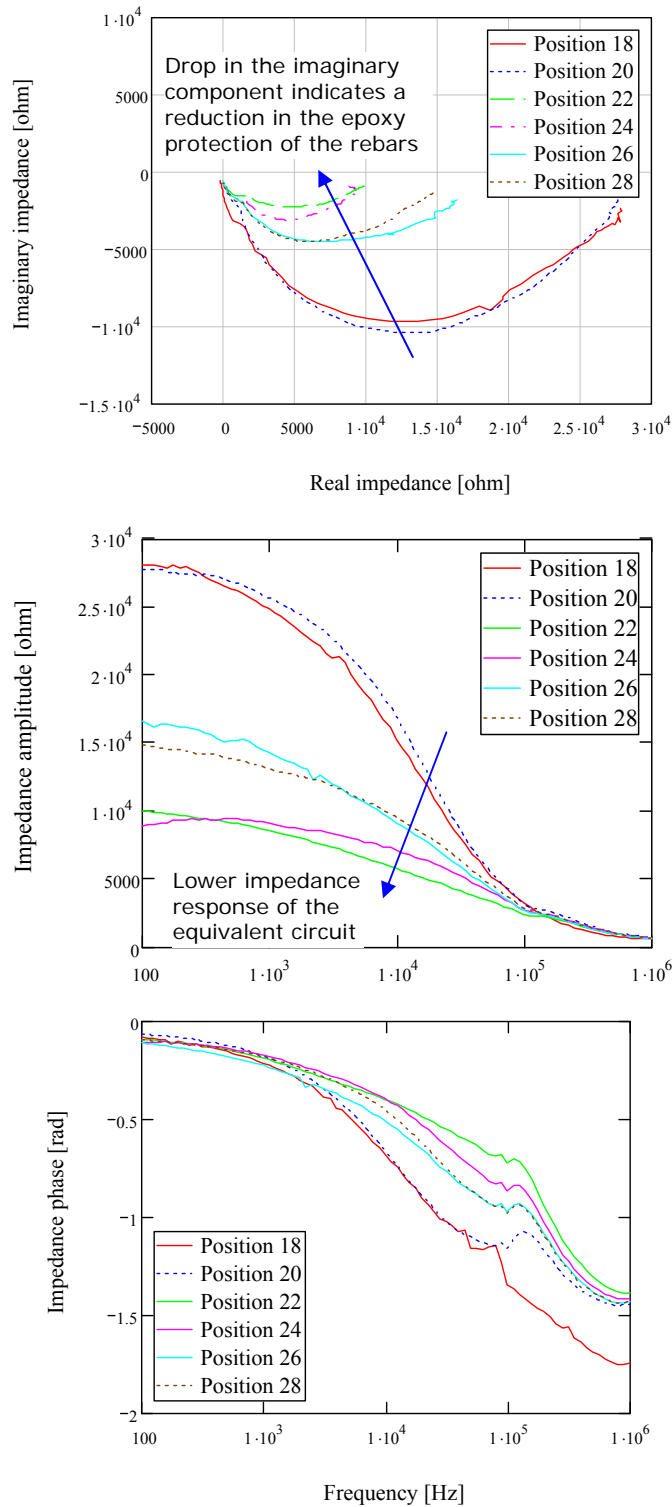
#### **6.2.4 Electrochemical impedance spectroscopy**

Impedance spectroscopy measurements were taken along the same grid used for the half cell readings (Figure 6.8). However, each of the measurements took approximately 5 minutes to be collected. Therefore, impedance data were collected only along the gridlines A, B, C, D, 2, and 4 as shown in Figure 6.8.

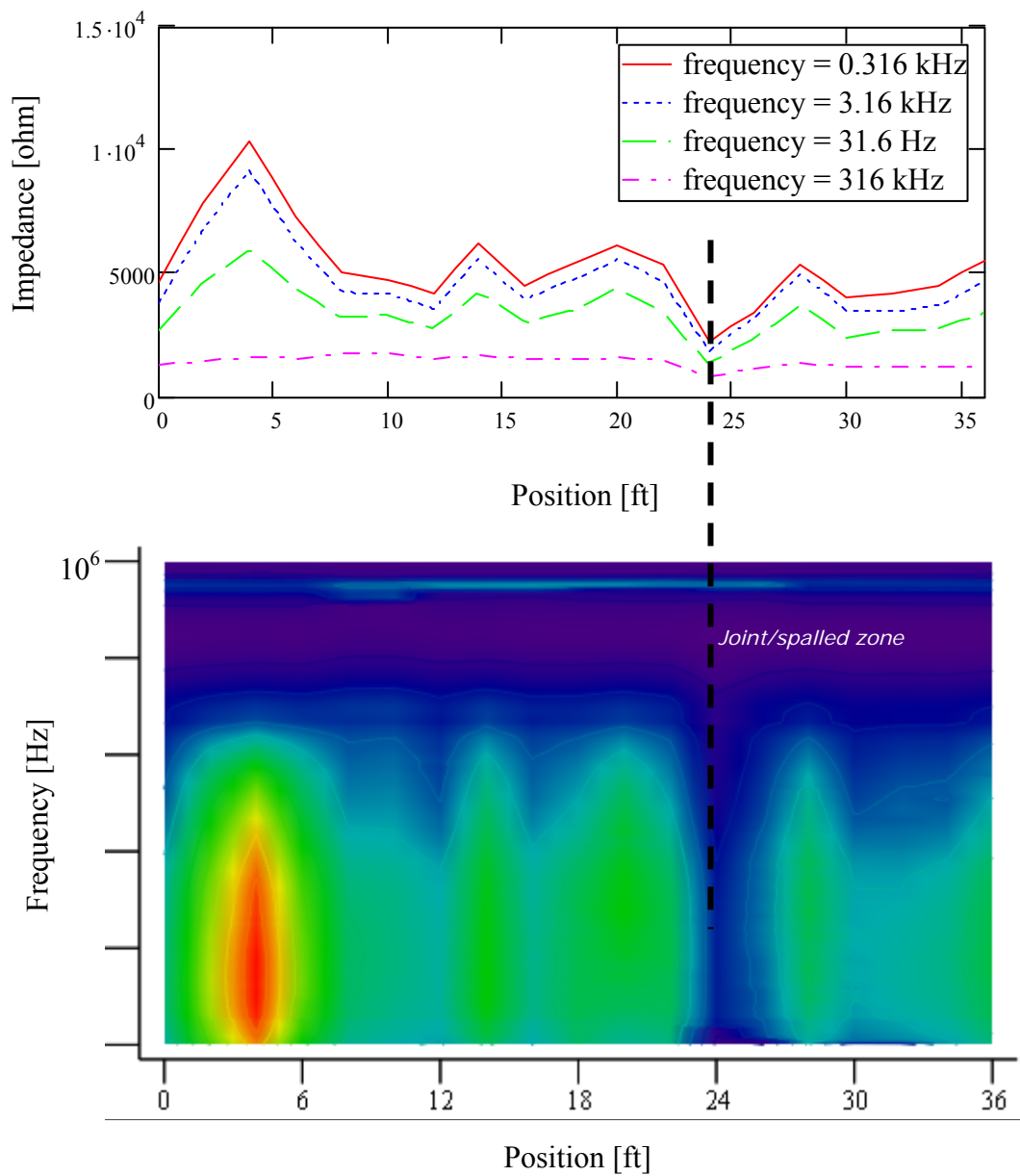
Typically, impedance spectroscopy data sets are presented as real vs. imaginary components and magnitude and phase of the measured impedance spectra as shown in Figure 6.9. These data are then fitted with equivalent electrical circuits in an attempt to determine the capacitive (negative imaginary component of impedance) or resistive behavior (real component of impedance) of epoxy-coated rebars (see Section 2.5.3). In an effort to correlate the impedance spectroscopy and the half-cell potential measurements, impedance measurements are presented as 2D plots of impedance amplitude versus frequency and measurement positions as shown in Figure 6.9, Figure 6.10, and Figure 6.11. The dashed line indicates the presence of a spalled area that coincides with a sharp drop in the impedance amplitude. These electrochemical impedance spectroscopy data should be qualitatively evaluated as a condition necessary but not sufficient for the corrosion process to occur. That is, the measured impedance should decrease in areas where the epoxy coating has deteriorated to provide the needed continuity for corrosion to occur. The interpretation of the half-cell potential and electrochemical impedance spectroscopy data seems to confirm these results. However due to the lack of survey time, the surface areas do not completely overlap and further confirmation could not be reached. More research and measurements are needed.



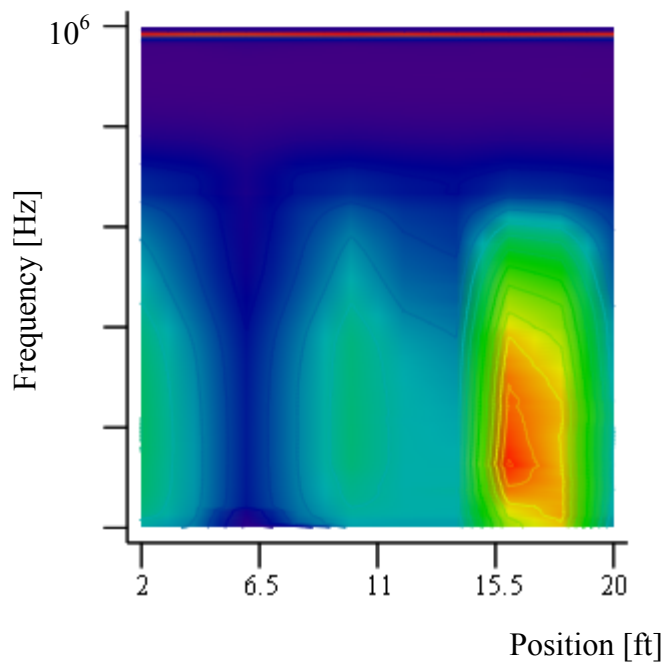
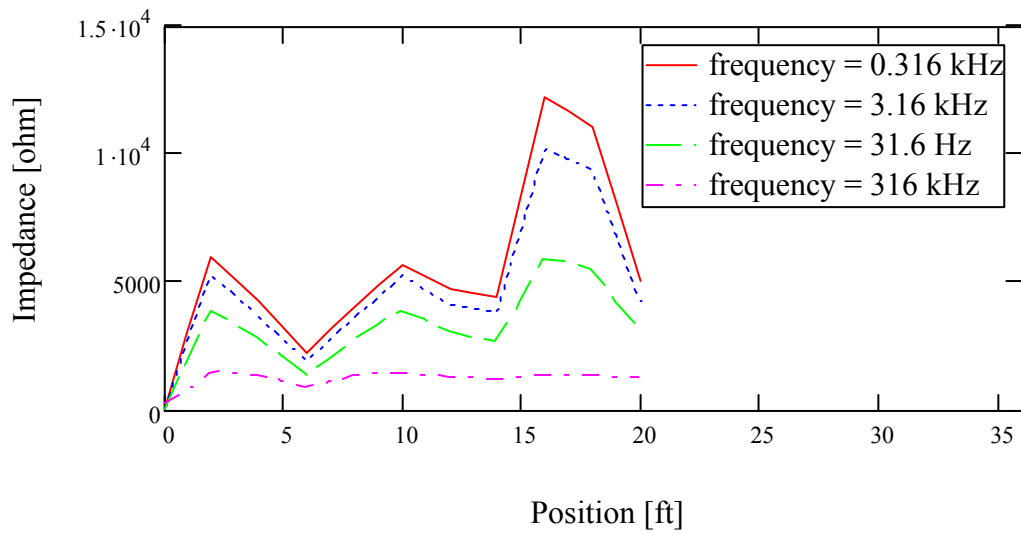
*Figure 6.8 Impedance spectroscopy grid used in bridge 19015.*



**Figure 6.9** Typical impedance spectroscopy results from bridge 19015 (Line B): (a) Cole-Cole plot and (b) amplitude and phase versus frequency.



**Figure 6.10** Electrical impedance spectroscopy along longitudinal line A. (a) Impedance magnitude at four frequencies and (b) Contour plot of impedance amplitude versus frequency and measurement position along the survey line.



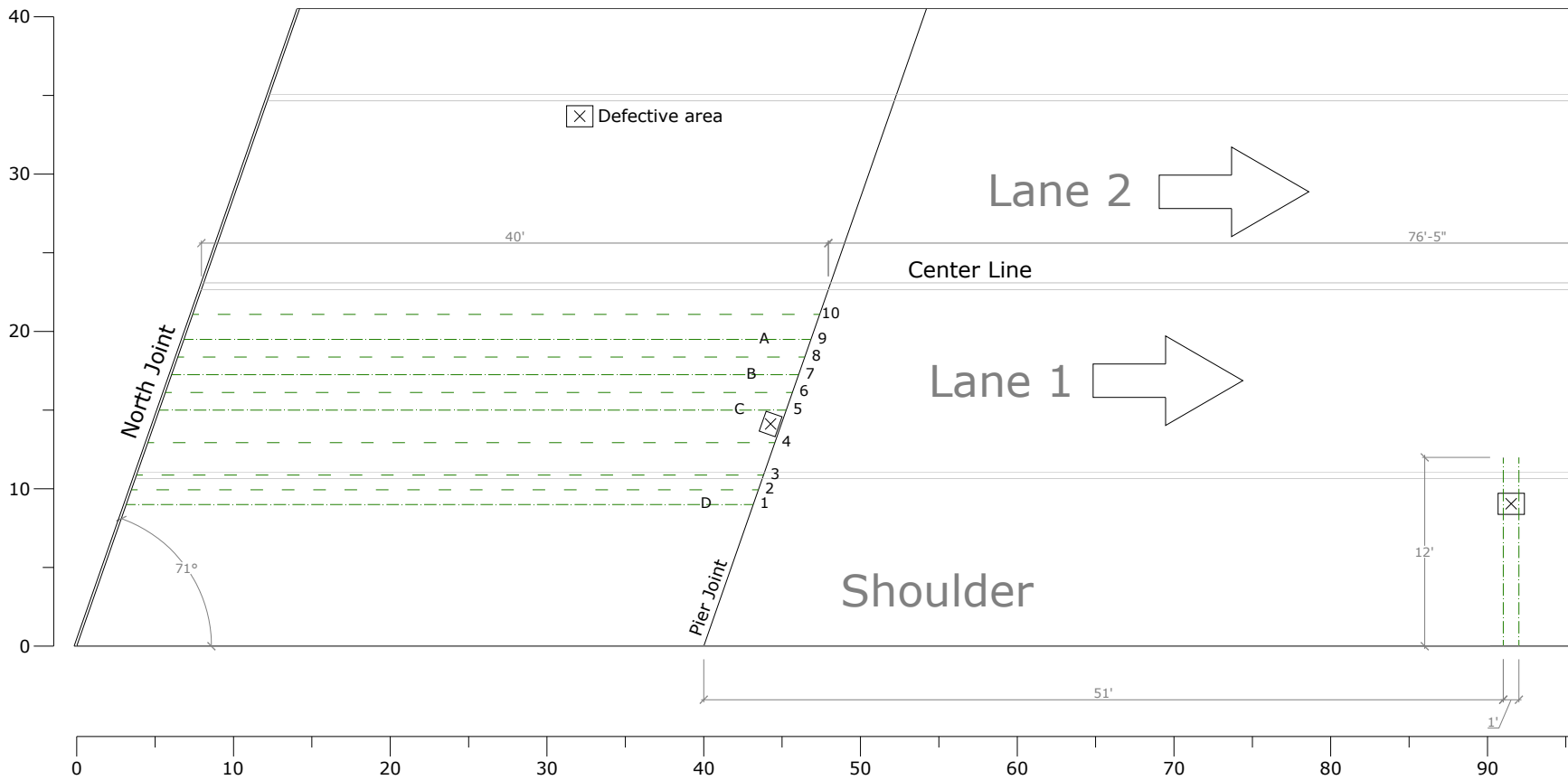
**Figure 6.11** Electrical impedance spectroscopy along longitudinal line 4. (a) Impedance magnitude at four frequencies and (b) Contour plot of impedance amplitude versus frequency and measurement position along the survey line.

### **6.2.5 *Ground penetrating radar measurements***

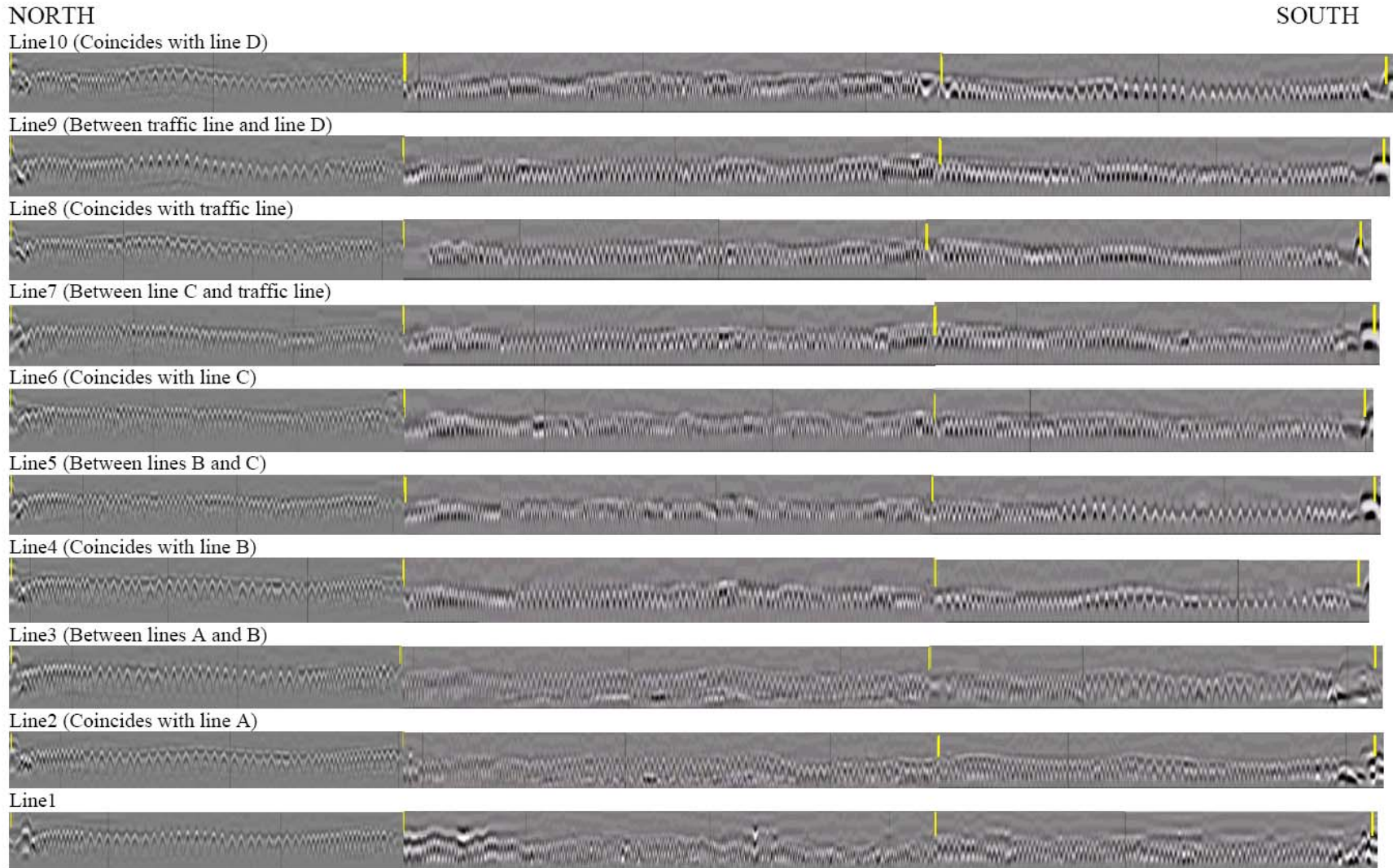
Dr. Mark Loken (Mn/DOT) collected GPR data along ten longitudinal survey lines between gridlines A and D in the bridge section between the North joint and the pier joint (see Figure 6.12). At a later date, Dr. Loken completed the GPR survey of the right lane and the shoulder of the southbound section of the bridge. The complete set of survey lines are presented in Figure 6.33.

Figure 6.14 shows the estimated distribution of the electromagnetic wave velocity on the bridge deck. Core “DCS2” is located at an area with low ELM wave velocity (highest water content). This result is matched well with trends obtained from other testing results. However, in the case of the core “CP”, the velocity contour and results from testing results do not show strong correlation (e.g., high water content and corresponding delamination). This lack of correlation may have been caused by the strong reflections from the metal at the pier joint.

The survey lines show a number of hyperbolas that correspond to the reflection signature of the rebars. The location and shape of these hyperbolas permit the evaluation of ELM wave velocity in the concrete and the depth of each rebar (Figure 6.15). The mapping of ELM wave velocity and the amplitude of the reflection are indicators of the volumetric water content and salt content in the concrete.



**Figure 6.12** Location of ground penetrating radar (GPR) survey.



**Figure 6.13** Ground penetrating radar (GPR) survey lines along the shoulder and left most lane on the southbound Bridge 19015.



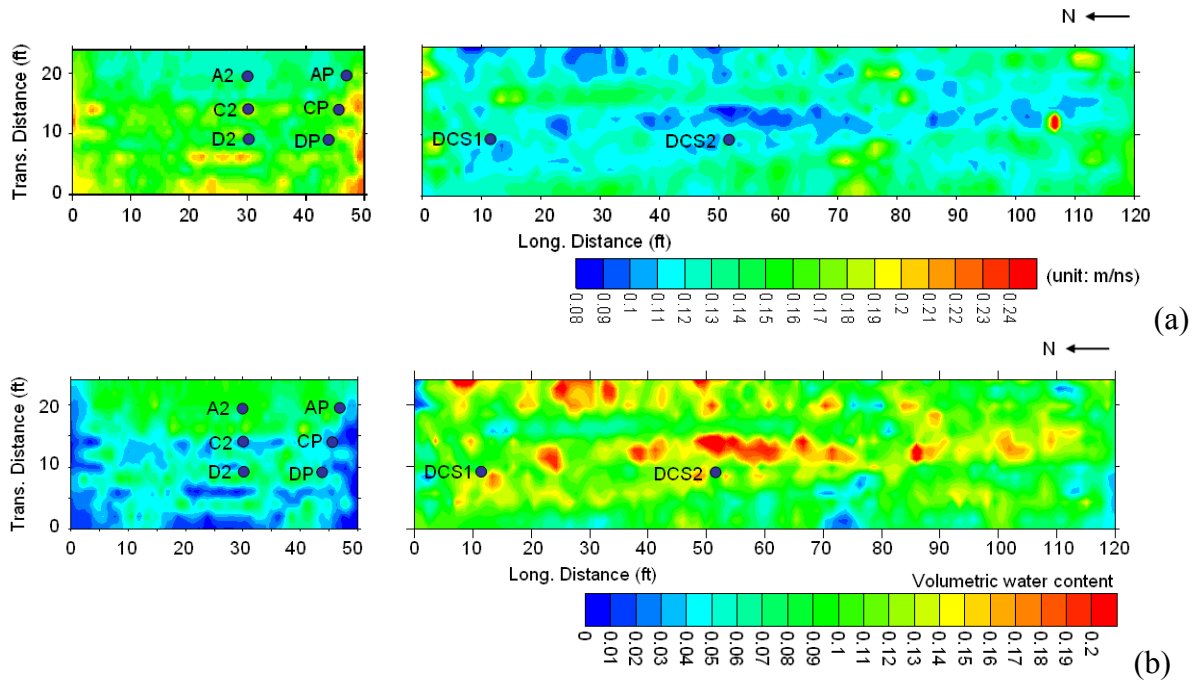


Figure 6.14 Distribution of (a) electromagnetic wave velocity and (b) calculated volumetric water content on Bridge 19015.

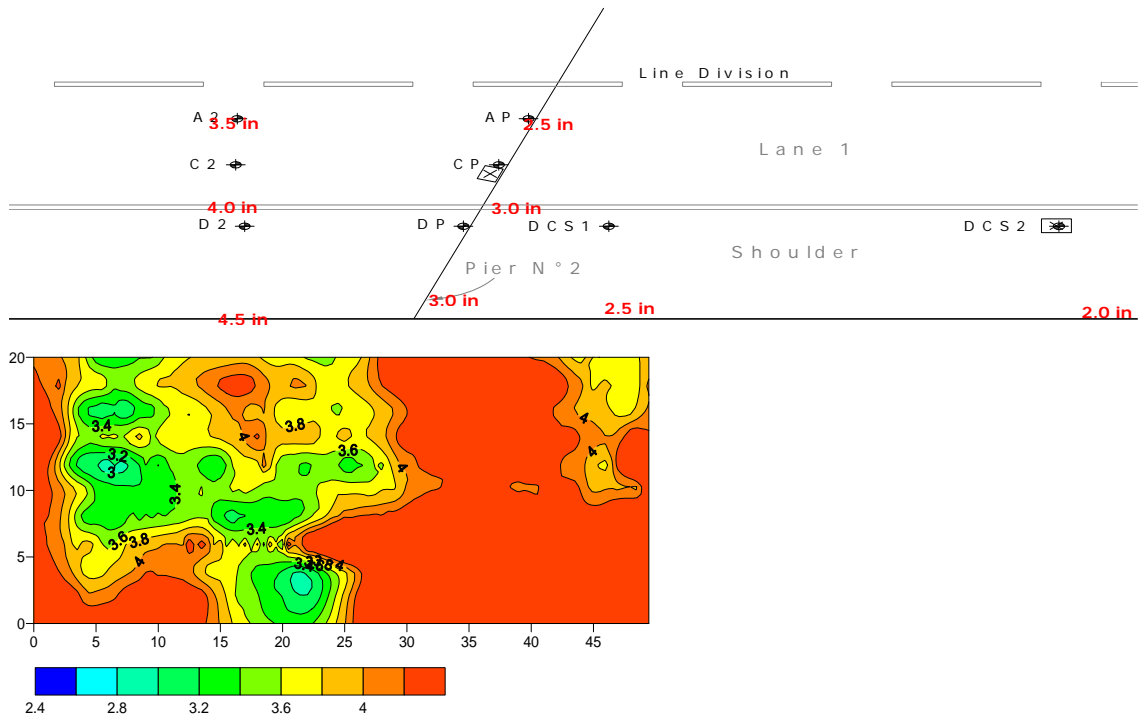


Figure 6.15 Distribution of rebar depths in Bridge 19015 as estimated from GPR measurements.

### 6.3 BRIDGE 27062

This bridge presented a good overall condition, however, several small delaminations were detected. Furthermore, patches and other maintenance work done on the deck indicated repairs for previous delamination damage.

#### 6.3.1 Visual inspection

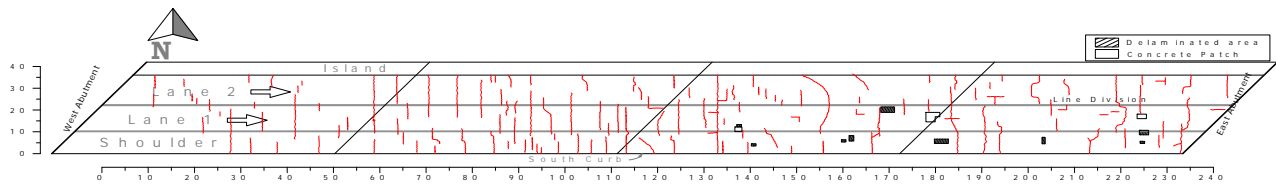
Visual inspection was performed in the shoulder and both eastbound lanes (lane 1 and lane 2). The deck had extensive cracking mainly along the transverse direction as shown in Figure 6.16. These cracks were sealed in the summer 2006, and as a result, it was not possible to measure any of the crack widths. The total crack length in the area inspected was 1134 ft, corresponding to a frequency of 0.129 ft/ft<sup>2</sup>. The deck also had a number of spalled and delaminated regions that had been already patched, mostly in the westbound lanes. There is also evidence of rebar corrosion at the bottom of the deck as shown in Figure 6.17. This corrosion evidence was observed in transverse cracks that coincide with the top of the deck. Figure 6.18 shows the crack layout of the entire bridge 27062 deck.



**Figure 6.16** Detailed view of transverse cracking on the deck of bridge 27062.



**Figure 6.17** Evidence of efflorescence and rust staining on the underside of the deck of bridge 27062.



**Figure 6.18** Crack Layout, Spalled and/or delaminated areas on bridge 27062.

### 6.3.2 Chain-drag survey

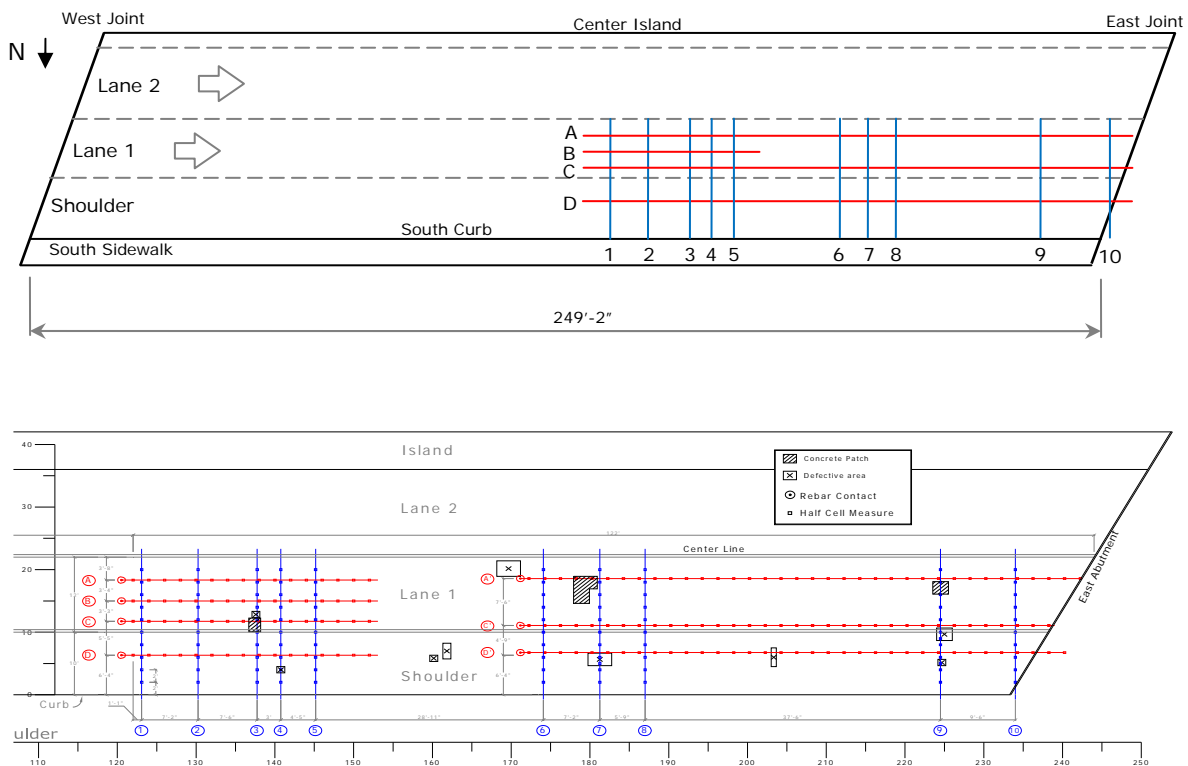
This survey was conducted by Mn/DOT personnel. It was performed in the right lane along the whole bridge length of the eastbound direction. The survey yielded a total of nine delaminated areas with 53 sq. ft., 1.0% of the inspected area. This span had several delaminated areas and recent patches that can be considered as an indication of potential corrosion activity in the reinforcing bars.

### 6.3.3 Half-cell potential survey

Based on visual inspection, the chain drag survey and results from the study conducted earlier in 1996, the second and third spans of the eastbound direction of the bridge were chosen for detailed evaluation. The half-cell potential survey was run along four grid lines in the longitudinal direction and ten grid lines in the transverse direction as shown in Figure 6.19.

Survey lines A and C were chosen to coincide approximately with the wheel paths of the vehicles. Survey line B was arbitrarily chosen to be in between grid lines A and C. Survey line D was placed on the shoulder about 6 ft from the bridge's curb. The location of survey lines 1 through 5 in the transverse direction was chosen to provide confirmation of the results obtained for the longitudinal rebars A, B, C, and D and to survey patches and delaminated areas detected during the chain drag survey. Grid lines 6 to 9 were chosen as additional lines of measurements to evaluate the health of the rebars at the center of the span and at the east most joint.

To identify potential differences in the corrosion activity between the shoulder and the right lane (lane 1), the transverse lines run from the south curb to the center line, as shown in Figure 6.19.



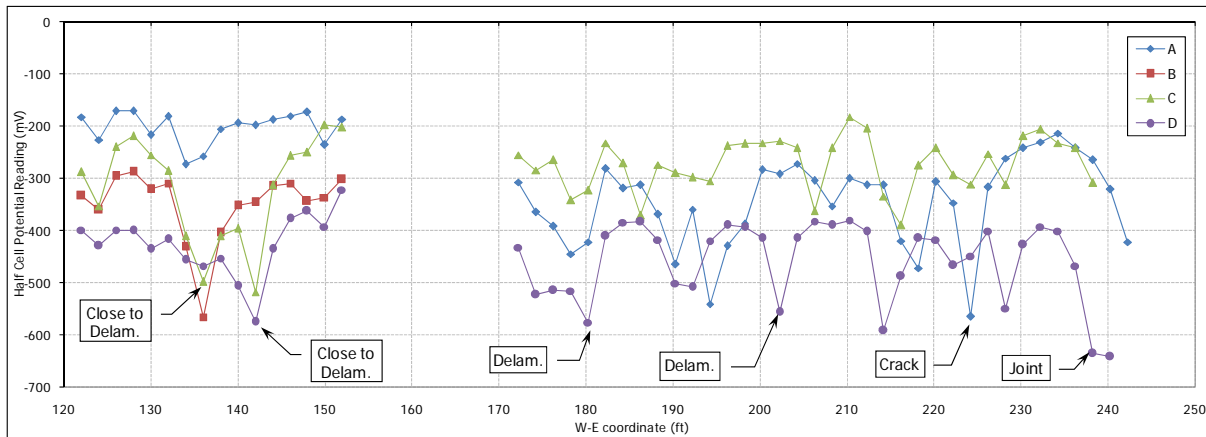
**Figure 6.19** Half-cell potential grid used in bridge 27062.

Results of the obtained half-cell potential readings along longitudinal and transversal grid lines are summarized in Figure 6.20, Figure 6.21, and Figure 6.22. Not surprisingly, the lowest voltage readings (-500mV or lower) indicating corrosion activity, correlate well with the presence of patches and delaminated areas, although this correlation does not apply to every single defect. Line D shows relative lower readings than other survey lines where most of the new delaminations detected are located in the shoulder. Corrosion activity was also found at crack locations and the joints.

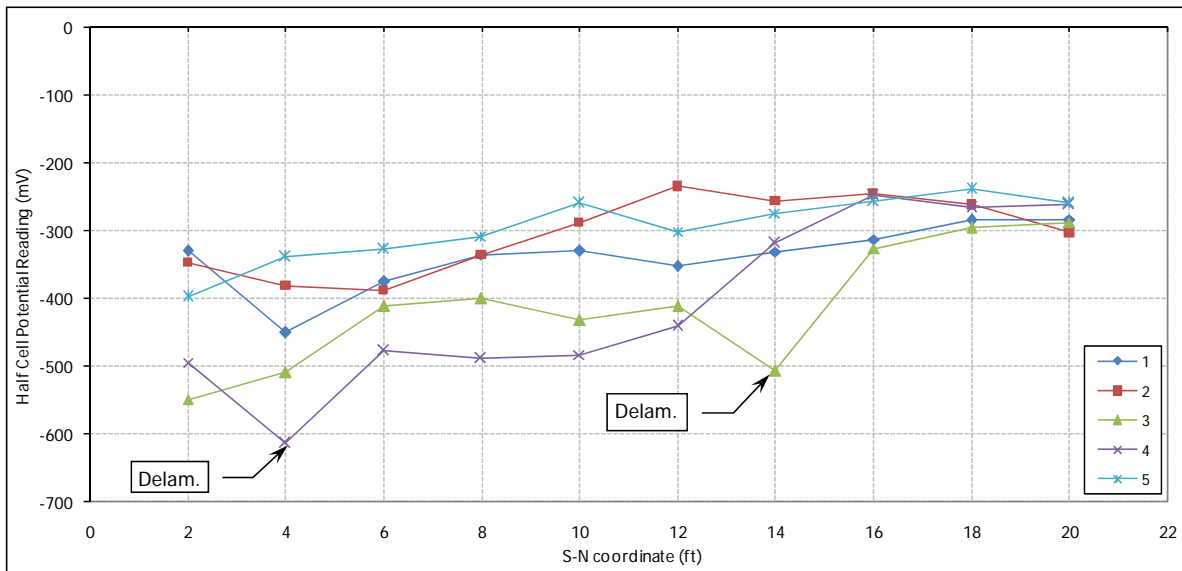
In the transverse direction, lines 4 and 7 show the lowest values (around -600mV), these two values are close to delaminated areas detected by the chain drag survey. Line 3 (represented by

triangles in the Figure 6.22) also shows a match between low reading and delamination. On the other hand, line 6 was selected in a healthy region of the deck and the readings are all above -150mV as shown in Figure 6.22.

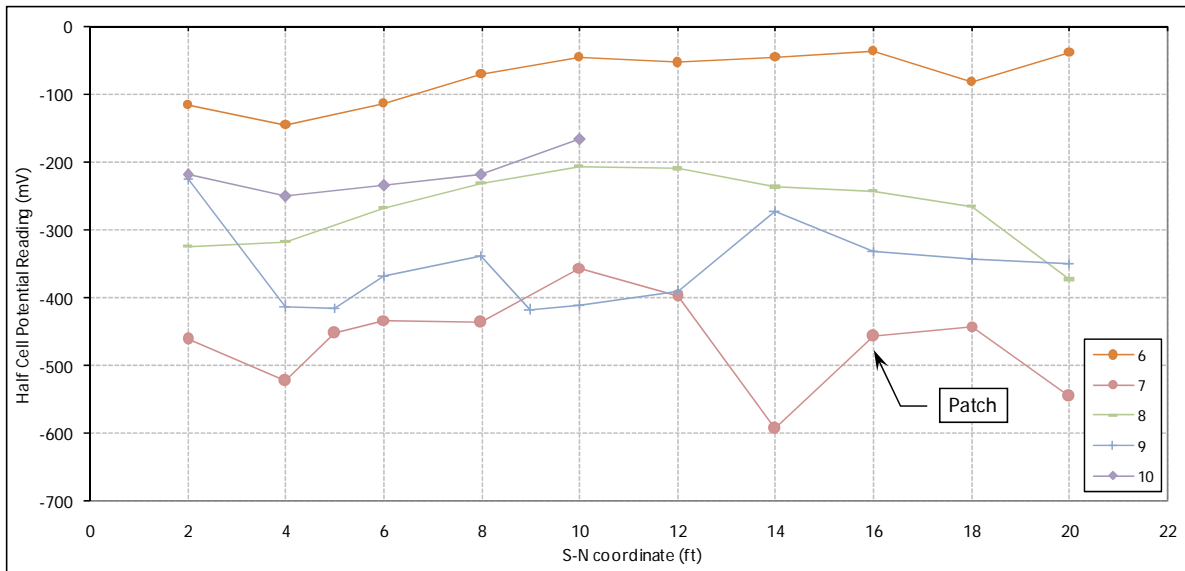
To have a global idea about how the HCP readings are distributed on the deck and to easily identify high and low readings on the deck, the half-cell potential results along the longitudinal and transversal gridlines are presented in the contour plots shown in Figure 6.23 and Figure 6.24. The delaminated areas identified by the chain drag survey are also displayed.



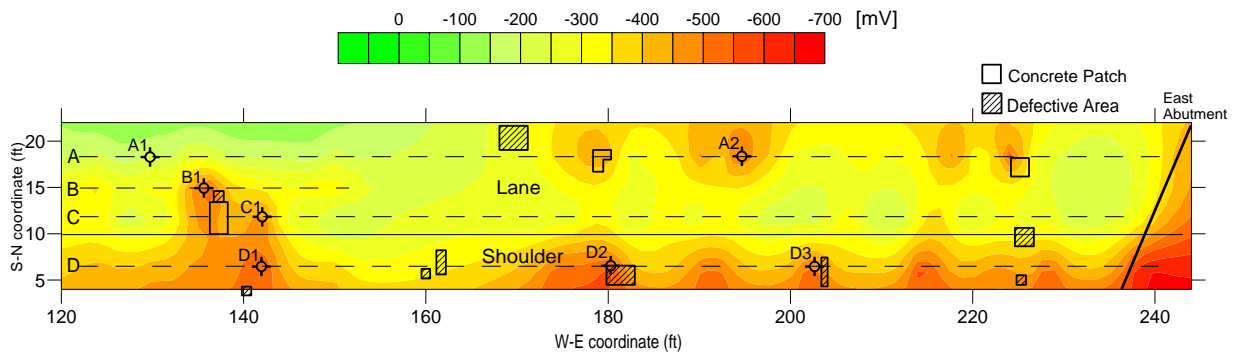
**Figure 6.20** Half-cell potential readings along grid line A, B, C and D in bridge 27062.



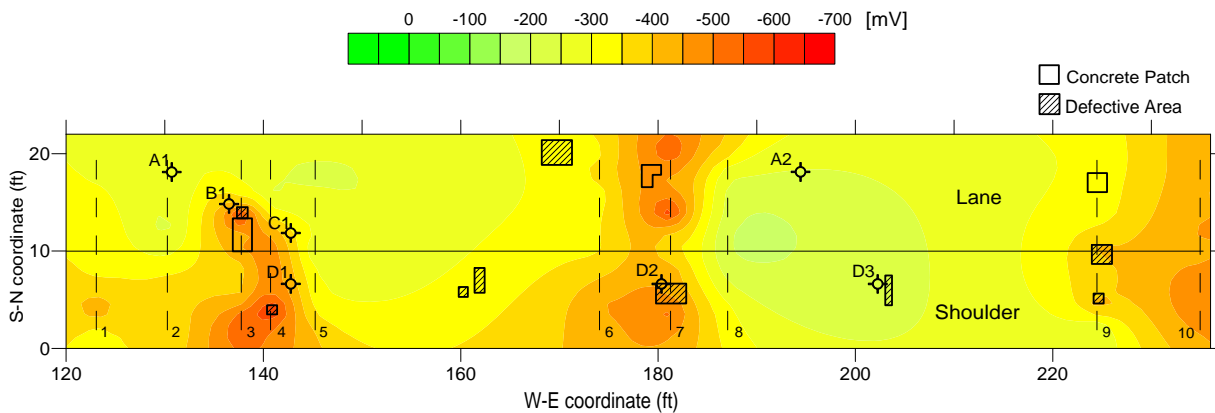
**Figure 6.21** Half-cell potential readings along grid line 1 to 5 in bridge 27062.



**Figure 6.22** Half-cell potential readings along grid line 6 to 10 in bridge 27062.



**Figure 6.23** Contour map of HCP readings in the longitudinal survey lines, bridge 27062.

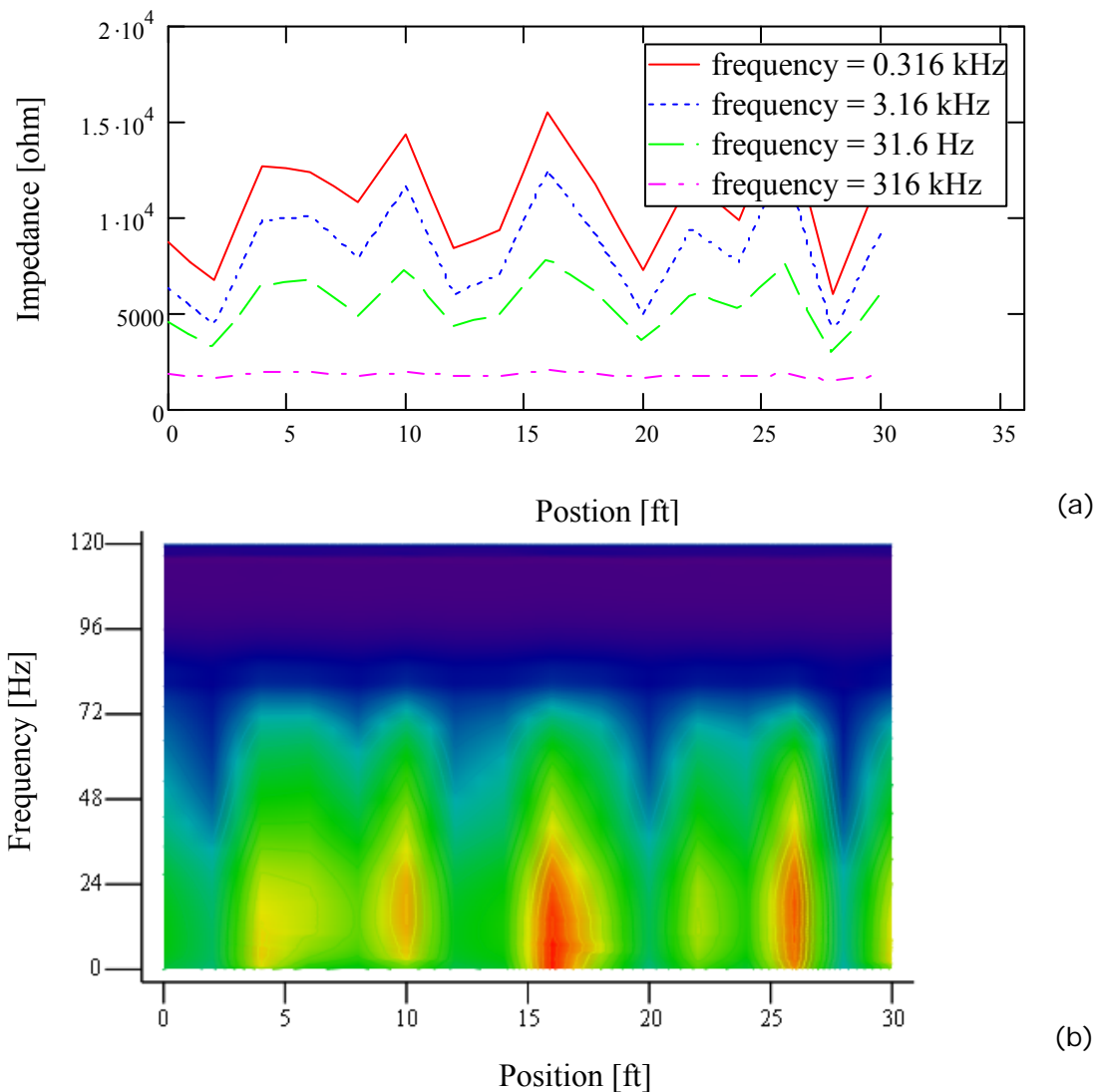


**Figure 6.24** Contour map of HCP readings in the transverse survey lines, bridge 27062.

The figures show how lower HCP readings are located and concentrated close to deck patches, delamination areas, cracks and joints. Therefore, these results suggest that HCP can be a valuable tool to identify corrosion activity in decks with ECR.

### 6.3.4 Electrochemical impedance spectroscopy

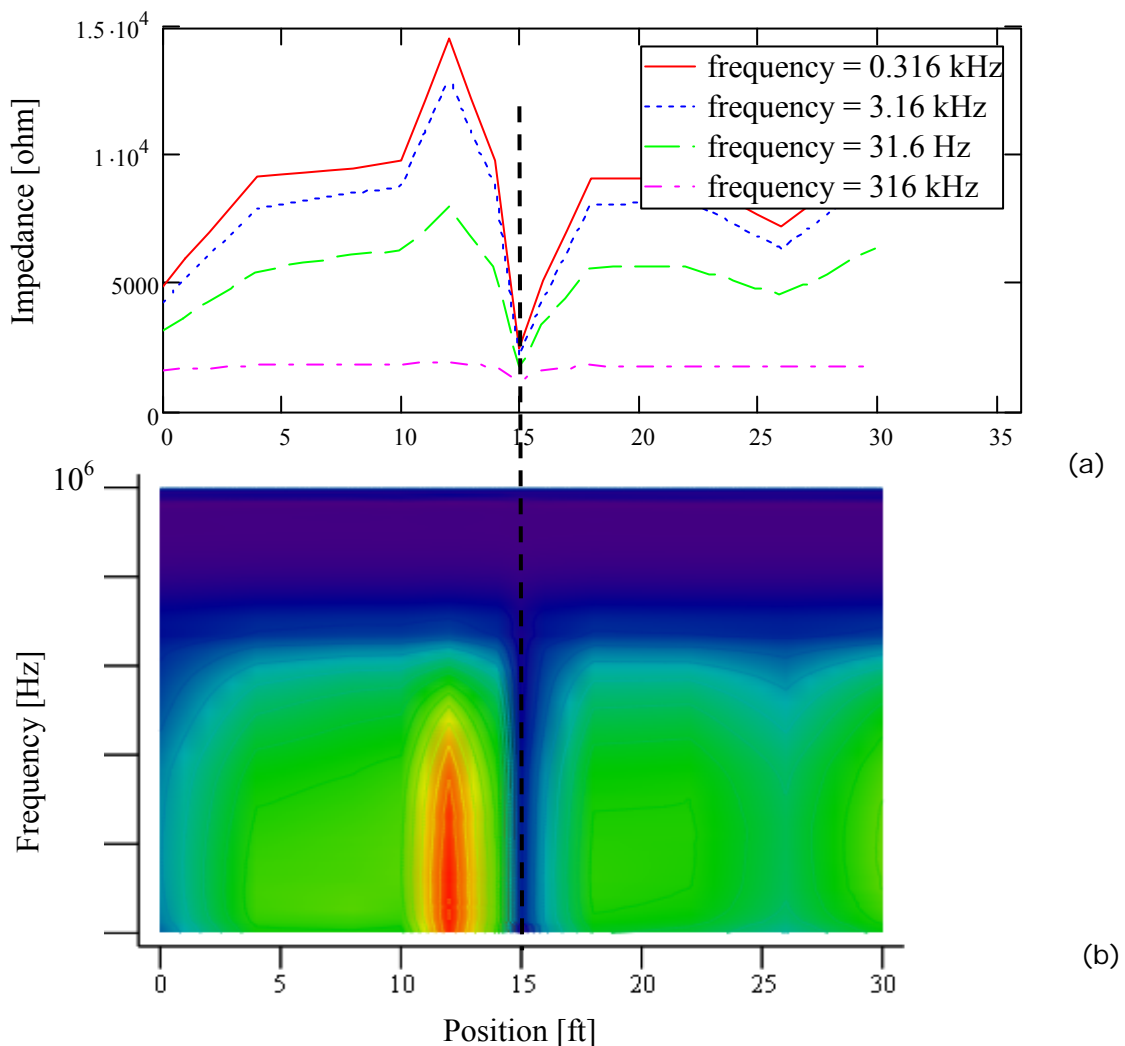
Due to slower data acquisition speeds, impedance spectroscopy data were only collected along the gridlines A, B and C (rain during the latter part of the survey day prevented the collection of data along transverse survey lines). In an attempt to correlate the impedance spectroscopy and the half-cell potential measurements, impedance measurements are presented as 2D plots of impedance amplitude versus frequency and measurement positions as shown in Figure 6.25 and Figure 6.26.



**Figure 6.25** Electrical impedance spectroscopy along longitudinal line A bridge 27062. (a) Impedance magnitude at four frequencies and (b) Contour plot of impedance amplitude versus frequency and measurement position along the survey line.

Figure 6.25 shows no sudden drops in electrical impedance along survey line A indicating that the bar has the same electrical properties through its length. These data coincide with half-cell potential data along line A where there is no indication of corrosion. That is no-corrosion activity on a rebar that seem to have healthy epoxy coating as indicated by the electrical impedance spectroscopy readings.

Figure 6.26 summarizes the electrical impedance along survey line C. The dashed line shows a sudden drop in impedance measurement coincides with the presence of a large concrete patch in the bridge deck (coordinate x=137 ft, y=12 ft in Figure 6.19). The response in the half-cell potential readings indicates active corrosion, while the low impedance measurement seems to indicate poor epoxy-coating protection in the reinforcing rebars.



**Figure 6.26** Electrical impedance spectroscopy along longitudinal line C, bridge 27062. (a) Impedance magnitude at four frequencies and (b) Contour plot of impedance amplitude versus frequency and measurement position along the survey line.

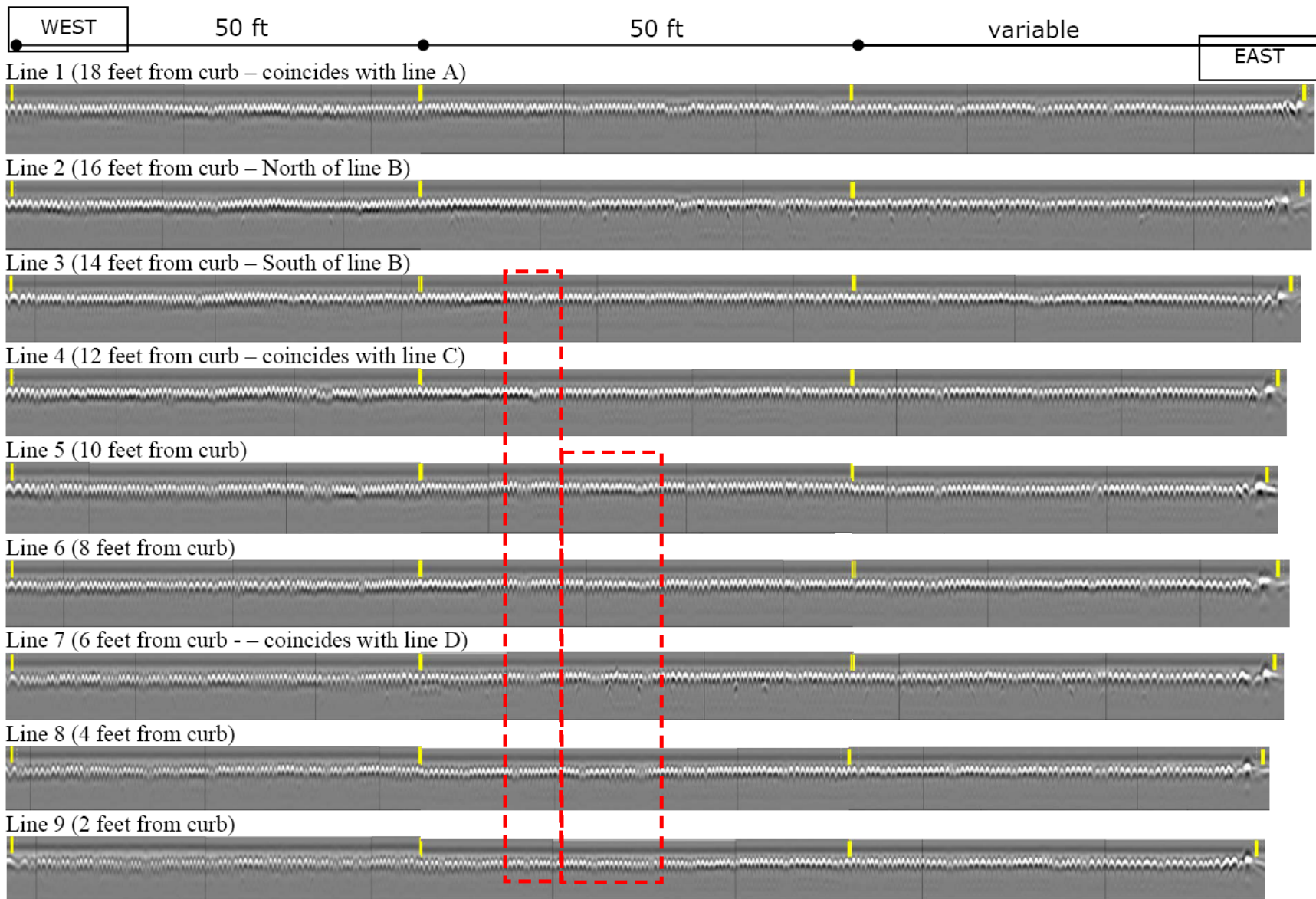


### **6.3.5 Ground penetrating radar measurements**

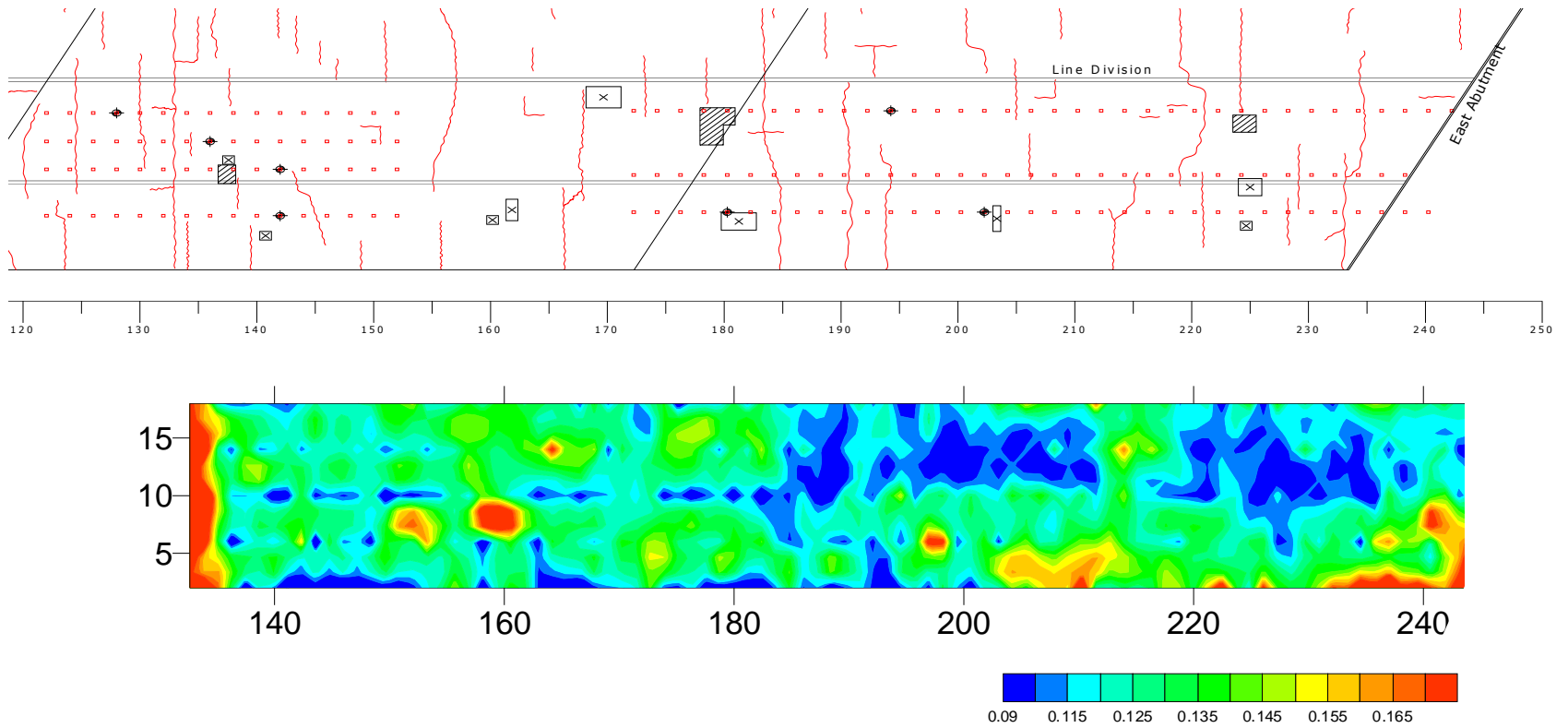
Mn/DOT personnel ran a (GPR) survey along the shoulder and right lane of the eastern most section of the eastbound direction of the bridge. Nine equally spaced longitudinal survey lines were collected. Figure 6.27 presents the collected survey lines. Each of these survey lines show hyperbolas that are the reflection signature of the reinforcing rebars.

The time analysis of these hyperbolas permit the evaluation of electromagnetic wave velocity in the concrete and the depth of each steel rebars. The mapping of EM wave velocity and the amplitude of the reflection provide an indication of the volumetric water content and salt content in the concrete. ELM wave velocity profiles allow the evaluation of the volumetric water content and the correlation with deteriorated areas in the bridge deck. Figure 6.28 and Figure 6.31 present a contour plot of the calculated ELM velocity on the bridge deck. The results are compared against the mapping of cracks, patches and delamination areas as these zones will tend to have concrete with greater water content.

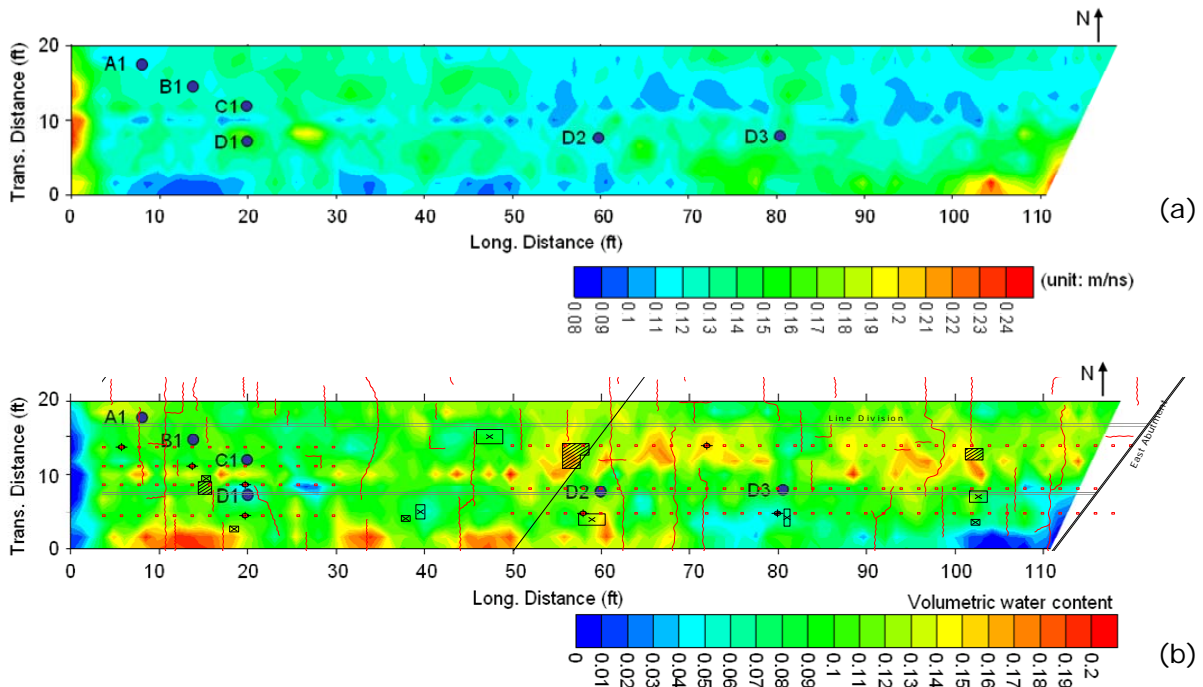
A reduction in the EM signal amplitude is an indication of high material attenuation. In the case of bridge deck that is related to the presence of moisture and  $\text{Cl}^-$  content. For example, the GPR survey consistently shows (dashed boxes in Figure 6.27) a sudden drop in amplitude and velocity (weaker signals and longer EM waves travel time at 60-70 ft coordinate). These signatures coincide with most negative half-cell potential measurements as shown in Figure 6.24. That is, high volumetric water and  $\text{Cl}^-$  content contribute to the corrosion environment. The problem with this interpretation is that the GPR survey show many other areas with similar signatures that do not correspond to half cell potential response. This is a clear indication of the complexity and interplay of many complex parameters including the quality of the epoxy coating in the rebars.



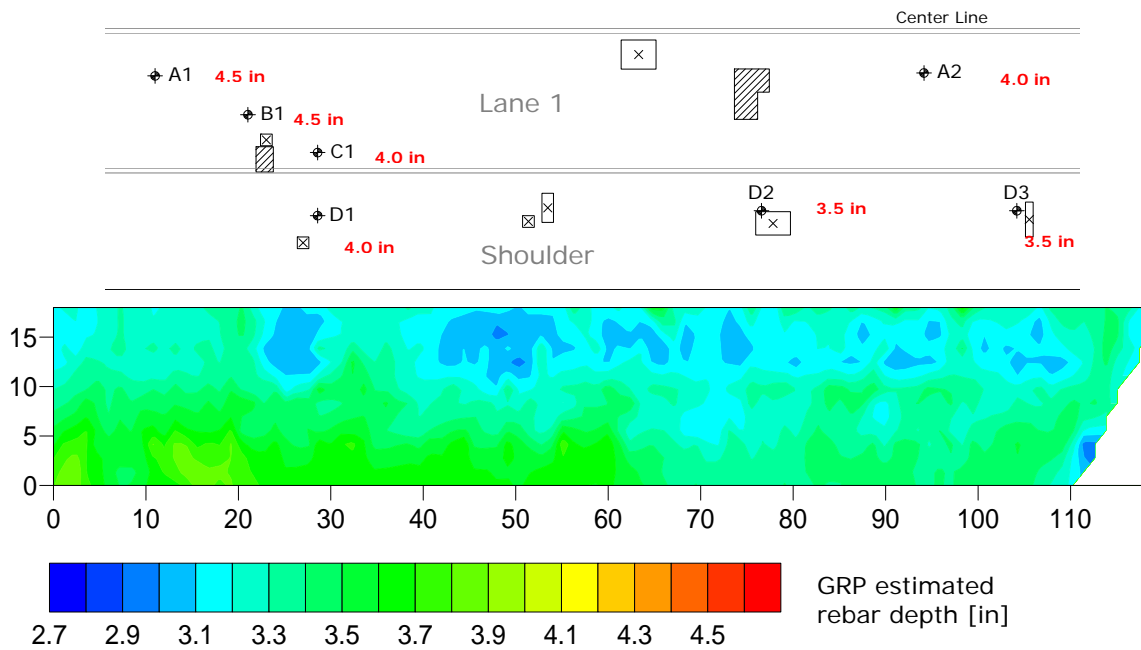
**Figure 6.27** GPR results along survey lines in bridge 27062.



**Figure 6.28** Bridge 27062 (a) Mapping of crack, patches and delamination areas and (b) Calculated velocity contours (m/ns).



**Figure 6.29** Distribution of (a) electromagnetic wave velocity and (b) volumetric water content on Bridge 27062 as determined by the GPR survey.



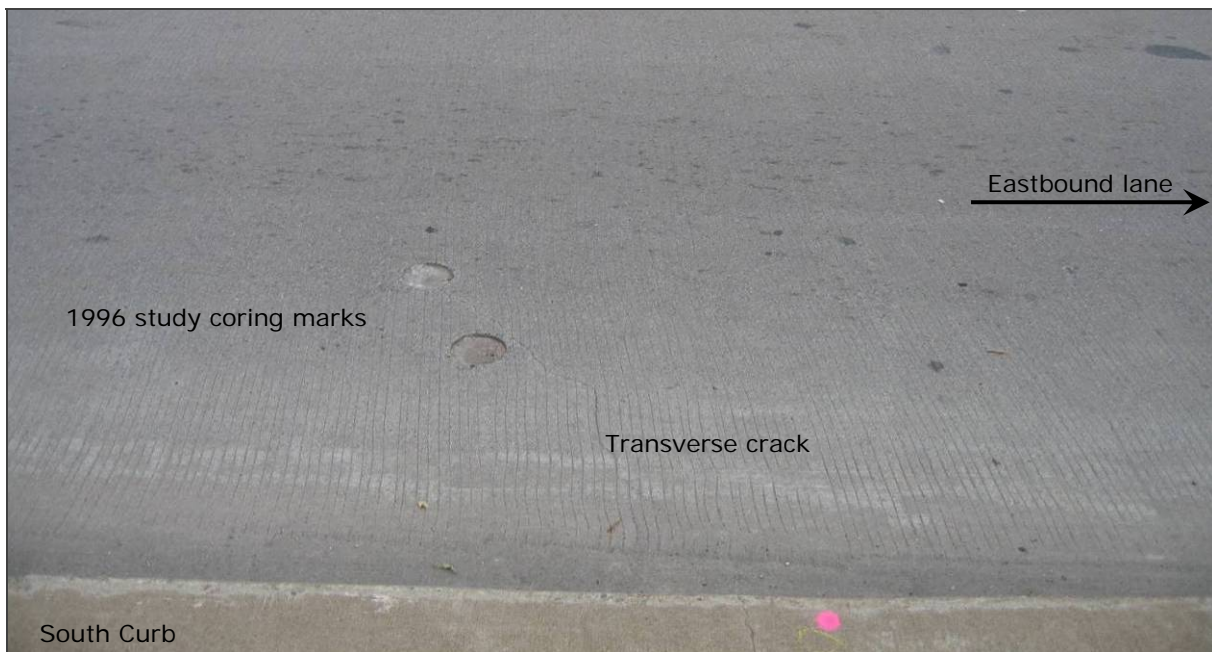
**Figure 6.30** Distribution of rebar depths in Bridge 27062 as estimated from GPR measurements.

## 6.4 BRIDGE 27812

This bridge presented good deck conditions in almost all its surface, with the exception of the west abutment joint, which presented concentrated cracking, delamination as determined by the chain drag survey and some minor spalling.

### 6.4.1 Visual inspection

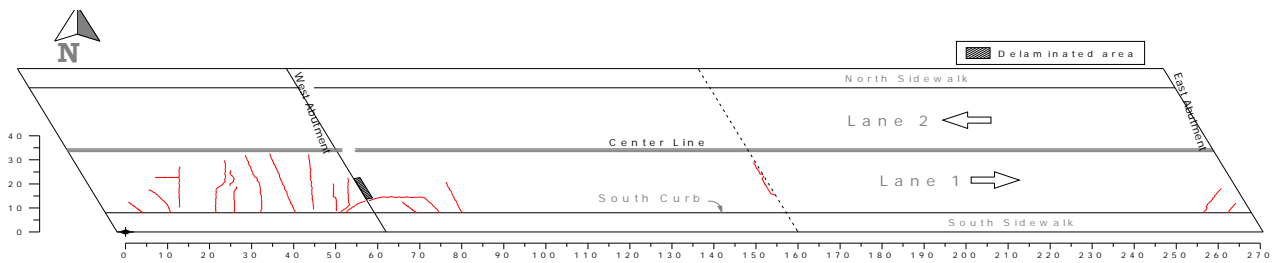
Visual inspection was performed only in the eastbound lane (lane 1). The deck showed minor longitudinal and transverse cracking as shown in Figure 6.31 and Figure 6.33. The total crack length in the area inspected was 263 ft, corresponding to a frequency of 0.038 ft/ft<sup>2</sup>. Crack widths ranged from 0.008 in. (0.2 mm) near the east abutment, to 0.080 in. (2.0 mm) in the longitudinal direction next to the delaminated area in the west abutment. There was also evidence of some efflorescence and light rust staining from the black bars of the bottom reinforcing mat. This efflorescence evidence was observed in a small area on the underside of the deck as shown in Figure 6.32.



*Figure 6.31 Detailed view of transversal cracking on the deck of bridge 27812.*



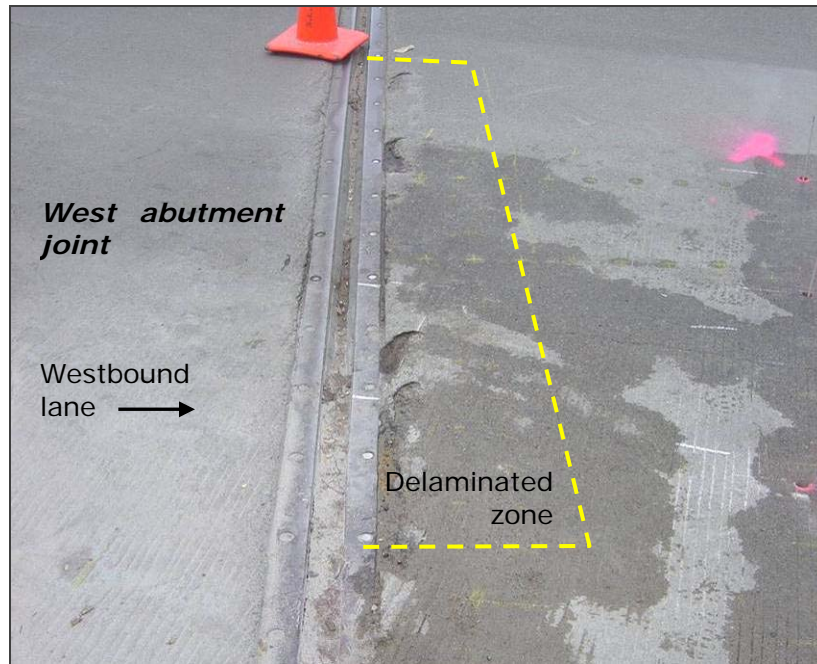
**Figure 6.32** Evidence of efflorescence and rust staining on the underside of the deck of bridge 27812.



**Figure 6.33** Layout of cracks, spalled and delaminated areas on bridge 27812.

#### 6.4.2 Chain-drag survey

This survey was conducted by Mn/DOT personnel and it was performed in only half the width of the right lane along the whole bridge length of the eastbound direction. In this bridge one delaminated area of 20 sq. ft. (2x10 ft) was detected, 0.3% of the inspected area. The delaminated area was located in the East side of the West abutment as shown in Figure 6.34.

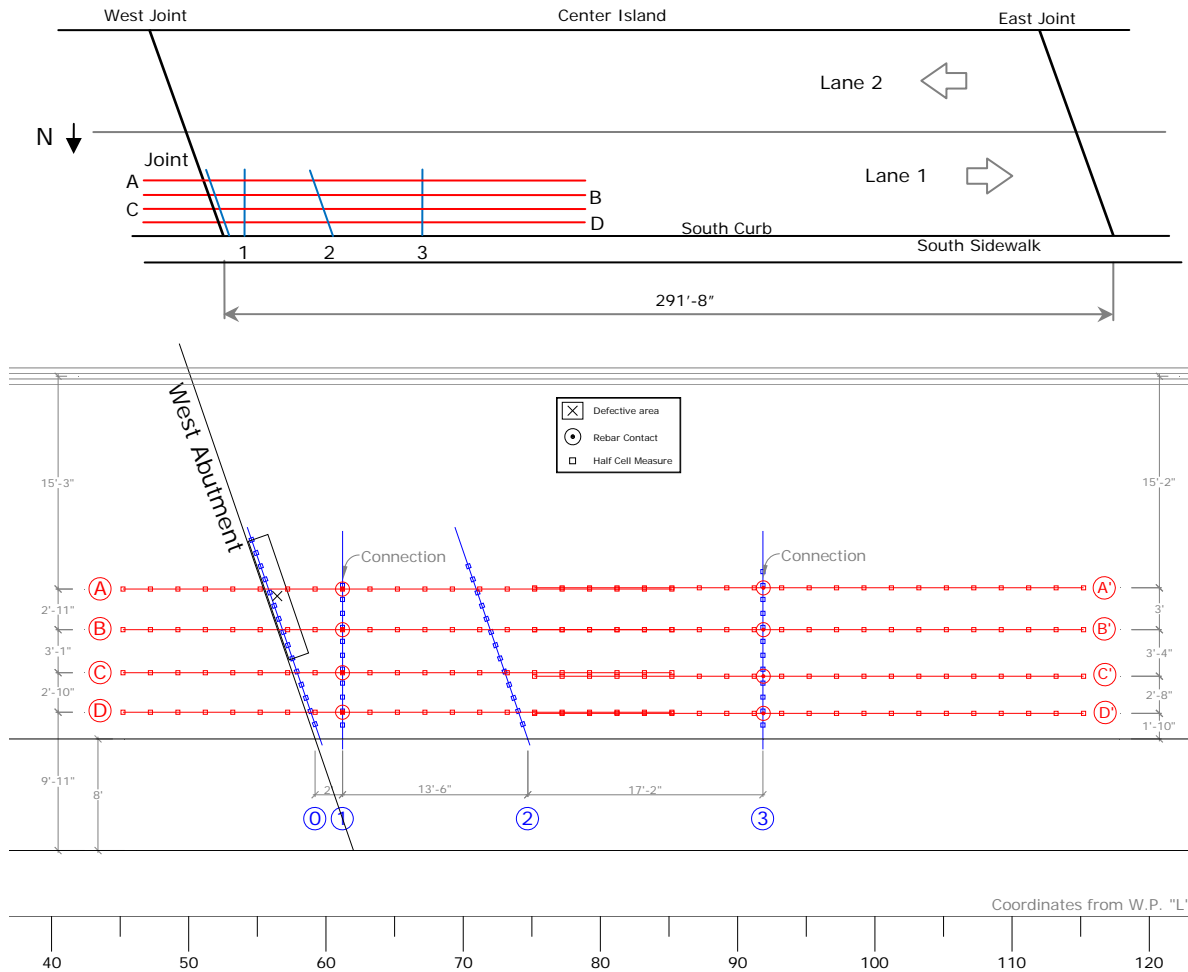


*Figure 6.34 Delaminated area detected in bridge 27812.*

### **6.4.3 Half-cell potential survey**

The half-cell potential survey was run along four equally spaced gridlines in the longitudinal direction and four gridlines in the transverse direction as shown in Figure 6.35. Two of the transverse lines were located to follow the west abutment joint and an existing crack (skew angle of  $70^{\circ}45'$ ). Two additional gridlines were chosen arbitrarily in areas of the deck that appeared to be corrosion free (with no delamination or crack free).

Due to traffic control restrictions, the gridlines were located in the south half of lane 1. Thus, the survey in the longitudinal direction could not be aligned with the wheel path of vehicles. Similarly, the survey in the transverse direction covered only half of lane width.



**Figure 6.35** Half-cell potential grid used in bridge 27812.

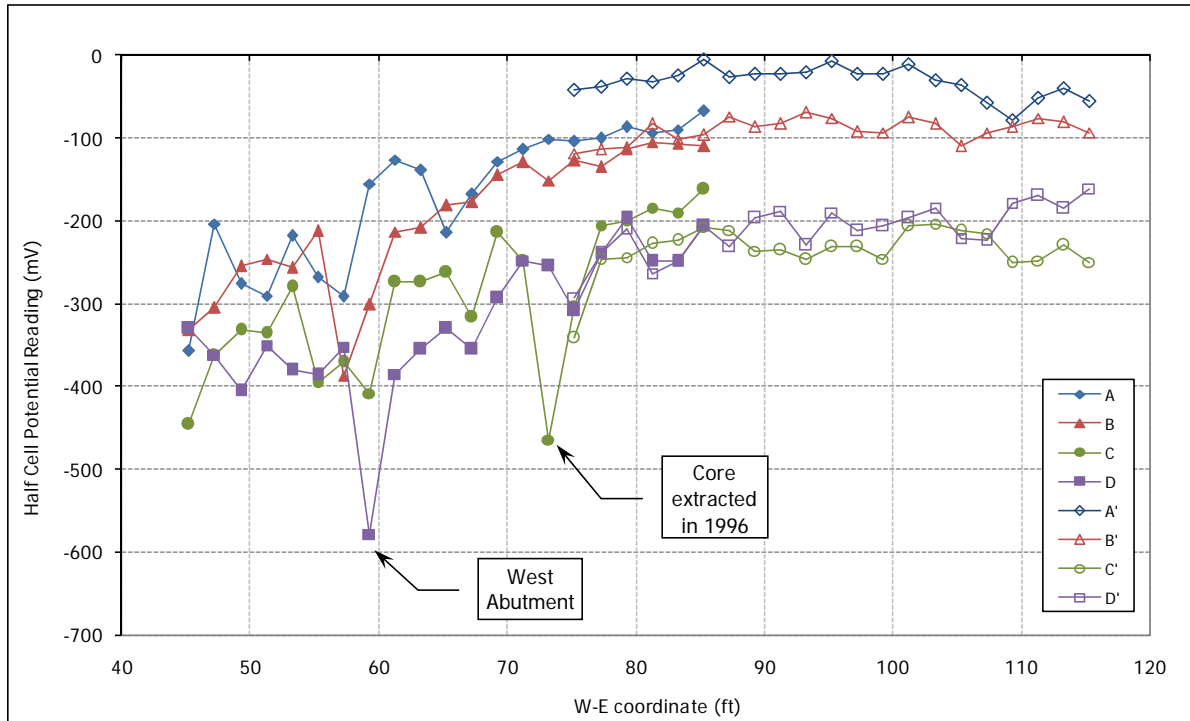
Figure 6.36 and Figure 6.37 show the half cell potential readings in the longitudinal and transverse directions, respectively. In the longitudinal direction, the data show potential readings that are above the value corresponding to a 90% probability of corrosion activity (-350mV) and are nearly constant along the gridline except at few locations. In general, it can be observed that the longitudinal readings are lower when they are close to the west abutment (left in Figure 6.36) and the potential increases gradually with the distance from abutment. These results suggest that corrosion activity is concentrated primarily near the joint abutment.

Survey lines D (closer to the south curb) and C presented the relative lower readings of almost -600mV and -500mV respectively; the lower reading in line D was from a reading taken on the west abutment and the lower reading in line C was from a reading taken right next to a core extracted in 1996 during WJE study [32].

Similar to bridge 27062, each longitudinal survey line (A, B, C and D) was connected to the upper mat in two connection points. To make a distinction of these two different set of readings,

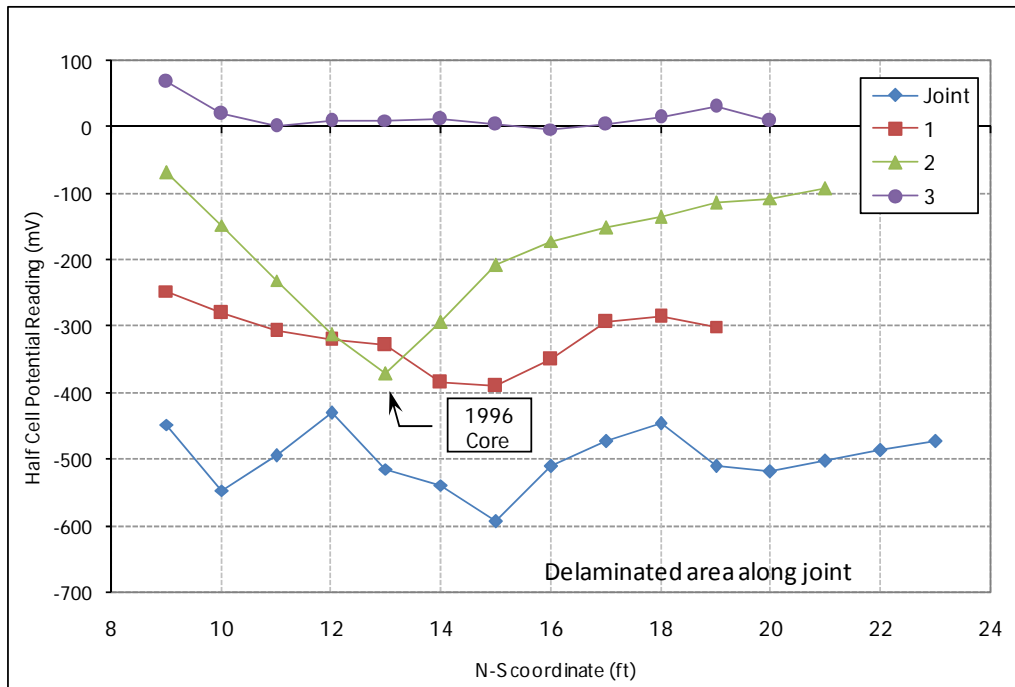


in Figure 6.36 the lines from the second set of readings were named A', B', C' and D' respectively.



**Figure 6.36** Half-cell potential readings along grid line A, B, C and D in bridge 27812.

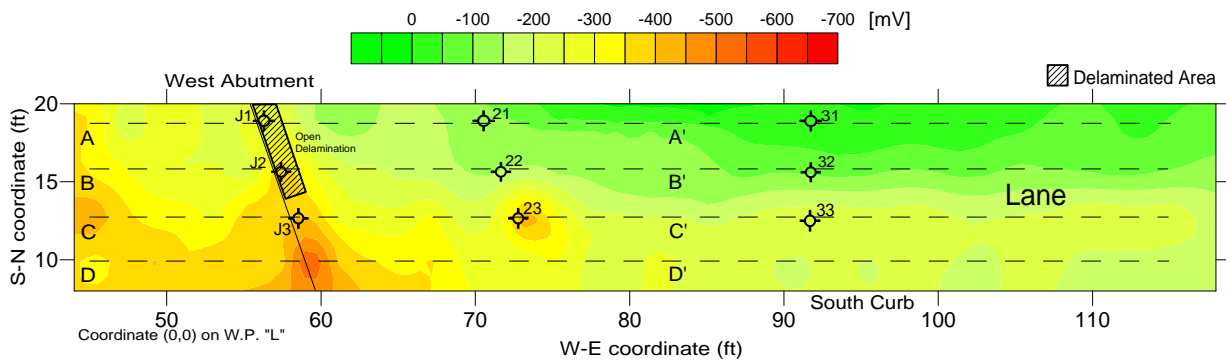
In the transverse direction, the readings along the joint gridline are all below -400mV, which suggest that corrosion activity is concentrated next to the west abutment joint where there is also a delaminated area. Line 3 showed particular higher readings, zero or positive potential, which may indicate a good electrical continuity in that section of the top mat. Survey line 2, which is located following a transverse crack, shows a relative low reading close to an old core sample extracted in 1996 during WJE study.



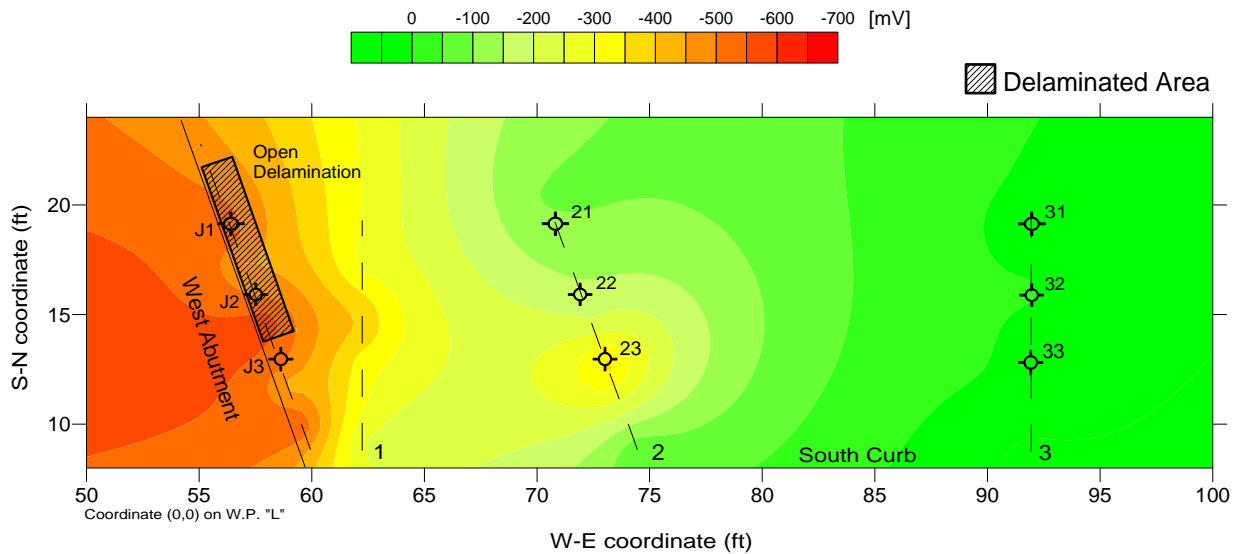
**Figure 6.37** Half-cell potential readings along grid lines Joint, 1, 2 and 3 in bridge 27812.

To have a global idea about how the HCP readings are distributed on the deck and to easily identify high and low readings on the deck, the half-cell potential results along the longitudinal and transversal gridlines are presented in the contour plots shown in Figure 6.38 and Figure 6.39. The delaminated areas identified by the chain drag survey are also displayed.

The figures show the good condition of the deck and the concentration of low HCP readings close to the west abutment. The extrapolation to the left of the west abutment joint in Figure 6.39 can not be considered as a prediction of the condition of the deck.



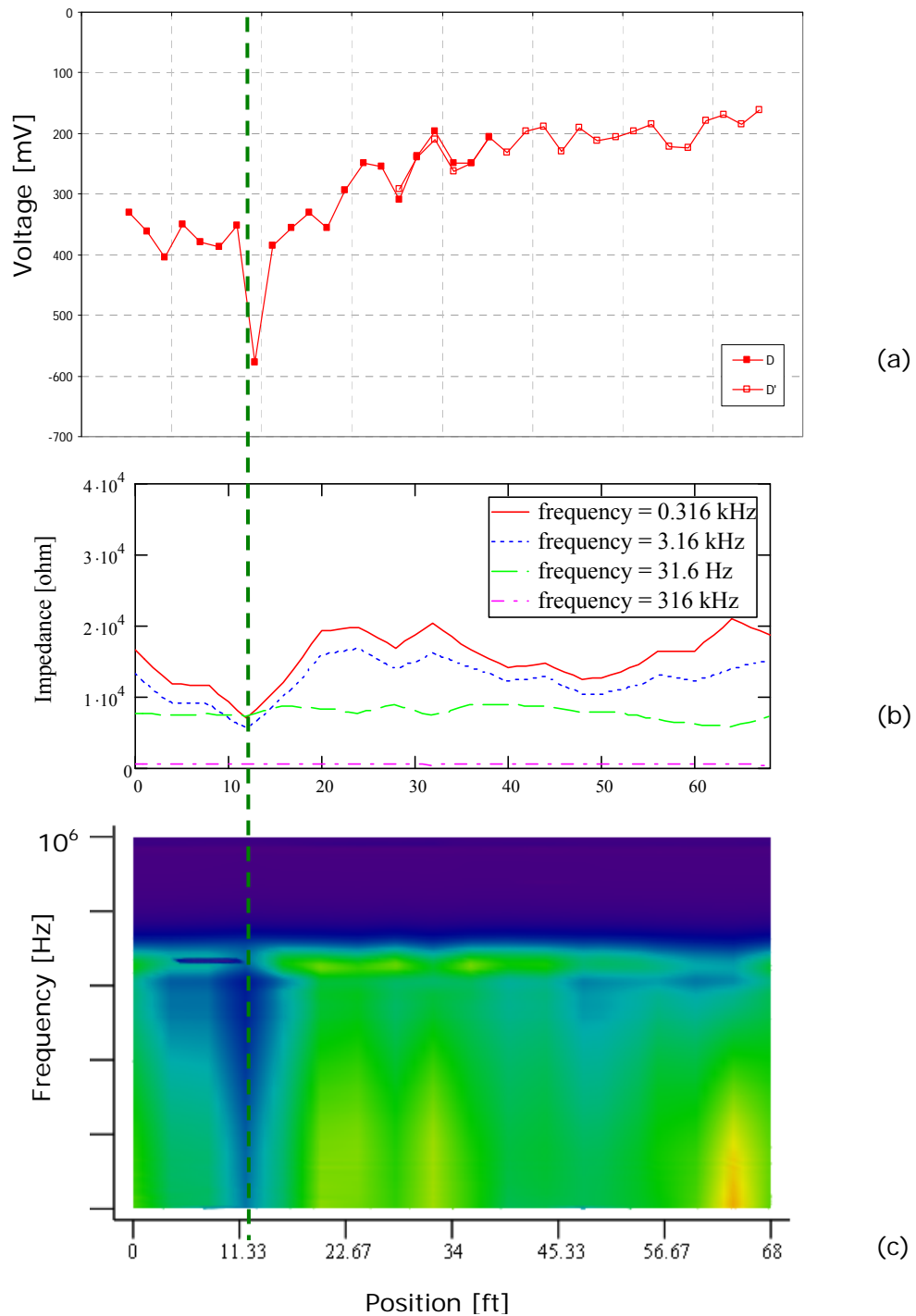
**Figure 6.38** Contour map of HCP readings in the longitudinal survey lines, bridge 27812.



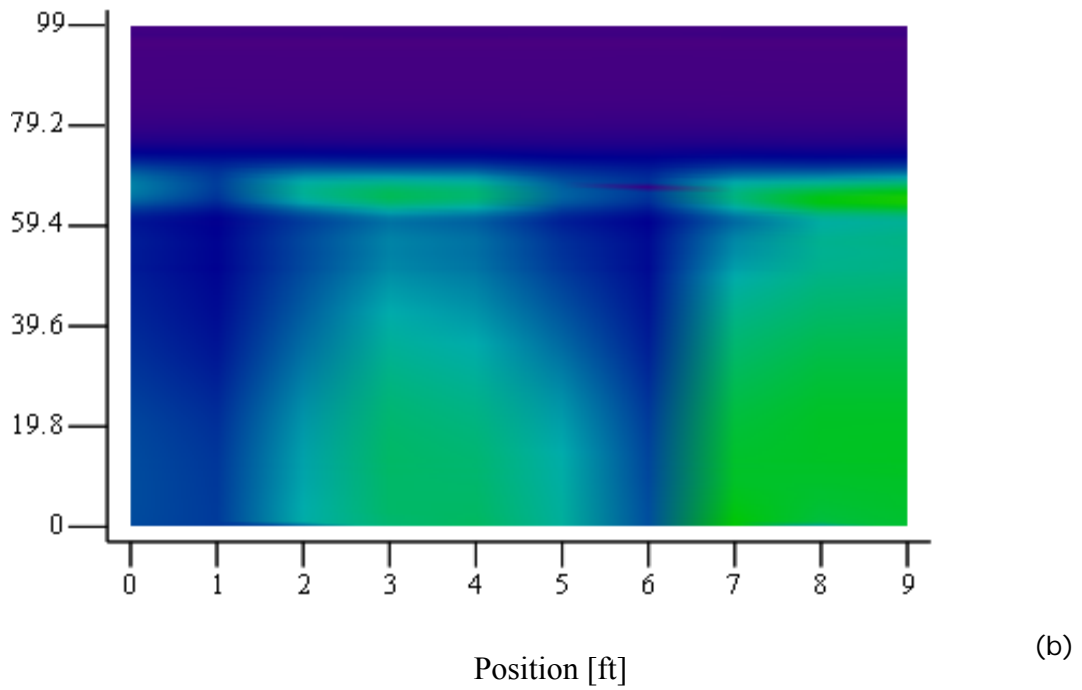
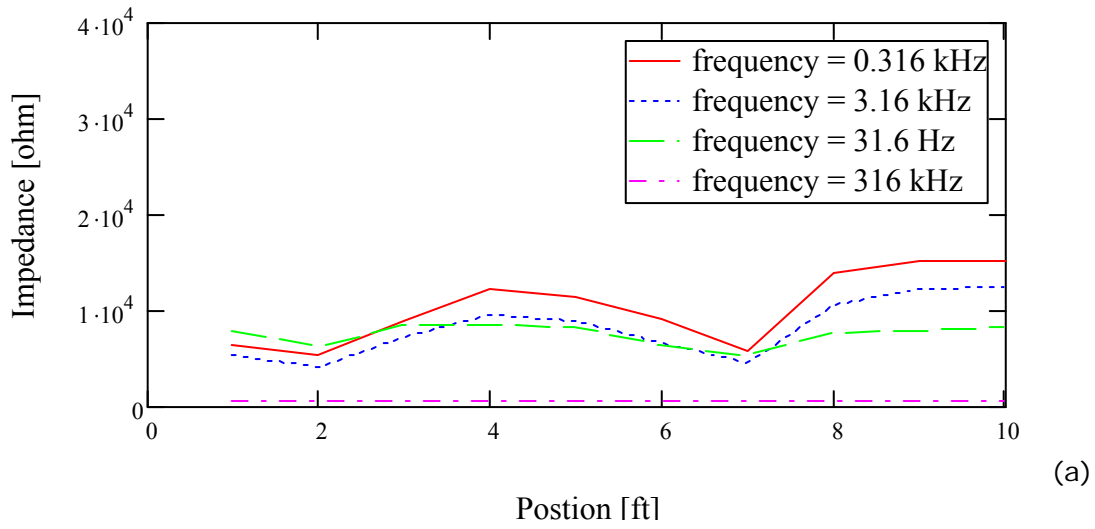
**Figure 6.39** Contour map of HCP readings in the transverse survey lines, bridge 27812.

#### 6.4.4 Electrochemical impedance spectroscopy

Impedance spectroscopy data were collected only along the half-cell potential longitudinal gridlines A-A', C-C' and D-D' and transversal gridlines "Joint", 1 and 2. The impedance spectroscopy results provide information about the quality of epoxy-coating of the rebars. That is, in areas with poor corrosion protection it is expected to have higher corrosion activity. For example, Figure 6.40 and Figure 6.41 show the correlation between corrosion activity and low impedance measurements. Areas with higher corrosion activity (low half potential measurements) coincide with a drop in electrical impedance measurements. Note that the impedance spectroscopy results on Figure 6.41 (Joint line) show low impedance at every single point. These results suggest that the epoxy coating has degraded, contributing to the corrosion activity found with the half cell potential measurements (see Figure 6.38 and Figure 6.39).



**Figure 6.40** Electrical impedance spectroscopy versus half-cell potential measurement along line D-D' in Bridge 27812. (a) half-cell potential measurements, (b) four-frequency impedance measurement, and (c) contour plots of impedance magnitude versus frequency and positions along the survey line.

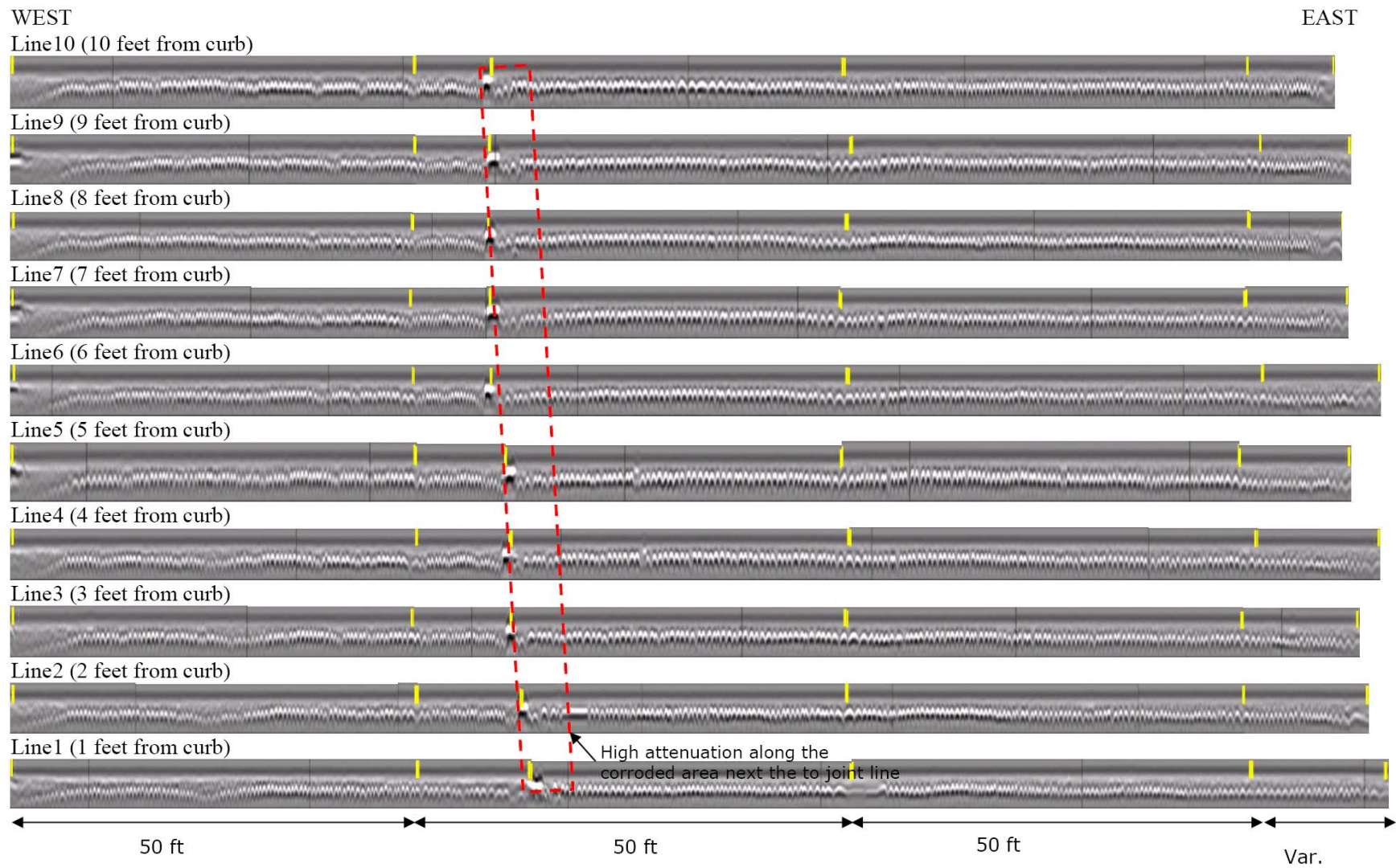


**Figure 6.41** Electrical impedance spectroscopy versus half-cell potential measurement along line Joint line in Bridge 27812. (a) four-frequency impedance measurement and (b) contour plots of impedance magnitude versus frequency and positions along the survey line.

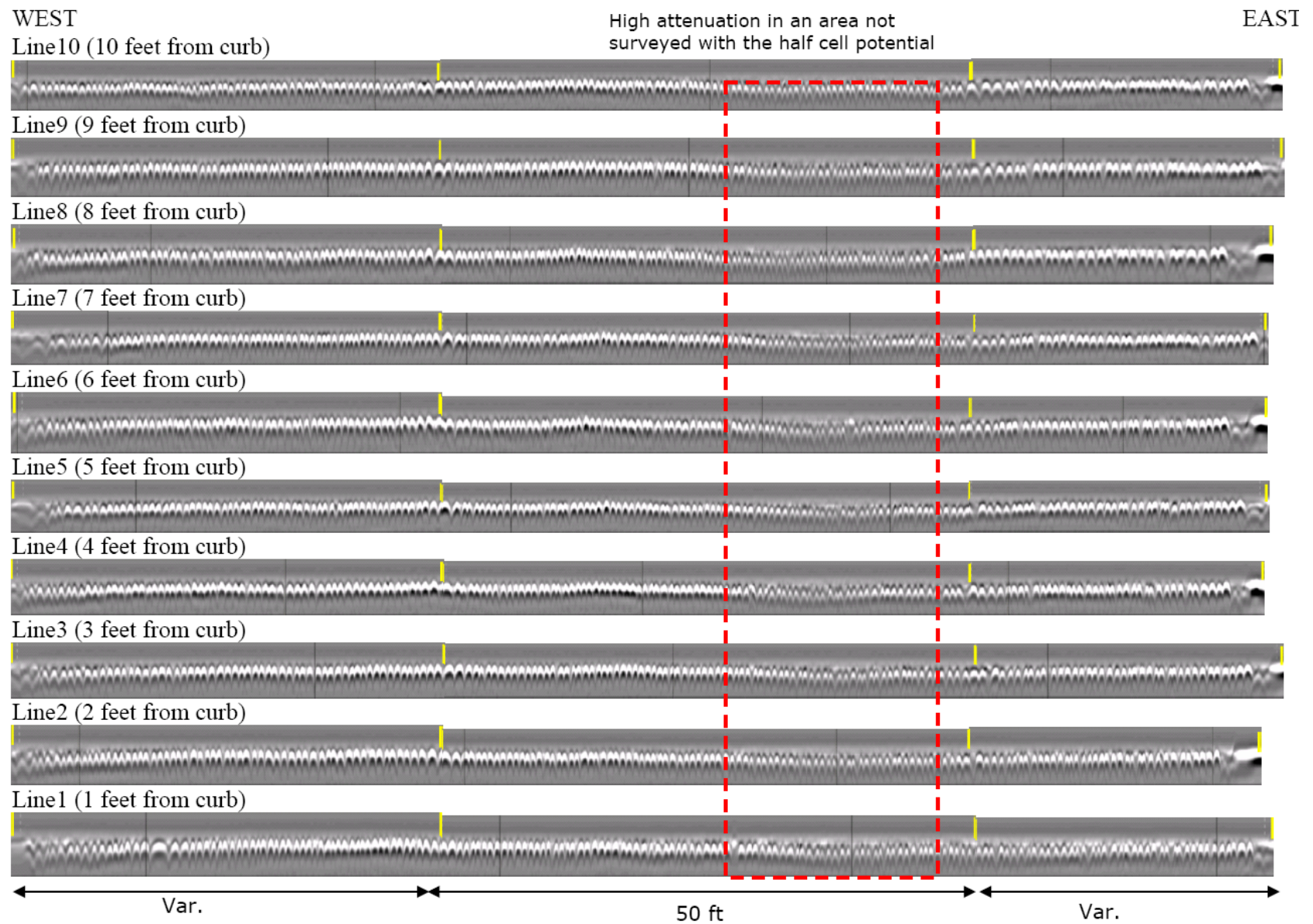
#### **6.4.5 *Ground penetrating radar measurements***

Mn/DOT personnel ran a ground penetrating radar (GPR) survey in the eastbound direction of the Bridge 27812. Ten equally spaced longitudinal survey lines were collected.

Figure 6.42 presents the collected survey lines. The time analysis of these hyperbolas in the survey permits the evaluation of electromagnetic (ELM) wave velocity and volumetric water content distribution in the concrete (Figure 6.43) and the depth of each steel rebar (Figure 6.44). The mapping of ELM wave velocity provides an indication of the volumetric water content and salt content in the concrete. The evaluation of the ELM wave velocity also helps in the evaluation of deteriorated areas in the bridge deck. The results are compared against the mapping of cracks, patches and delaminated areas as these zones will tend to have concrete with greater water content. For example Figure 6.43 shows the area next to the joint (cores “J1”, “J2”, and “J3”) shows the highest water content. These data correlates well with the high corrosion activity documented with the half-cell potential measurements (Figure 6.38 and Figure 6.39) and the low coating quality as detected by the half-cell potential measurements (Figure 6.41)

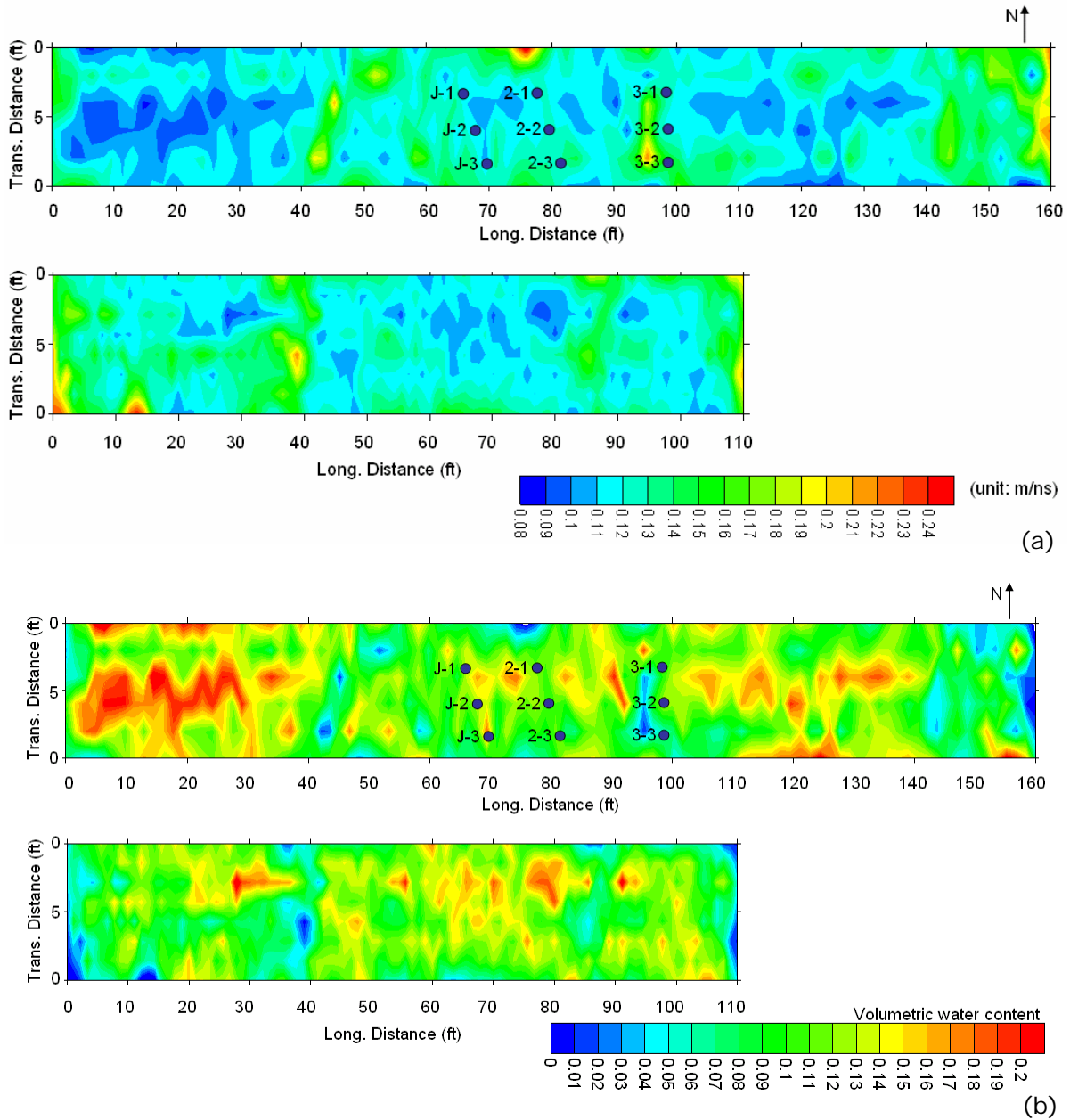


*Figure 6.42 GPR survey lines in east-most part of the eastbound direction of bridge 27812.*

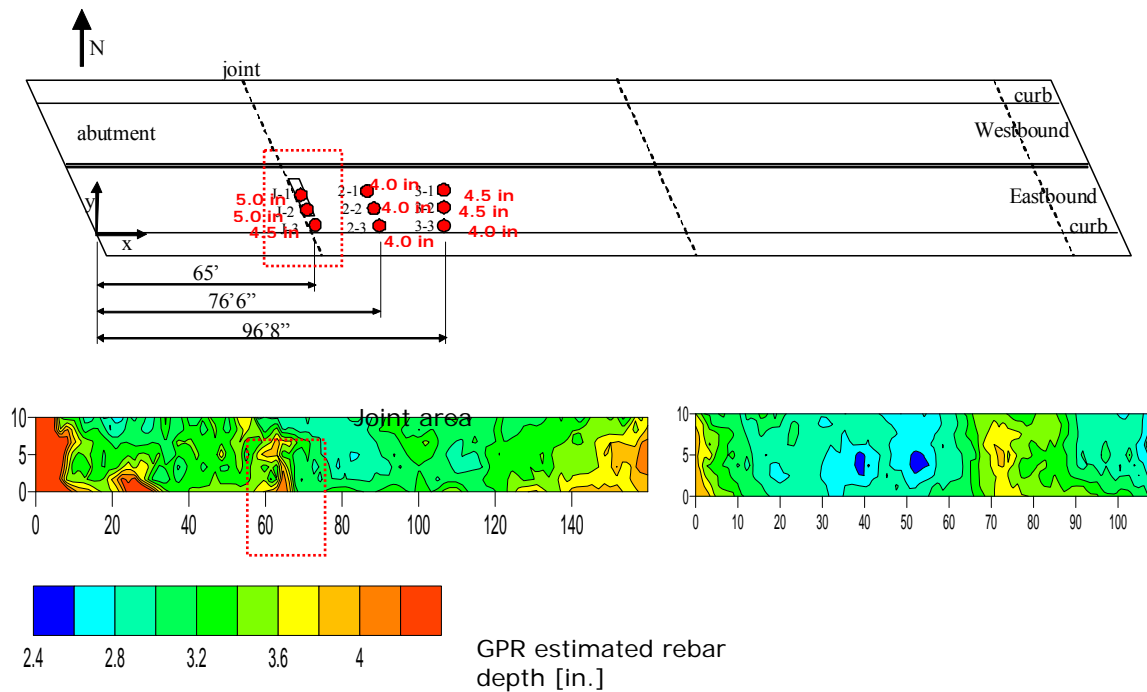


*Figure 6.42 (continuation)*





**Figure 6.43** Distribution of (a) electromagnetic wave velocity and (b) calculated volumetric water content.



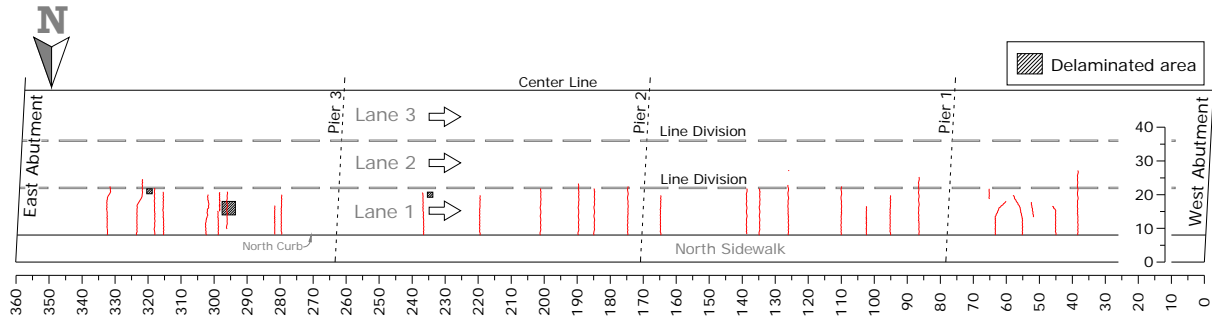
**Figure 6.44** Distribution of rebar depths in Bridge 27812 as estimated from GPR measurements. For comparison, the rebar depths obtained from extracted cores are presented in the top figure.

## 6.5 BRIDGE 27815

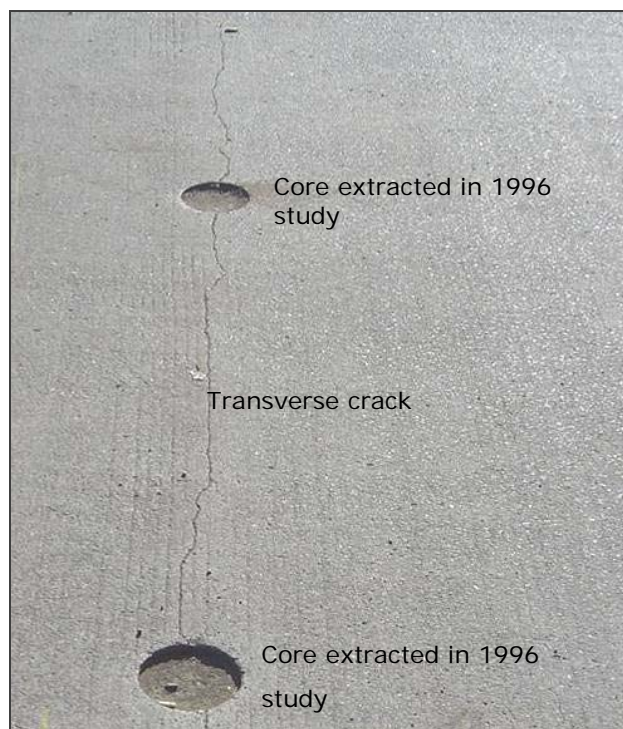
The deck of this bridge had few delaminated areas and extensive transverse cracks were detected in the right lane. Corrosion activity in this bridge appears to be concentrated in transverse cracks.

### 6.5.1 Visual inspection

Visual inspection was performed only in the right lane (lane 1). This deck showed mostly transverse cracking (see Figure 6.45). The total crack length in the area inspected was 373 ft, corresponding to a frequency of 0.073 ft/ft<sup>2</sup>. Although the predominant crack width was 0.039 in. (1.0 mm), crack widths ranged from 0.008 in. (0.2 mm) in small cracks close to the north curb, to 0.080 in. (2.0 mm) in a transverse crack where core samples were extracted in the previous study (see Figure 6.46). Signs of efflorescence were observed on the underside of the deck along with several transverse cracks as shown in Figure 6.46. There was also evidence of rebar corrosion of the bottom mat in many sections of the deck, as indicated by light rust staining on the underside of the bridge as shown in Figure 6.47. This figure shows that despite the visual inspection was conducted only in the right lane, the cracks observed on the underside of the bridge are presented in the three lanes of the westbound.



**Figure 6.45** Crack layout, spalled and/or delaminated areas on bridge 27815.



**Figure 6.46** Transverse crack in bridge 27815.



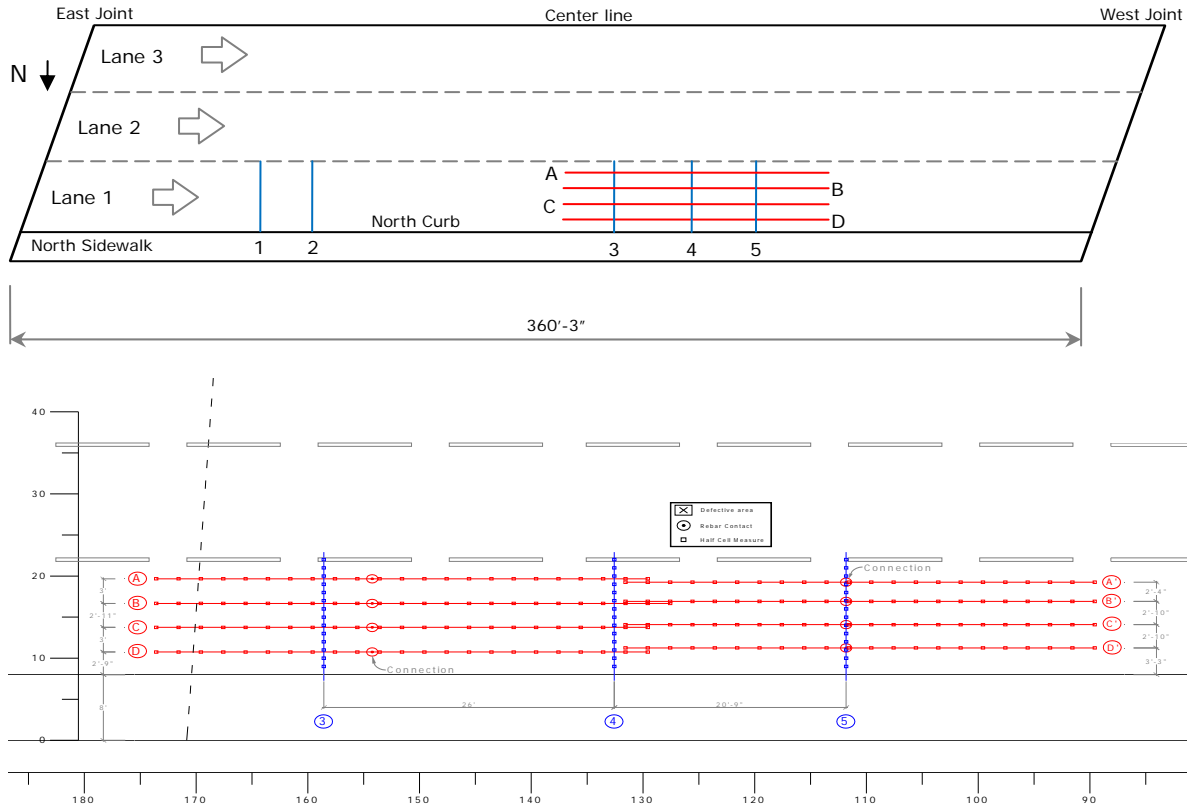
**Figure 6.47** Evidence of efflorescence and rust staining on the underside of the deck of bridge 27815.

### **6.5.2 Chain-drag survey**

This survey was conducted by Mn/DOT personnel and it was performed in the right lane along the whole bridge length of the westbound direction. In this bridge, four delaminated areas were identified by the chain drag survey, totaling 21 sq. ft. (0.4% of the inspected area).

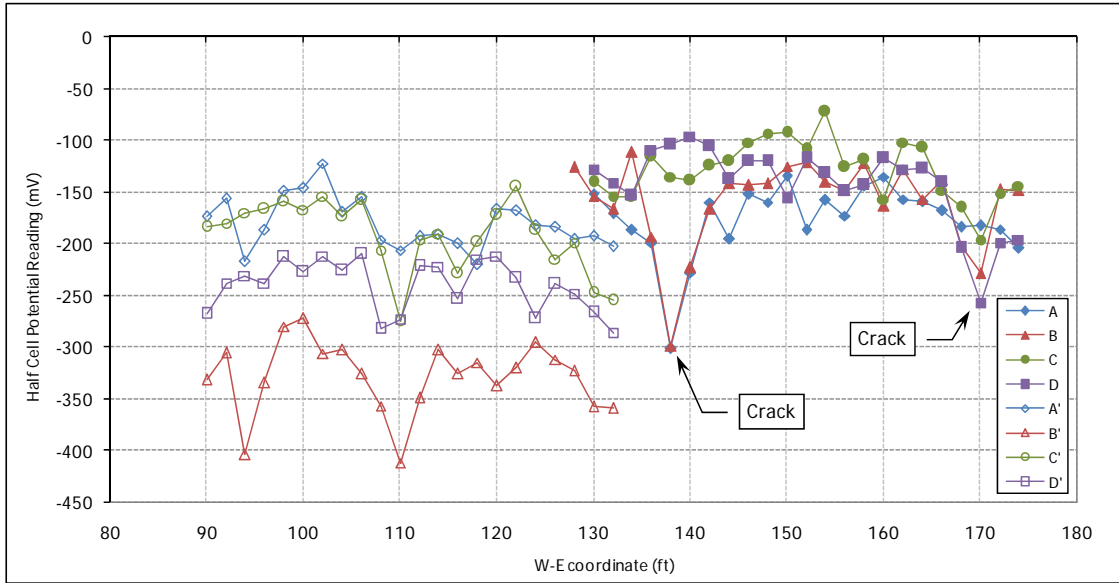
### **6.5.3 Half-cell potential survey**

The half-cell potential survey was run along four equally spaced gridlines in the longitudinal direction and five gridlines in the transverse direction as shown in Figure 6.48. The grid lines in the transverse direction were chosen to measure the corrosion activity in two separate areas of the deck. Gridlines A, B, C and D were chosen to be equidistant and nearly coincident with their similar gridlines A', B', C' and D', respectively. The readings were obtained, however, by independent electrical connections to the bars at two different points along the gridline.

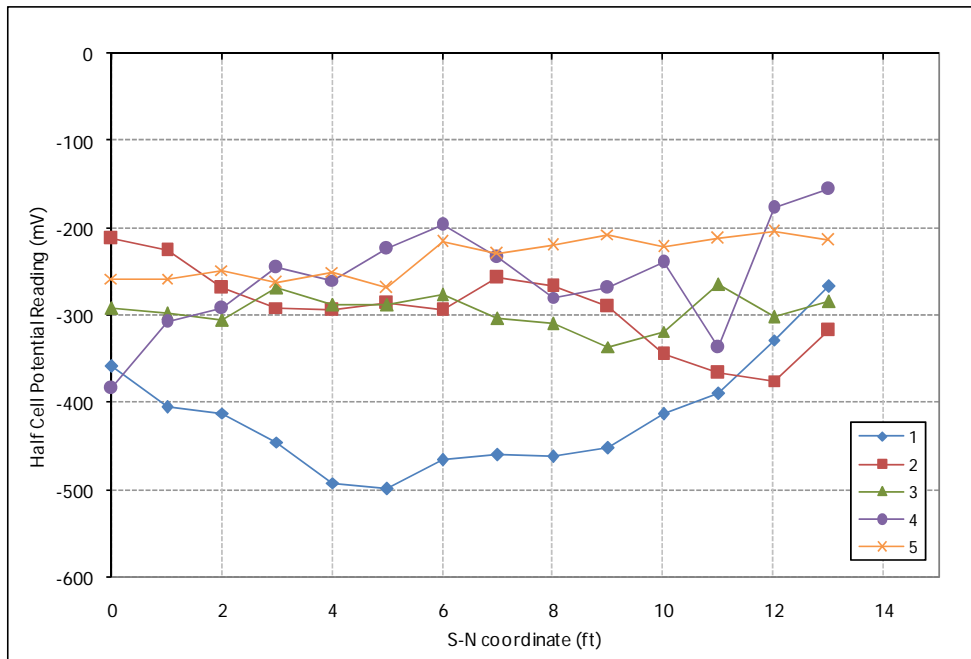


**Figure 6.48** Half-cell potential grid used in bridge 27815.

Figure 6.49 and Figure 6.50 show the half-cell potential readings in the longitudinal and transverse directions, respectively. The data show that the potentials are generally above the threshold value of -350 mV (corresponding to a 90% probability of corrosion activity in the bars), except along gridline B' in the longitudinal direction and along gridline 1 in the transverse direction. The data along gridline 1 were obtained next to a transverse crack and over an area reported to be delaminated by the chain drag survey. Overall, the half-cell potential measurements obtained in this bridge are less negative than the measurements from the other three bridges, which suggest low or no corrosion activity in the area surveyed.

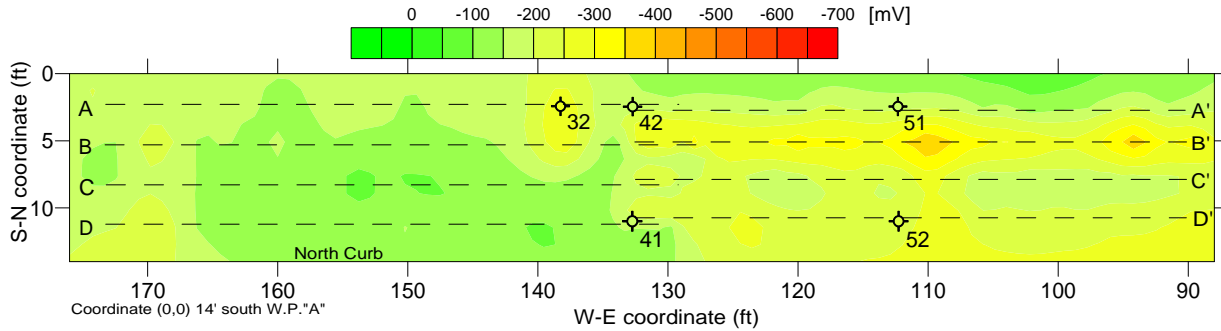


**Figure 6.49** Half-cell potential readings along grid line A, B, C and D in bridge 27815.

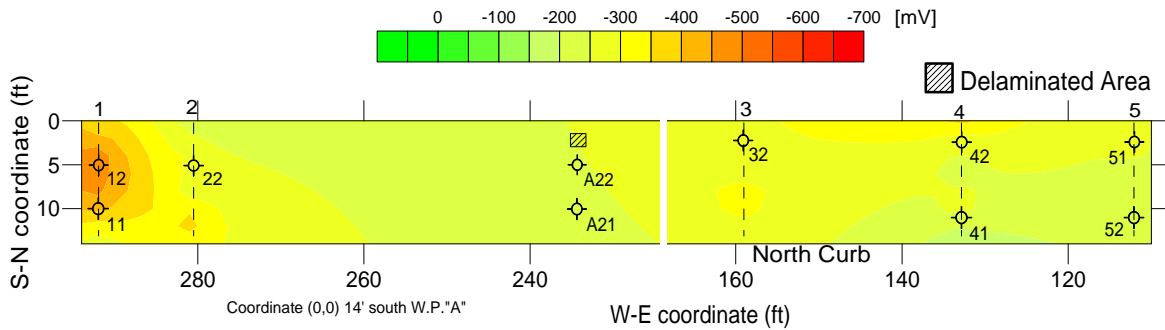


**Figure 6.50** Half-cell potential readings along grid line 1 to 5 in bridge 27815.

To have a global idea about how the HCP readings are distributed on the deck and to easily identify high and low readings on the deck, the half-cell potential results along the longitudinal and transversal gridlines are presented in the contour plots shown in Figures 6.51 and 6.52. The delaminated areas identified by the chain drag survey are also displayed. In this case, because the origin was located in the West abutment, the traffic runs from right to left in the figure. In Figure 6.52, due to the significant distance between transverse survey lines, which is more than 120 ft between line 3 and line 2, a split contour map is presented.



**Figure 6.50** Contour map of HCP readings in the longitudinal survey lines, bridge 27815.

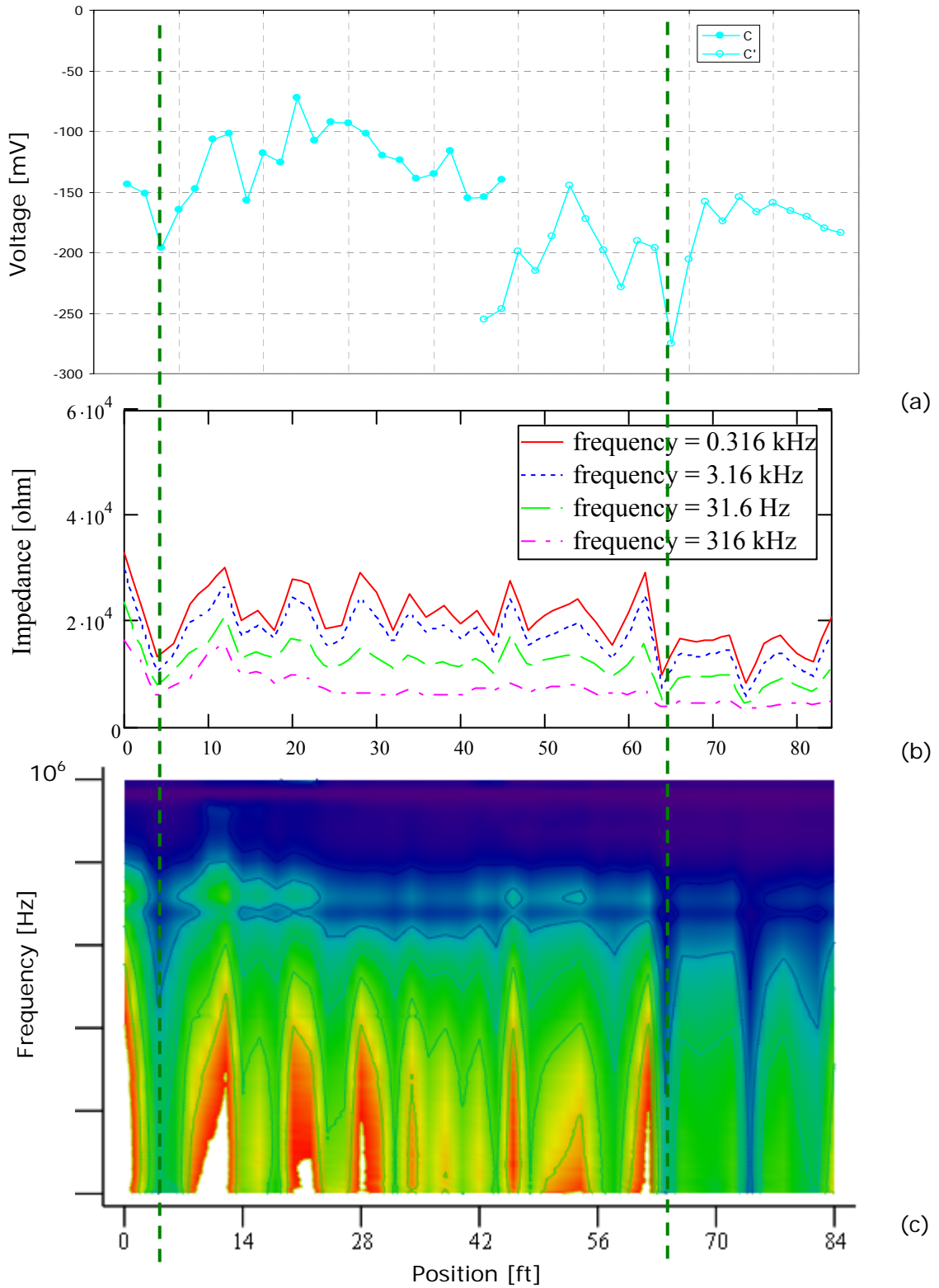


**Figure 6.51** Contour map of HCP readings in the transverse survey lines, bridge 27815.

As shown in the figures, only few areas indicate corrosion activity (potentials of -350mV or higher). The interpolation cannot be considered as a prediction of the deck condition in most of the area studied.

#### 6.5.4 Electrochemical impedance spectroscopy

Impedance spectroscopy data were collected only along the half-cell potential longitudinal gridlines C-C' and D-D' and transversal gridlines 3 and 4. The impedance spectroscopy results provide information about the quality of epoxy-coating of the rebars. That is, in areas with poor corrosion protection it is expected to have higher corrosion activity. For example, Figure 6.53 shows this correlation between corrosion activity and low impedance measurements. Areas with higher corrosion activity (very negative half cell potential measurements) coincide with a drop in electrical impedance measurements.

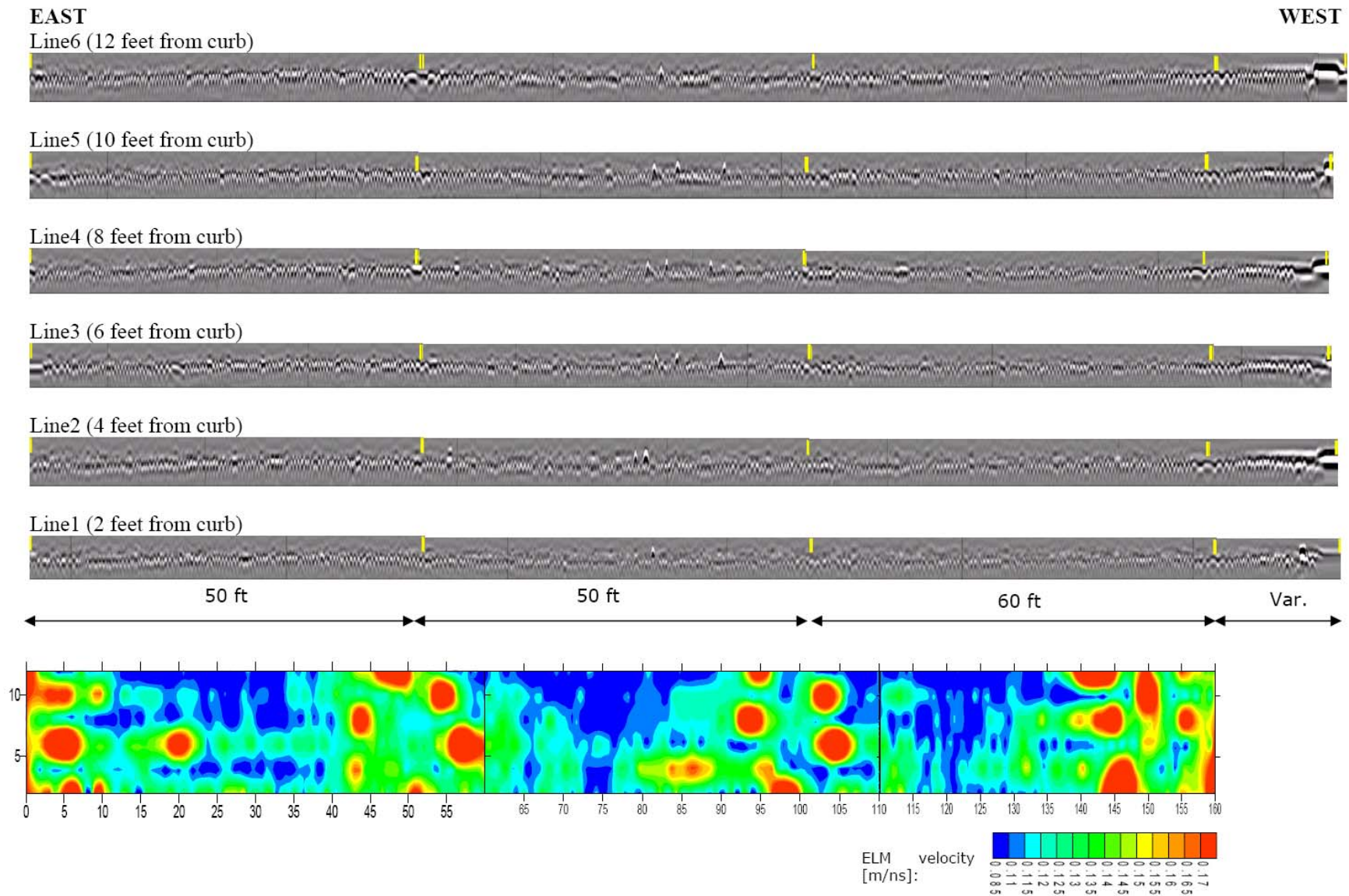


**Figure 6.53** Electrical impedance spectroscopy versus half-cell potential measurement along line C-C'. Bridge 27815: (a) half-cell potential measurements, (b) four-frequency impedance measurement, and (c) contour plots of impedance magnitude versus frequency and positions along the survey line.

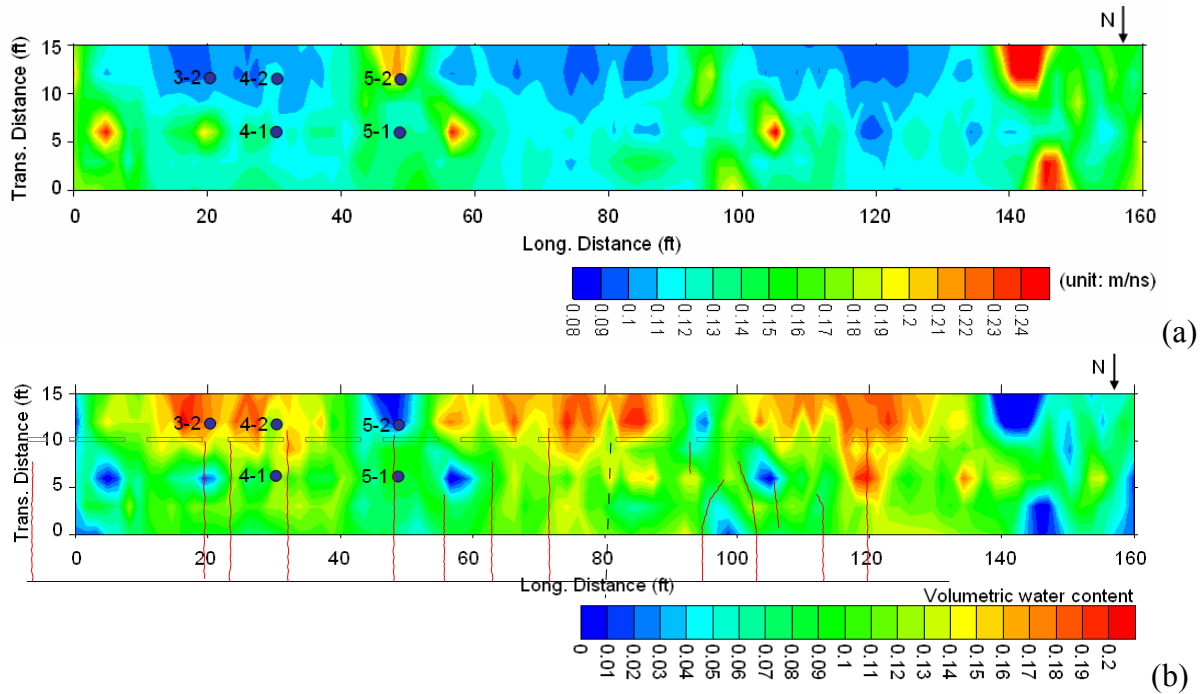


### **6.5.5 *Ground penetrating radar***

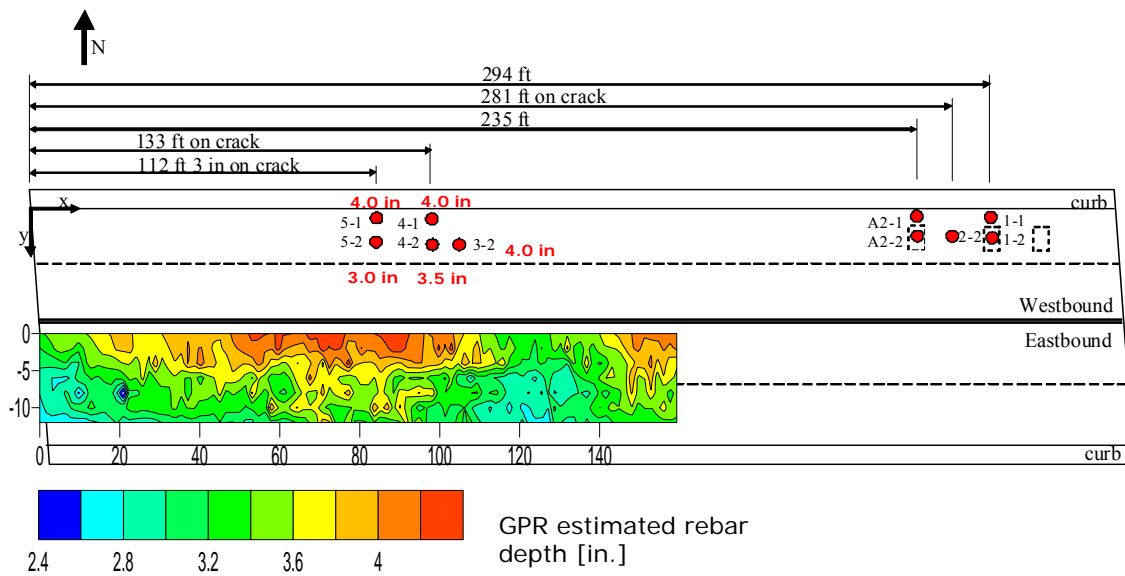
Mn/DOT personnel ran a ground penetrating radar (GPR) survey along the west section of the westbound direction of the Bridge 27815. Six equally spaced longitudinal survey lines were collected. Figure 6.54 presents the collected survey lines. The time analysis of these hyperbolas permit the evaluation of electromagnetic (ELM) wave velocity and volumetric water content in the concrete (Figure 6.55) and the depth of each steel rebar. The mapping of ELM wave velocity provides an indication of the volumetric water content and salt content in the concrete. The results are compared against the mapping of cracks, patches and delaminated areas as these zones will tend to have concrete with greater water content.



*Figure 6.54 GPR survey lines in bridge 27815 and interpretation of the distribution of electromagnetic wave velocity.*



**Figure 6.55** Distribution of (a) electromagnetic wave velocity and (b) volumetric water content (overlapped with crack mapping) on Bridge 27815 as determined by the GPR survey.



**Figure 6.56** Distribution of rebar depths in Bridge 27815 as estimated from GPR measurements. For comparison, the rebar depths obtained from extracted cores are presented in the top figure.

## 6.6 CORE SELECTION

Upon evaluation of the data in the field, the locations for at least 7 cores to be extracted by Mn/DOT personnel at later date (per bridge) were identified as described in section 4.4. Core samples were selected close to delaminated areas, joints, spalls, cracks and healthy areas of the deck.

Table 6.1 shows a summary of all cores extracted. The x and y coordinates refer to the local coordinate axis as defined in Figure 6.3, Figure 6.19, Figure 6.35 and Figure 6.48, for bridges 19015, 27062, 27812 and 27815 respectively. In the table, cores extracted where the half-cell potential readings show a minimum are indicated as “Minimum HCP”.

A detailed description of each core, including pictures, map of locations, number of bars, cover depth, presence of cracks and other important information, is presented in Appendix A: Detailed Core Description.

Although only 6 field cores from bridge 27815 were drilled through visual surface cracks over an ECR bar, subsequent laboratory assessment of all the cores demonstrated that one core from bridge 19015 also contained a vertical crack. Crack widths of the cores ranged from 0.008 to 0.039 in. (0.2 to 1.0 mm). Crack depths in core samples from bridge 27815 were all penetrating to at least the depth of the reinforcing steel; crack in core sample from 19015 was only 2 in. depth, 2 in. above rebar face.

Some of the cores were intentionally taken at locations representing a worst case. Therefore, these cores may not be representative or indicative of the overall performance of the deck nor the performance that can be obtained from ECR.

*Table 6.1 Summary of coordinates by core selected*

| <b>Bridge No.</b> | <b>Designation</b> | <b>Location</b>               | <b>X</b> | <b>Y</b> |
|-------------------|--------------------|-------------------------------|----------|----------|
| 19015             | A2                 |                               | 30'-1"   | 19'-6"   |
|                   | AP                 | Joint                         | 46'-5"   | 19'-6"   |
|                   | C2                 |                               | 30'-0"   | 15'-0"   |
|                   | CP                 | Joint, Spall                  | 44'-9"   | 15'-0"   |
|                   | D2                 |                               | 30'-6"   | 9'-0"    |
|                   | DP                 | Joint                         | 42'-9"   | 9'-0"    |
|                   | DCS1               |                               | 50'-11"  | 9'-0"    |
|                   | DCS2               | Delaminated area              | 91'-8"   | 9'-0"    |
| 27062             | A1                 |                               | 138'-9"  | 18'-4"   |
|                   | A2                 | Minimum HCP                   | 205'-0"  | 18'-7"   |
|                   | B1                 | Minimum HCP                   | 146'-9"  | 15'-0"   |
|                   | C1                 | Minimum HCP, Delaminated area | 152'-9"  | 11'-9"   |
|                   | D1                 | Minimum HCP, Delaminated area | 152'-9"  | 6'-4"    |
|                   | D2                 | Minimum HCP, Delaminated area | 191'-0"  | 6'-9"    |
|                   | D3                 | Minimum HCP, Delaminated area | 213'-0"  | 6'-9"    |
| 27812             | 21                 | Crack                         | 76'-6"   | 10'-9"   |
|                   | 22                 | Crack                         | 76'-6"   | 7'-10"   |
|                   | 23                 | Crack                         | 76'-6"   | 4'-9"    |
|                   | 31                 |                               | 96'-8"   | 10'-10"  |
|                   | 32                 |                               | 96'-8"   | 7'-10"   |
|                   | 33                 |                               | 96'-8"   | 4'-6"    |
|                   | J1                 | Joint, Minimum HCP            | 65'-0"   | 10'-9"   |
|                   | J2                 | Joint                         | 65'-0"   | 7'-10"   |
|                   | J3                 | Joint                         | 65'-0"   | 4'-9"    |
| 27815             | 11                 | Crack, Delaminated area       | 294'-0"  | 4'-0"    |
|                   | 12                 | Crack, Delaminated area       | 294'-0"  | 9'-0"    |
|                   | 22                 | Crack                         | 281'-0"  | 9'-0"    |
|                   | 32                 |                               | 138'-0"  | 11'-8"   |
|                   | 41                 | Crack                         | 133'-0"  | 3'-0"    |
|                   | 42                 | Crack                         | 133'-0"  | 11'-8"   |
|                   | 51                 | Crack                         | 112'-3"  | 3'-0"    |
|                   | 52                 | Crack                         | 112'-3"  | 11'-8"   |
|                   | A21                |                               | 235'-0"  | 4'-0"    |
|                   | A22                |                               | 235'-0"  | 9'-0"    |

## 6.7 REBAR COVER DEPTH

From half-cell potential connections and concrete core samples, a total of 84 cover depths measurements were made at various locations in the four bridge decks. Table 6.2 shows the average depth of concrete cover of the bars in the longitudinal and transverse direction of the top mat.

*Table 6.2 Average measured bar cover depth*

| <b>Bridge No.</b> | <b>Bar Direction</b> | <b>Average Depth (in)</b> | <b>Low Slump Overlay</b> |
|-------------------|----------------------|---------------------------|--------------------------|
| 19015             | Longitudinal         | 3.1                       | No                       |
|                   | Transverse           | 3.2                       |                          |
| 27062             | Longitudinal         | 4.0                       | No                       |
|                   | Transverse           | 3.5                       |                          |
| 27812             | Longitudinal         | 4.4                       | Yes                      |
|                   | Transverse           | 4.0                       |                          |
| 27815             | Longitudinal         | 4.9                       | Yes                      |
|                   | Transverse           | 4.2                       |                          |

As shown in the table, the bridges with an overlay (bridges 27812 and 27815) show a higher average depth of cover. On the other hand, bars in bridge 19015 (which is the oldest bridge surveyed here) had the smallest cover depth, which is in accordance with the design practice at the time of construction of this bridge. This situation was especially evident close to the joint where the depth of cover was between 2.0 and 2.5 in. The joint also had the most deterioration.

## 6.8 SUMMARY OF FIELD RESULTS

### 6.8.1 Cracks, spalls and patches

Fine hairline cracks were detected on the top surface of all four decks. In the areas inspected, transverse cracks were predominant over longitudinal ones, the only exceptions was bridge 19015 where the longitudinal cracks were predominant. The bridges presented few cracks in terms of length per area, with a total average crack frequency of 0.08 ft/ft<sup>2</sup> considering all four bridges. Crack widths of decks were in general rated between 0.02 in. (0.5 mm) and 0.04 in. (1.0 mm), only few cracks presented widths of 0.08 in. (2.0 mm) or larger.

It was observed that the cracks and spalls were located, in general, close or next to joints or abutments. Table 6.3 shows the deck and inspected areas with the calculated crack density (total crack length divided by area inspected).

**Table 6.3 Crack density**

| <b>Bridge</b> | <b>Deck Area<br/>(ft<sup>2</sup>)</b> | <b>Area<br/>Inspected<br/>(ft<sup>2</sup>)</b> | <b>Crack Density<br/>(ft/ft<sup>2</sup>)</b> |
|---------------|---------------------------------------|--|--|
| 19015         | 6,622                                 | 3,550  | 0.06   |
| 27062         | 28,488                                | 7,375  | 0.13   |
| 27812         | 15,167                                | 6,925  | 0.04   |
| 27815         | 31,222                                | 5,114  | 0.07   |
| Total         | 81,498                                | 22,964   |  |

The table shows less crack density on bridges 19015 and 27812, coincidentally, these bridges decks are supported on concrete girders. These results show that the bridge decks are in general in good condition, and the results are below the typical crack densities for decks of similar ages, which average values between 0.12 and 0.15 ft/ft<sup>2</sup> (0.40 and 0.50 m/m<sup>2</sup> respectively) [21].

### 6.8.2 Chain-drag survey

The suspect areas in each bridge were, in general, small rectangles (typically 2 x 2 ft). This could mean that delamination is at an early stage caused by localized corrosion at the bar level. When delaminated areas were located close to cracks or joints, the size of the area detected was greater.

Table 6.4 shows the areas of delamination, open spalls, and good patches and the total delaminated area (including open spalls and patches) as a percentage of the inspected area.

**Table 6.4 Delaminated areas identified by chain-drag**

| <b>Bridge<br/>No.</b> | <b>Delamination<br/>(ft<sup>2</sup>)</b> | <b>Open Spall<br/>(ft<sup>2</sup>)</b> | <b>Good<br/>Patches<br/>(ft<sup>2</sup>)</b> | <b>Percent<br/>(%)</b> |
|-----------------------|--|--|--|------------------------|
| 19015                 | 36                                       | 3                                      | 0  | 1.1%                   |
| 27062                 | 14                                       | 0                                      | 70   | 1.1%                   |
| 27812                 | 20                                       | 0                                      | 0  | 0.3%                   |
| 27815                 | 21                                       | 0                                      | 0  | 0.4%                   |

The data show that the delaminated area in all bridges after 30 years of service was very low. It should be noted that the amount of delamination was even lower in both bridge decks with low slump, high density overlays (bridges 27812 and 27815).

It was expected that delaminated areas would be concentrated close to cracks, joints or on the shoulder. This is because cracks and joints allow an easy ingress of chloride ions to the rebars, and shoulders accumulate more deicing salt on the surface than traffic lanes, increasing the chloride ion ingress through the concrete. However, the delaminated areas observed varied in

location, with no identifiable trend. It should be noted that no delaminated areas were detected during the survey in 1996 [32], except for 2 sq. ft. in bridge 27062.

### **6.8.3 *Half-cell potential readings***

In general, lower voltage readings (i.e., higher corrosion activity) seem to coincide well with the presence of cracks, joints, patches and delaminated areas. As shown in previous figures showing half-cell readings, the down peaks are located accurately in joints, cracks or delaminated areas. Also, HCP surveys conducted in shoulders showed a relative lower reading, indicating greater probability of corrosion. However, a weak side of the HCP survey is that does not give indication of the rate of corrosion, nor of how long the steel has been corroding.

In a study conducted by WJE in Illinois in 2003 [21], the HCP readings in bridge decks containing ECRs in both mats did not show electrical continuity, and thus HCP measurements were abandoned. However, in the present study, due to the use of several connections points to the top mat, HCP showed effectiveness identifying corrosion activity when the deck has ECRs in both mats or only at the top.

The survey provided good information in terms of corrosion detection; this should be an incentive to use this test covering an entire lane, or if it is possible, the entire deck.

### **6.8.4 *Electrochemical impedance spectroscopy***

A limited electrochemical impedance spectroscopy survey was collected in all four bridges. The coverage was limited by the time needed to take and save each set of measurements. For this reason a complete comparison of all results cannot be developed.

Electrochemical impedance spectroscopy measurements yield an indication of the quality of the epoxy coating of the rebars. That is, the impedance spectroscopy yield *Good quality epoxy coating* ratings (higher resistance, capacitive impedance response) versus *Poor quality epoxy coating* ratings (lower resistance, capacitive impedance response). That is, a poor epoxy coating rating yields a necessary but not sufficient condition for the epoxy coated rebar to corrode. The assumption in this analysis is that properly epoxy coated rebars would not corrode.

However, the obtained ratings have to be combined with high moisture content and chloride ion content and/or large carbonation depth for corrosion to occur. In most examples described in this section, when half-cell potential readings indicated the presence of corrosion activity, the associated electrochemical impedance spectroscopy readings yielded poor quality rating of epoxy coating on the rebars. However, a more systematic survey needs to be implemented to carefully evaluate epoxy degradation throughout the whole bridge deck.

### **6.8.5 *Ground penetrating radar***

Ground penetrating radar surveys were collected on all four bridges with the support of Mn/DOT personnel and equipment. The collected reflection travel times in the GPR traces were used to measure the distribution of EM velocity on the bridge decks and to estimate the volumetric water



content and rebar depths. The reflected amplitudes in the GPR traces were used to qualitatively evaluate areas with large Cl<sup>-</sup> content.

As GPR surveys yield qualitative information about some of the corrosion controlling parameters, GPR data need to be used along with other corrosion monitoring tests (e.g., chain drag, half cell potential, and chloride ion content) to provide a better understating the structural health of bridge decks.

In general, areas with larger estimated water content yield higher corrosion activity as indicated by high negative half-cell potential measurements. Certain areas that also show high attenuation (an indication of high salt content) correlated well with corrosion process as shown in half-cell potential surveys. Finally, GPR data provides a rapid methodology for the evaluation of rebar depths throughout bridge decks without the need for core extraction.

## CHAPTER 7. LABORATORY EVALUATION - TEST RESULTS AND DISCUSSION

### 7.1 INTRODUCTION

In this chapter, 34 core samples and the 45 bars extracted within the cores are presented and discussed. The results are presented separately for each bridge and include the data obtained from the chloride ion analysis and the evaluation of the condition of the epoxy coated bars. Then, the results are discussed and compared among the bridges studied.

### 7.2 CHLORIDE ION CONTENT

A total of 384 samples were tested. Table 7.1 shows a summary of the number of tests conducted per bridge.

*Table 7.1 Number of samples tested for chloride ion content*

| <b>Bridge</b> | <b>Total Number of Tests</b> |
|---------------|------------------------------|
| 19015         | 106                          |
| 27062         | 82                           |
| 27812         | 78                           |
| 27815         | 118                          |

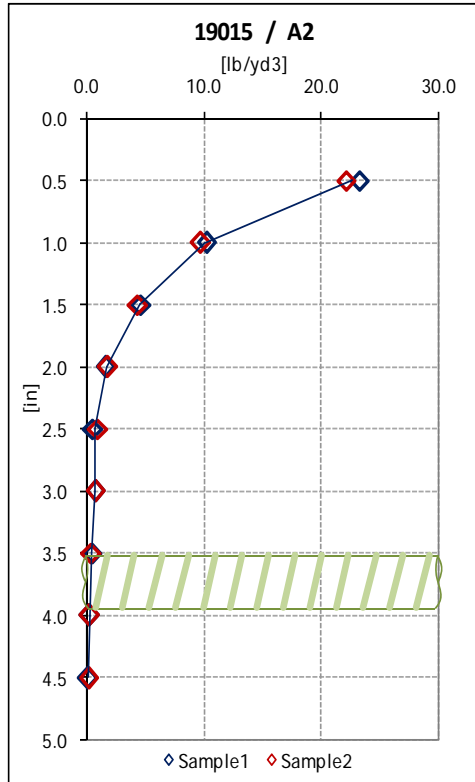
In the following sections a detailed description of the measured chloride ion content is shown.

### 7.3 CHLORIDE CONTENT PROFILES

#### 7.3.1 *Uncracked cores*

As described in section 5.3.1 (Sample retrieval), measurements of the chloride ion content were taken every 0.5 in (12.6 mm) below the surface up to the bar level, typically at 4 in (100 mm). For each sample, the chloride ion content in pounds of chloride per cubic yard of concrete was calculated for each depth. In Figure 7.1, the chloride content is shown as a function of depth. As expected, larger concentrations of chloride exist close to the surface (about 23 lb/cy at 0.5 in) and the concentrations decrease rapidly with depth. For this core, the measured chloride content is about 0.4 lb/cy at the bar level (3.5 in). It may be recalled that two samples were taken at each depth to confirm the measurements.

Chloride ion contents obtained from samples 1 and 2 (Figure 7.1) were nearly identical at each depth. This result was typical for all the tests conducted in uncracked cores. Although the results from samples tested from the same level exhibited virtually no scatter, and nearly all the scatter in results could be attributed to the inherent test error, the number of two samples tested from each level was not modified. Enough material was still retrieved from each hole to allow a third sample to be tested if results from the first two samples conflicted.

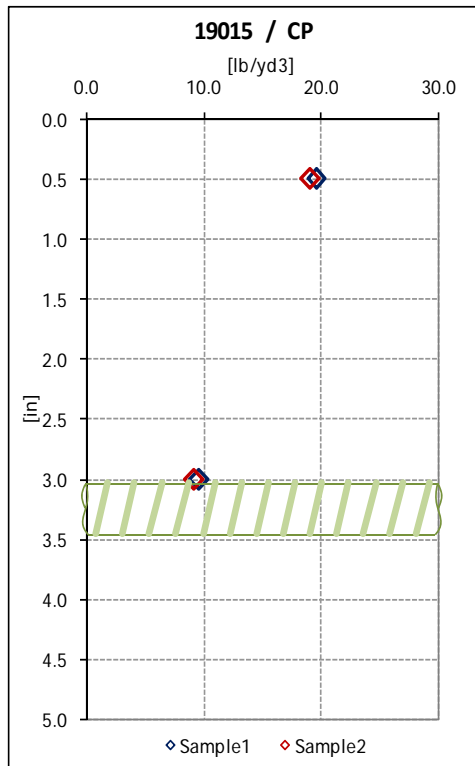


*Figure 7.1 Example of chloride content taken from a non-delaminated core at different depths.*

### 7.3.2 Cracked cores

In cracked cores, measurements of the chloride ion content were taken only at two locations, 0.5 in (12.6 mm) and at the bar level. However, in some cores with vertical cracks, samples were taken every 0.5 in. increments.

Figure 7.2 shows the chlorine ion content for cracked core “CP” of bridge 19015. Note that the chlorine ion concentration at the bar level (3 in) is much greater than that measured in uncracked cores at the same bar level (see Figure 7.1).



*Figure 7.2 Example of chloride content taken from a delaminated core at different depths.*

Although the results from samples tested from the same level exhibited virtually no scatter, and nearly all the scatter in results could be attributed to the inherent test error, the number of two samples tested from each level was not modified. Enough material was still retrieved from each hole to allow a third sample to be tested if results from the first two samples conflicted.

Overall, it was observed that the chloride ion content at the bar level was much higher than that obtained from non-delaminated or uncracked cores. However, there are few exceptions where cores extracted with cracks presented a low chloride content value at bar level.

## **7.4 BRIDGE 19015**

### **7.4.1 Chloride ion content**

Table 7.2 documents the measured chloride ion content versus the depth for the cores extracted from bridge 19015. The values shown in the table correspond to the average chloride ion content measured at each depth.

**Table 7.2 Chloride ion content in bridge 19015 cores**

| Depth<br>(in) | Chloride ion content (lb/cy) |                            |                           |                           |                           |                           |                           |                            |    |
|---------------|------------------------------|----------------------------|---------------------------|---------------------------|---------------------------|---------------------------|---------------------------|----------------------------|----|
|               | A2 <sup>(1)</sup>            | AP <sup>(2)</sup>          | C2 <sup>(3)</sup>         | CP <sup>(2)</sup>         | D2 <sup>(1)</sup>         | DP <sup>(2)</sup>         | DCS1 <sup>(1)</sup>       | DCS2 <sup>(4)</sup>        |    |
| 0.5           | 22.7                         | 22.2                       | 15.2                      | 19.3                      | 33.2                      | 21.6                      | 27.7                      | 19.6                       |    |
| 1.0           | 10.0                         | 17.0                       | 9.7                       | 12.5*                     | --                        | 22.8                      | 16.5                      | 18.7                       | -- |
| 1.5           | 4.6                          | 8.4                        | 6.3                       | --                        | 15.6                      | 13.1                      | 13.4                      | --                         |    |
| 2.0           | 1.7                          | 10.2                       | 6.3                       | --                        | 11.3                      | 10.2                      | 8.5                       | 21.5                       |    |
| 2.5           | 0.8                          | <b>14.1</b><br>(bar level) | 4.3                       | --                        | 5.9                       | 10.9                      | <b>5.3</b><br>(bar level) | --                         |    |
| 3.0           | 0.8                          | --                         | 2.2                       | <b>9.4</b><br>(bar level) | 4.7                       | <b>8.3</b><br>(bar level) | 2.7                       | --                         |    |
| 3.5           | <b>0.4</b><br>(bar level)    | --                         | 1.1                       | --                        | 3.0                       | --                        | 0.9                       | <b>24.3</b><br>(bar level) |    |
| 4.0           | 0.3                          | --                         | <b>0.5</b><br>(bar level) | --                        | 0.6                       | --                        | 0.5                       | --                         |    |
| 4.5           | 0.1                          | --                         | 0.1                       | --                        | <b>0.5</b><br>(bar level) | --                        | 0.5                       | --                         |    |

(1): Cores “A2”, “D2” and “DCS1” presented no cracks.

(2): Cores “AP”, “CP” and “DP” were adjacent to joint over pier No2.

(3): Core “C2” presented a hairline vertical crack.

(4): Core “DCS2: was taken over a delaminated area and presented a diagonal crack.

\*: value measured at a vertical crack.

Table 7.2 shows that the measured chloride ion content near the surface of the deck (0.5 in below the surface) varied between 19 and 33 lb/cy with an average value of 23 lb/cy. The chloride ion content at the rebar level varied significantly depending on the condition of the core. In general, cores without vertical cracks, away from the joint or a delaminated area had chloride ion content of 0.5 lb/cy or less (cores “A2”, “C2” and “D2”). This value is well below the reported values for corrosion initiation of 1.2 lb/cy for black steel [6]. The chloride ion content at the bar level in core “DCS1”, however, was much higher than in the other uncracked cores. This result is attributed however to the proximity of the bar to the surface in this core (only 2.5 in. of bar cover), as the chloride ion content at this depth is comparable to that in core “D2” at the same depth.

On the other hand, the chloride ion content at the bar level in cores near the joint and over the delaminated area (“AP”, “CP”, “DP”, and “DCS2”) were much higher and varied between 8.3 and 24.3 lb/cy. These values, and also that in core “DCS1”, are all above the threshold chloride

ion content for corrosion initiation of black bars, and are consistent with the rust observed on the surface of the bars in these cores.

Core “C2” also had a 2.5 in. (63.5 mm) deep vertical crack from the surface. The chloride ion content measured inside the crack at a depth of 1 in. was 12.5 lb/cy, and as was expected, it was larger than that outside of the crack at the same depth.

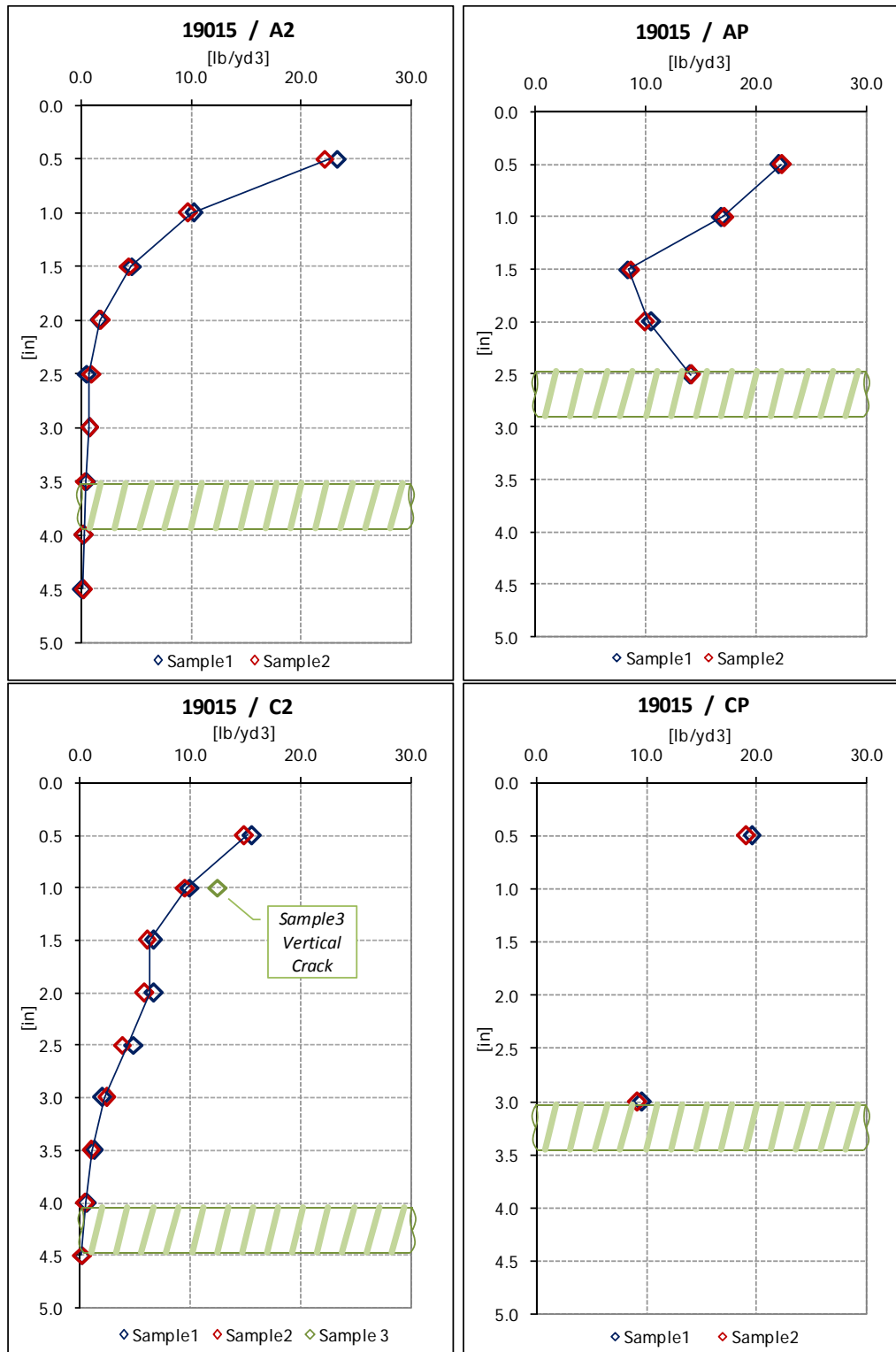
Figure 7.3 and Figure 7.4 show a set of plots obtained from cores extracted from bridge 19015, displaying the chloride ion content as a function of depth.

#### **7.4.2 Diffusion coefficient**

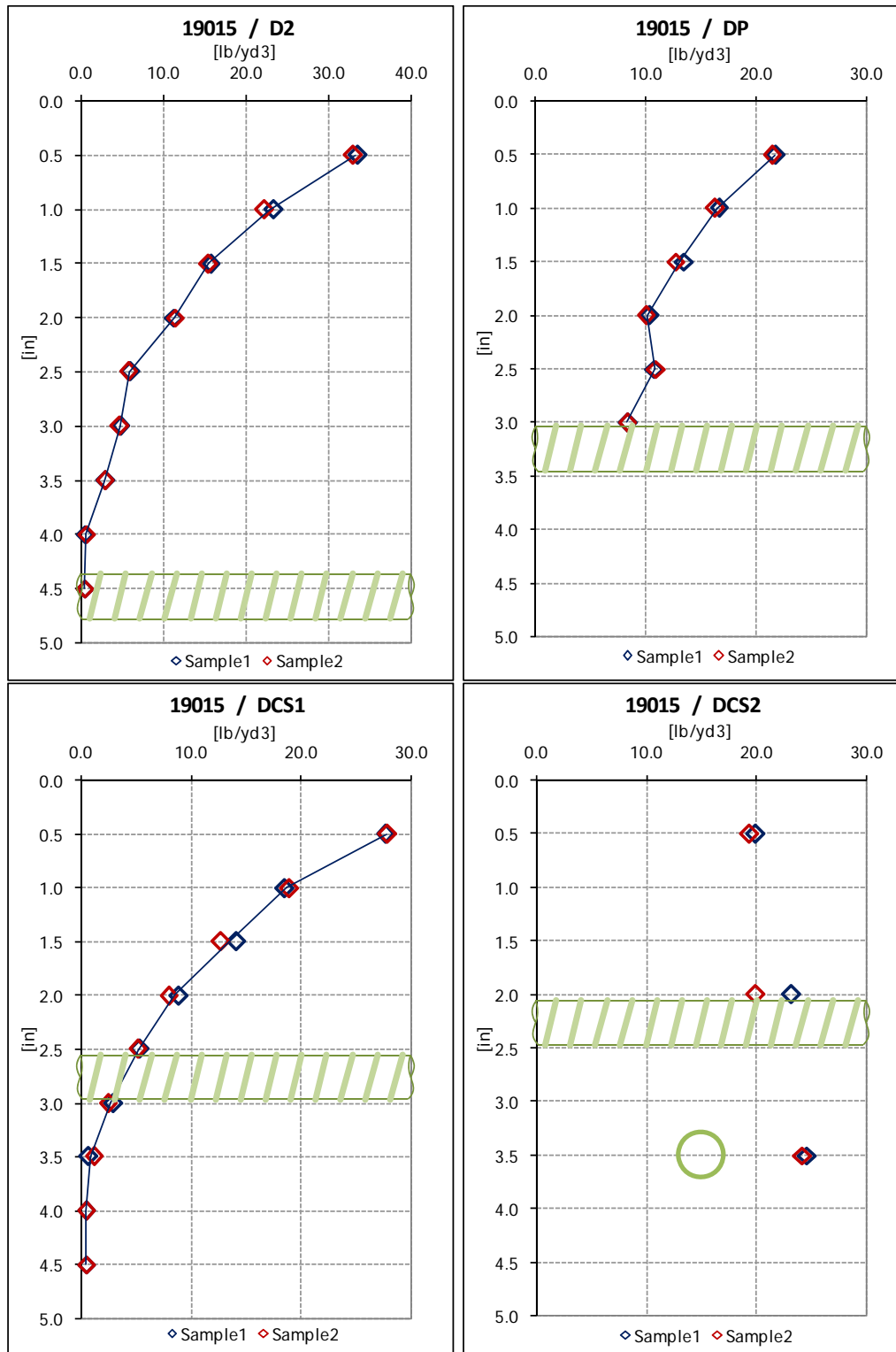
Table 7.3 presents the calculated diffusion coefficient using the method described in Appendix D (Diffusion Coefficient Calculation), for this calculation were used the data of chloride ion content profiles obtained from the cores without or away from vertical cracks, joints or delaminated areas (cores “A2”, “C2”, “D2” and “DCS1”). The computed values range between 0.013 and 0.055 in<sup>2</sup>/year with an average of 0.039 in<sup>2</sup>/year, which compares well with values reported in the literature for similar decks [2].

**Table 7.3 Diffusion coefficient in bridge 19015 cores**

| <b>Core</b> | <b>D</b><br>(in <sup>2</sup> /year) |
|-------------|-------------------------------------|
| A2          | 0.013                               |
| C2          | 0.055                               |
| D2          | 0.045                               |
| DCS1        | 0.043                               |



**Figure 7.3** Chloride ion content profile results for Bridge 19015, Cores “A2”, “AP”, “C2” and “CP”.



**Figure 7.4** Chloride ion content profile results for Bridge 19015, Cores “D2”, “DP”, “DCS1” and “DCS2”.



### 7.4.3 Carbonation depth

Table 7.4 shows the average measured carbonation depth,  $d_k$ , in millimeters from the surface. The measured carbonation depths were very small, ranging from 0.3 to 2.8 mm (1/100 in. to 1/10 in.), with an average carbonation of 1.0 mm (1/25 in.) for this deck. The carbonation depths are much smaller than the rebar cover (see Table 7.4) and thus carbonation cannot be considered to be a source of bar deterioration.

*Table 7.4 Measured carbonation depth in bridge 19015 cores*

| Core | $d_k$<br>(mm) | Bar cover<br>(mm) |
|------|---------------|-------------------|
| A2   | 1.6           | 89                |
| AP   | 0.5           | 64                |
| C2   | 0.3           | 102               |
| CP   | 0.6           | 76                |
| D2   | 2.8           | 114               |
| DP   | 0.2           | 76                |
| DCS1 | 1.0           | 64                |
| DCS2 | 0.7           | 89                |

### 7.4.4 Epoxy coating hardness

Table 7.5 shows the epoxy coating hardness expressed in terms of the standard lead grade. The common value observed was between H and 2H which is comparable with the hardness of 2H of a new and intact ECR. It must be noted that the coating of the bar extracted from core “C2” showed an unusually high hardness value (5H). These results suggest that the quality of the coating itself is in good condition and as good as that of a new ECR.

*Table 7.5 Measured coating hardness of bars extracted from bridge 19015 cores*

| Core | Upper bar<br>(#4) | Lower bar<br>(#6 or #5) |
|------|-------------------|-------------------------|
| A2   | H                 | --*                     |
| AP   | H                 | --*                     |
| C2   | H                 | 5H                      |
| CP   | H                 | --*                     |
| D2   | 2H                | 2H                      |
| DP   | 2H                | --*                     |
| DCS1 | 2H                | 2H                      |
| DCS2 | HB                | H                       |

\*: no bar extracted with core.

#### 7.4.5 Epoxy coating adherence

Table 7.6 shows the measured adhesion of the epoxy coating given by the lowest rating obtained from the three test locations over the length of the extracted bars. The values range between 1 (no adherence) and 3 (moderate adherence), with no bar having a rating of 4 (well adhered coating). According with Sagüés [25] these results suggest that the coating had been subject of moisture absorption and may be an indication of aging of the epoxy-coating adhesion.

**Table 7.6** Coating adhesion of bars extracted from bridge 19015 cores

| Core | Upper bar<br>(#4) | Lower bar<br>(#6 or #5) |
|------|-------------------|-------------------------|
| A2   | 2                 | --*                     |
| AP   | 2                 | --*                     |
| C2   | 2                 | 2                       |
| CP   | 1                 | --*                     |
| D2   | 2                 | 3                       |
| DP   | 1                 | --*                     |
| DCS1 | 2                 | 2                       |
| DCS2 | 1                 | 2                       |

\*: no bar extracted with core.

#### 7.4.6 Epoxy coating thickness

Table 7.7 shows the measured thickness of the epoxy coating in four bars. The values range between 6 and 11 mils, with an average of 7 mils among the bars measured. As described in section 5.5.3, the ASTM A775 standard requires that the coating thickness be between 7 and 16 mils (0.007-0.016 inches), therefore, results suggest that the coating thickness is, in general, below current standards in this deck.

**Table 7.7** Measured coating thickness of bars extracted from bridge 19015 cores

| Core | Upper bar<br>(#4) | Lower bar<br>(#6 or #5) |
|------|-------------------|-------------------------|
| C2   | 7                 | 6                       |
| D2   | 6                 |                         |
| DP   | 11                | --*                     |
| DCS1 | 6                 | 6                       |

\*: no bar extracted with core.

It is important to mention that, as was described in section 2.4, in 1991 CRSI started the epoxy coating applicator plant certification, where plants have shown a continual and dramatic improvement in quality since the program's inception. Therefore, the coating thickness measured for the bars in this deck may not be representative of those found in the ECR manufactured today (2008).

### 7.4.7 Corrosion condition

Table 7.8 shows the state of corrosion condition of the bar using the rating system described in section 5.5.4. The numbers shown in the table represent the lowest rating obtained from three test locations over the length of the bar. The values range between 0 (no corrosion) and 3 (severe corrosion). The bars in cores “A2”, “C2”, “D2” and “DCS1” presented a better condition than bars in cores “AP”, “CP”, “DP” and “DCS2”. In general, when present, the lower bar showed a similar corrosion condition than the upper bar. Overall, bars located near the joint or in the delaminated area showed light to moderate levels of corrosion (see Table 5.4 that describes levels of corrosion).

**Table 7.8** Bar corrosion condition in bars extracted from bridge 19015 cores

| Core | Upper bar (#4) | Lower bar (#6 or #5) | Surface Defect or Location |
|------|----------------|----------------------|----------------------------|
| A2   | 0              | --*                  | None                       |
| AP   | 2              | --*                  | Joint                      |
| C2   | 1              | 1                    | None                       |
| CP   | 3              | --*                  | Joint, Spall               |
| D2   | 0              | 0                    | None                       |
| DP   | 3              | --*                  | Joint                      |
| DCS1 | 1              | 0                    | None                       |
| DCS2 | 3              | 2                    | Delamination               |

\*: no bar extracted with core.

## 7.5 BRIDGE 27062

### 7.5.1 Chloride ion content

Table 7.9 shows the average measured chloride ion content versus depth for the cores extracted from bridge 27062 (average of two samples). It can be seen that the measured chloride ion content on the surface of this deck varied between 19 and 27 lb/cy with an average value of 23 lb/cy. At the bar level, cores without vertical cracks, away from the joint or a delaminated area had chloride ion content between 0.2 and 0.4 lb/cy (cores “A1”, “B1”, “C1” and “D1”). These values are below the common chloride ion content threshold for corrosion initiation [6]. On the other hand, in cores adjacent to delaminated areas, the chloride ion content at the bar level was 1.0 lb/cy (cores “D2” and “D3”). This value of chloride ion content is not above the threshold for corrosion initiation, and is consistent with the good condition observed on the surface of the bars in these cores.

In particular, core “D2” had a diagonal crack from 0.5 to 3.0 in. depth. To measure the chloride ion content in that crack, a third and four samples at a depth of 1.5 in. were retrieved from the internal face of the crack (see chloride content profile core “D2” in Appendix C). The chloride ion content result inside the crack was 20 lb/cy, and as was expected, it was larger than that outside of the crack at the same depth. This may implies that cracks help to increase the overall chloride ion content in concrete.

**Table 7.9 Chloride ion content in bridge 27062 cores**

| Depth<br>(in) | Chloride ion content (lb/cy) |                           |                           |                           |                           |                           |
|---------------|------------------------------|---------------------------|---------------------------|---------------------------|---------------------------|---------------------------|
|               | A1 <sup>(1)</sup>            | B1 <sup>(1)</sup>         | C1 <sup>(1)</sup>         | D1 <sup>(1)</sup>         | D2 <sup>(2,3)</sup>       | D3 <sup>(3)</sup>         |
| 0.5           | 27.4                         | 22.0                      | 21.2                      | 25.2                      | 21.0                      | 18.8                      |
| 1.0           | 18.3                         | 13.1                      | 11.6                      | 12.4                      | --                        | --                        |
| 1.5           | 12.4                         | 7.5                       | 5.9                       | 6.8                       | 14.5<br>20.0*             | --                        |
| 2.0           | 7.7                          | 3.5                       | 2.2                       | 3.3                       | --                        | --                        |
| 2.5           | 4.0                          | 1.4                       | 0.8                       | 1.3                       | --                        | --                        |
| 3.0           | 1.7                          | 0.6                       | 0.9                       | 0.9                       | --                        | --                        |
| 3.5           | 0.7                          | 0.4                       | 0.3                       | 0.6                       | --                        | --                        |
| 4.0           | 0.4                          | 0.4                       | <b>0.4</b><br>(bar level) | <b>0.3</b><br>(bar level) | <b>1.0</b><br>(bar level) | <b>1.0</b><br>(bar level) |
| 4.5           | <b>0.2</b><br>(bar level)    | <b>0.3</b><br>(bar level) | 0.5                       | 0.2                       | --                        | --                        |

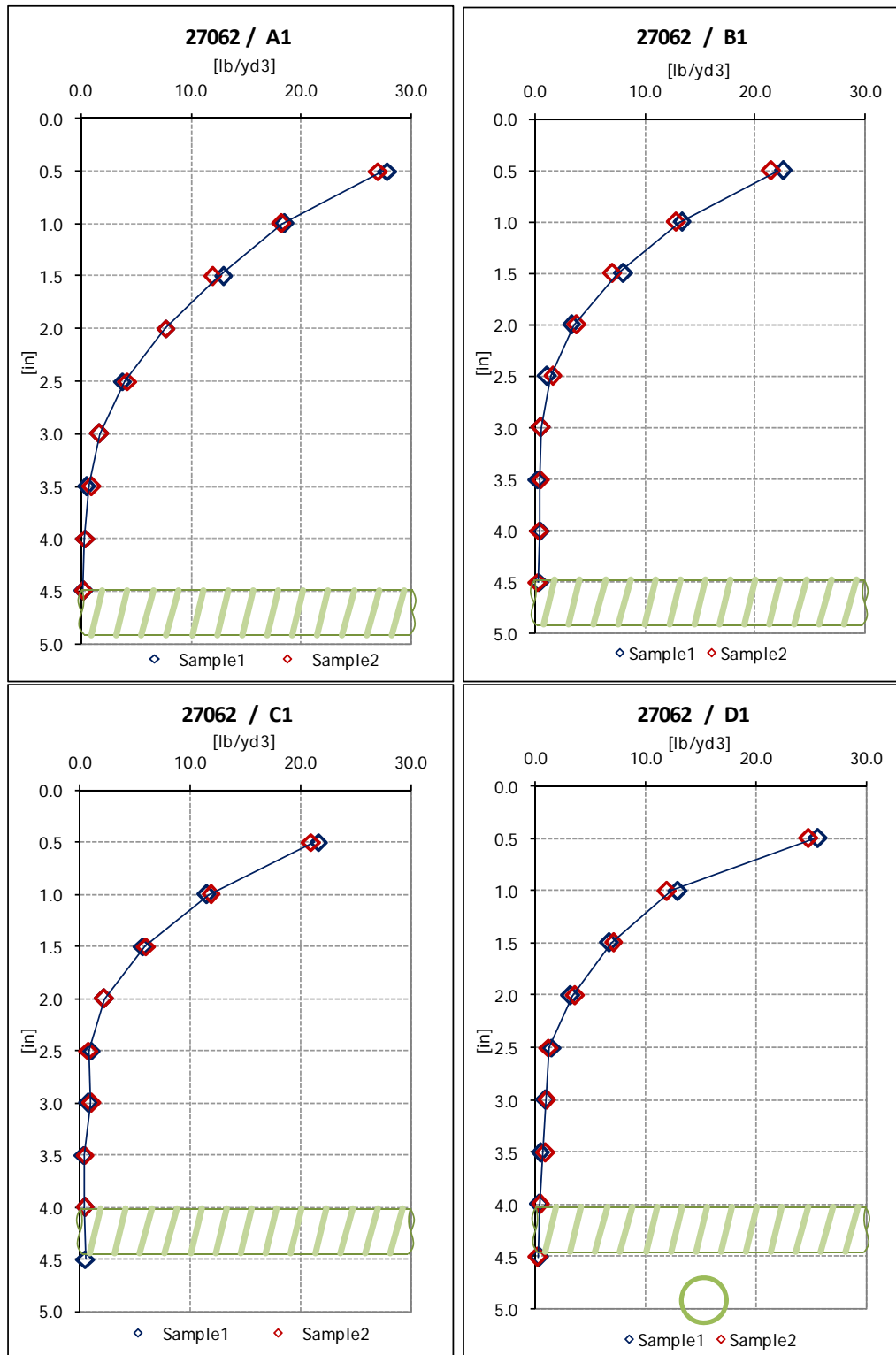
(1): Cores “A1”, “B1”, “C1” and “D1” presented no cracks.

(2): Core “D2” presented a diagonal crack.

(3): Cores “D2” and “D3” were adjacent to delaminated areas.

\*: value measured at a crack.

Near the surface, the chloride ion content of this bridge are similar than in bridge 19015. However, the chloride ion content at the bar level are much lower. These results may suggest that having a greater cover depth it would helps to reduce the chloride ion content at the bar level. Figure 7.5 and Figure 7.6 show a set of plots obtained from cores extracted from bridge 27062, displaying the chloride ion content as a function of depth.



**Figure 7.5** Chloride ion content profile results for Bridge 27062, Cores “A1”, “B1”, “C1” and “D1”.

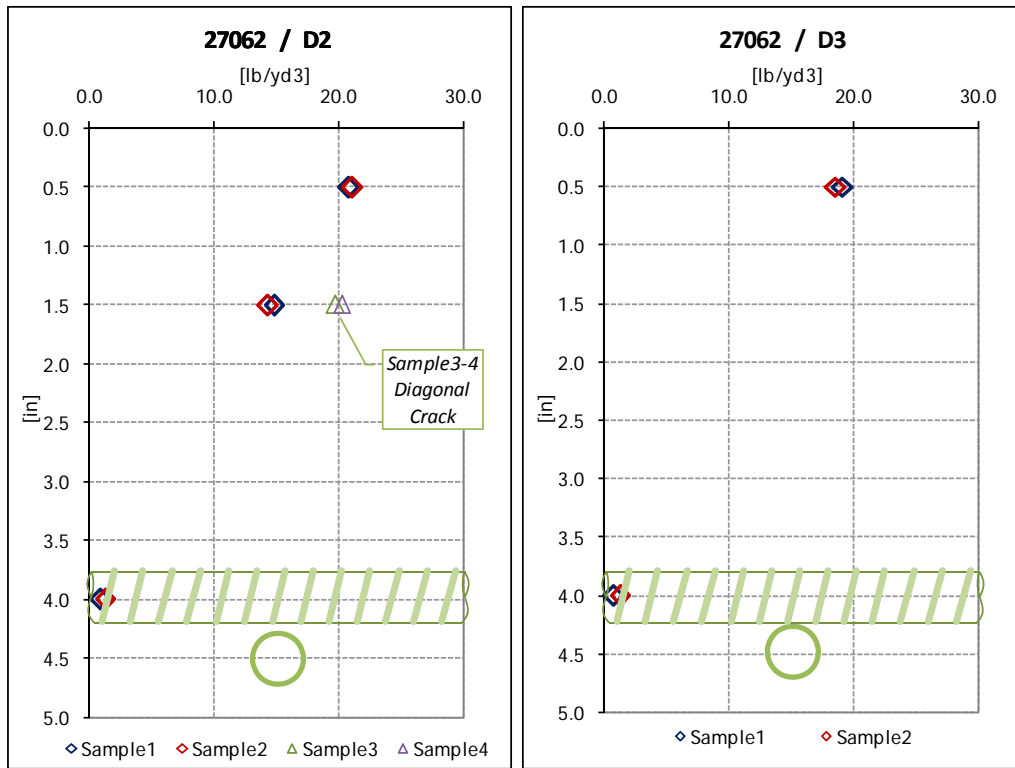


Figure 7.6 Chloride ion content profile results for Bridge 27062, Cores “D2” and “D3”.

### 7.5.2 Diffusion coefficient

Table 7.10 shows the calculated coefficient of diffusion using the chloride ion content profiles obtained from cores “A1”, “B1”, “C1” and “D1”. The computed values range between 0.022 and 0.048 in<sup>2</sup>/year with an average value of 0.030 in<sup>2</sup>/year. Although these values are lower than presented in bridge 19015, compare well with typical values reported in the literature. These lower values may be an indication of a low water-to-cement ratio where the cores were extracted.

Table 7.10 Diffusion coefficient in bridge 27062 cores

| Core | D<br>(in <sup>2</sup> /year) |
|------|------------------------------|
| A1   | 0.048                        |
| B1   | 0.028                        |
| C1   | 0.022                        |
| D1   | 0.028                        |

### 7.5.3 Carbonation depth

Table 7.11 shows the average carbonation depth,  $d_k$ , measured from the surface. The carbonation depths were again very small, ranging from 0.3 to 1.4 mm (1/100 in. to 1/20 in.), such smaller than the reinforcement cover. The average carbonation depth observed in this bridge was 0.9 mm (1/25 in.). Similarly than bridge 19015, these results of carbonation may not be considered to be a source of bar deterioration.

*Table 7.11 Measured carbonation depth in bridge 27062 cores*

| Core | $d_k$<br>(mm) | Bar cover<br>(mm) |
|------|---------------|-------------------|
| A1   | 0.6           | 114               |
| B1   | 1.4           | 114               |
| C1   | 1.2           | 102               |
| D1   | 0.8           | 102               |
| D2   | 1.0           | 102               |
| D3   | 0.3           | 102               |

### 7.5.4 Epoxy coating hardness

Table 7.12 shows the epoxy coating hardness expressed as standard lead grade. The predominant value observed was between H and 2H. These values are comparables with those presented in new ECRs, therefore indicates that coating is in good condition.

*Table 7.12 Measured coating hardness in bars extracted from bridge 27062 cores*

| Core | Upper bar<br>(#6 or #7) | Lower bar<br>(#4) |
|------|-------------------------|-------------------|
| A1   | H                       | --*               |
| B1   | 2H                      | H                 |
| C1   | H                       | --*               |
| D1   | H                       | H                 |
| D2   | --*                     | H                 |
| D3   | H                       | 2H                |

\*: no bar extracted with core.

### 7.5.5 Epoxy coating adherence

Table 7.13 shows the epoxy coating adhesion expressed as the lowest rating observed in the bar. The values range between 2 (poor adherence) and 3 (moderate adherence), with no bar found with well adhered coating. These results indicate that the deterioration of the epoxy-coating adhesion had begun.

**Table 7.13** Coating adherence in bars extracted from bridge 27062 cores

| <b>Core</b> | <b>Upper bar<br/>(#6 or #7)</b> | <b>Lower bar<br/>(#4)</b> |
|-------------|---------------------------------|---------------------------|
| A1          | 3                               | --*                       |
| B1          | 3                               | 3                         |
| C1          | 3                               | --*                       |
| D1          | 2                               | 2                         |
| D2          | --*                             | 2                         |
| D3          | 3                               | 2                         |

\*: no bar extracted with core.

### 7.5.6 Epoxy coating thickness

Table 7.14 shows the measured thickness of the epoxy coating in three bars. The values range between 9 and 11 mils, with an average around 10 mils among the bars measured. In this case, the bars are according with the coating thickness standard (between 7 and 16 mils), therefore, the results suggest that the quality of the coating thickness in this deck is in good condition and is comparable with the thickness of a new ECR.

**Table 7.14** Measured coating thickness in bars extracted from bridge 27062 cores

| <b>Core</b> | <b>Upper bar<br/>(#6 or #7)</b> | <b>Lower bar<br/>(#4)</b> |
|-------------|---------------------------------|---------------------------|
| D1          | 11                              | 9                         |
| D2          | --*                             | 10                        |
| D3          |                                 | 11                        |

\*: no bar extracted with core.

### 7.5.7 Corrosion condition

Table 7.15 shows the measured corrosion condition of the bar given by the lowest rating obtained from the three test locations over the length of the bar. The values range between 0 (no corrosion) and 1 (light corrosion). In general the bars were in good condition and only the bar in core “D2” presented a rating 1 (light corrosion) due to some spotting. In this bridge, the lower bar in cores “B1”, “D1” and “D3” showed the same corrosion condition than the upper bar. Cores “D2” and “D3”, located adjacent to a delaminated area, showed light and no corrosion respectively. However, in this deck was not clear the difference in levels of corrosion between bars located in delaminated areas or away from them.



**Table 7.15** Corrosion condition in bars extracted from bridge 27062 cores

| <b>Core</b> | <b>Upper bar<br/>(#6 or #7)</b> | <b>Lower bar<br/>(#4)</b> | <b>Surface Defect or<br/>Location</b> |
|-------------|---------------------------------|---------------------------|---------------------------------------|
| A1          | 0                               | --*                       | None                                  |
| B1          | 0                               | 0                         | None                                  |
| C1          | 0                               | --*                       | None                                  |
| D1          | 0                               | 0                         | None                                  |
| D2          | --*                             | 1                         | Adjacent to a<br>delaminated area     |
| D3          | 0                               | 0                         | Adjacent to a<br>delaminated area     |

\*: no bar extracted with core.

## **7.6 BRIDGE 27812**

### **7.6.1 Chloride ion content**

Table 7.16 shows the measured chloride ion content over the depth for the cores extracted from bridge 27812. The values shown in the table correspond to the average chloride ion content measured at each depth. The values obtained on the surface of this deck varied between 7 and 14 lb/cy with an average value of 11 lb/cy. These values are much lower than those measured on the surface of the decks of bridges 19015 and 27062.

Cores adjacent to a transverse crack (cores “22” and “23”) presented higher chloride ion content at the bar level than cores away from the crack (“31”, “32”, and “33”). These higher values are both above the reported value for corrosion initiation of 1.2 lb/cy [21], however, only core 23 had some rust staining on the surface.

Cores near to the joint and over a delaminated area (“J1”, “J2”, and “J3”) presented diagonal and horizontal cracks above the bar level, however, low chloride ion content values were detected at the bar level. These values were all below the corrosion initiation value of 1.2 lb/cy.

Figure 7.7 and Figure 7.8 show a set of plots obtained from cores extracted from bridge 27812, displaying the chloride ion content as a function of depth.

**Table 7.16 Chloride ion content in bridge 27812 cores**

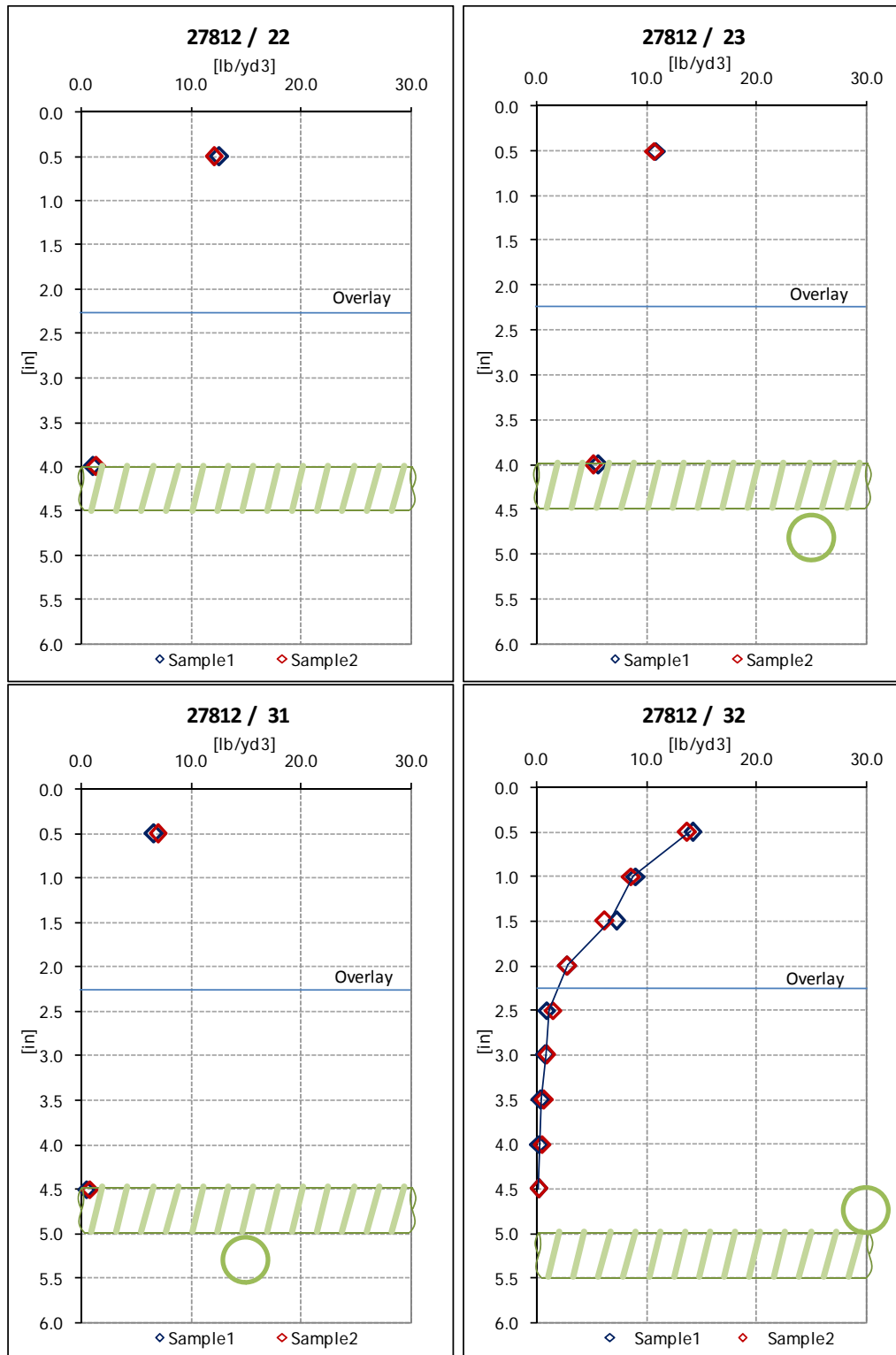
| Depth<br>(in) | Chloride ion content (lb/cy) |                           |                           |                           |                           |                           |                           |                           |
|---------------|------------------------------|---------------------------|---------------------------|---------------------------|---------------------------|---------------------------|---------------------------|---------------------------|
|               | 22 <sup>(1,2)</sup>          | 23 <sup>(1,2)</sup>       | 31 <sup>(3)</sup>         | 32 <sup>(3)</sup>         | 33 <sup>(3)</sup>         | J1 <sup>(2,4)</sup>       | J2 <sup>(2,4)</sup>       | J3 <sup>(3,4)</sup>       |
| 0.5           | 12.3                         | 10.8                      | 6.8                       | 14.0                      | 9.9                       | 11.6                      | 7.9                       | 12.1                      |
| 1.0           | --                           | --                        | --                        | 8.8                       | 3.7                       | --                        | --                        | 4.4                       |
| 1.5           | --                           | --                        | --                        | 6.7                       | 1.4                       | --                        | 1.6                       | 1.2                       |
| 2.0           | --                           | --                        | --                        | 2.8                       | 1.1                       | --                        | --                        | 1.8                       |
| 2.5           | --                           | --                        | --                        | 1.2                       | 1.2                       | --                        | 0.9                       | 1.4                       |
| 3.0           | --                           | --                        | --                        | 0.9                       | 0.9                       | --                        | --                        | 1.2                       |
| 3.5           | --                           | --                        | --                        | 0.5                       | 0.7                       | --                        | 0.7                       | 0.5                       |
| 4.0           | <b>1.3</b><br>(bar level)    | <b>5.4</b><br>(bar level) | --                        | 0.4                       | <b>0.5</b><br>(bar level) | --                        | --                        | 0.5                       |
| 4.5           | --                           | --                        | <b>0.6</b><br>(bar level) | <b>0.2</b><br>(bar level) | --                        | --                        | --                        | <b>0.4</b><br>(bar level) |
| 5.0           | --                           | --                        | --                        | --                        | --                        | <b>0.8</b><br>(bar level) | <b>0.4</b><br>(bar level) | --                        |

(1): Cores “22” and “23” were adjacent to a transverse crack.

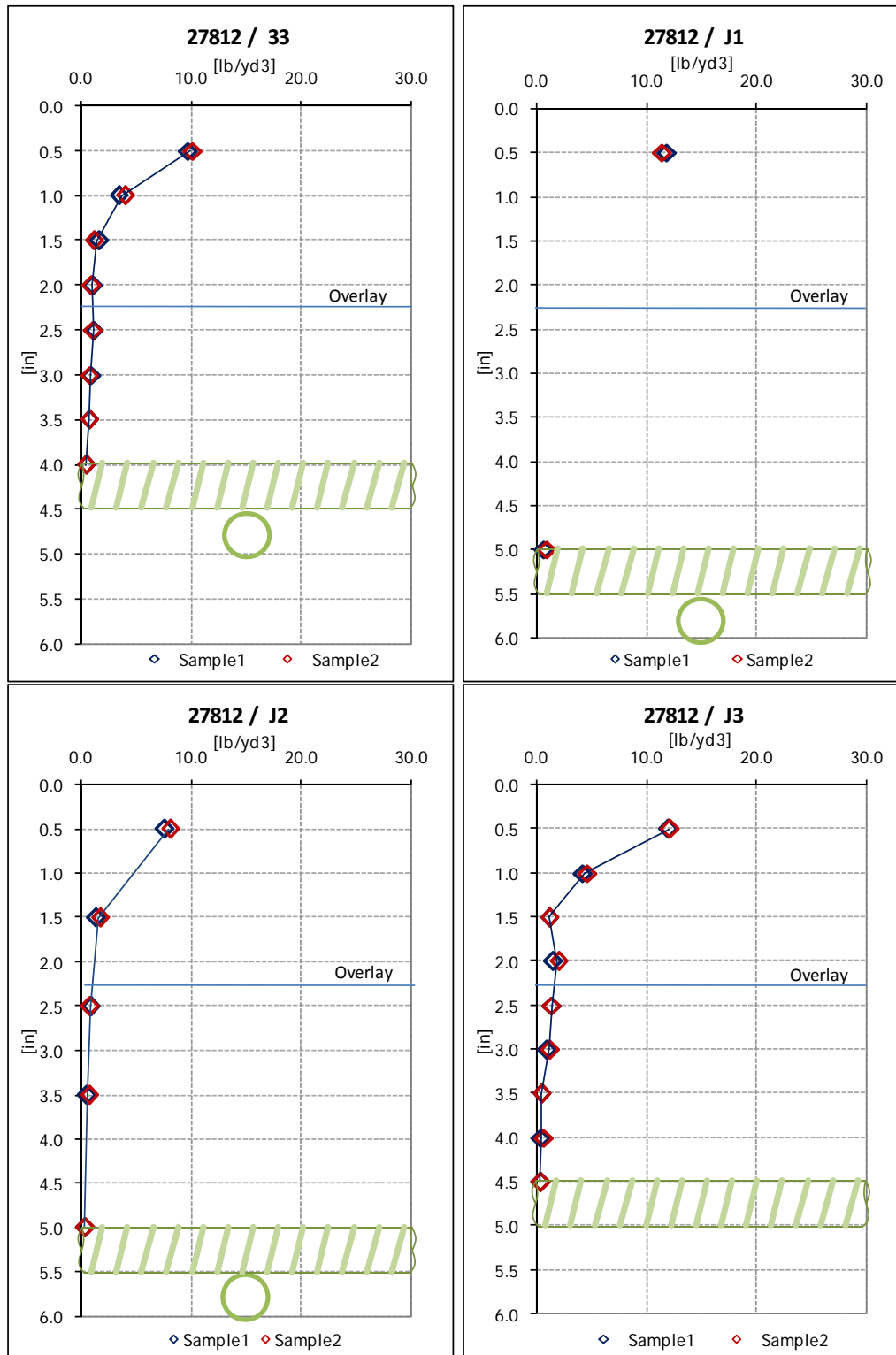
(2): Cores “22”, “23”, “J1” and “J2” presented cracks.

(3): Cores “31”, “32”, “33” and “J3” presented no cracks.

(4): Cores “J1”, “J2” and “J3” were adjacent to the west joint.



**Figure 7.7** Chloride ion content profile results for Bridge 27812, Cores “22”, “23”, “31” and “32”.



**Figure 7.8** Chloride ion content profile results for Bridge 27812, Cores “33”, “J1”, “J2” and “J3”.

### 7.6.2 Diffusion coefficient

Table 7.17 shows the calculated coefficient of diffusion using the chloride ion content profiles obtained from cores “32”, “33”, and “J3”. The computed values range between 0.011 and 0.037 in<sup>2</sup>/year with an average value of 0.020 in<sup>2</sup>/year. The values observed are lower than those obtained in bridges 19015 and 27062. This may suggest that the higher density, lower slump concrete overlay present in this deck contributes to decreasing the chloride ingress into the concrete. Diffusion coefficient values of cores “33” and “J3” are below the values reported in the literature for similar decks [2], this may be an indication of an unusual low water-to-cement ratio in their locations.

**Table 7.17** Diffusion coefficient in bridge 27812 cores

| Core | D<br>(in <sup>2</sup> /year) |
|------|------------------------------|
| 32   | 0.037                        |
| 33   | 0.012                        |
| J3   | 0.011                        |

The use of high performance concrete should lower concrete’s permeability and reduce the rate of ingress of carbon dioxide and chlorides and, thereby, increase the effectiveness of the physical barrier.

### 7.6.3 Carbonation depth

Table 7.18 shows the average measured carbonation depth,  $d_k$ , from the surface. The measured carbonation depths were extremely small, ranging from 0.0 to 0.5 mm (0 in. to 1/50 in.), which is well below the reinforcement cover. The average carbonation depth observed in this bridge was 0.1 mm (1/250 in.). This low carbonation depth observed is probably because of the higher density, lower slump concrete used in the upper 2¼ in. of the deck.

**Table 7.18** Measured carbonation depth in bridge 27812 cores

| Core | $d_k$<br>(mm) | Bar cover<br>(mm) |
|------|---------------|-------------------|
| 22   | 0.3           | 102               |
| 23   | 0.0           | 102               |
| 31   | 0.0           | 114               |
| 32   | 0.5           | 114               |
| 33   | 0.0           | 102               |
| J1   | 0.0           | 127               |
| J2   | 0.3           | 127               |
| J3   | 0.0           | 114               |

#### 7.6.4 Epoxy coating hardness

Table 7.19 shows the measured epoxy coating hardness in terms of a standard lead grade. The predominant observed grade was Grade H. The bar in core “22” showed a slightly lower hardness (HB), just one level below Grade H. Visual inspection showed, however, that the condition of the coating in this bar was similar to that of the other bars. These values are comparable with those presented in new ECRs, therefore indicates that coating is in good condition.

*Table 7.19 Measured coating hardness in bars extracted from bridge 27812 cores*

| <b>Core</b> | <b>Upper bar<br/>(#5)</b> | <b>Lower bar<br/>(#4)</b> |
|-------------|---------------------------|---------------------------|
| 22          | HB                        | --*                       |
| 23          | H                         | H                         |
| 31          | H                         | 2H                        |
| 32          | H                         | H                         |
| 33          | H                         | 2H                        |
| J1          | H                         | H                         |
| J2          | 2H                        | H                         |
| J3          | H                         | --*                       |

\*: no bar extracted with core.

#### 7.6.5 Epoxy coating adherence

Table 7.20 shows the epoxy coating adherence expressed as the minimum rating observed in the bar. The values range between 2 (poor adherence) and 4 (well adherence) and there was no bar with a rating of one (no adherence). Only in cores “J1” and “J2”, the lower bar presented lower adherence than the upper bar, which in both cases the upper bar was rated 4 well adhered. Overall, the coating adherence observed in this deck was better than observed in the two previous bridges (19015 and 27062). This suggests that the coating adherence is in better condition than other bridges in this study and the coating may have different rate of deterioration than those bridges.

**Table 7.20** Coating adherence in bars extracted from bridge 27812 cores

| Core | Upper bar<br>(#5) | Lower bar<br>(#4) |
|------|-------------------|-------------------|
| 22   | 2                 | --*               |
| 23   | 2                 | 2                 |
| 31   | 4                 | 4                 |
| 32   | 2                 | 3                 |
| 33   | 3                 | 4                 |
| J1   | 4                 | 2                 |
| J2   | 4                 | 3                 |
| J3   | 2                 | --*               |

\*: no bar extracted with core.

### 7.6.6 Epoxy coating thickness

Table 7.21 shows the measured thickness of the epoxy coating in three bars. The values range between 8 and 11 mils, with an average around 9 mils among the bars measured. Similarly than bridge 27062, the bars are according with the coating thickness standard (between 7 and 16 mils), therefore, the results suggest that the quality of the coating thickness in this deck is in good condition and is as good as that of a new ECR.

**Table 7.21** Measured coating thickness in bars extracted from bridge 27812 cores

| Core | Upper bar<br>(#5) | Lower bar<br>(#4) |
|------|-------------------|-------------------|
| 22   | 9                 | --*               |
| 32   | 8                 |                   |
| J3   | 11                | --*               |

\*: no bar extracted with core.

### 7.6.7 Corrosion condition

Table 7.22 shows the measured corrosion condition of the bar given by the lowest rating obtained from the three test locations over the length of the bar. The values range between 0 (no corrosion) and 2 (moderate corrosion). The lower bar showed the same corrosion condition than the upper bar with the only exception of core 23. In general the bars were in good condition with a predominant rating 0 (no corrosion) and only the bars in cores 23 and J3 showed some level of corrosion, these two cores were located adjacent to a crack and near a join and over a delaminated area respectively.

**Table 7.22 Corrosion condition in bars extracted from bridge 27812 cores**

| <b>Core</b> | <b>Upper bar<br/>(#5)</b> | <b>Lower bar<br/>(#4)</b> | <b>Surface Defect<br/>or Location</b> |
|-------------|---------------------------|---------------------------|---------------------------------------|
| 22          | 0                         | - - *                     | Adjacent to a<br>transverse crack     |
| 23          | 2                         | 1                         | Adjacent to a<br>transverse crack     |
| 31          | 0                         | 0                         | None                                  |
| 32          | 0                         | 0                         | None                                  |
| 33          | 0                         | 0                         | None                                  |
| J1          | 0                         | 0                         | Joint                                 |
| J2          | 0                         | 0                         | Joint                                 |
| J3          | 1                         | - - *                     | Joint                                 |

\*: no bar extracted with core.

(-) no surface defect

## **7.7 BRIDGE 27815**

### **7.7.1 Chloride ion content**

Table 7.13 shows the measured chloride ion content over the depth for the cores extracted from bridge 27815. The values shown in the table correspond to the average chloride ion content measured at each depth.

Cores “22”, “32”, “41”, “42”, “51” and “52” presented a vertical crack from the surface to the bar (see Figure 7.9). Thus, the values reported in the table show the chloride ion content away from the crack (left) and inside the crack (right). Near the surface, the measured chloride ion content varied between 9 and 19 lb/cy with an average value of 15 lb/cy. Again, the average chloride ion content was lower than that observed in the decks of bridges 19015 and 27062. At the bar level, the chloride ion content varied between 0.4 and 0.5 lb/cy in cores with no vertical crack (cores “11”, “12” and “A21”). The chloride ion content at the bar level in cores with vertical cracks (“22”, “32”, “41”, “42”, “51” and “52”) were much higher and varied between 7.4 and 13.4 lb/cy. These values are all above the threshold chloride ion content for corrosion initiation of epoxy coated bars, and are consistent with the rust observed on the surface of the bars.

Particularly, on cores “32”, “42” and “51”, once the vertical crack was opened, two additional samples were retrieved from the internal face of the crack at all depths. The average of these two samples is presented to the right of the data collected away from the crack.



**Table 7.23 Chloride ion content in bridge 27815 cores**

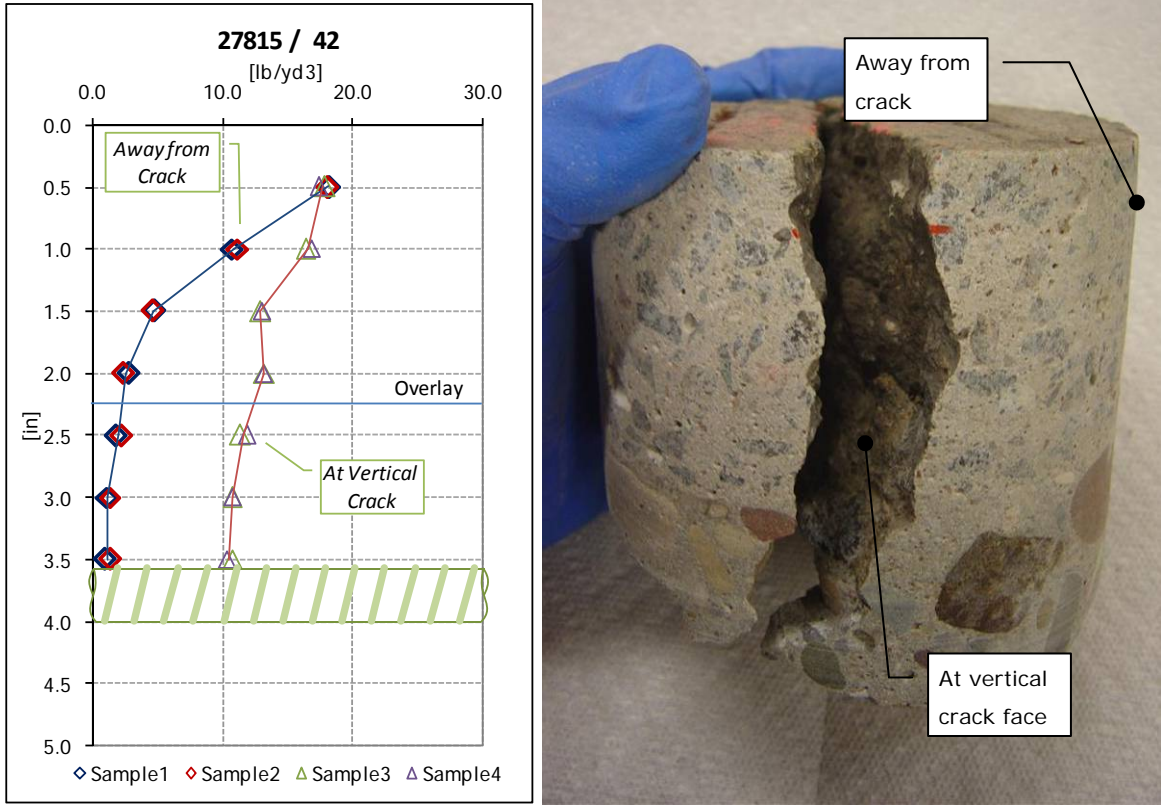
| Depth<br>(in) | Chloride ion content (lb/cy) |                           |                   |                           |                   |                     |                   |                           |                   |                     |                   |                     |                   |                           |                           |
|---------------|------------------------------|---------------------------|-------------------|---------------------------|-------------------|---------------------|-------------------|---------------------------|-------------------|---------------------|-------------------|---------------------|-------------------|---------------------------|---------------------------|
|               | 11 <sup>(1)</sup>            | 12 <sup>(1)</sup>         | 22 <sup>(2)</sup> |                           | 32 <sup>(2)</sup> |                     | 41 <sup>(2)</sup> |                           | 42 <sup>(2)</sup> |                     | 51 <sup>(2)</sup> |                     | 52 <sup>(2)</sup> |                           | A21 <sup>(1)</sup>        |
| 0.5           | 9.0                          | 14.1                      | 15.1              | *<br>12.7                 | 19.4              | *<br>17.4           | 15.5              | *<br>16.2                 | 18.1              | *<br>17.7           | 16.9              | *<br>17.5           | 15.6              | *<br>15.9                 | 15.8                      |
| 1.0           | 2.6                          | 9.2                       |                   |                           | 9.2               | 14.3                |                   |                           | 10.9              | 16.6                | 9.8               | 13.7                |                   |                           | 8.8                       |
| 1.5           | 1.0                          | 6.8                       |                   |                           | 4.3               | 13.2                |                   |                           | 4.7               | 12.9                | 6.7               | 10.6                |                   |                           | 5.0                       |
| 2.0           | 1.2                          | 4.5                       |                   |                           | 2.2               | 13.1                |                   |                           | 2.6               | 13.2                | 4.0               | 10.4                |                   |                           | 3.3                       |
| 2.5           | 0.7                          | 1.7                       |                   |                           | 1.2               | 11.6                |                   |                           | 2.0               | 11.6                | 2.1               | 10.5                |                   |                           | 1.2                       |
| 3.0           | 0.9                          | 1.0                       |                   |                           | 0.8               | 11.9                |                   |                           | 1.2               | 10.7                | 1.2               | 8.8                 |                   | <b>8.8</b><br>(bar level) | 1.1                       |
| 3.5           | 0.4                          | 0.5                       |                   |                           | 0.7               | 12.0                |                   |                           | 1.2               | 10.5<br>(bar level) | 1.2               | 10.1                |                   | --                        | 0.9                       |
| 4.0           | 0.3                          | <b>0.4</b><br>(bar level) |                   | <b>7.4</b><br>(bar level) | 0.5               | 13.4<br>(bar level) |                   | <b>9.6</b><br>(bar level) |                   | --                  | 0.9               | 11.3<br>(bar level) |                   | --                        | 0.7                       |
| 4.5           | 0.4                          | --                        |                   | --                        | --                | --                  |                   | --                        | --                | --                  | --                | --                  |                   | --                        | <b>0.5</b><br>(bar level) |

(1): Cores “11”, “12” and “A21” presented no cracks.

(2): Cores “22”, “32”, “41”, “42”, “51” and “52” presented a vertical crack.

\*: value measured at a vertical crack.

Figure 7.10 and Figure 7.11 show chloride ion content as a function of depth for cores extracted from bridge 27815.



**Figure 7.9** Example of chloride ion content at vertical crack and away from crack.

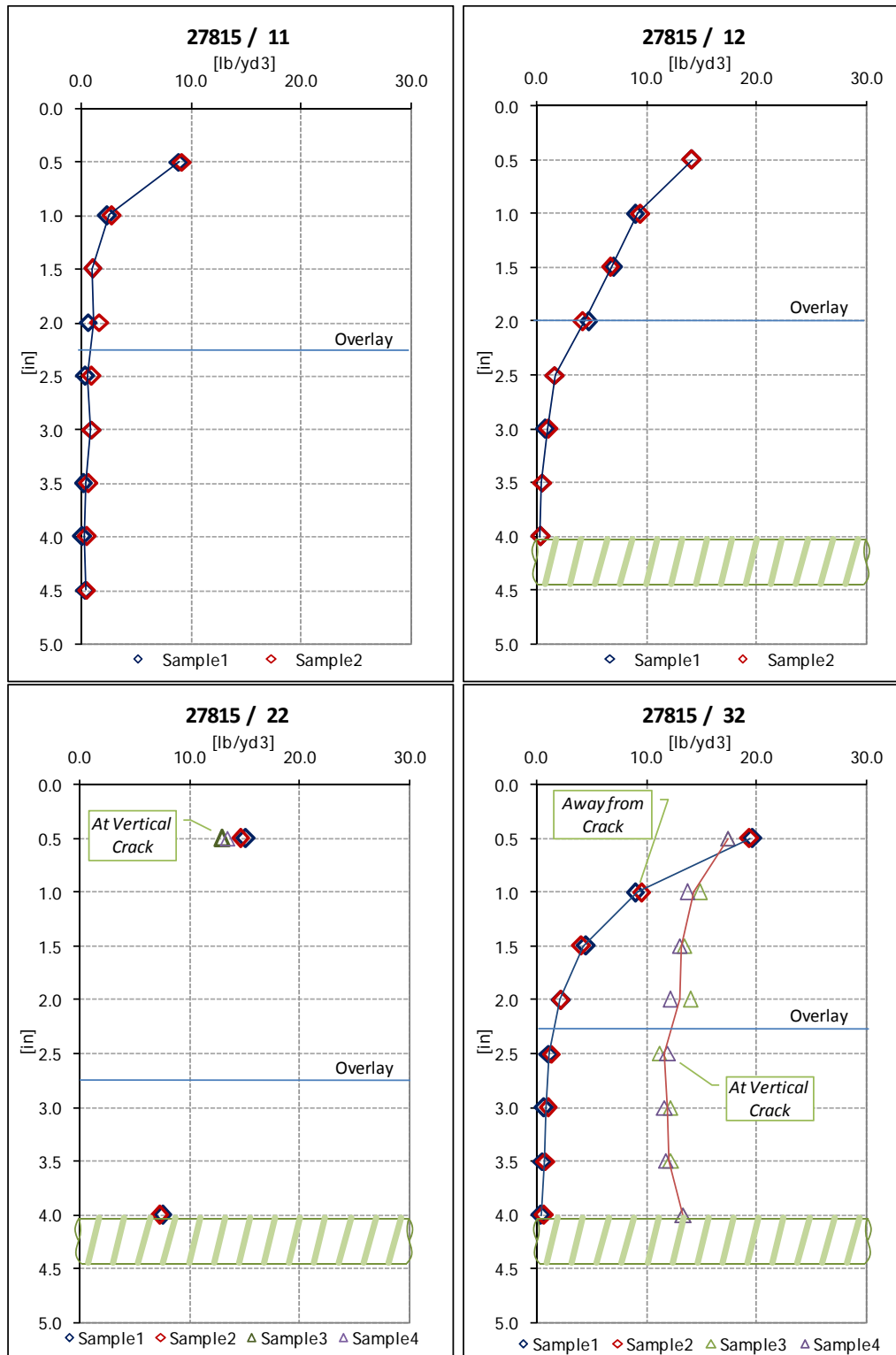


Figure 7.10 Chloride ion content profile results for Bridge 27815, Cores “11”, “12”, “22” and “32”.

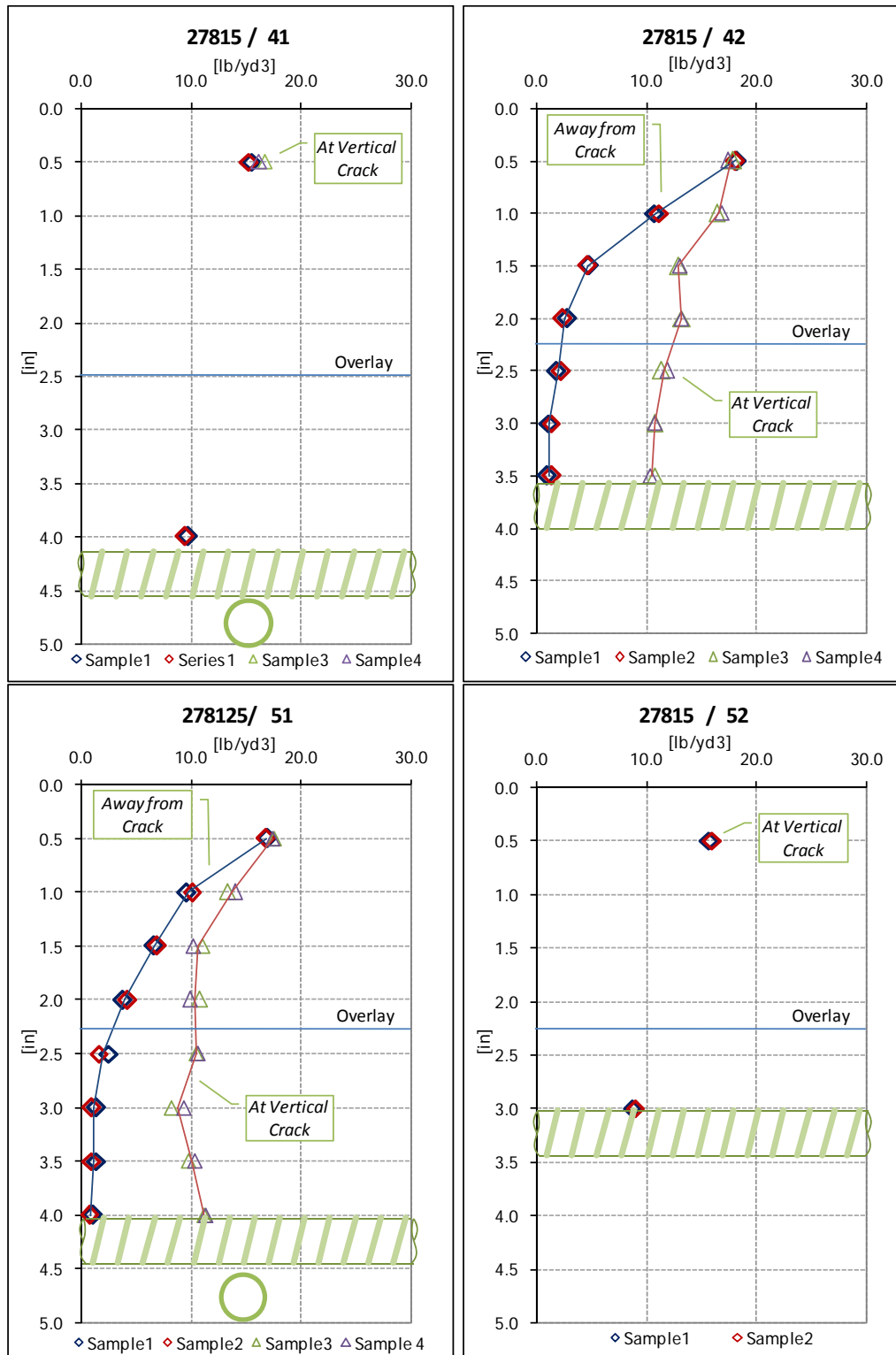


Figure 7.11 Chloride ion content profile results for Bridge 27815, Cores “41”, “42”, “51” and “52”.

### 7.7.2 Diffusion coefficient

Table 7.24 shows the calculated coefficient of diffusion using the chloride ion content profiles obtained from cores “11”, “12” and “A21”. The computed values range between 0.009 and 0.045 in<sup>2</sup>/year with an average value of 0.027 in<sup>2</sup>/year. The computed values from cores “12” and “A21” compare well with values reported in the literature for similar decks; however, the diffusion coefficient of core “11” was the lowest detected in this study, this may be an indication of a very low water-to-cement ratio in the lower slump concrete overlay.

**Table 7.24** Diffusion coefficient in bridge 27815 cores

| Core | D<br>(in <sup>2</sup> /year) |
|------|------------------------------|
| 11   | 0.009                        |
| 12   | 0.045                        |
| A21  | 0.029                        |

### 7.7.3 Carbonation depth

The average measured carbonation depth,  $d_k$ , from the surface is shown in Table 7.25. The measured carbonation depths were very small, ranging from 0.0 to 0.4 mm (0 in. to 1/60 in.), which is well below the reinforcement cover. The average carbonation depth observed in this bridge was 0.2 mm (1/10 in.). This low carbonation depth observed is probably because of the higher density, lower slump concrete used in the upper 2¼ in. of the deck, and these results of carbonation may not be considered to be a source of bar deterioration.

**Table 7.25** Measured carbonation depth in bridge 27815 cores

| Core | $d_k$<br>(mm) | Bar cover<br>(mm) |
|------|---------------|-------------------|
| 12   | 0.3           | 102               |
| 22   | 0.0           | 102               |
| 32   | 0.0           | 102               |
| 41   | 0.3           | 102               |
| 42   | 0.0           | 89                |
| 51   | 0.3           | 102               |
| 52   | 0.4           | 76                |
| A21  | 0.5           | 114               |

An additional carbonation depth test was conducted in cores with vertical cracks, and the test was performed immediately when the both crack surfaces were exposed. Carbonation was detected in the whole crack surface, and none horizontal carbonation was detected from the crack to inside the concrete.

#### 7.7.4 Epoxy coating hardness

Table 7.26 shows the epoxy coating hardness expressed in terms of a standard lead grade. Different to the other three bridges, the predominant value observed was Grade HB, which indicates some softening or deterioration of the coating comparing with the hardness of 2H of a new and intact ECR.

**Table 7.26** Measured coating hardness in bars extracted from bridge 27815 cores

| Core | Upper bar<br>(#5) | Lower bar<br>(#4 or #6) |
|------|-------------------|-------------------------|
| 12   | H                 | --*                     |
| 22   | HB                | --*                     |
| 32   | HB                | --*                     |
| 41   | H                 | H                       |
| 42   | HB                | --*                     |
| 51   | HB                | 2H                      |
| 52   | HB                | --*                     |
| A21  | 2H                | --*                     |

\*: no bar extracted with core.

#### 7.7.5 Epoxy coating adherence

Table 7.27 shows the epoxy coating bond or adhesion expressed as the minimum rating observed in the bar. The predominant rating is 2 (poor adhesion), with one bar from core “51” assigned a rating of 1 (no adhesion), which correspond to severe deterioration of the coating bond, with essentially no adhesion to the bar. These results indicate that the coating had been subject of moisture absorption [25] and suggest aging of the coating adhesion.

**Table 7.27** Coating adherence in bars extracted from bridge 27815 cores

| Core | Upper bar<br>(#5) | Lower bar<br>(#4 or #6) |
|------|-------------------|-------------------------|
| 12   | 2                 | --*                     |
| 22   | 2                 | --*                     |
| 32   | 2                 | --*                     |
| 41   | 2                 | 2                       |
| 42   | 2                 | --*                     |
| 51   | 1                 | 2                       |
| 52   | 2                 | --*                     |
| A21  | 2                 | --*                     |

\*: no bar extracted with core.

### 7.7.6 Epoxy coating thickness

Table 7.28 shows the measured thickness of the epoxy coating. The values range between 8 and 11 mils, with an average around 9 mils among the bars measured. These results suggest that the quality of the coating thickness in this deck is in good condition and is comparable with the thickness of a new ECR.

**Table 7.28** Measured coating thickness in bars extracted from bridge 27815 cores

| Core | Upper bar<br>(#5) | Lower bar<br>(#4 or #6) |
|------|-------------------|-------------------------|
| 12   | 8                 | --*                     |
| 22   | 11                | --*                     |
| 52   | 9                 | --*                     |
| A21  | 9                 | --*                     |

\*: no bar extracted with core.

### 7.7.7 Corrosion condition

Table 7.19 shows the measured corrosion condition of the bar given by the lowest rating obtained from the three test locations over the length of the bar. The values range between 0 and 3. There was only one case, the bar in core “51”, with severe corrosion (rating 3). On the other hand, the bars in cores “12” and “A21” presented no signs of corrosion. In the cores with two bars found in this bridge, the lower bar showed lower corrosion level than the upper bar. In general, bars located in vertical cracks showed light to severe levels of corrosion, and cores located away from vertical cracks showed no corrosion.

**Table 7.29** Corrosion condition in bars extracted from bridge 27815 cores

| Core | Upper bar<br>(#5) | Lower bar<br>(#4 or #6) | Surface Defect or<br>Location |
|------|-------------------|-------------------------|-------------------------------|
| 12   | 0                 | --*                     | None                          |
| 22   | 1                 | --*                     | Vertical crack                |
| 32   | 2                 | --*                     | Vertical crack                |
| 41   | 2                 | 1                       | Vertical Crack                |
| 42   | 2                 | --*                     | Vertical Crack                |
| 51   | 3                 | 0                       | Vertical Crack                |
| 52   | 2                 | --*                     | Vertical Crack                |
| A21  | 0                 | --*                     | -                             |

\*: no bar extracted with core.

(-) no surface defect

## 7.8 SUMMARY OF LABORATORY RESULTS

### 7.8.1 Visual inspection of cores

The data collected from the core samples was combined with the HCP readings in an attempt to correlate bar condition and chlorine ion content with field corrosion activity and surface delamination and spalling. Table 7.30 shows the probability of corrosion activity obtained from the HCP readings and the number of cores which presented delamination.

*Table 7.30 Cores by probability of corrosion*

| Probability of corrosion activity (HCP) | Delaminated cores | Non delaminated cores | Total     |
|---|-------------------|-----------------------|-----------|
| High                                    | 14                | 3                     | <b>17</b> |
| Likely                                  | 4                 | 0                     | <b>4</b>  |
| Low                                     | 3                 | 8                     | <b>11</b> |
| Not measured                            | 1                 | 1                     | <b>2</b>  |
| <b>Total</b>                            | <b>22</b>         | <b>12</b>             | <b>34</b> |

The fourteen delaminated cores with high probability of corrosion and the eight non delaminated cores with low probability of corrosion give a good relationship between these two independently obtained data sets. Also four delaminated cores were detected as “likely” to present corrosion.

### 7.8.2 Chloride content values

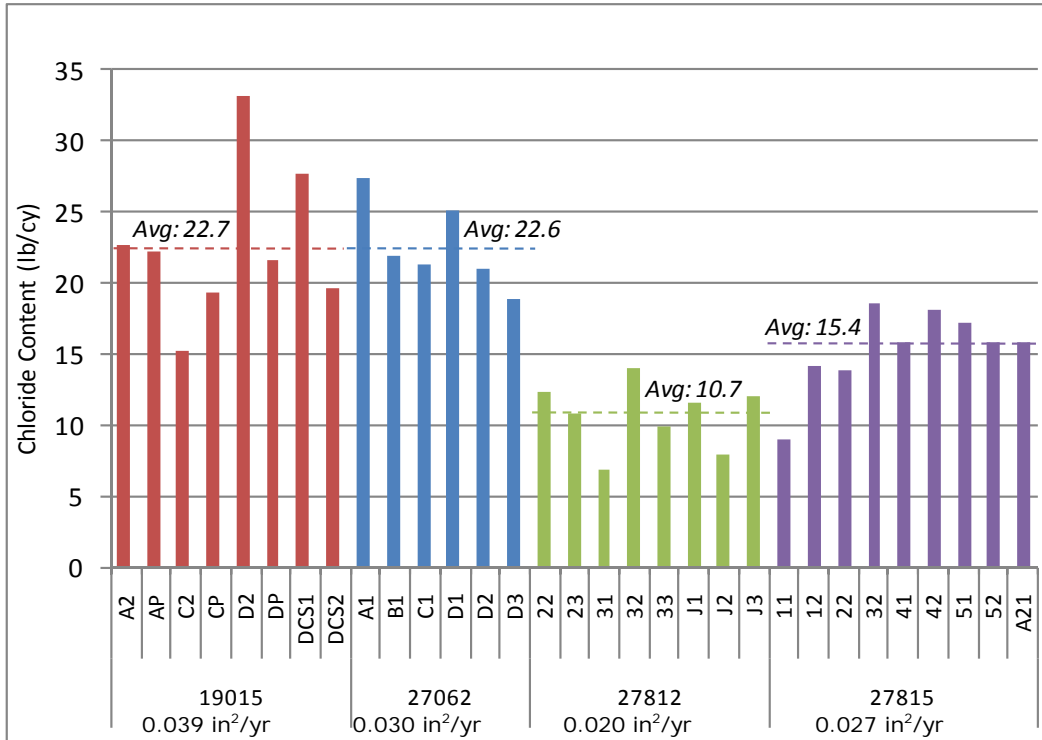
Table 7.31 shows the average chloride content per bridge measured at 0.5 in. below the surface and the average chloride content per bridge measured at bar level separated by cracked and uncracked cores. These results are also plotted in Figure 7.12 and Figure 7.13, respectively.

*Table 7.31 Average chloride ion content per bridge for non-delaminated cores*

| Bridge | Avg Cl <sup>-</sup> content at 0.5” depth (lb/yd <sup>3</sup> ) | Avg Cl <sup>-</sup> content at bar level (lb/yd <sup>3</sup> ) |                 | Average Bar Depth (in) |
|--------|---|--|-----------------|------------------------|
|        |   | Cracked Cores  | Uncracked Cores |                        |
| 19015  | 22.7  | 14.0   | 1.7             | 3.2                    |
| 27062  | 22.6  | 1.0  | 0.3             | 3.8                    |
| 27812  | 10.7  | 2.0  | 0.4             | 4.2                    |
| 27815  | 15.5  | 10.2   | 0.4             | 4.6                    |

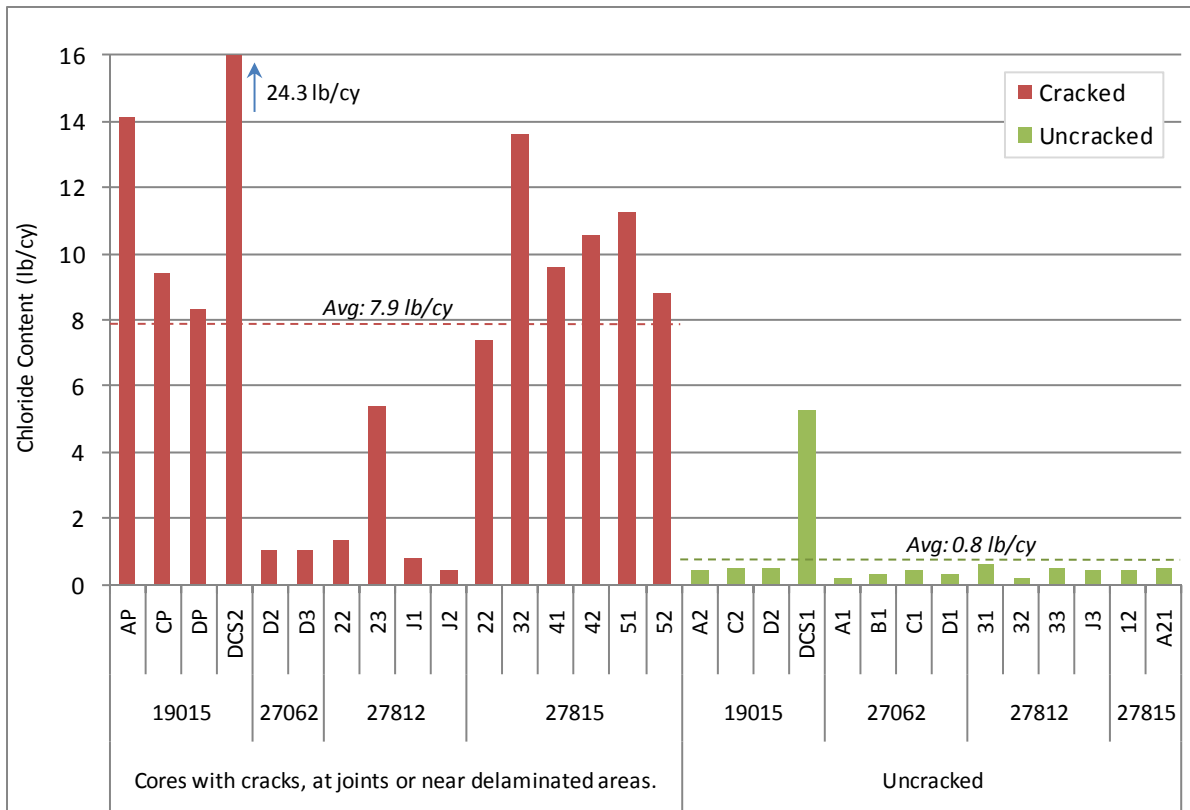
Table 7.31 and Figure 7.12 show that bridges 19015 and 27062 have much higher chloride concentrations on the surface than the other two decks. The standard deviation of these averages varied between 2 and 5 lb/cy.





**Figure 7.12 Chloride ion content at 0.5 in.**

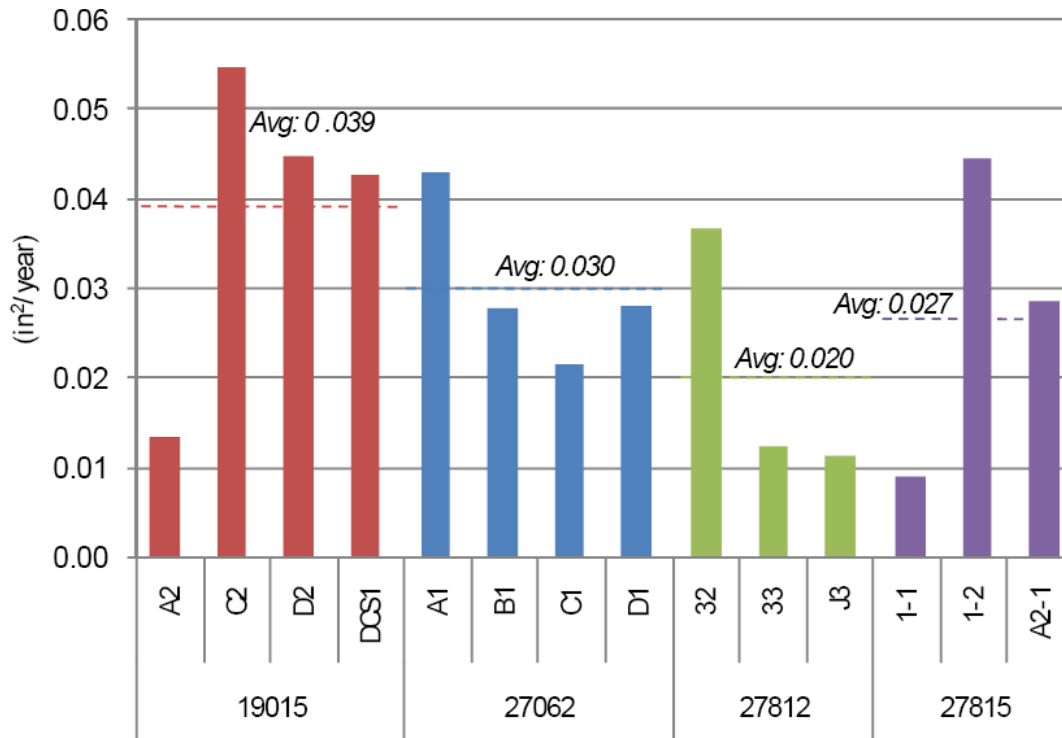
Figure 7.13 shows the values of chloride ion content at the bar level, grouped by the type of core, i.e., cracked and uncracked. This figure shows that at joints or near delaminated areas the chloride ion content in cores with cracks was much higher than in uncracked cores. Furthermore, the chloride ion content exceeds the reported value for corrosion initiation of 1.2 lb/cy for black steel [6] in nearly every cracked core. On the other hand, the chloride content in uncracked cores does not reach this threshold value, with the exception of the value in core “DCS1” from bridge 19015, which had a chloride ion content of about 5 lb/cy. However, the bar in this core was much closer to the surface with a bar cover of 2.5 in., which may explain the larger chloride ion content measured at the bar level. In fact, the chloride ion content is comparable to that at similar depths in other uncracked cores of the same deck (see Figure 7.3 and Figure 7.4).



**Figure 7.13** Chloride ion content at the upper bar level for cracked and uncracked cores.

There was more corrosion activity on ECR segments extracted from cracked cores than in those bars taken from uncracked cores. In all cases, with chloride concentrations from 5.3 lb/cy, some visible level of corrosion was found. This suggests that cracks give both, chlorides and moisture, easy and direct access to ECR, which appears to accelerate the corrosion process.

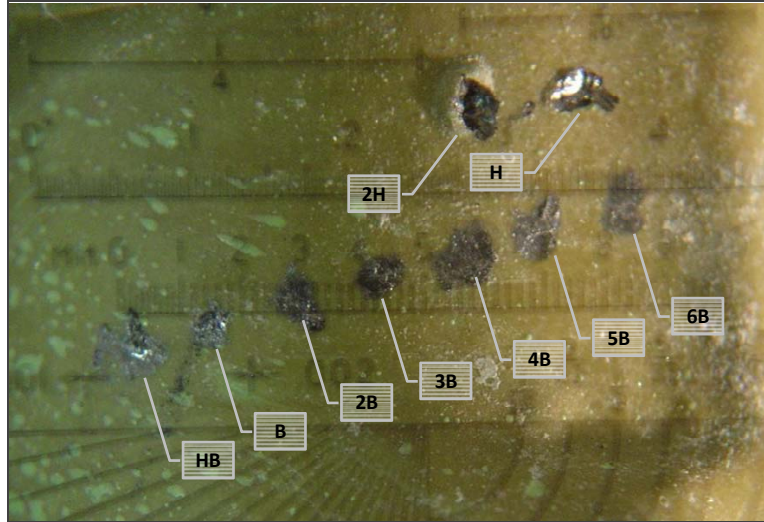
In Figure 7.14, the calculated chloride ion diffusion coefficients obtained from uncracked core specimens are compared. The data show that the average diffusion coefficient is smaller for decks with low slump, high density overlays (bridges 27812 and 27815) than for the other two decks (bridges 19015 and 27062). Note, however, that the scatter in the data is as large as the difference among the calculated averages.



**Figure 7.14** Calculated chloride ion diffusion coefficient in concrete for all four bridge decks.

### 7.8.3 Coating hardness

The purpose of this test was to evaluate the performance of protective coatings, and the test was conducted in both, corroded and non corroded bars. Figure 7.15 shows an example of the pencil hardness test where pencils from 6B (softest) to 2H were used. The figure presents different lead spots produced by the pencil, and only the last two (H and 2H) produced a clear damage to the coating. The hardness test showed to be very precise in terms of representing the coating resistance when the bar was in good condition. However, it was seen that coating disbondment and corrosion activity underneath the coating can greatly affect the hardness test results. The rust underneath the coating develops a soft millscale bed that helps the pencil lead to make coating damage easily than other coatings over steel in good condition.



*Figure 7.15 Example of pencil hardness test.*

As was explained in section 5.5.1, coating hardness was classified by lead nominations (from 6B to 6H). Converting the hardness rating into a numerical scale from 1 to 14 (softest to hardest), it was possible to average the hardness measured per bridge; these results are presented in Table 7.32.

*Table 7.32 Hardness test results per bridge*

| <b>Bridge</b> | <b>Average of Hardness (lead grade)</b> | <b>Standard Deviation</b> |
|---------------|---|---------------------------|
| 19015         | 7 (H)                                   | 0.71                      |
| 27062         | 7 (H)                                   | 0.52                      |
| 27812         | 7 (H)                                   | 0.53                      |
| 27815         | 7 (H)                                   | 0.76                      |

Despite the variation of hardness among bars, the average was the same for all four bridges. Furthermore, the majority of the bars (37 over 45 tested) presented hardness H or 2H, which is comparable to the hardness of new bars.

#### **7.8.4 Coating adherence**

From the 45 bars examined, 69% presented none or poor coating adherence (rating 1 and 2) while the rest presented some resistance to be peeled (rating 3 and 4). Overall, the test showed that all four bridge decks had bars with loss of coating adherence. It was also found that disbondment can occur with or without corrosion underneath the coating. This situation was also observed by other researchers evaluating epoxy coated bars performance [10, 26]. Table 7.33 shows the average and the standard deviation of the adherence rating for each bridge.

**Table 7.33 Adherence test results per bridge**

| <b>Bridge</b> | <b>Average of Adherence (1-4)</b> | <b>Standard Deviation</b> |
|---------------|-----------------------------------|---------------------------|
| 19015         | 2                                 | 0.52                      |
| 27062         | 3                                 | 0.52                      |
| 27812         | 3                                 | 0.99                      |
| 27815         | 2                                 | 0.35                      |

### **7.8.5 Coating thickness**

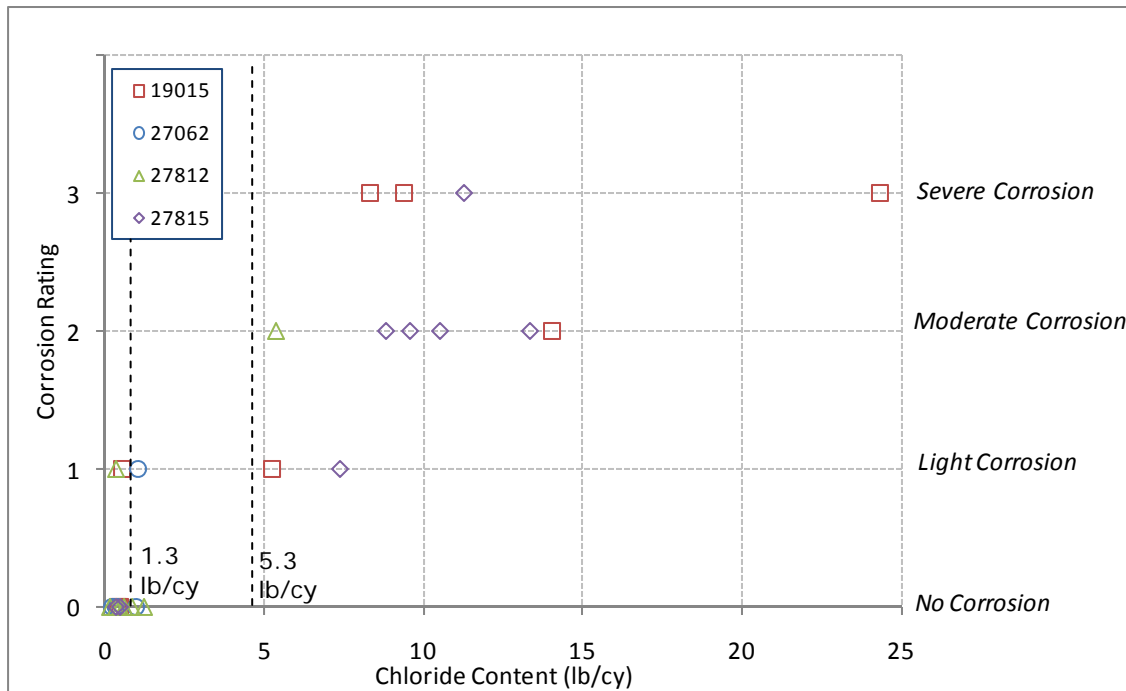
A total of 17 bars in good condition (with no corrosion observed) were tested. Coating thicknesses, as an average thickness between ribs varied from 6 to 11 mils (see Table 7.7, Table 7.14, Table 7.21 and Table 7.28), where 6 mils was the lowest thickness found only in bars from bridge 19015. The ASTM A775 standard [36] requires that the coating thickness be between 7 and 16 mils (0.007-0.016 inches). Therefore, the bar coating thickness met the current standards in all decks, except some bars (four out six) in bridge 1905.

### **7.8.6 Relationship between chloride ion content and bar corrosion condition**

Figure 7.16 shows the corrosion condition of all (upper and lower) bars examined against the measured chloride ion content at the bar level. The figure shows that all of the bars without corrosion had a chloride ion content at the bar level of 1.3 lb/cy or less. On the other hand, all bars that exhibited some level of corrosion, had a bar level, chloride ion content of 5.3 lb/cy or larger. There were three exceptions to these observations: two upper bars that showed light corrosion, one from core “C2” of bridge 19015 and the other from core J3 in bridge 27812. These bars had bar level chloride ion contents of 0.5 and 0.4 lb/cy, respectively. There was also a lower bar from core “D2” in bridge 27062 that had a bar level, chloride ion content of 1.0 lb/cy. Two of these bars were extracted only a few feet away from a delaminated area. This observation suggests that the presence of corrosion in the bar may have been initiated elsewhere and it may not be related to the chloride ion content measured at the bar level. The third bar is not close to a delaminated area, joint or a crack, but the millscale brown stains can be seen only with a magnifier lens which means that the bar is in its very early stage of corrosion.

It should also be noted, however, that there were a few bars with very high chloride ion content values that showed no or light corrosion, such as the lower bars of cores “41” and “51” of bridge 27815 which had chloride ion contents of 9.6 and 11.3 lb/cy, respectively. Therefore, these results show that a high chloride ion content level is a necessary, but not sufficient condition to initiate corrosion of epoxy coated bars.

Although the data show considerable scatter, Figure 7.16 shows that the larger the chloride ion content, the more severe the level of corrosion of the bar, as might be expected.



**Figure 7.16** Relationship between chloride ion content and corrosion condition.

In summary, the data show that the majority of the bars with a chloride ion content of 5.3 lb/cy or larger showed corrosion, while most of the bars with a chloride ion content of 1.3 lb/cy showed no corrosion. There were no bars, with or without corrosion, that had a chloride ion content at the bar level between 1.3 and 5.3 lb/cy. Therefore, it is not possible to establish a threshold value for the onset of corrosion. The data suggest, however, that bars with a chloride ion content of 5 lb/cy or higher are likely to exhibit corrosion provided that other conditions favorable to induce it also exist.

## CHAPTER 8. COMPARISON OF BRIDGE DECK CONDITION BETWEEN 1996 AND 2006

### 8.1 INTRODUCTION

This chapter presents a comparison between the results of the study conducted by Wiss, Janney, Elstner Associates, Inc. (WJE) in 1996 [32] with those from this study. These comparisons are presented separately for each bridge deck and include the data obtained from the field inspections, the chloride ion content analyses, and the assessment of the condition of the epoxy coated bars.

### 8.2 FIELD INSPECTION

A comparison of the field inspection of the decks in 1996 and 2006 showed that despite the appearance of new cracks the overall level of cracking in the areas inspected remained about the same. The rust stains and efflorescence observed in 1996 on the underside of the decks of bridges 27062, 27812, and 27815 are comparable to those in 2006. Bridge 19015, which has a bottom mat of ECR, did not show rust stains or efflorescence on the underside in 2006. The overall condition of the decks has not changed significantly since 1996. However, an increment in the area of delamination was observed.

Table 8.1 shows the amounts of delaminated areas detected on the decks with a chain drag in square feet and as a percentage of the inspected areas for this project.

*Table 8.1 Comparison of delaminated areas in 1996 and 2006*

| Bridge | Total Delaminated Area 1996 |      | Total Delaminated Area 2006 |      |
|--------|-----------------------------|------|-----------------------------|------|
|        | (ft <sup>2</sup> )          | (%)  | (ft <sup>2</sup> )          | (%)  |
| 19015  | 0                           | 0.0% | 39                          | 1.1% |
| 27062  | 2                           | 0.0% | 84                          | 1.1% |
| 27812  | 0                           | 0.0% | 20                          | 0.3% |
| 27815  | 0                           | 0.0% | 21                          | 0.4% |

The table shows that the delamination process has begun in all four bridges during the last ten years and, according to the Mn/DOT Bridge Inspection Manual [37] the total delamination area may be considered as “Condition State 2”.

As presented in section 6.8.2, the total delaminated area is very low in all bridges, notably in the decks of bridges 27812 and 27815 both of which had a 2.5 in. low slump, high density overlay. Given the current condition of the decks, it may be expected that delamination area would exceed increase in the next ten years unless some preventive or repair work is performed. Delamination would be expected to occur in areas where corrosion activity was detected by the half cell potential survey, or indirectly by high chloride ion content measurements at the bar level.

### 8.3 CHLORIDE ION CONTENT

In Table 8.2 the chloride ion content obtained from cores extracted in close proximity (within 3 ft.) in the decks of bridges 19015, 27812, and 27815 during the 1996 and the present study are compared (there were no cores extracted in 2006 in close proximity to cores extracted in 1996 in bridge deck 27062). The chloride ion content is shown at 0.5 in. in depth and at the bar level.

*Table 8.2 Comparison of chloride ion content test results 1996-2006*

| Bridge | Core Designation |      | Cl <sup>-</sup> 0.5" depth<br>(lb/cy) |      | Cl <sup>-</sup> Bar depth<br>(lb/cy) |      |
|--------|------------------|------|---------------------------------------|------|--------------------------------------|------|
|        | 1996             | 2006 | 1996                                  | 2006 | 1996                                 | 2006 |
| 19015  | 3                | DP   | 19.1                                  | 21.6 | 2.3                                  | 8.3  |
|        | 5                | DCS2 | 13.1                                  | 19.6 | 0.3                                  | 24.3 |
| 27812  | 10               | 22   | 9.6                                   | 12.3 | 5.7                                  | 1.3  |
|        | 11               | 23   | 6.7                                   | 10.8 | 0.5                                  | 5.4  |
| 27815  | 9                | 52   | 9.1                                   | 15.8 | 5.5                                  | 8.8  |

Note: Interpolated from readings taken at 0.2 and 0.6 in. depth (5 and 15 mm respectively)

The data show that the chloride ion content at a depth 0.5 in. has increased since 1996 as it would be expected. A similar result is observed for the chloride ion content at the bar level, except in core "22" of bridge 27812 (compared to core No. 10 in the 1996 study). During the 1996 study, the chloride ion content was measured at 5.7 lb/cy, while in this study the value was only 1.3 lb/cy. This result, however, is explained by the fact that the core extracted in 1996 was right on a vertical crack, while core "22" extracted in this study, was extracted a few inches away from that crack.

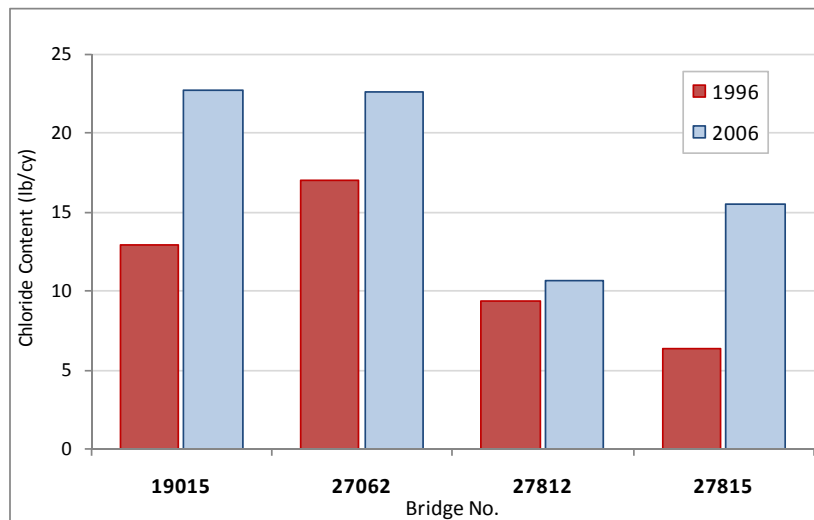
In Table 8.3, the average chloride ion content in each bridge deck at a depth of 0.5 in. from the surface is compared. The values shown correspond to measurements taken from cores without vertical cracks, or away from joints or delaminated areas. Also shown in the table is the standard deviation of each value. The last column in the table shows the percent increment in chloride ion content measured in 1996 and 2006. The same data is also plotted in Figure 8.1.



**Table 8.3 Comparison of average chloride ion content 1996-2006**

| Bridge | Avg. Cl <sup>-</sup> Content 0.5" depth<br>(lb/yd <sup>3</sup> ) |             | Increment<br>(%) |
|--------|--|-------------|------------------|
|        | 1996 (WJE) *   | 2006 (UW-M) |                  |
| 19015  | 12.9 (5.9)   | 22.7 (5.5)  | 76%              |
| 27062  | 17.0 (3.9)   | 22.6 (3.1)  | 33%              |
| 27812  | 9.4 (1.9)  | 10.7 (2.4)  | 14%              |
| 27815  | 6.4 (2.1)  | 15.5 (2.9)  | 142%             |

\*: Values interpolated from measurements taken at 0.2 and 0.6 in. depth (5 and 15 mm respectively) in the 1996 study.

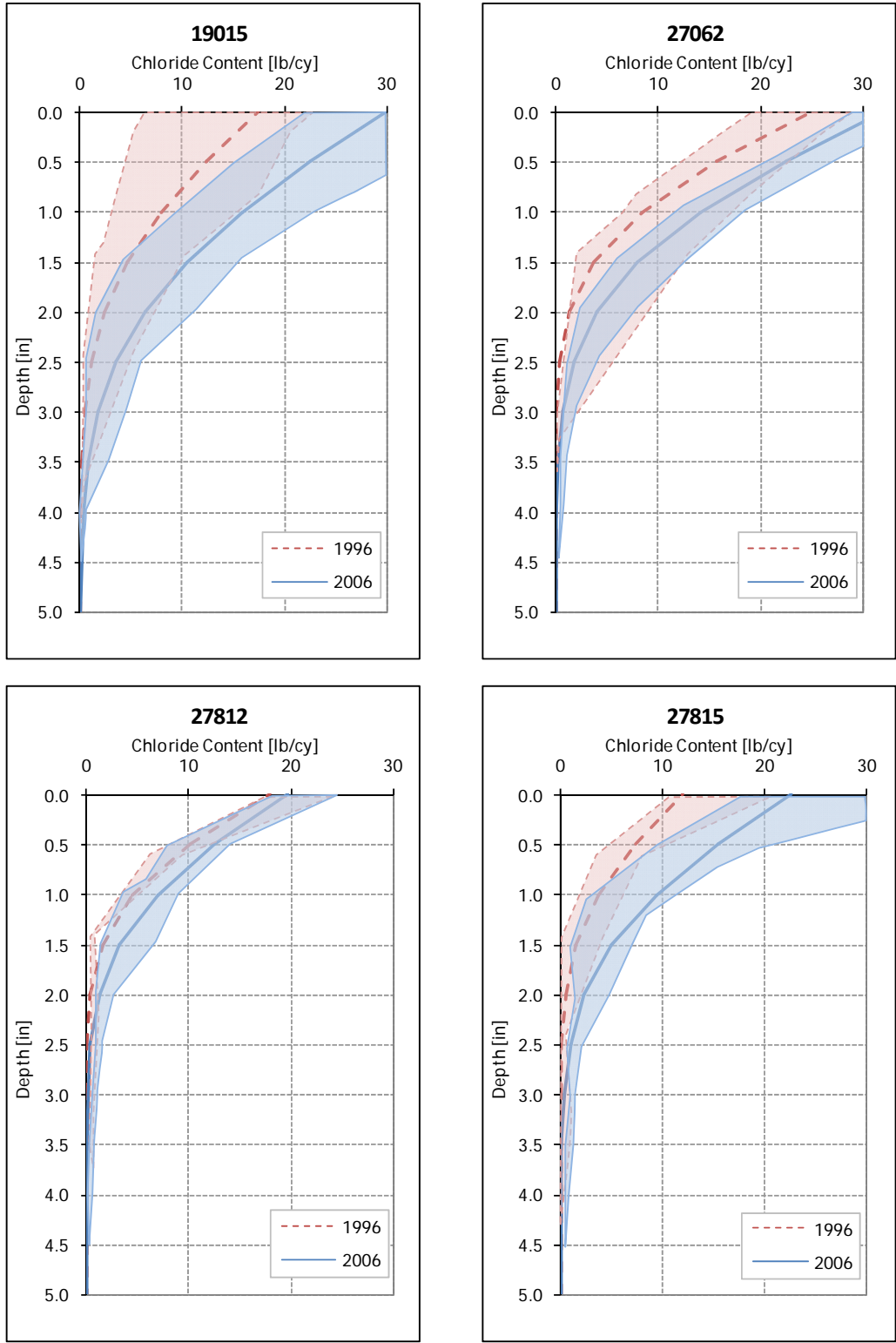


**Figure 8.1 Comparison of average measured chloride ion content at 0.5 in. below the surface in 1996 and in 2006.**

Table 8.3 and Figure 8.1 show that the chloride ion content has increased significantly in the last ten years in all bridges, but in particular in bridge 27815, which showed almost 2.5 times the chloride content detected in 1996. On the other hand, bridge 27812 showed a small variation remaining around 10 lb/cy. The larger increase in the near surface chloride ion content in bridge 27815 suggest that this deck may have been exposed to a larger salt rate application than the other decks.

In Figure 8.2, the envelopes of minimum and maximum values of the chloride ion content measured in 1996 and 2006 are shown. The shaded areas show the range of values measured for the chloride ion content over the depth in 1996 (shown in light red) and in 2006 (shown in light blue). Also shown in the figure is the average chloride ion content over the depth in 1996 (light red dashed line) and in 2006 (light blue continuous line). These averages were calculated on the basis of the chloride ion content at the surface and the measured diffusion coefficient. These average values are also shown at 0.5 in. increments in Table 8.4. These data show a significant

slump, high density overlays (bridges 27812 and 27815). As shown earlier in Figure 7.14, decks with low slump, high density overlays had, on average, concrete diffusion coefficients 30% smaller than decks without overlays. Thus, the lower chloride ion concentration measured at the near surface (Figure 8.1) combined with a lower diffusion coefficient help explain the lower chloride ion content at a given depth in decks with overlays.



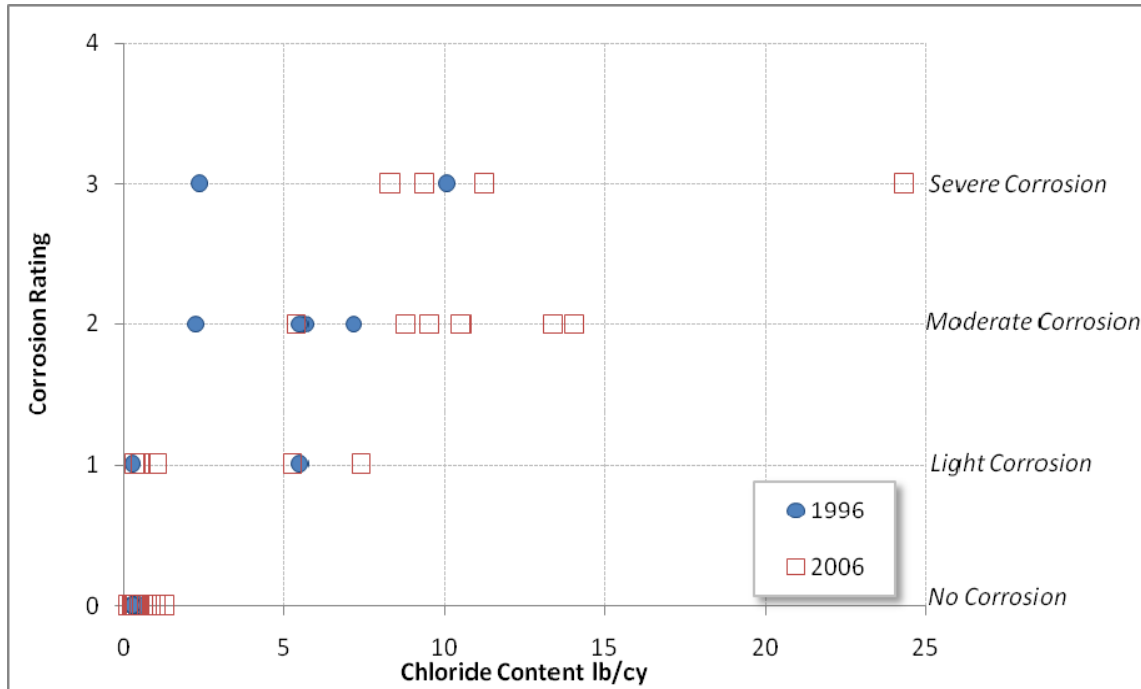
*Figure 8.2 Envelope of chloride ion content profiles in 1996 and 2006.*

**Table 8.4 Comparison of average chloride ion content**

| Bridge | Depth (in.) | Avg. Cl <sup>-</sup> Content (lb/yd <sup>3</sup> ) |             | Increment (%) |
|--------|-------------|--|-------------|---------------|
|        |             | 1996 (WJE)   | 2006 (UW-M) |               |
| 19015  | 0.0         | 17.50  | 29.90       | 71%           |
|        | 0.5         | 12.41  | 22.58       | 82%           |
|        | 1.0         | 7.97   | 15.94       | 100%          |
|        | 1.5         | 4.60   | 10.46       | 127%          |
|        | 2.0         | 2.37   | 6.36        | 168%          |
|        | 2.5         | 1.08   | 3.56        | 229%          |
|        | 3.0         | 0.44   | 1.84        | 319%          |
|        | 3.5         | 0.16   | 0.87        | 455%          |
|        | 4.0         | 0.05   | 0.38        | 666%          |
| 27062  | 0.0         | 25.00  | 32.10       | 28%           |
|        | 0.5         | 15.76  | 22.46       | 43%           |
|        | 1.0         | 8.40   | 14.14       | 68%           |
|        | 1.5         | 3.72   | 7.93        | 113%          |
|        | 2.0         | 1.36   | 3.94        | 190%          |
|        | 2.5         | 0.40   | 1.73        | 328%          |
|        | 3.0         | 0.10   | 0.66        | 581%          |
|        | 3.5         | 0.02   | 0.22        | 1074%         |
|        | 4.0         | 0.00   | 0.07        | --            |
| 27812  | 0.0         | 18.00  | 19.60       | 9%            |
|        | 0.5         | 10.19  | 12.59       | 24%           |
|        | 1.0         | 4.52   | 6.92        | 53%           |
|        | 1.5         | 1.54   | 3.21        | 109%          |
|        | 2.0         | 0.39   | 1.24        | 217%          |
|        | 2.5         | 0.07   | 0.40        | 434%          |
|        | 3.0         | 0.01   | 0.10        | 905%          |
|        | 3.5         | 0.00   | 0.02        | --            |
|        | 4.0         | 0.00   | 0.00        | --            |
| 27815  | 0.0         | 12.00  | 22.50       | 88%           |
|        | 0.5         | 7.34   | 15.40       | 110%          |
|        | 1.0         | 3.73   | 9.36        | 151%          |
|        | 1.5         | 1.54   | 5.01        | 226%          |
|        | 2.0         | 0.51   | 2.34        | 358%          |
|        | 2.5         | 0.13   | 0.95        | 603%          |
|        | 3.0         | 0.03   | 0.33        | 1076%         |
|        | 3.5         | 0.00   | 0.10        | --            |
|        | 4.0         | 0.00   | 0.03        | --            |

Figure 8.3 shows the corrosion condition of the extracted bars in both studies against the measured chloride ion content at the bar level. The figure shows that the chloride ion content at

the bar level has, on average, increased since 1996. This result is consistent with the increased chloride ion content measured at the surface of the decks (see Figure 8.1). Although the core location was non-randomly selected and the core area represents only a small fraction of the total bridge deck area, the fact that the present study detected more bars with light, moderate and severe corrosion than in 1996, is strong an indication that corrosion activity has increased in the last ten years.



**Figure 8.3** Relationship between chloride ion content at the bar level and corrosion condition of the bars.

It must be noted that the chloride ion concentration at the bar level in the majority of the bars that showed corrosion (light, moderate or severe) was about 5 lb/cy or greater. On the other hand, all bars without signs of corrosion had chloride ion concentrations at or below 1.3 lb/cy. There are, however, four exceptions to these results: one corroded bar from the 1996 WJE study that had a chloride ion content of 0.3 lb/cy and three corroded bars from the present study with chloride ion contents of 0.4 lb/cy, 0.5 lb/cy and 1.0 lb/cy. However, corrosion in two of these last bars is believed to have initiated elsewhere as discussed in section 7.8.6. On the other hand, the 1996 study showed two bars with moderate and severe corrosion where the chloride ion content was 2.3 and 2.4 lb/cy, respectively. These results suggest that corrosion may begin in ECRs at chloride ion contents between 1.3 lb/cy and 5.3 lb/cy.

## 8.4 EPOXY COATING EVALUATION

### 8.4.1 Coating deterioration

The lost of adherence, or disbondment, between the steel and the epoxy coating is relevant in this study because it may facilitate the initiation of the corrosion process. Therefore, a comparison of the change in coating adherence to the bar, if significant, can be an indicator of coating

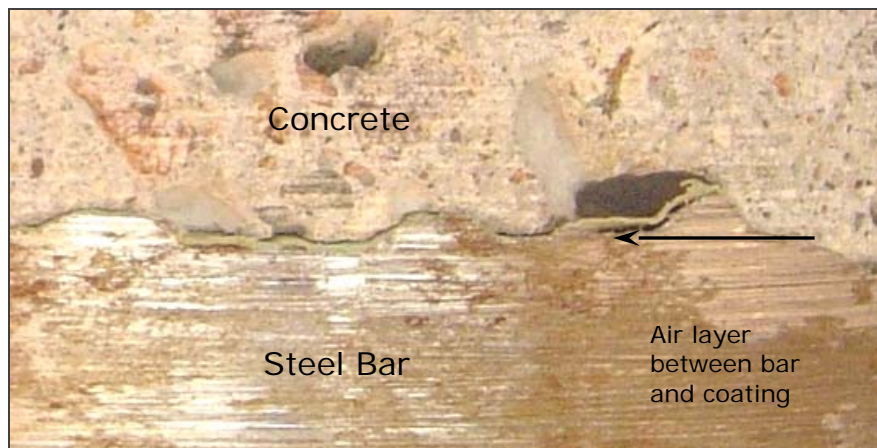
protection deterioration. To compare the results from both studies, the rating used in the WJE report (from 1 to 5) was converted, albeit approximately, to the ratings used in this study from 1 to 4 (see Table 5.3). Table 8.5 shows a comparison of the adherence test results of uncracked cores from the two studies. The table presents the minimum and maximum rating observed in all extracted bars.

**Table 8.5 Comparison of adherence test results 1996-2006**

| Bridge | Adherence Test<br>(1 no adherence – 4 good adherence) |      |             |          |
|--------|---|------|-------------|----------|
|        | 1996 (WJE)  |      | 2006 (UW-M) |          |
|        | Min.  | Max. | Min.        | Max.     |
| 19015  | moderate  | good | no          | poor     |
| 27062  | no  | good | poor        | moderate |
| 27812  | poor  | good | poor        | good     |
| 27815  | no  | good | no          | poor     |

It can be observed that in 1996 all bridges presented some bars with good adherence (rating 4), while the present study found bars with good adherence only in the bridge 27812. These results suggest that the adherence of the coating has deteriorated in the last ten years.

Poor adherence (rating 2) could be considered the limit after which coating disbondment develop a thin air layer between the steel and the coating (see Figure 8.4), and upon the arrival of chloride ions, corrosion underneath the coating could develop at a faster rate than with moderate or good adherence. However, the service life extension provided by coatings in various states of adhesion loss has not been studied in detail. Therefore, the level of protection provided by the epoxy coating with poor or moderate adherence is unknown at this time.



**Figure 8.4 Detail of coating disbondment in core.**

#### 8.4.2 Bar corrosion condition

The corrosion condition of the bars used in the WJE report [32] was described qualitatively as follows:

- Good or clean
- Minor rust, slight rust
- Corroded, corrosion
- Very corroded, heavy corrosion

This description is not the same as the one used in this study, but it is very similar (see Table 5.4). To compare the observed condition of the bars in both studies, the description used in the WJE study [32] was converted to that used here as presented in Table 8.6.

**Table 8.6** Conversion of corrosion condition between both studies

| Rating | This Study         | WJE Study                      |
|--------|--------------------|--------------------------------|
| 0      | No corrosion       | Good or clean                  |
| 1      | Light corrosion    | Minor rust, slight rust        |
| 2      | Moderate corrosion | Corroded, corrosion            |
| 3      | Heavy corrosion    | Very corroded, heavy corrosion |

In Table 8.7, the bar corrosion condition observed in the 1996 and 2006 studies are compared. The table presents the minimum and maximum ratings observed in all extracted bars for each bridge deck.

**Table 8.7** Comparison of the bar corrosion condition in 1996 and 2006

| Bridge | Corrosion Condition |          |              |          |
|--------|---------------------|----------|--------------|----------|
|        | 1996 (WJE)          |          | 2006 (UW-M)  |          |
|        | Min.                | Max.     | Min.         | Max.     |
| 19015  | No corrosion        | moderate | No corrosion | heavy    |
| 27062  | No corrosion        | heavy    | No corrosion | light    |
| 27812  | No corrosion        | moderate | No corrosion | moderate |
| 27815  | No corrosion        | heavy    | No corrosion | heavy    |

In general, the table shows that after three decades of service, there are still bars in good condition, with no signs of corrosion. These bars were generally located away from cracks, joints or delaminated areas. On the other hand, clear indications of bar corrosion were generally observed at or near cracks and at joints. In 1996, 31% of the extracted bars had some level of

corrosion, while in 2006, 50% of the extracted bars were corroded. This result, however, should not be construed as indicator of the performance of epoxy-coated bars over the entire deck because a) the number of bars extracted represent a small fraction of the total bar area in the decks and b) many of the extracted bars were purposely extracted at locations where corrosion activity was suspected. Nonetheless, the higher level of corrosion activity in the extracted bars observed in 2006 is consistent with the increase in chloride content measured in the decks and suggests that corrosion activity has increased.

A holiday count of the bars was not conducted in this study (see section 5.5). The 1996 WJE study show an extremely high count for the bar in all decks (an average value ranging from 22 to 40 per foot). In that study, however, it was not possible to establish the source of the holidays, i.e., manufacturing-related or due to coring or bar removal. Therefore, it cannot be determined whether the corrosion activity observed in the bars was initiated by the presence of holidays or by deterioration of the epoxy coating, or both.

It is important to emphasize that some of the cores were intentionally taken at locations representing a worst case. Of the nineteen corroded bars found in the cores, only four bars showed severe coating disbondment with corrosion (e.g., Figure 2.1). However, no section loss could be measured in any of these bars. Therefore, these cores may not be representative or indicative of the overall condition of the ECRs.

## **8.5 ESTIMATING THE CORROSION CONDITION OF ECR IN BRIDGE DECKS**

The results of the present and the 1996 study show that ECR surrounded by a chloride ion content of 5.0 lb/cy or greater presented corrosion, while bars with a chloride ion concentration of 1.3 lb/cy or less presented no signs of corrosion. The data also show that the chloride ion content profile can be approximated well using the second Fick's law. Using this law, the time it takes chloride ions to migrate through the concrete from the surface to the bar level may be estimated.

For this approximation, it is necessary to know three parameters:

- a) The age of the bridge
- b) The chloride content near the surface
- c) The diffusion coefficient

In the following, the procedure to estimate the corrosion condition of the ECR is described. This procedure involves two main steps:

- a) Estimation of the chloride ion content profiles over time.
- b) Estimation of the chloride ion content at the bar level corresponding to the onset of corrosion.

### **8.5.1 Estimation of chloride ion depth profiles**

In practice, the chloride content near the surface may be measured in the field by drilling and taking powder samples directly from the bridge deck, as was done in this study. Similarly, the diffusion coefficient may be calculated by taking chloride ion content at different depths from cores without or away from vertical cracks, joints or delaminated areas. In the absence of field



data, the near surface chloride ion content may be obtained from other studies on bridges of similar age, weather and maintenance conditions. Typical values for the diffusion coefficient can be assumed between 0.01 and 0.05 in/yr<sup>2</sup> [2, 7], with 0.05 in/yr<sup>2</sup> as a conservative value.

Knowing the near surface chloride ion content and the diffusion coefficient, the chloride ion content at the surface is calculated (*i.e.*, at 0 in. depth). This calculation is made by solving the equation *D.2* (see Appendix D) for  $C_s$  using the near surface chloride ion content (taken at 0.5 in. deep in this study). Some researchers [2, 21, 6, 7, 7, 40, 38 and 39] do not follow this step and assume the value of the chloride ion content near the surface as  $C_s$ . However, this assumption may lead to errors that may affect the computed values of chloride ion content in 10% to 20% for bridges with more than 40 years of service, and 20% to 50% for bridges with less than 40 years.

Table 8.8 shows the parameters used to calculate the profile for each bridge deck studied, *i.e.*, the average measured of chloride ion content at 0.5 in. deep, the age of the bridge, the average measured diffusion coefficient, and the computed chloride ion content at the surface. Figure 8.5 shows the different profiles curves obtained.

**Table 8.8** Parameters used to calculate the chloride ion profiles

| <b>Bridge No.</b> | <b>C (lb/cy)</b> | <b>Age (years)</b> | <b>D<sub>eff</sub> (in/yr<sup>2</sup>)</b> | <b>C<sub>s</sub> (lb/cy)</b> |
|-------------------|------------------|--------------------|--|------------------------------|
| 19015             | 22.7             | 34                 | 0.039                                      | 29.9                         |
| 27062             | 22.6             | 29                 | 0.030                                      | 32.1                         |
| 27812             | 10.7             | 30                 | 0.020                                      | 16.5                         |
| 27815             | 15.5             | 29                 | 0.027                                      | 22.5                         |

It may be recalled that this model represents the chloride ion ingress into the concrete in healthy areas of the deck, *i.e.*, away from vertical cracks, joints or delaminated areas. Any of these defects will affect the one-dimensional diffusion phenomenon increasing the chloride ion content at lower depths (see for example core “AP” in Figure 7.3).

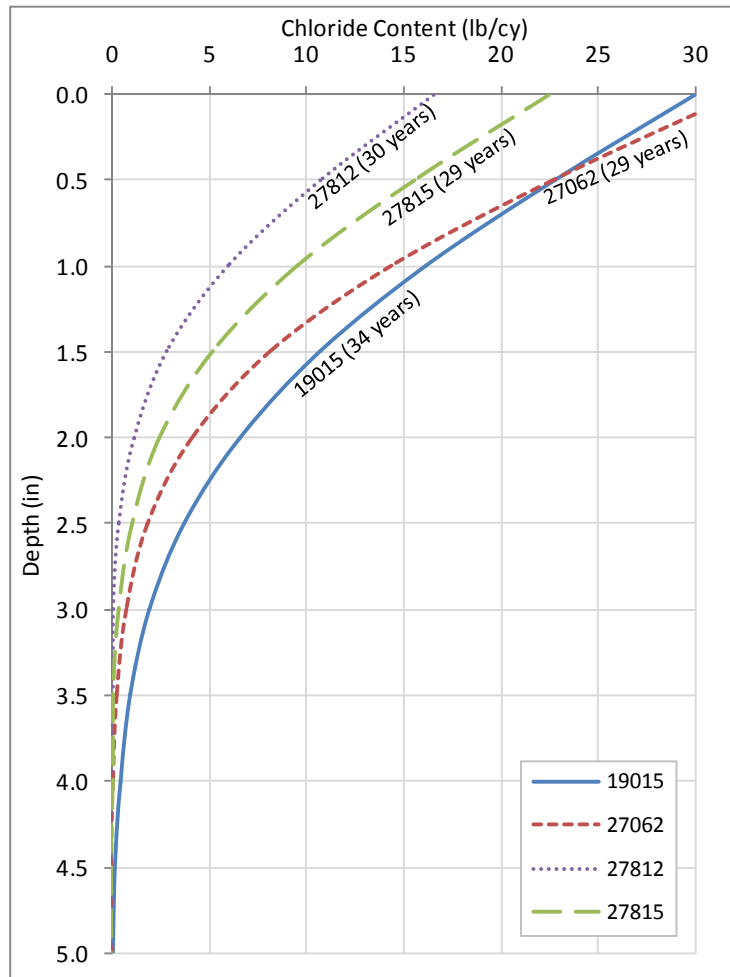
### **8.5.2 Estimation of the chloride content at the bar level corresponding to a given corrosion activity level**

Once the chloride ion depth profile is estimated, the calculation of the chloride ion content at the bar level is a direct application of equation *D.2* (see appendix D). As an example, in Figure 8.5, the chloride ion content at 4 in. deep in 2006 has maximum value of 0.4 lb/cy. This content is well below the values observed for corrosion and suggests that no bar located at 4 in. deep from the surface and away from cracks or joints should have begun corroding in 2006, a result that is consistent with field observations from this and the 1996 study.

The level of corrosion activity in the bar can be described by the relationship between chloride ion content and corrosion condition as presented in section 7.8.6 and in Figure 8.3. Based on the

data obtained in this investigation and the 1996 study, this relationship will be simplified using the following thresholds of corrosion activity:

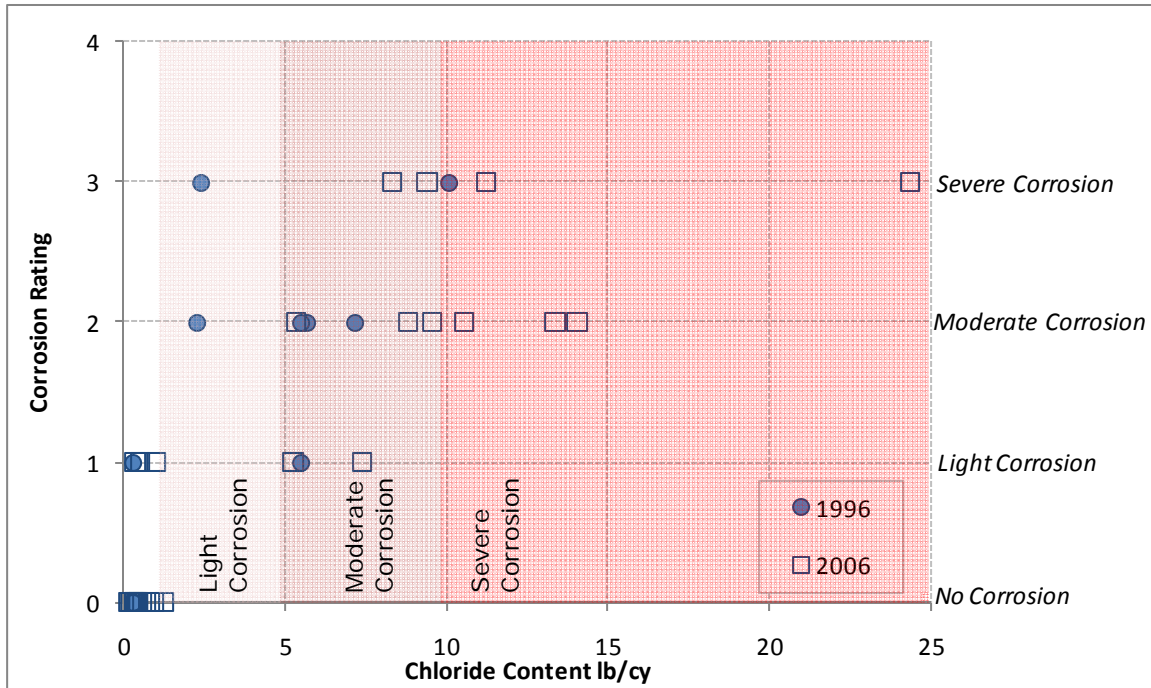
| Corrosion Activity Level    | Chloride Content Threshold (lb/cy) |
|-----------------------------|------------------------------------|
| Onset of or light corrosion | 1.2 - 5.0                          |
| Moderate                    | 5.0-10.0                           |
| Severe                      | >10.0                              |



**Figure 8.5** Estimated chloride ion content profiles in 2006 for the decks studied.

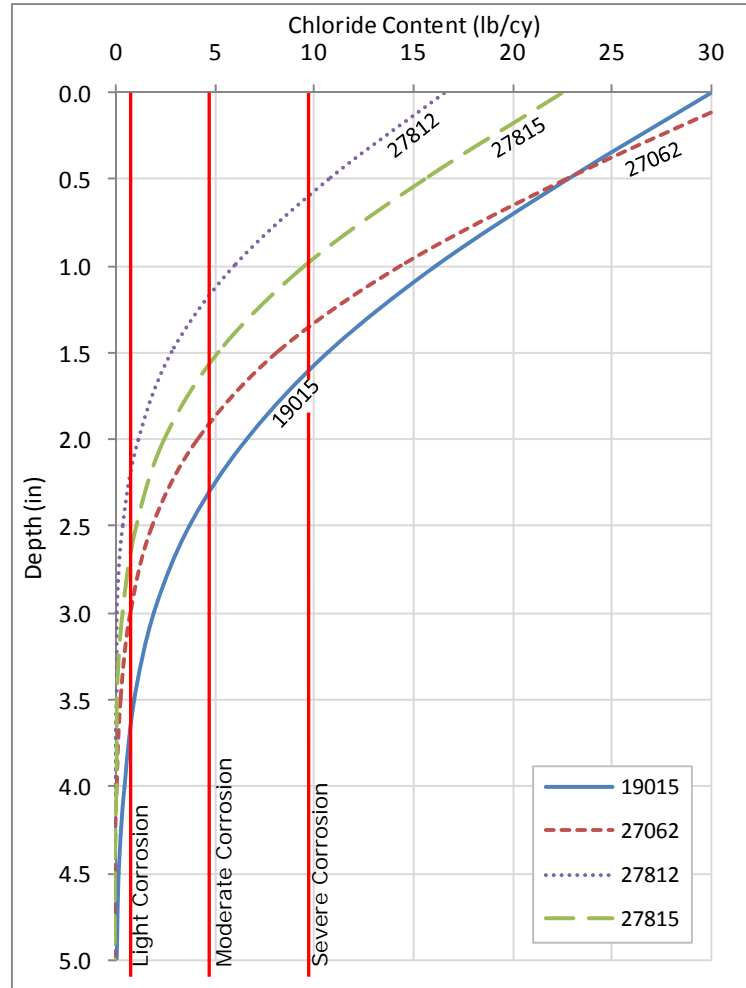
Note that a range of values is provided, rather than a single value for the threshold of chloride ion content corresponding to a given level of corrosion activity, which reflects the observations gathered from the 1996 and 2006 studies. Also, while the data obtained here is insufficient to provide a statistically reliable average value in each range, the data suggest that light corrosion is more likely to be encountered toward the higher end of the provided range, i.e., at chloride ion contents closer to 5 lb/cy.

Figure 8.6 shows the data from the two studies (1996 and 2006) and the range of chloride ion content values defined above for each corrosion condition. These values are an approximation based on the data collected in this study; however, it is consistent with data from other studies.



**Figure 8.6** Regression of chloride ion content and corrosion condition.

Using the lower limit of chloride ion content corresponding to a given corrosion condition in each range, and the average chloride ion profiles of each bridge, the relation between chloride ion concentrations and corrosion activity can be plotted. In Figure 8.7, the estimated chloride ion content profiles in 2006 and the chloride ion content thresholds levels defined above are shown for all four bridges studied. For example, in Fall 2006 the bars at a depth of cover of 3 in. in bridge 19015 would have begun to corrode. At a depth of cover of 2.5 in., the bars in bridge decks 19015, 27062 and 27815 would be above the lower limit of chloride content for light corrosion and at a depth of cover of 2 in. or less, the bars in all four bridges would be above that lower limit.



**Figure 8.7** Estimated chloride ion content profiles in 2006 and bar corrosion threshold levels for the bridges studied.

To estimate the service life of a deck in years, the addition of two terms is commonly used [2,21,6,7,40,39]: Time of corrosion initiation ( $T_{ini}$ ) and time of corrosion propagation ( $T_{prop}$ ).

$$Service\ Life = T_{ini} + T_{prop} \quad (8.1)$$

The time of propagation is commonly expressed as the number of years required to reach a state of generalized corrosion. This estimation is described in section 2.2.4. The time of corrosion initiation can be estimated by solving the Fick's equation (see appendix D) for time  $t$  until the chloride ion content at the bar level reaches the threshold for corrosion initiation. For this example, the onset of corrosion will be conservatively assumed to be 1.2 lb/cy, with the caveat that initiation of corrosion is likely to occur a higher contents as discussed above.

$$C(x) = C_s \left[ 1 - erf \left( \frac{x}{2\sqrt{tD_{eff}}} \right) \right] \quad (8.2)$$

where  $x$  (in) is the depth,  $t$  (yr) is the time in years,  $C_s$  (lb/cy) is the chloride surface concentration,  $D_{eff}$  (in<sup>2</sup>/year) is the effective diffusion coefficient, and  $erf()$  is the Gaussian error function. Some investigators assume that the chloride ion content at the surface ( $C_s$ ) remains constant during the service life of the deck. In Figure 8.2 it was shown, however, that the chloride ion content at the surface increases over time. Lindquist et al. [40] presented several linear regressions of chloride content values at different depths. These regressions were developed using data from more than 500 bridges studied. One of these linear regressions establishes that chloride content at 1 in. depth will increase 0.57 lb/cy per year in deck areas away from cracks. In areas at cracks the chloride concentration expected at 1 in. depth will be 1.76 lb/cy for the first year and will increase 0.66 lb/cy per year. This means that chloride content would show the same increment at any year. However, the chloride ion concentration values obtained using the approximation proposed by Lindquist et al. do not agree with typical values reported in the literature.

Because the solution needs to consider the chloride ion concentration  $C(x)$  as function of depth and time ( $C(x,t)$ ), it is necessary to use of a different approach. To model the chloride ion content profiles over the time, the main and most significant variable is the chloride ion concentration at the surface. The prediction of this progression over the time is beyond the scope of this study and further research is needed. However, as a first approximation, the increment of chloride ion content at the surface can be modeled using the following equation:

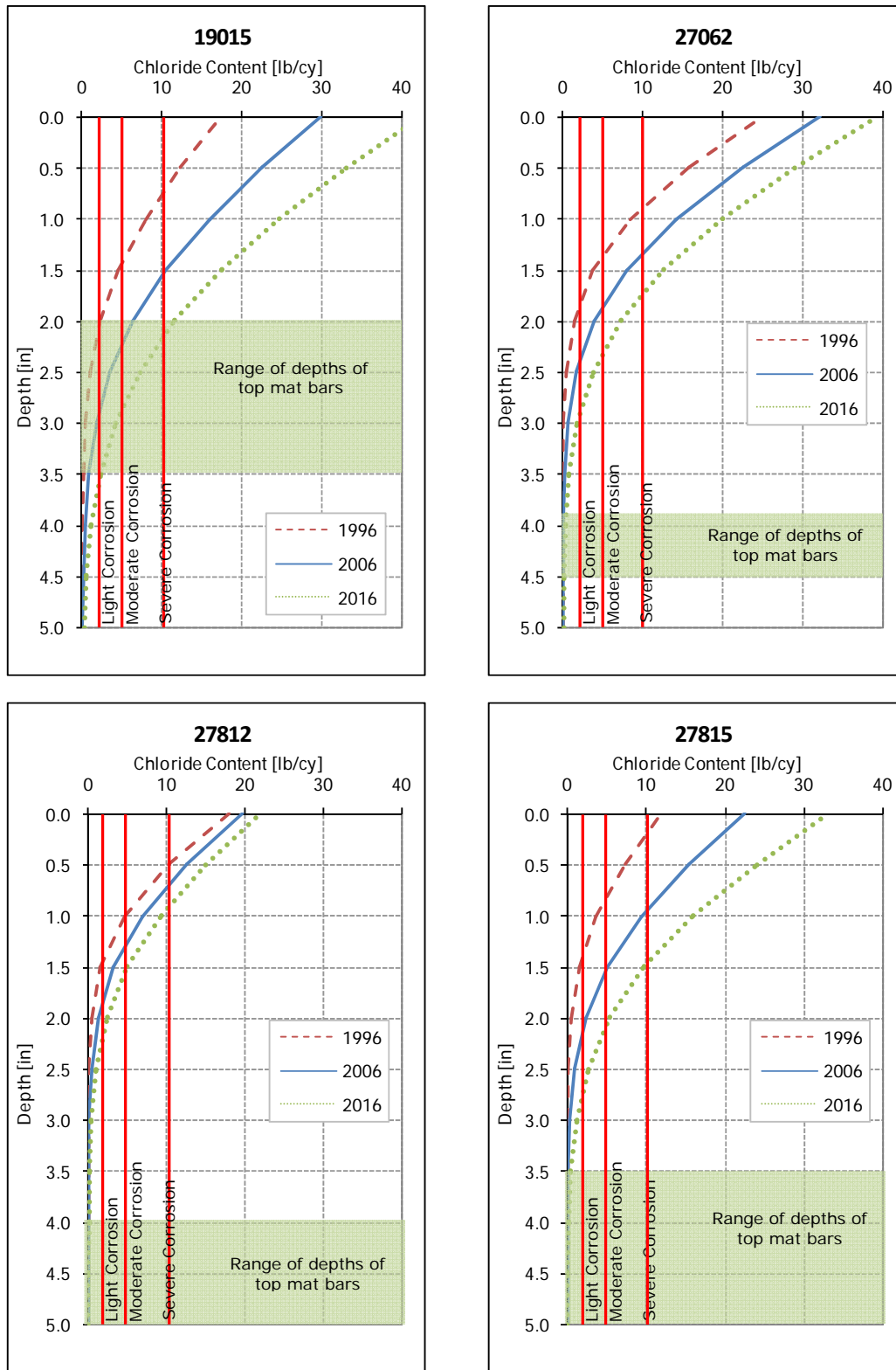
$$C_s(t) = C_{\max} \left[ 1 - e^{-t/t_{\max}} \right] \quad (8.3)$$

where  $C_s(t)$  (lb/yd<sup>3</sup>) is the chloride surface concentration,  $C_{\max}$  (lb/yd<sup>3</sup>) is the maximum chloride surface concentration,  $t$  (yr) is the time, and  $t_{\max}$  (yr) is the maximum modeling time. Using finite differences approximation to solve the Fick's equation (equation D.1 in Appendix D) and the progression of chloride ion content at the surface with equation 8.3, the chloride ion concentration progression over time may be calculated (see Figure 8.8). The figure also shows the lower limit of chloride ion concentration for each range of corrosion activity level defined earlier. This is conservative. The figure is presented in different scales to emphasize the relation between light corrosion, cover depth and service years. These curves were calculated using a conservative diffusion coefficient of 0.05 in/yr<sup>2</sup>.

Figure 8.8 shows a comparison between chloride ion profiles from 1996, 2006 and the predicted curve for year 2016. The predicted profile was calculated assuming the same increment in chloride ion content observed in the period 1996-2006. The figure also shows the range of depths where the top mat bars were found. It can be observed that bars in bridges 27062, 27812 and 27815 show a very low probability of light corrosion by 2016. However, the bars in bridge 19015 show high probability of moderate to severe corrosion by 2016.

Note that at a depth of 3 in. in Bridge 19015, light corrosion will be expected at about 30 years of service (2003). However, at a depth of 2 in. (the minimum cover depth measured in this study), light corrosion is expected to occur only after 20 years of service. This means that, increasing the concrete cover by 1 in. can delay the onset of corrosion by about 10 years. These curves estimate the variation of chloride ion content in time and depth accordingly to the data obtained in this

study. This approach is semi-empirical and must be corroborated with a larger amount of data from several bridges in different conditions.



**Figure 8.8** Example of chloride ion content profiles predicted for year 2016.

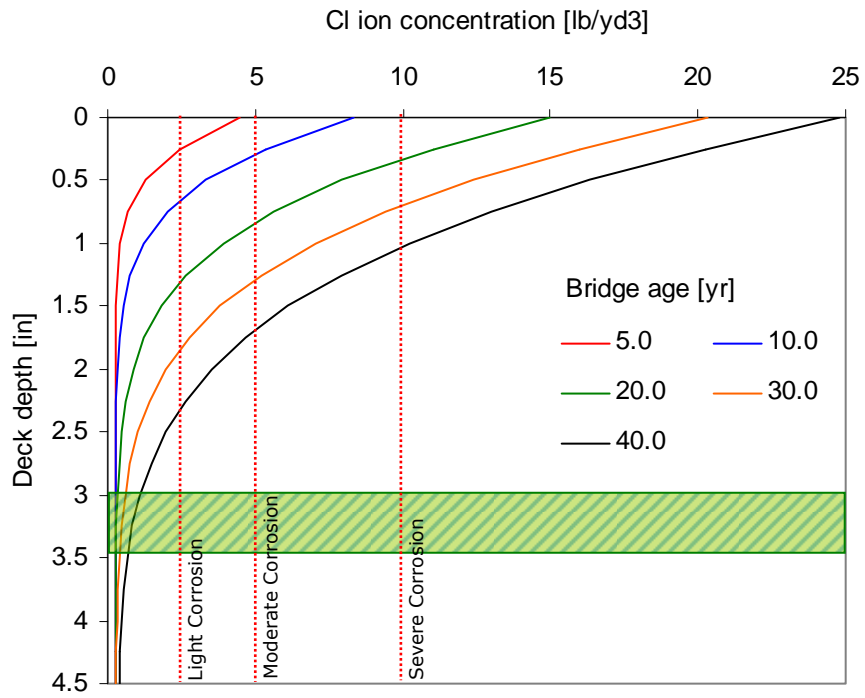
It should be emphasized that the data presented in Figure 8.8 do not incorporate the effect of cracks on the chlorine ion concentration profiles. The presence of cracks is extremely important in the estimation of the remaining service life of bridge decks as they act as discontinuities that

greatly increase the chlorine ion concentration adjacent to the bar. If cracks are present on the deck surface, the chloride ion concentration distribution changes as cracks allow direct ingress of chlorides into the concrete. Conservatively, the chloride concentration over the crack depth may be assumed to be the same as that at the surface. This assumption is supported by the measurements made over the depth the crack which showed that the chloride ion content remains nearly constant with depth at a crack (see Figure 7.9). To evaluate the effect of cracks in the chloride ion content and the reduction in service life, a simple example is presented next.

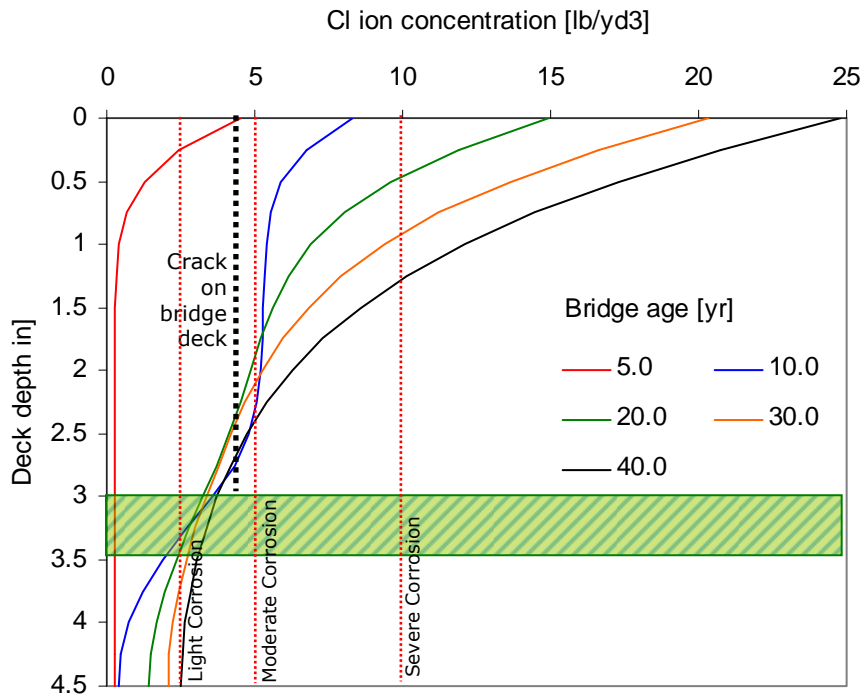
Figure 8.9a shows the theoretical chloride ion distribution versus depth for an uncracked bridge deck surface at 5, 10, 20, 30 and 40 years of service using a diffusion coefficient of  $0.039 \text{ in}^2/\text{yr}$ . For a 3 in. deep coated rebar, no corrosion would be expected to occur in 40 years of service in the uncracked deck. The chloride ion distribution for a cracked deck is shown in Figure 8.9b. For example, if at the fifth year a crack is formed, the surface chloride ion concentration will rapidly propagate along the face of the crack. Assuming that the concentration at the bar level is the same as that on the surface in that year, a new chloride content distribution will occur over the depth (see distribution at ten years – blue line). The chloride content at the bar level increases drastically and the bar is expected to show light to moderate corrosion shortly after the crack is formed. If the crack is sealed after one year, the chlorides at the bar level will gradually diffuse into the surrounding concrete areas and the chloride content distribution profiles will, in the long-term, become similar to those calculated for the uncracked deck (see profiles for 30 and 40 years in Figure 8.9b).

Given the variability of the parameters of ECR condition and chloride content profiles that may be encountered in practice, the number of decks surveyed in this study is insufficient to provide a statistically reliable assessment of service life estimates. The complex interaction of epoxy coating adhesion deterioration, the presence of holidays and/or surface defects of the coating, and the formation and sealing of cracks (corrosion deterioration can be greatly slow down by sealing cracks as soon as they occur) must also be estimated. Furthermore, the influence of a bottom mat of black steel on the onset of corrosion and corrosion propagation was not studied here and is unknown. Nonetheless, the procedures presented together with the field data gathered in this and the 1996 studies provide a tool for making reasonable estimates of the condition of the epoxy coated bars in a given year.





(a)



(b)

**Figure 8.9** Effect of a surface crack in year 5 (and sealed in year 6) on the chloride ion concentration distribution. (a) non-cracked bridge deck chloride ion distribution and (b) cracked bridge deck chloride ion distribution.

## **CHAPTER 9. SUMMARY AND CONCLUSIONS**

### **9.1 SUMMARY**

Exposure of reinforced concrete to chloride ions is the primary cause of premature corrosion of steel reinforcement in bridge decks. The use of epoxy-coated bars in bridge structures became a standard procedure by the early 1980s; however, few field studies have been conducted to assess the long term performance of epoxy coated bars in bridge decks.

The primary objective of this study was to evaluate the performance of epoxy coated bars (ECR) in four bridge decks built in the early 1970s in the Minneapolis/St. Paul, MN metropolitan area. The study included field measurements and laboratory tests. The field investigation included: (1) visual inspection, chain drag surveys, and documentation of existing damage; (2) half-cell potential measurements, electrochemical impedance spectroscopy, and ground penetrating radar surveys, and (3) extraction of core samples at selected locations. In the laboratory, carbonation depth and acid-soluble chloride ion concentrations at various depths were measured from the cores extracted in the field. The condition of the extracted ECRs was evaluated in terms of coating hardness, adhesion and thickness, and the corrosion level of the bars.

Based on the results of the present investigation and those from a 1996 study conducted on the same bridge decks, the changes in the corrosion condition of the bars, the amount of delamination, and the chloride ion content in the decks was assessed. In addition, a procedure for estimating the service life of the decks to reach a given corrosion level in the bars is proposed. Recommendations for future studies and test methods are also provided.

### **9.2 MAIN FINDINGS**

#### **9.2.1 *ECR performance***

- a) The data gathered in this study showed that the majority of the bars with chloride ion content at the bar level of 1.3 lb/cy or lower, had no signs of corrosion. On the other hand, most bars with chloride ion content of 5.3 lb/cy or higher, showed corrosion.
- b) Most corroded bars were found at or near vertical cracks, joints or delaminated areas, where the chloride ion content was 5.3 lb/cy or greater. Bars away from these areas were in good condition.
- c) Coating disbondment was found with and without rebar corrosion.
- d) The measured coating thickness of all bars extracted from bridges 27062, 27812 and 27815 was within the limits specified in current standards. In bridge 19015, however, 60% of the extracted bars had a coating thickness of 6 mils, slightly less than the minimum of 7 mils required by today's standards. The rest of the bars had coating thicknesses within the limits. Overall, however, the results suggest that the coating hardness and thickness of the bars extracted from these decks are comparable to those of the bars used today.

#### **9.2.2 *Chloride Ion Content***

- a) The average measured chloride ion content near the surface (at 0.5 in. depth) varied between 10 and 23 lb/cy.

- b) The chloride ion content at the bar level at a vertical crack was, on average, 20 times greater than that away from the crack at the same depth.
- c) In vertical cracks, the value of chloride ion content was found to be nearly constant with depth and similar to the concentration measured at the surface.
- d) The average measured chloride ion content near the surface (0.5 in. deep) in decks with a low slump, high density concrete overlay (bridges 27812 and 27815) was less than in the other two bridges without overlays (bridges 19015 and 27062).
- e) The measured average diffusion coefficient was found to be 30% lower in decks with a low slump, high density concrete overlay than in decks without overlays.
- f) Carbonation depth measurements were found to be very small (i.e., 3 mm or less), much smaller than the rebar cover in all four decks studied.

### **9.2.3 Observations from field inspections and surveys**

- a) The amount of delamination measured in all decks was very low. The maximum extent of the delaminated area was less than 1.1% of the inspected deck surfaces. Also, the amount of delamination in decks with low slump, high density concrete overlays (bridges 27812 and 27815) was smaller (less than 0.4%) than in the decks without overlays (bridges 19015 and 27062).
- b) Decks supported on concrete girders (19015 and 27812) presented fewer cracks than decks supported on steel girders.
- c) Bridge 19015, which had both top and bottom mats with ECRs, had no efflorescence or rust staining on the underside of the deck. The three other bridges, which had black bars for the bottom mat, all showed some level of efflorescence and rust staining on the underside of the bridge.
- d) The use of the half-cell potential (HCP) method was found to be very effective to identify the corrosion activity, even when the deck had ECRs in both mats. This result, however, is mainly due the use in this study of several electrical connections points to the top mat rather than a single point as is commonly done in bridge decks with black bars.
- e) Some of the cores were intentionally taken at locations representing a worst case. Therefore, these cores may not be representative or indicative of the overall performance of the deck nor of the overall condition of the ECRs.

## **9.3 CONCLUSIONS**

- a) After 30 years of service, the overall condition of epoxy-coated bars in these decks is good to very good, with no or modest levels of corrosion activity. In only one bridge (bridge 19015), corrosion activity appears to be moderate to severe. Furthermore, the amount of delamination in all decks is very low.
- b) The epoxy coated bars used in the bridge decks studied are likely to show corrosion when the bar level chloride ion content level is 5.3 lb/cy or greater. The mechanism by which corrosion will initiate, i.e., deterioration of the epoxy coating, the presence of holidays or surface defects in the coating or a combination of these, is unknown.
- c) The lower chloride ion content measured near the surface, the lower diffusion coefficient, and the smaller amount of delamination observed in decks with overlays suggest that a low slump, high density overlay can extend the service life of concrete bridge decks.

- d) Based on the observed performance of ECRs and using a model for predicting the rate of increase in chloride concentration at the bar level for the bridge decks studied here, the bars away from cracks or joints, and with depths of cover of 3.5 in. or greater (bridges 27062, 27812, and 27815) should exhibit no corrosion for another 20 to 25 years. In bridge 19015, where cover depth is less (2 in. minimum) corrosion activity is expected to have already begun, but has not caused significant delamination.
- e) At cracks or joints, the bar level chloride ion content may be conservatively assumed to be the same as the near surface chloride ion content.
- f) In this study, the bars showed loss of coating adherence in both corroded and non-corroded bars. Therefore, disbondment of the coating may not only be related to corrosion of the bar, but also to the aging of the coating under sustained moisture environment.
- g) In all bridge decks studied, the carbonation depth was much smaller than the rebar cover (less than 3 mm). Thus, carbonation cannot be considered to contribute to corrosion of the ECRs nor be the source of bar coating deterioration.
- h) In this study, one bridge deck (bridge 19015) had epoxy-coated bars in both the top and bottom mats, while the other three decks studied had epoxy-coated bars only in the top mat. The results showed no evidence that a bottom mat of black bars causes more or less corrosion on the top mat of epoxy-coated bars.
- i) Electrochemical impedance spectroscopy (EIS) is an effective method to identify rebar coating deterioration or defects.
- j) Ground penetrating radar measurements provided rapid rebar location, depth measurements, and distribution of volumetric water content on the bridge deck studied.

#### **9.4 RECOMMENDATIONS**

- a) Joints and cracks should be sealed immediately to prevent direct ingress of deicing salts and humidity to the reinforcing bars.
- b) The current practice of providing 3.0 in. bar cover or more should be continued to delay the ingress of high levels of chlorine ions to the bar level.
- c) The current Mn/DOT practice of using epoxy-coated bars for both the top and bottom mats should enhance the overall health of the bridge deck and should be continued.
- d) Because of the strong dependence between chloride ion content and bar corrosion initiation, near-surface powder samples should be monitored regularly (e.g., every 10 years). Fick's law may be used to estimate the chloride content at the bar level.
- e) For future studies, it is recommended that cores should be extracted from healthy and delaminated areas. This will provide detailed information about bars with corrosion activity in its propagation stage. Furthermore, a follow up study should be conducted in 2016 to assess the conditions of the deck and corroborate the findings of this study.
- f) Systematic monitoring of corrosion activity (using some of the methods used in this study) should be implemented to closely evaluate the structural health of these aging bridge decks.

#### **9.5 FINAL REMARKS**

After approximately 30 years of service, the bridge decks are in overall good condition. The decks showed light cracking and few delaminated areas, and only one deck (bridge 19015) had

an open spalled area. Overall delaminated and spalled surfaces represented a small fraction of the total bridge deck area (less than 1.1 % of the total surveyed areas).

The data obtained in this and the 1996 studies show that epoxy coated bars used in the bridge decks studied are likely to show corrosion when the chloride ion content in the surrounding concrete reaches 5.3 lb/cy. Only a few bars (three bars in this study and one bar in the 1996 study) showed corrosion at a chloride ion content level comparable to that of black bars (i.e., 1.2 lb/cy). The procedures for coating fabrication and application, as well as storage and handling of the bars in the field have improved significantly in the last 30 years through tighter specifications and plant certification programs. As a result, the quality of the epoxy coating and therefore the performance of the bars used today are expected to be as good as or better than that observed in this study.

## REFERENCES

1. Gannon, E.J. and Cady, P.D., *Condition Evaluation of Concrete Bridges Relative to Reinforcement Corrosion, Volume 1: State of the Art of Existing Methods*, Strategic Highway Research Program, Publication No. SHRP-S/FR-92-103, National Research Council, Washington, D.C., 1992.
2. Fanous, F., Wu, H., and Pape, J., *Impact of Deck Cracking on Durability*, CTRE Management Project 97-05, Iowa DOT project TR-405, Iowa, 2000.
3. Smith, J.L. and Virmani, Y.P., *Performance of Epoxy Coated Rebars in Bridge Deck*, Report FHWA-RD-96-092, Federal Highway Administration, Washington, D.C., 1996.
4. Xi, Y., Abu-Hejleh, N., Asiz, A., and Suwito A., *Performance Evaluation of Various Corrosion Protection Systems of Bridges in Colorado*, Report No. CDOT-DTD-R-2004-1, CDOT, Research Branch, 2004.
5. Page, C.L., Bamforth, P.B., and Figg, J.W., Editors, *Corrosion of Reinforcement in Concrete Construction*, Royal Society of Chemistry, Cambridge, U.K., 1996.
6. Weyers, R.E., Pyc, W., Zemajtis, J., Liu, Y., Mokarem, D., and Sprinkel, M.M., "Field Investigation of Corrosion-Protection Performance of Bridge Decks Constructed with Epoxy-coated Reinforcing Steel in Virginia", *Transportation Research Record*, No. 1597, Washington, D.C., 1997, pp. 82-90.
7. Weyers, R.E., Sprinkel, M.M., and Brown, M.C., *Summary Report on the Performance of Epoxy-Coated Reinforcing Steel in Virginia*, Report VTRC 06-R29, Virginia Transportation Research Council, 2006.
8. Cady, P.D. and Weyers, R.E., "Chloride Penetration and the Deterioration of Concrete Bridge Decks", *Cement, Concrete and Aggregate*, Vol. 5, No. 2, 1983, pp. 81-87.
9. Munjal, S.K., *Evaluation of Epoxy-Coated Reinforcing Steel in Bridge Decks*, Interim Report No. FHWA-MD-82/03, Maryland State Highway Administration, Brooklandville, Maryland, March 1981, 137 pp.
10. Sagüés, A.A., Chang, C., Pickering, H., Nystron, E., Carpenter, W., Kranc, S.C., Simmons, T., Boucher, B., and Heirholzer, S., *Corrosion of Epoxy-coated Rebar on Florida Bridges*, Report WPI No. 0510603, State Job No. 99700-7556-010, Florida Department of Transportation, 1994.
11. Malasheskie, G.J., Maurer, D.A., Mellott, D.B., and Avellano, J.L., *Bridge Deck Protective Systems*, Report No. FHWA-PA-88-001+85-17, Federal Highway Administration, Washington, D.C., July 1988, 61 pp.
12. Berke, N.S., "The Use of Anodic Polarization to Determine the Effectiveness of Calcium Nitrite as an anodic Inhibitor", *Corrosion Effect of Stray Currents and the Techniques for Evaluating Corrosion of Rebars in Concrete*, ASTM STP 906, V. Chaker, Ed., American Society for Testing and Materials, Philadelphia, PA, 1986, pp. 78-91.
13. Sohahngpurwala, A.A., Scannell, W.T., and Viarengo, J., *Verification of Effectiveness of Epoxy-coated Rebar*, Project 94-05, Pennsylvania Department of Transportation, 1997.
14. Weyers, R.E. and Cady, P.D., "Deterioration of Concrete Bridge Decks from Corrosion of Reinforcing Steel", *ACI Concrete International*, Vol. 9, No. 1, January 1987, pp. 15-20.
15. Al-Qadi, I.L., Peterson, J.E., and Weyers, R.E., "A Time to Cracking Model for Critically Contaminated Reinforced Concrete Structures", *Proceedings of 5<sup>th</sup> International Conference on Structural Faults and Repairs*. V.3, June 29, 1993, Venue, University of Edinburgh, Edinburgh, Scotland, pp. 91-99.

16. Hagen, M.G., *Bridge Deck Deterioration and Restoration*, Report No. FHWA-MN/RD-83/01, Federal Highway Administration, Washington, D.C., November 1982, 39 pp.
17. Fraczek, J., "A Review of Electromechanical Principles as Applied to Corrosion of Steel in a Concrete or Grout Environment", *Corrosion, Concrete and Chlorides*, ACI SP 102, F.W. Gibson, Ed., American Concrete Institute, Detroit, MI, 1987, pp. 13-24.
18. World Construction, "Gulf Concrete Under Scrutiny", *World Construction*, July 1986, pp. 22-24.
19. Concrete Reinforcing Steel Institute, *Guidelines for Inspection and Acceptance of Epoxy-Coated Reinforcing Bars at the Job Site*, CRSI, Schaumburg, IL, 1986.
20. Clear, K.C., *Time-to-Corrosion of Reinforcing Steel in Concrete Slabs*, Report FHWA-RD-76-70, Federal Highway Administration, Washington, D.C., 1976.
21. Wiss, Janney, Elstner Associates, Inc., *Service Life Extension of Northern Bridge Decks Containing Epoxy-Coated Reinforcing Bars*, Concrete Reinforcing Steel Institute, Northbrook, IL, 2003.
22. Federal Highway Administration, *Corrosion Detection in Reinforced Concrete Bridge Structures*, Demonstration Project 84, Federal Highway Administration, Washington, D.C., 1992.
23. Weyers, R.E., Prowell, B.D., Sprinkel, M.M., and Vorster, M., *Concrete Bridge Protection, Repair and Rehabilitation Relative to Reinforcement Corrosion: A Methods Application Manual*, Strategic Highway Research Program report SHRP-S-360, Transportation Research Board: Washington, D.C., 1997.
24. Torres, A.A. and Sagüés, A.A., "Concrete Cracking by Localized Steel Corrosion-Geometric Effects", American Concrete Institute, *ACI Materials Journal*, Vol. 101, No. 6, November–December 2004, pp. 501–507.
25. Jana, D. and Erlin, B., "Carbonation as an Indicator of Crack Age", *ACI Concrete International*, May 2007, pp. 61-64.
26. Sagüés, A.A., *Mechanism of Corrosion of Epoxy-Coated Reinforcing Steel in Concrete*, Report No. FL/DOT/RMC/0543-3296, National Technical Information Service, Springfield, VA., 1991.
27. Zemajtis, J., Weyers, R.E., Sprinkel, M.M., and McKeel, Jr., W.T., *Epoxy-Coated Reinforcement - A Historical Performance Review*, VTRC 97-IR1, Virginia Transportation Research Council, 1996.
28. Babei, K. and Hawkins, N.M., "Evaluation of Bridge Deck Protective Strategies", *ACI Concrete International*, 1988, pp. 56-66.
29. Weyers, R.E., "Protocol for In-Service Evaluation of Bridges with Epoxy-coated Reinforcing Steel", *NCHRP Research Results Digest*, No. 215, 1996.
30. ENR, "Rebar Coating Plants to be Certified", *Engineering News Record*, The McGraw-Hill Construction Weekly, July 1976, pp 14-17.
31. Concrete Reinforcing Steel Institute, *Voluntary Certification Program for Fusion Bonded Epoxy Coating Application Plants*, CRSI, Schaumburg, IL, 1991, 97 pp.
32. Wiss, Janney, Elstner Associates, Inc., *Corrosion Investigation of Four Bridges Built Between 1973 and 1978 Containing Epoxy-Coated Reinforcing Steel*, Report No.96-25, Minnesota Department of Transportation, St. Paul, MN, 1996.
33. RILEM, "Measurement of hardened concrete carbonation depth", *Recommendations for the Testing and Use of Constructions Materials*. Paper - CPC 18. RILEM (Réunion

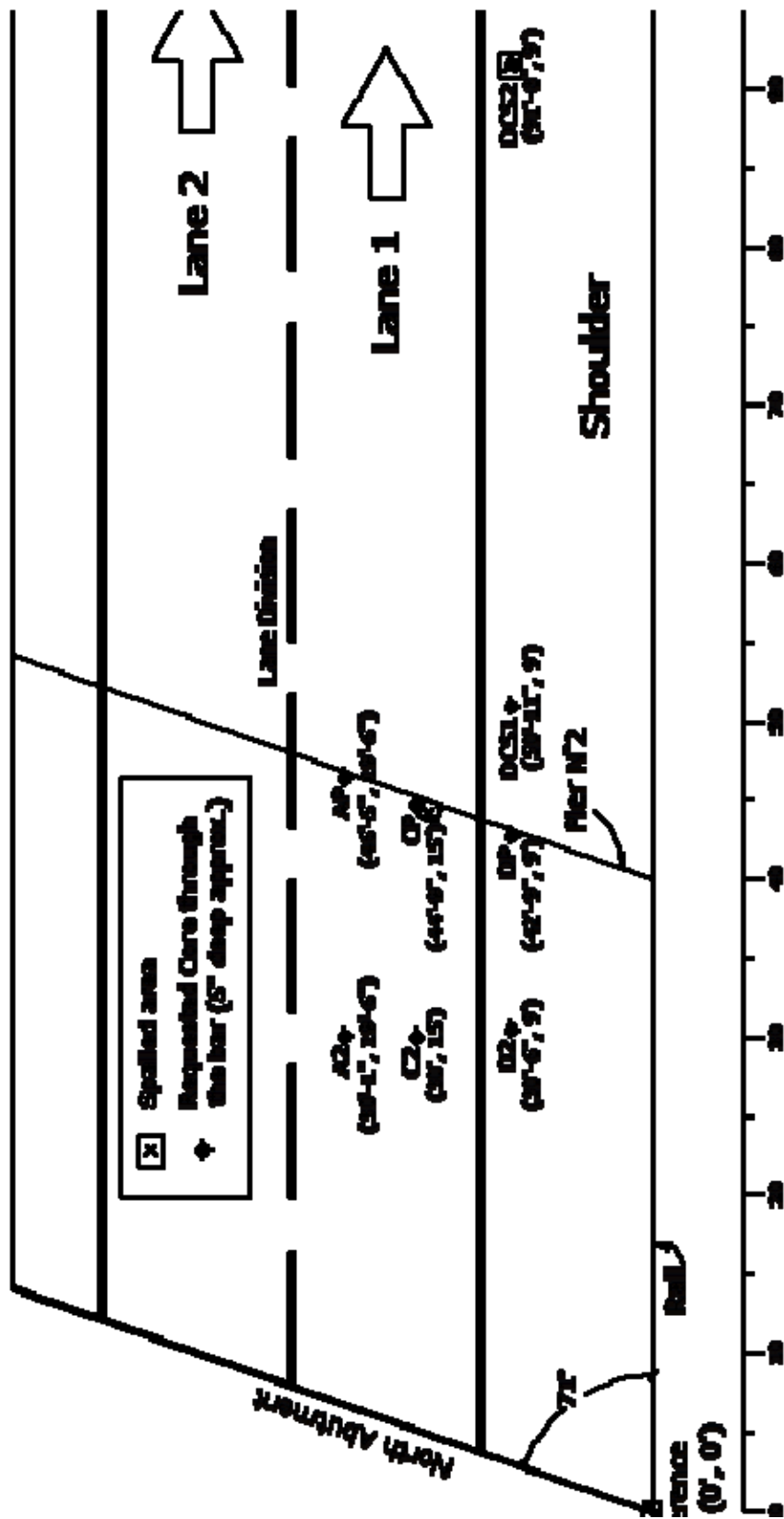
- Internationale des Laboratoires et Experts des Matériaux, Systèmes de Construction et Ouvrages), 1988.
34. National Association of Corrosion Engineers (NACE), *TM0174 - Laboratory methods for the evaluation of protective coatings used as lining materials in immersion service*, The Corrosion Society, Houston, TX, 2002.
  35. National Association of Corrosion Engineers (NACE), *TM0185 - Evaluation of Internal Plastic Coatings for Corrosion*, The Corrosion Society, Houston, TX, 2000.
  36. American Association of Testing and Materials (ASTM), *Standard Specification for Epoxy-Coated Steel Reinforcing Bars*, ASTM A775/A775M-07, West Conshohocken, PA., 2007.
  37. Minnesota Department of Transportation, *Bridge Inspection Manual*. Version 1.4, May 2007.
  38. Thomas, M.D.A. and Bamforth, P.B., “Modelling chloride diffusion in concrete, Effect of fly ash and slag”, *Cement and Concrete Research*, Vol. 29, 1999, pp. 487–495.
  39. Sohangpurwala, A.A., *Manual on Service Life of Corrosion-Damaged Reinforced Concrete Bridge Superstructure Elements*, National Cooperative Highway Research Program (NCHRP), Report 558, Washington, D.C., 2006.
  40. Weyers, R.E., Fitch, M.G., Larsen, E.P., Al-Qadi, I.L., Chamberlin, W.P., and Hoffman, P.C., *Service Life Estimate*, Strategic Highway Research Program, Report SHRP-S-668, National Research Council, Washington, D.C., 1994, 144 pp.
  41. Lindquist, W.D., Darwin, D., Browning, J., Miller, G.G., “Effect of Cracking on Chloride Content in Concrete Bridge Decks”, *ACI Materials Journal*, Title no. 103-M52. November-December 2006.
  42. Kosmatka, S.H. and Panarese, W.C., *Design and Control of Concrete Mixtures*, 13th ed. Skokie, IL, Portland Cement Association, 1994.
  43. Berke, N.S., Escalante, E., Nmai, C.K., and Whiting, D., *Techniques to Assess the Corrosion Activity of Steel Reinforced Concrete Structures*, ASTM PCN 04-012760- 07, West Conshohocken, PA, 1996.
  44. Broomfield, J.P. *Corrosion of Steel in Concrete: Understanding, Investigation, and Repair*. E & FN Spon, London, U.K., 1997.
  45. Barnes, C. L. and Trottier, J.-F., “Effectiveness of Ground Penetrating Radar in Predicting Deck Repair Quantities”, *Journal of Infrastructure Systems*, Vol. 10, No. 2, 2004, pp. 69-76.
  46. Jana, D. and Erlin, B., “Carbonation as an Indicator of Crack Age”, *ACI Concrete International*, May 2007, pp. 39-42.
  47. American Association of State Highway and Transportation Officials (AASHTO), *Standard Test Method for Sampling and Testing for Total Chloride Ion in Concrete and Concrete Raw Materials*, AASHTO T 260-02, Washington, D.C., 2004.
  48. Pincheira, J.A. and Dorshorst, M., *Evaluation of Concrete Deck and Cracks Sealers*, SPR #0092-03-09, Wisconsin Highway Research Program, Madison, WI, 2005.
  49. Brown, T.L., LeMay, Jr., H.M., and Bursten, B.E., *Chemistry, The Central Science*, 6th ed. Englewood Cliffs: Prentice Hall, NJ, 1994, 756 pp.
  50. Gu, P. and Beaudoin, J.J., *Obtaining Effective Half-Cell Potential Measurements in Reinforced Concrete Structures*, Construction Technology Update No. 18, National Research Council of Canada, Ottawa, Canada, 1998.



51. Scannell, W.T., Sohanchpurwala, A.A., and Islam, M., *FHWA-SHRP Showcase: Assessment of Physical Condition of Concrete Bridge Components*, Federal Highway Administration, Washington, D.C., 1996.
52. Larson, T.D., Cady, P.D., and Theisen, J.C., *Durability of Bridge Deck Concrete*, Report 7, Pennsylvania State University, University Park, PA, April 1969, 173 pp.
53. Clear, K.C., *Reinforcing Bar Corrosion in Concrete: Effect of Special Treatments*, Special Publication 49, American Concrete Institute, Detroit, MI, 1975, pp. 77–82.
54. Brown, R.D., *Mechanisms of Corrosion of Steel in Concrete in Relation to Design, Inspection, and Repair of Offshore and Coastal Structures*, Special Publication 65-11, American Concrete Institute, Detroit, MI, 1980, pp. 169–204.
55. Marcotte, T. D. and Hansson, C. M., “The Influence of Silica Fume on the Corrosion Resistance of Steel in High Performance Concrete Exposed to Simulated Sea Water”, *J. Materials Science*, Vol. 38, 2003, pp. 4765-4776.
56. Walter, G. W., “A Review of Impedance Plot Methods Used for Corrosion Performance Analysis of Painted Metals”, *Corrosion Science*, Vol. 26, No. 9, 1986, pp. 671-703.
57. Mansfeld, F., “Electrochemical Impedance Spectroscopy (EIS) as a New Tool for Investigating Methods of Corrosion Protection”, *Electrochimica Acta*, Vol. 35, No. 10, 1990, pp. 1533-1544.
58. Qiao, G., and Ou, J., “Corrosion monitoring of reinforcing steel in cement mortar by EIS and ENA”, *Electrochimica Acta*, Vol. 52, 2007, pp. 8008–8019.
59. Reynolds, J. M., *An Introduction to Applied and Environmental Geophysics*, Wiley, Chichester, UK, 1997, 796 pp.
60. Annan, P., “Ground Penetrating Radar”, *Near Surface Geophysics*, D. Buttler, Ed. SEG, Tulsa, OK, 2005, pp. 357-438.

**APPENDIX A:  
DETAILED CORE DESCRIPTION**

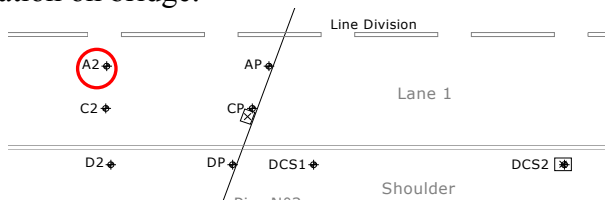
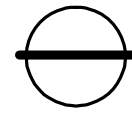
**BRIDGE 19015**



Bridge: 19015

Core: A2



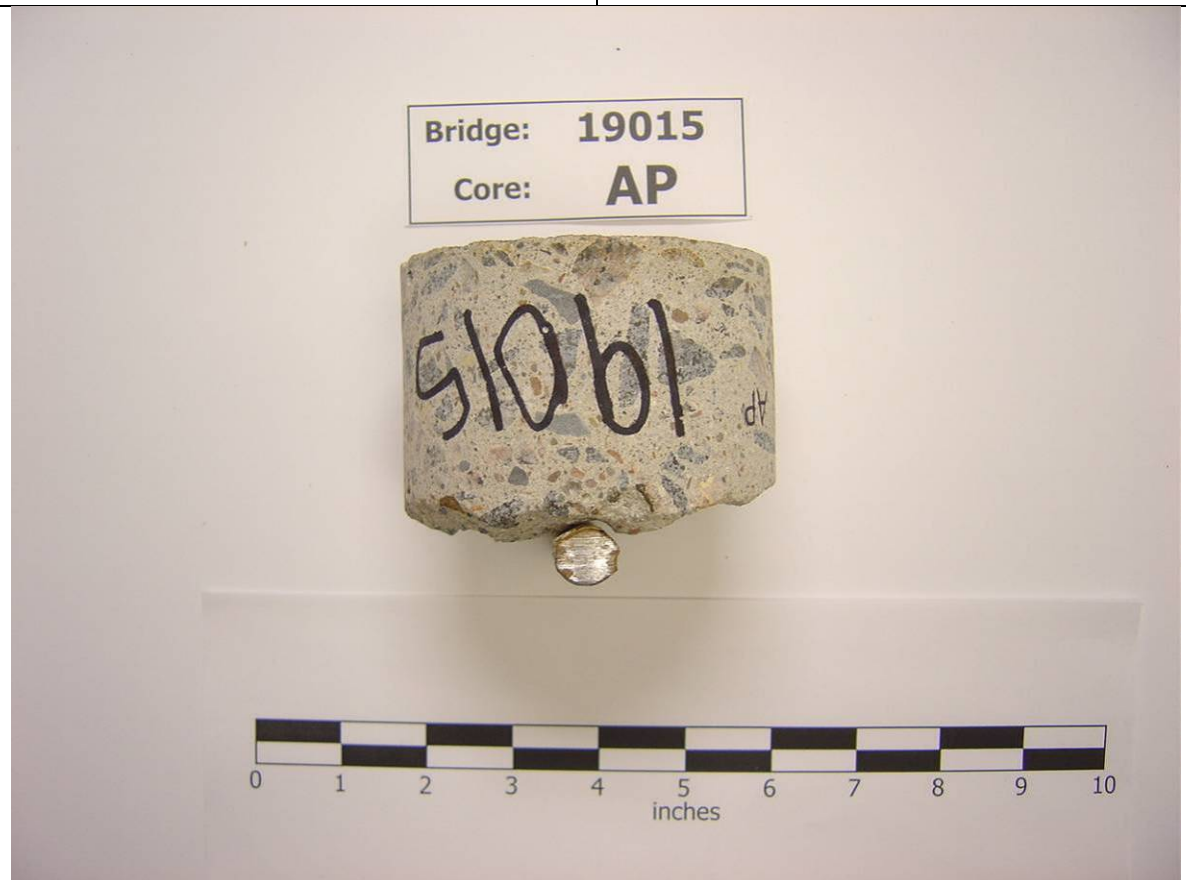
|  |                            |  |                             |
|--|----------------------------|--|-----------------------------|
| Cracks:<br><b>None observed</b>  | Corroded Bar:<br><b>No</b> | Delamination:<br><b>None</b>   | Core diameter:<br><b>4"</b> |
| <b>Bar Size</b>  |                            | Cover to rebar face:<br><b>3½"</b>   | Core length:<br><b>5½"</b>  |
| Longitudinal: <b>#4</b>  | Transverse: <b>#6</b>      |  |                             |
| Location on bridge:<br> |                            | Bar location inside core:<br> |                             |

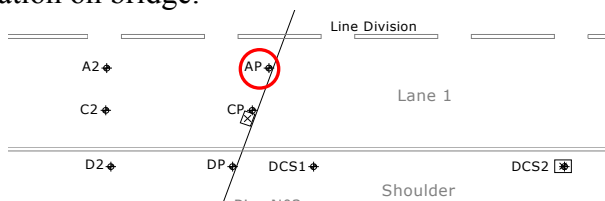
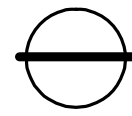
Notes:

- The chain drag survey indicated no signs of delamination at this location
- Half cell potential readings indicated a low probability of corrosion activity at this location
- Bar shows no evidence of corrosion

Bridge: 19015

Core: AP



|  |                             |  |                             |
|--|-----------------------------|--|-----------------------------|
| Cracks:<br><b>None observed</b>  | Corroded Bar:<br><b>Yes</b> | Delamination:<br><b>Yes</b>  | Core diameter:<br><b>4"</b> |
| <b>Bar Size</b>  |                             | Cover to rebar face:<br><b>3"</b>  | Core length:<br><b>3"</b>   |
| Longitudinal: <b>#4</b>  | Transverse: <b>#6</b>       |  |                             |
| Location on bridge:<br> |                             | Bar location inside core:<br> |                             |

Notes:

- Cracks at bar level (possible delamination)
- The chain drag survey indicated no signs of delamination at this location
- Half cell potential readings indicated a high probability of corrosion activity at this location
- Bar shows evidence of corrosion

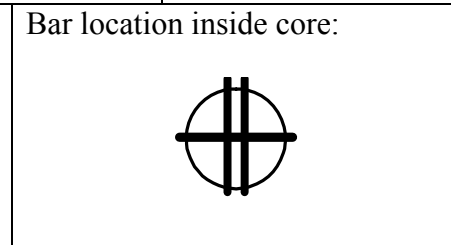
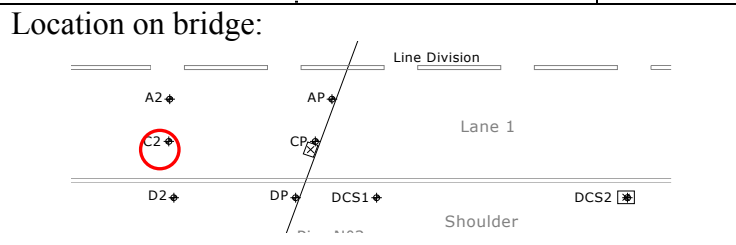
Bridge: 19015

Core: C2



|                                 |                             |                             |                             |
|---------------------------------|-----------------------------|-----------------------------|-----------------------------|
| Cracks:<br><b>None observed</b> | Corroded Bar:<br><b>Yes</b> | Delamination:<br><b>Yes</b> | Core diameter:<br><b>4"</b> |
|---------------------------------|-----------------------------|-----------------------------|-----------------------------|

|                         |                       |                                   |                           |
|-------------------------|-----------------------|-----------------------------------|---------------------------|
| <b>Bar Size</b>         |                       | Cover to rebar face:<br><b>4"</b> | Core length:<br><b>5"</b> |
| Longitudinal: <b>#4</b> | Transverse: <b>#6</b> |                                   |                           |



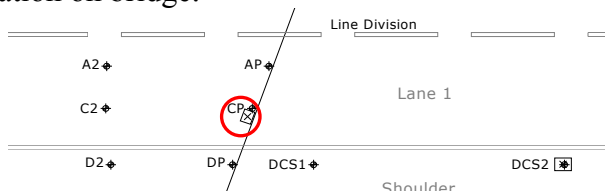
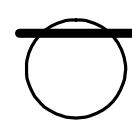
Notes:

- The chain drag survey indicated no signs of delamination at this location
- Half cell potential readings indicated a low probability of corrosion activity at this location
- Bar shows evidence of corrosion

Bridge: 19015

Core: CP



|  |                             |  |                             |
|--|-----------------------------|--|-----------------------------|
| Cracks:<br><b>Observed</b>   | Corroded Bar:<br><b>Yes</b> | Delamination:<br><b>Yes</b>  | Core diameter:<br><b>4"</b> |
| <b>Bar Size</b>  |                             | Cover to rebar face:<br><b>3"</b>  | Core length:<br><b>3"</b>   |
| Longitudinal: <b>#4</b>  | Transverse: <b>#6</b>       |  |                             |
| Location on bridge:<br> |                             | Bar location inside core:<br> |                             |

Notes:

- Cracks at bar level (possible delamination)
- The chain drag survey indicated a spall at this location
- Half cell potential readings indicated a high probability of corrosion activity at this location
- Bar shows evidence of corrosion



Bridge: **19015**

Core: **D2**



Cracks:  
**None observed**

Corroded Bar:  
**No**

Delamination:  
**None**

Core diameter:  
**4"**

**Bar Size**

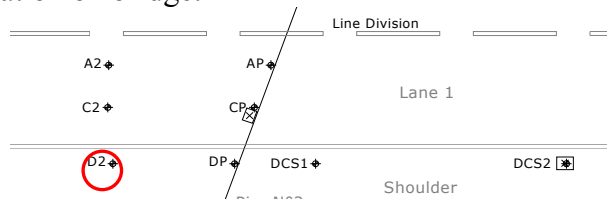
Longitudinal: **#4**

Transverse: **#6**

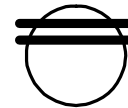
Cover to rebar face:  
**4½"**

Core length:  
**5½"**

Location on bridge:



Bar location inside core:



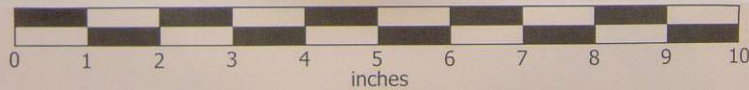
Notes:

- The chain drag survey indicated no signs of delamination at this location
- Half cell potential readings indicated a low probability of corrosion activity at this location
- Bar shows no evidence of corrosion

Bridge: **19015**

Core: **DP**

Bridge: **19015**  
Core: **DP**



Cracks:  
**None observed**

Corroded Bar:  
**Yes**

Delamination:  
**Yes**

Core diameter:  
**4"**

**Bar Size**

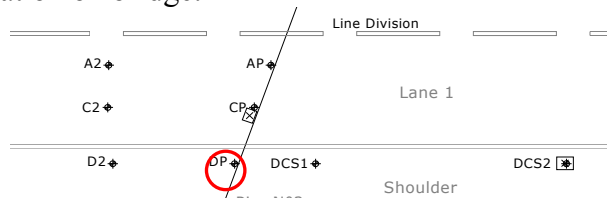
Cover to rebar face:  
**3"**

Core length:  
**3"**

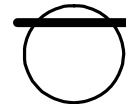
Longitudinal: **#4**

Transverse: **#6**

Location on bridge:



Bar location inside core:



Notes:

- The chain drag survey indicated no signs of delamination at this location
- Half cell potential readings indicated a high probability of corrosion activity at this location
- Bar shows evidence of corrosion

Bridge: **19015**

Core: **DCS1**



|                                 |                             |                                   |                             |
|---------------------------------|-----------------------------|-----------------------------------|-----------------------------|
| Cracks:<br><b>None observed</b> | Corroded Bar:<br><b>Yes</b> | Delamination:<br><b>None</b>      | Core diameter:<br><b>4"</b> |
| <b>Bar Size</b>                 |                             | Cover to rebar face:<br><b>3"</b> | Core length:<br><b>5½"</b>  |
| Longitudinal: <b>#4</b>         | Transverse: <b>#6</b>       |                                   |                             |
| Location on bridge:<br>         |                             | Bar location inside core:<br>     |                             |

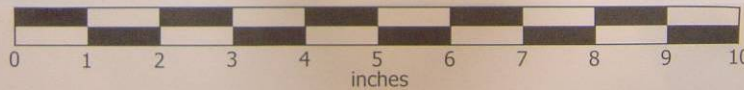
Notes:

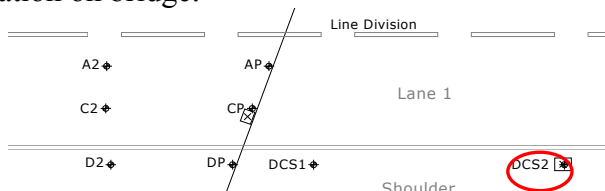
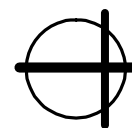
- The chain drag survey indicated no signs of delamination at this location
- Half cell potential readings indicated a low probability of corrosion activity at this location
- Bar shows evidence of corrosion

Bridge: 19015

Core: DCS2

Bridge: 19015  
Core: DCS2

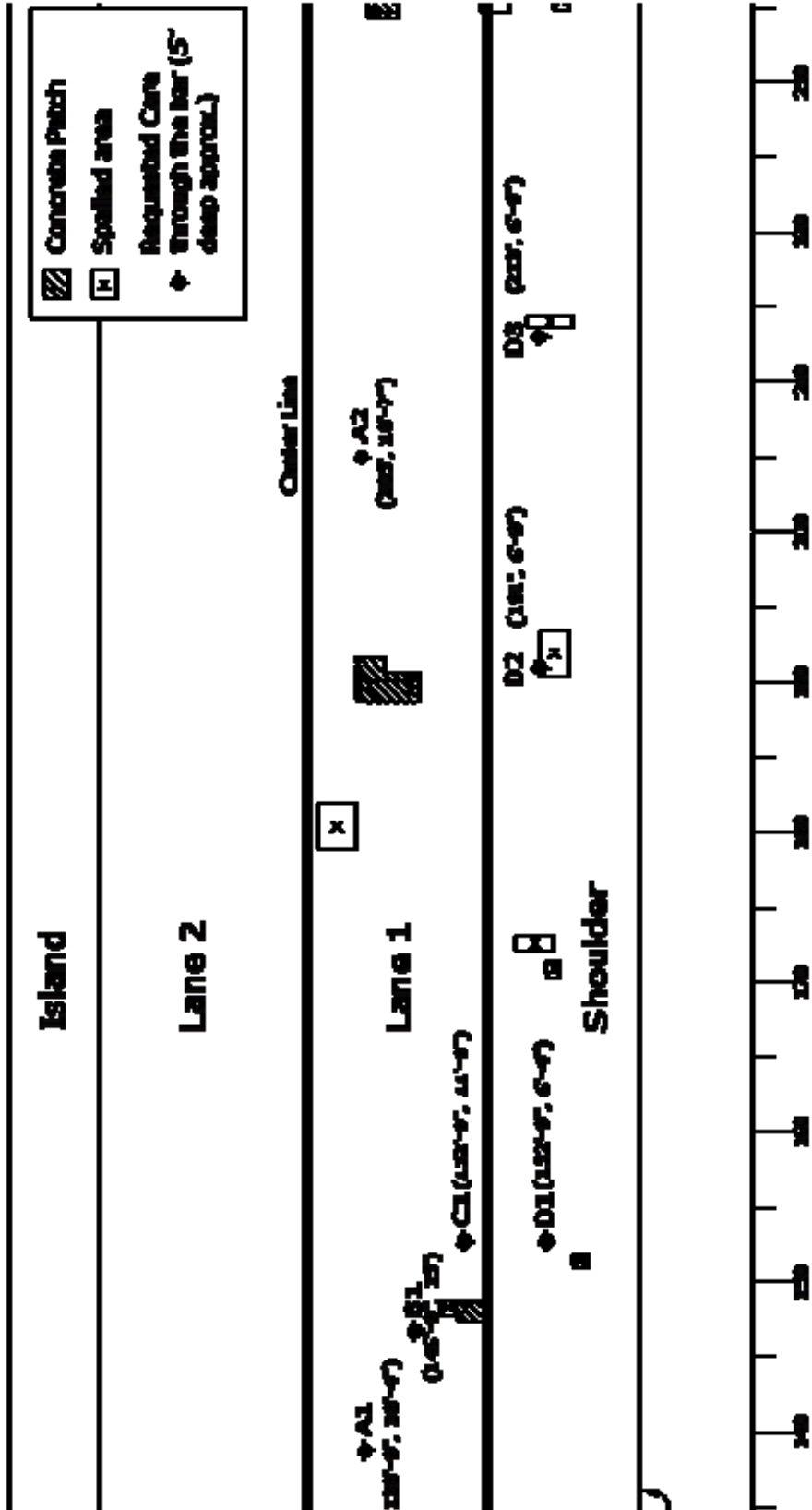


|  |                             |  |                             |
|--|-----------------------------|--|-----------------------------|
| Cracks:<br><b>Observed</b>   | Corroded Bar:<br><b>Yes</b> | Delamination:<br><b>Yes</b>  | Core diameter:<br><b>4"</b> |
| <b>Bar Size</b>  |                             | Cover to rebar face:<br><b>2"</b>  | Core length:<br><b>6"</b>   |
| Longitudinal: <b>#4</b>  | Transverse: <b>#6</b>       |  |                             |
| Location on bridge:<br> |                             | Bar location inside core:<br> |                             |

Notes:

- Delamination cracks at the bar level
- The chain drag survey indicated delamination at this location
- Half cell potential readings indicated a high probability of corrosion activity at this location
- Bar shows evidence of corrosion

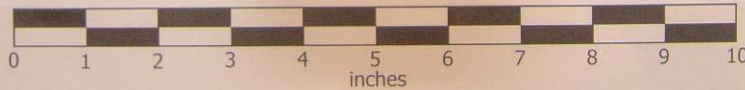
**BRIDGE 27062**



Bridge: 27062

Core: A1

Bridge: 27062  
Core: A1



Cracks:  
**None observed**

Corroded Bar:  
**No**

Delamination:  
**None**

Core diameter:  
**4"**

**Bar Size**

Longitudinal: **#4**

Transverse: **#6**

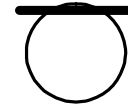
Cover to rebar face:  
**4½"**

Core length:  
**5½"**

Location on bridge:



Bar location inside core:



Notes:

- The chain drag survey indicated no signs of delamination at this location
- Half cell potential readings indicated a low probability of corrosion activity at this location
- Bar shows no evidence of corrosion

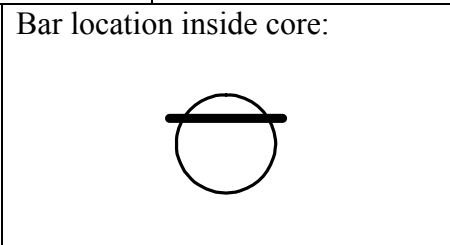
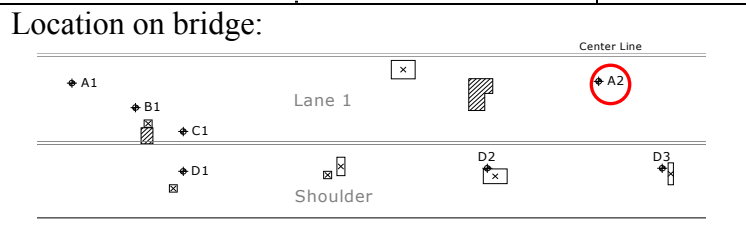
Bridge: 27062

Core: A2



|                                 |                            |                              |                             |
|---------------------------------|----------------------------|------------------------------|-----------------------------|
| Cracks:<br><b>None observed</b> | Corroded Bar:<br><b>No</b> | Delamination:<br><b>None</b> | Core diameter:<br><b>4"</b> |
|---------------------------------|----------------------------|------------------------------|-----------------------------|

|                         |                       |                                   |                            |
|-------------------------|-----------------------|-----------------------------------|----------------------------|
| <b>Bar Size</b>         |                       | Cover to rebar face:<br><b>4"</b> | Core length:<br><b>5½"</b> |
| Longitudinal: <b>#4</b> | Transverse: <b>#6</b> |                                   |                            |



Notes:

- The chain drag survey indicated no signs of delamination at this location
- Half cell potential readings indicated a high probability of corrosion activity at this location
- Bar shows no evidence of corrosion



Bridge: 27062

Core: B1



Cracks:  
**None observed**

Corroded Bar:  
**No**

Delamination:  
**Yes**

Core diameter:  
**4"**

**Bar Size**

Longitudinal: **#4**

Transverse: **#6**

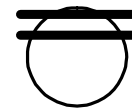
Cover to rebar face:  
**4 1/2"**

Core length:  
**5"**

Location on bridge:



Bar location inside core:



Notes:

- The chain drag survey indicated no signs of delamination at this location (Jose there is an inconsistency here)
- Half cell potential readings indicated a high probability of corrosion activity at this location
- Bar shows no evidence of corrosion

Bridge: 27062

Core: C1



Cracks:  
**None observed**

Corroded Bar:  
**No**

Delamination:  
**No**

Core diameter:  
**4"**

**Bar Size**

Longitudinal: **#4**

Transverse: **#6**

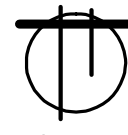
Cover to rebar face:  
**4"**

Core length:  
**5"**

Location on bridge:



Bar location inside core:



Notes:

- The chain drag survey indicated no signs of delamination at this location
- Half cell potential readings indicated a high probability of corrosion activity at this location
- Bar shows no evidence of corrosion

Bridge: 27062

Core: D1



Cracks:  
**None observed**

Corroded Bar:  
**No**

Delamination:  
**Yes**

Core diameter:  
**4"**

**Bar Size**

Longitudinal: **#4**

Transverse: **#6**

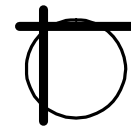
Cover to rebar face:  
**4"**

Core length:  
**6"**

Location on bridge:



Bar location inside core:



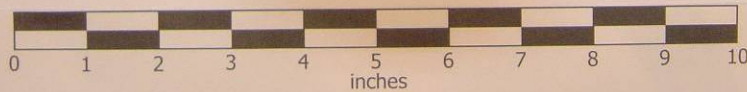
Notes:

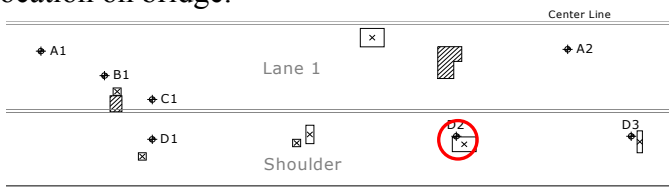
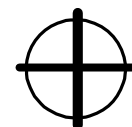
- The chain drag survey indicated delamination 2' from this location
- Half cell potential readings indicated a high probability of corrosion activity at this location
- Bar shows no evidence of corrosion

Bridge: 27062

Core: D2

Bridge: 27062  
Core: D2



|  |                             |  |                             |
|--|-----------------------------|--|-----------------------------|
| Cracks:<br><b>Observed</b>   | Corroded Bar:<br><b>Yes</b> | Delamination:<br><b>Yes</b>  | Core diameter:<br><b>4"</b> |
| <b>Bar Size</b>  |                             | Cover to rebar face:<br><b>3½"</b>   | Core length:<br><b>4½"</b>  |
| Longitudinal: <b>#4</b>  | Transverse: <b>#6</b>       |  |                             |
| Location on bridge:<br> |                             | Bar location inside core:<br> |                             |

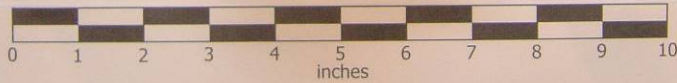
Notes:

- Diagonal crack from ½" to 2-½" below surface, delamination above rebar
- The chain drag survey indicated delamination at this location
- Half cell potential readings indicated a high probability of corrosion activity at this location
- Bar shows evidence of corrosion

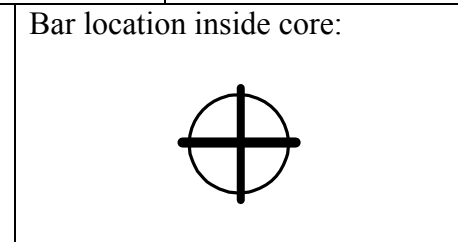
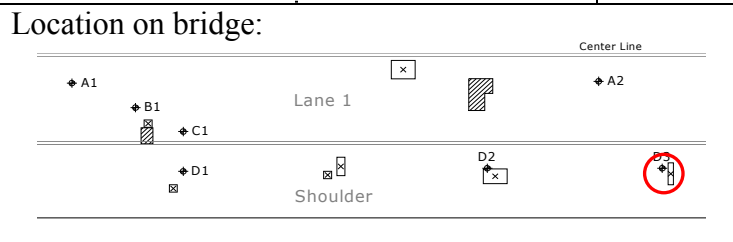
Bridge: 27062

Core: D3

Bridge: 27062  
Core: D3



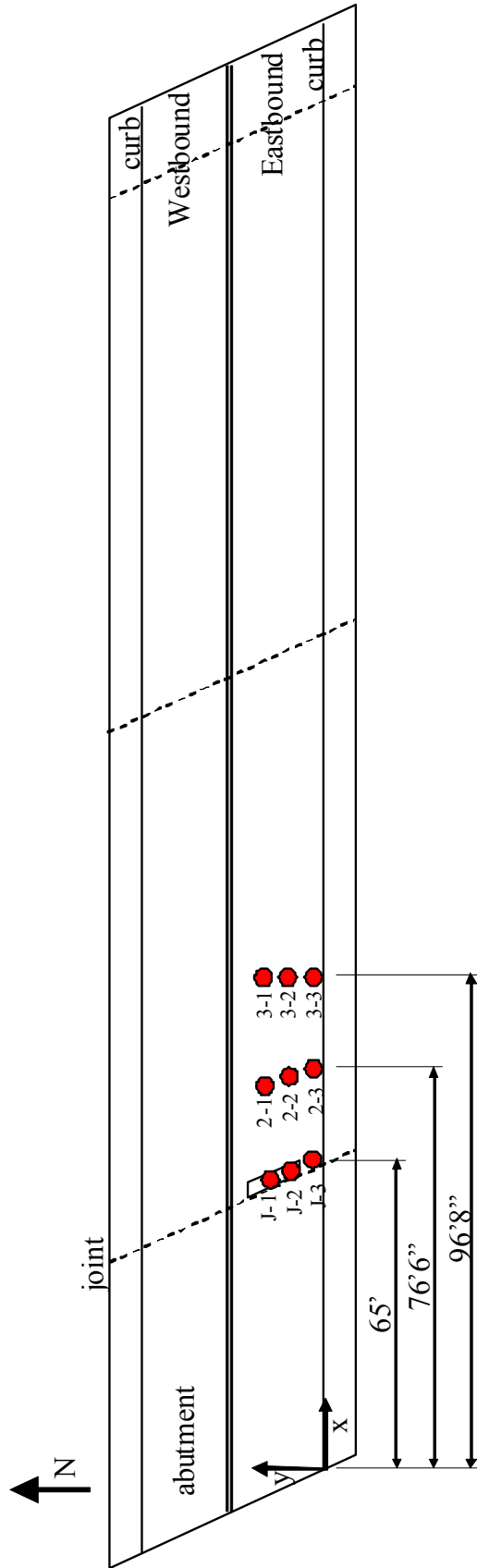
|                            |                            |                                    |                             |
|----------------------------|----------------------------|------------------------------------|-----------------------------|
| Cracks:<br><b>Observed</b> | Corroded Bar:<br><b>No</b> | Delamination:<br><b>Yes</b>        | Core diameter:<br><b>4"</b> |
| <b>Bar Size</b>            |                            | Cover to rebar face:<br><b>3½"</b> | Core length:<br><b>4½"</b>  |
| Longitudinal: <b>#4</b>    | Transverse: <b>#6</b>      |                                    |                             |



Notes:

- Cracks at bar level (possible delamination)
- The chain drag survey indicated delamination 1' from this location
- Half cell potential readings indicated a high probability of corrosion activity at this location

**BRIDGE 27812**



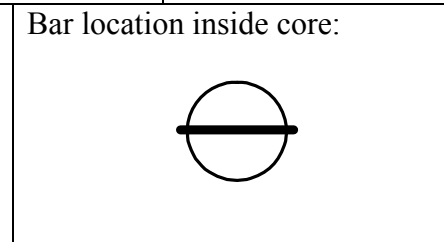
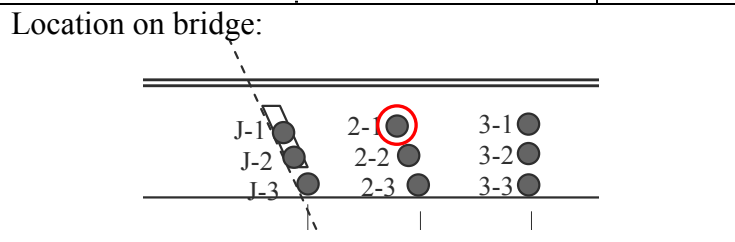
Bridge: 27812

Core: 2-1



|                                 |                            |                              |                             |
|---------------------------------|----------------------------|------------------------------|-----------------------------|
| Cracks:<br><b>None observed</b> | Corroded Bar:<br><b>No</b> | Delamination:<br><b>None</b> | Core diameter:<br><b>4"</b> |
|---------------------------------|----------------------------|------------------------------|-----------------------------|

|                         |                       |                                   |                           |
|-------------------------|-----------------------|-----------------------------------|---------------------------|
| <b>Bar Size</b>         |                       | Cover to rebar face:<br><b>4"</b> | Core length:<br><b>7"</b> |
| Longitudinal: <b>#4</b> | Transverse: <b>#5</b> |                                   |                           |



Notes:

- The chain drag survey indicated no signs of delamination at this location
- Half cell potential readings indicated a low probability of corrosion activity at this location
- Bar shows no evidence of corrosion

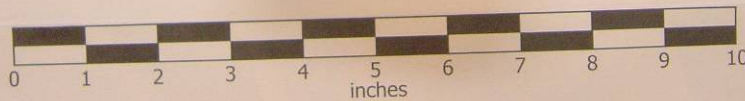


Bridge: 27812

Core: 2-2

Bridge: 27812

Core: 22



Cracks:  
**Observed**

Corroded Bar:  
**No**

Delamination:  
**Yes**

Core diameter:  
**4"**

**Bar Size**

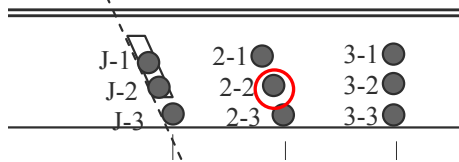
Cover to rebar face:  
**4"**

Core length:  
**6"**

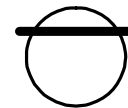
Longitudinal: **#4**

Transverse: **#5**

Location on bridge:



Bar location inside core:



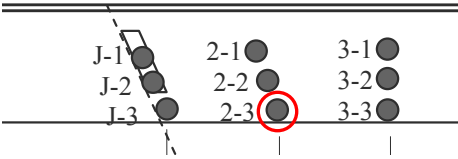

Notes:

- Delamination cracks at the bar level
- The chain drag survey indicated no signs of delamination at this location
- Half cell potential readings indicated that is likely to find corrosion activity at this location
- Bar shows no evidence of corrosion

Bridge: 27812

Core: 2-3



|  |                             |  |                             |
|--|-----------------------------|--|-----------------------------|
| Cracks:<br><b>Observed</b>   | Corroded Bar:<br><b>Yes</b> | Delamination:<br><b>Yes</b>  | Core diameter:<br><b>4"</b> |
| <b>Bar Size</b>  |                             | Cover to rebar face:<br><b>4"</b>  | Core length:<br><b>6½"</b>  |
| Longitudinal: <b>#4</b>  | Transverse: <b>#5</b>       |  |                             |
| Location on bridge:<br> |                             | Bar location inside core:<br> |                             |

Notes:

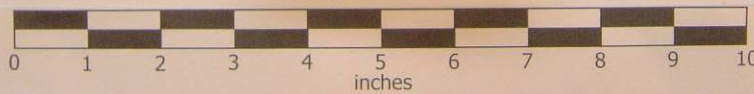
- Delamination cracks at the bar level
- The chain drag survey indicated no signs of delamination at this location
- Half cell potential readings indicated a high probability of corrosion activity at this location
- Bar shows evidence of corrosion

Bridge: 27812

Core: 3-1

Bridge: 27812

Core: 31



Cracks:  
**None observed**

Corroded Bar:  
**No**

Delamination:  
**Yes**

Core diameter:  
**4"**

**Bar Size**

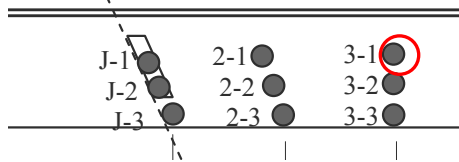
Longitudinal: **#4**

Transverse: **#5**

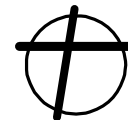
Cover to rebar face:  
**4½"**

Core length:  
**6½"**

Location on bridge:



Bar location inside core:



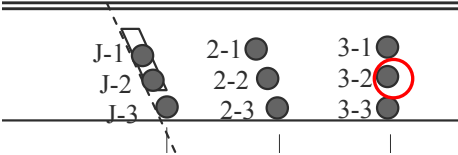
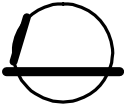
Notes:

- Horizontal crack 2" below surface (at overlay-deck interface)
- The chain drag survey indicated no signs of delamination at this location
- Half cell potential readings indicated a low probability of corrosion activity at this location
- Bar shows no evidence of corrosion

Bridge: 27812

Core: 3-2



|  |                            |  |                             |
|--|----------------------------|--|-----------------------------|
| Cracks:<br><b>Observed</b>   | Corroded Bar:<br><b>No</b> | Delamination:<br><b>None</b>   | Core diameter:<br><b>4"</b> |
| <b>Bar Size</b>  |                            | Cover to rebar face:<br><b>5"</b>  | Core length:<br><b>5½"</b>  |
| Longitudinal: <b>#4</b>  | Transverse: <b>#5</b>      |  |                             |
| Location on bridge:<br> |                            | Bar location inside core:<br> |                             |

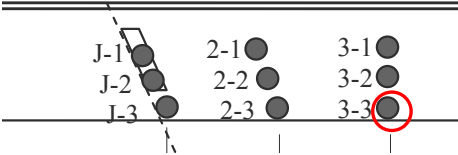
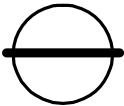
Notes:

- The chain drag survey indicated no signs of delamination at this location
- Half cell potential readings indicated a low probability of corrosion activity at this location
- Bar shows no evidence of corrosion

Bridge: 27812

Core: 3-3



|  |                            |  |                             |
|--|----------------------------|--|-----------------------------|
| Cracks:<br><b>None observed</b>  | Corroded Bar:<br><b>No</b> | Delamination:<br><b>None</b>   | Core diameter:<br><b>4"</b> |
| <b>Bar Size</b>  |                            | Cover to rebar face:<br><b>4"</b>  | Core length:<br><b>7½"</b>  |
| Longitudinal: <b>#4</b>  | Transverse: <b>#5</b>      |  |                             |
| Location on bridge:<br> |                            | Bar location inside core:<br> |                             |

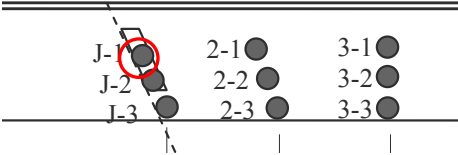
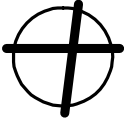
Notes:

- The chain drag survey indicated no signs of delamination at this location
- Half cell potential readings indicated a low probability of corrosion activity at this location
- Bar shows no evidence of corrosion

Bridge: 27812

Core: J-1



|  |                            |  |                             |
|--|----------------------------|--|-----------------------------|
| Cracks:<br><b>Observed</b>   | Corroded Bar:<br><b>No</b> | Delamination:<br><b>Yes</b>  | Core diameter:<br><b>4"</b> |
| <b>Bar Size</b>  |                            | Cover to rebar face:<br><b>5"</b>  | Core length:<br><b>6½"</b>  |
| Longitudinal: <b>#4</b>  | Transverse: <b>#5</b>      |  |                             |
| Location on bridge:<br> |                            | Bar location inside core:<br> |                             |

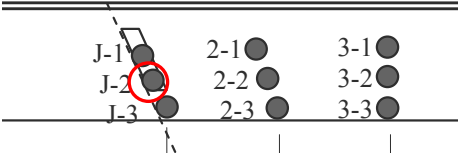
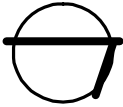
Notes:

- Horizontal crack 4" below surface
- The chain drag survey indicated delamination at this location
- Half cell potential readings indicated a high probability of corrosion activity at this location
- Bar shows no evidence of corrosion

Bridge: 27812

Core: J-2



|  |                            |  |                             |
|--|----------------------------|--|-----------------------------|
| Cracks:<br><b>Observed</b>   | Corroded Bar:<br><b>No</b> | Delamination:<br><b>Yes</b>  | Core diameter:<br><b>4"</b> |
| <b>Bar Size</b>  |                            | Cover to rebar face:<br><b>5"</b>  | Core length:<br><b>6½"</b>  |
| Longitudinal: <b>#4</b>  | Transverse: <b>#5</b>      |  |                             |
| Location on bridge:<br> |                            | Bar location inside core:<br> |                             |

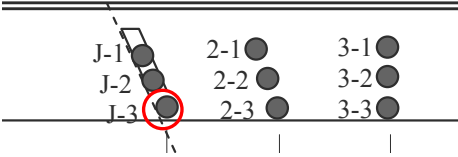
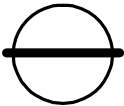
Notes:

- Dipping crack ½" below surface
- Cracks at the bar level (possible delamination)
- The chain drag survey indicated delamination and spall at this location
- Half cell potential readings indicated a high probability of corrosion activity at this location
- Bar shows no evidence of corrosion

Bridge: 27812

Core: J-3



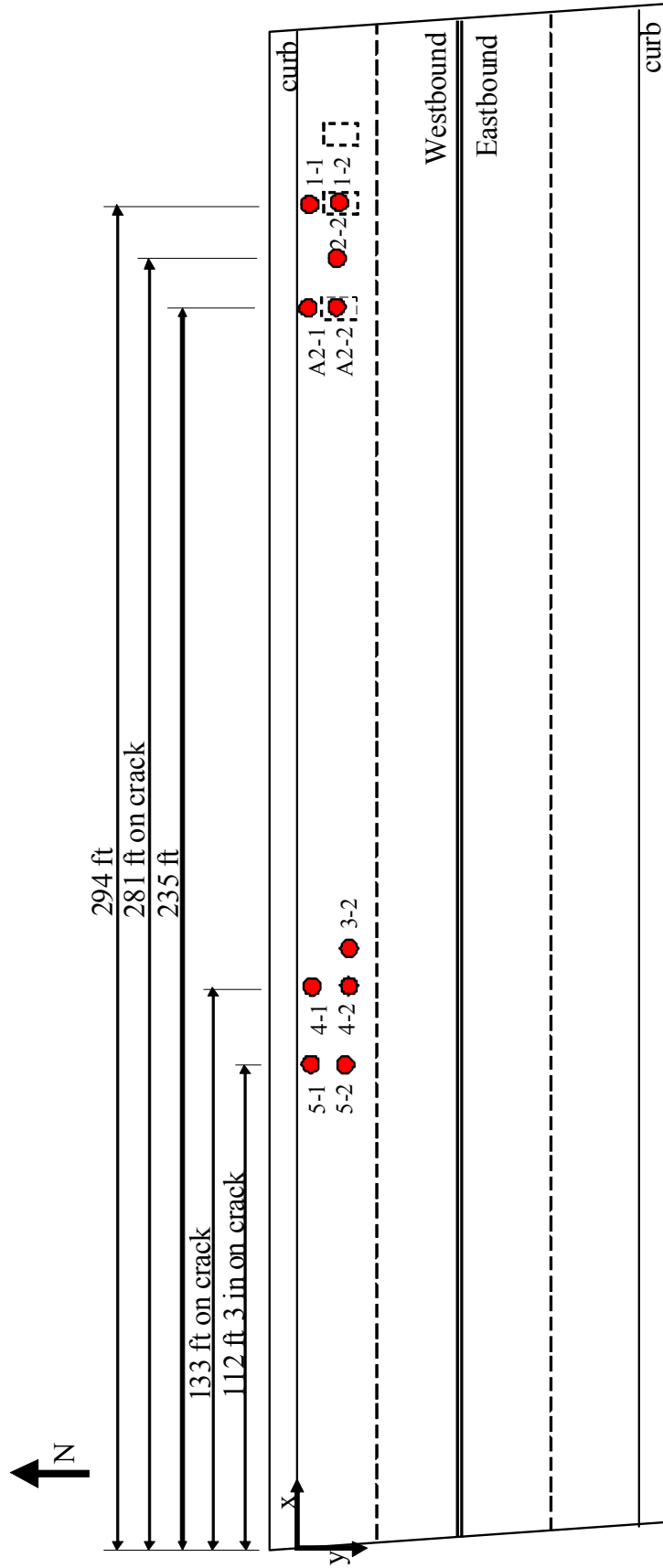
|  |                             |  |                             |
|--|-----------------------------|--|-----------------------------|
| Cracks:<br><b>None observed</b>  | Corroded Bar:<br><b>Yes</b> | Delamination:<br><b>Yes</b>  | Core diameter:<br><b>4"</b> |
| <b>Bar Size</b>  |                             | Cover to rebar face:<br><b>5"</b>  | Core length:<br><b>5"</b>   |
| Longitudinal: <b>#4</b>  | Transverse: <b>#5</b>       |  |                             |
| Location on bridge:<br> |                             | Bar location inside core:<br> |                             |

Notes:

- Cracks at the bar level (possible delamination)
- The chain drag survey indicated delamination 1' from this location
- Half cell potential readings indicated a high probability of corrosion activity at this location
- Bar shows evidence of corrosion



**BRIDGE 27815**



Bridge: 27815

Core: 1-1



Cracks:  
**None observed**

Corroded Bar:  
**No**

Delamination:  
**None**

Core diameter:  
**4"**

**Bar Size**

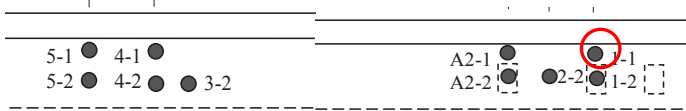
Cover to rebar face:

Core length:  
**6"**

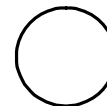
Longitudinal: **#4**

Transverse: **#5**

Location on bridge:



Bar location inside core:



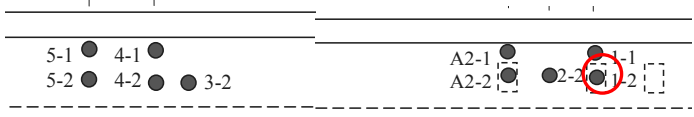
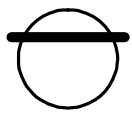
Notes:

- No bar observed
- The chain drag survey indicated no signs of delamination at this location
- Half cell potential readings indicated a high probability of corrosion activity at this location

Bridge: 27815

Core: 1-2



|  |                            |  |                             |
|--|----------------------------|--|-----------------------------|
| Cracks:<br><b>None observed</b>  | Corroded Bar:<br><b>No</b> | Delamination:<br><b>Yes</b>  | Core diameter:<br><b>4"</b> |
| <b>Bar Size</b>  |                            | Cover to rebar face:<br><b>4"</b>  | Core length:<br><b>4½"</b>  |
| Longitudinal: <b>#4</b>  | Transverse: <b>#5</b>      |  |                             |
| Location on bridge:<br> |                            | Bar location inside core:<br> |                             |

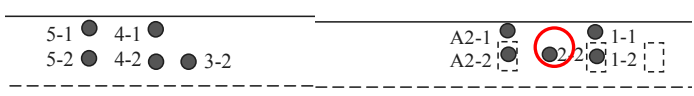
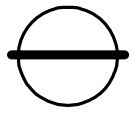
Notes:

- The chain drag survey indicated no signs of delamination at this location
- Half cell potential readings indicated a high probability of corrosion activity at this location
- Bar shows no evidence of corrosion

Bridge: 27815

Core: 2-2



|  |                             |  |                             |
|--|-----------------------------|--|-----------------------------|
| Cracks:<br><b>Observed</b>   | Corroded Bar:<br><b>Yes</b> | Delamination:<br><b>Yes</b>  | Core diameter:<br><b>4"</b> |
| <b>Bar Size</b>  |                             | Cover to rebar face:<br><b>4"</b>  | Core length:<br><b>7"</b>   |
| Longitudinal: <b>#4</b>  | Transverse: <b>#5</b>       |  |                             |
| Location on bridge:<br> |                             | Bar location inside core:<br> |                             |

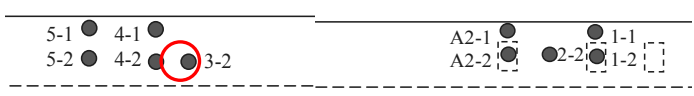
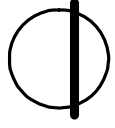
Notes:

- Vertical crack at center of core, 2" length from surface
- Delamination cracks at bar level
- The chain drag survey indicated no signs of delamination at this location
- Half cell potential readings indicated that is likely to find corrosion activity at this location
- Bar shows evidence of corrosion

Bridge: 27815

Core: 3-2



|  |                             |  |                             |
|--|-----------------------------|--|-----------------------------|
| Cracks:<br><b>Observed</b>   | Corroded Bar:<br><b>Yes</b> | Delamination:<br><b>Yes</b>  | Core diameter:<br><b>4"</b> |
| <b>Bar Size</b>  |                             | Cover to rebar face:<br><b>4"</b>  | Core length:<br><b>7"</b>   |
| Longitudinal: <b>#4</b>  | Transverse: <b>#5</b>       |  |                             |
| Location on bridge:<br> |                             | Bar location inside core:<br> |                             |

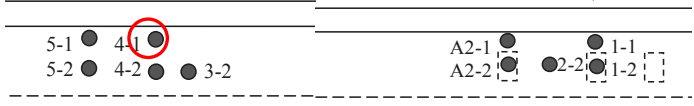
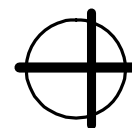
Notes:

- Delamination cracks at the bar level
- The chain drag survey indicated no signs of delamination at this location
- Half cell potential readings indicated that is likely to find corrosion activity at this location
- Bar shows evidence of corrosion

Bridge: 27815

Core: 4-1



|  |                             |  |                             |
|--|-----------------------------|--|-----------------------------|
| Cracks:<br><b>Observed</b>   | Corroded Bar:<br><b>Yes</b> | Delamination:<br><b>Yes</b>  | Core diameter:<br><b>4"</b> |
| <b>Bar Size</b>  |                             | Cover to rebar face:<br><b>4"</b>  | Core length:<br><b>7"</b>   |
| Longitudinal: <b>#4</b>  | Transverse: <b>#5</b>       |  |                             |
| Location on bridge:<br> |                             | Bar location inside core:<br> |                             |


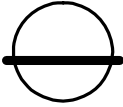
Notes:

- Vertical crack at center of core, from top to bottom
- Cracks below the bar
- The chain drag survey indicated no signs of delamination at this location
- Half cell potential readings indicated a high probability of corrosion activity at this location
- Bar shows evidence of corrosion

Bridge: 27815

Core: 4-2



|  |                             |  |                             |
|--|-----------------------------|--|-----------------------------|
| Cracks:<br><b>Observed</b>   | Corroded Bar:<br><b>Yes</b> | Delamination:<br><b>Yes</b>  | Core diameter:<br><b>4"</b> |
| <b>Bar Size</b>  |                             | Cover to rebar face:<br><b>4"</b>  | Core length:<br><b>7"</b>   |
| Longitudinal: <b>#4</b>  | Transverse: <b>#5</b>       |  |                             |
| Location on bridge:<br> |                             | Bar location inside core:<br> |                             |

Notes:

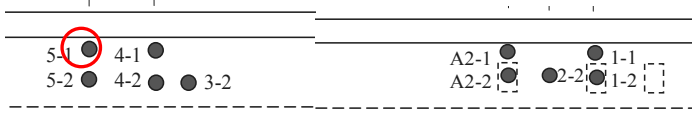
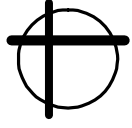
- Vertical crack at center of core, from surface to bar level
- Delamination cracks at the bar level
- The chain drag survey indicated no signs of delamination at this location
- Half cell potential readings indicated that is likely to find corrosion activity at this location
- Bar shows evidence of corrosion



Bridge: 27815

Core: 5-1



|  |                             |  |                             |
|--|-----------------------------|--|-----------------------------|
| Cracks:<br><b>Observed</b>   | Corroded Bar:<br><b>Yes</b> | Delamination:<br><b>Yes</b>  | Core diameter:<br><b>4"</b> |
| <b>Bar Size</b>  |                             | Cover to rebar face:<br><b>4"</b>  | Core length:<br><b>7"</b>   |
| Longitudinal: <b>#4</b>  | Transverse: <b>#5</b>       |  |                             |
| Location on bridge:<br> |                             | Bar location inside core:<br> |                             |

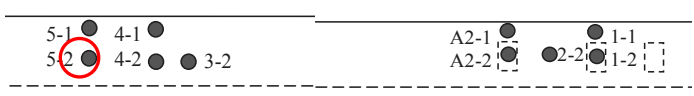
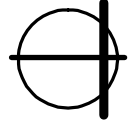
Notes:

- Vertical crack at center of core, from surface to bar level
- Delamination cracks at the bar level
- The chain drag survey indicated no signs of delamination at this location
- Half cell potential readings indicated a low probability of corrosion activity at this location
- Bar shows evidence of corrosion

Bridge: 27815

Core: 5-2



|  |                             |  |                             |
|--|-----------------------------|--|-----------------------------|
| Cracks:<br><b>Observed</b>   | Corroded Bar:<br><b>Yes</b> | Delamination:<br><b>Yes</b>  | Core diameter:<br><b>4"</b> |
| <b>Bar Size</b>  |                             | Cover to rebar face:<br><b>3½"</b>   | Core length:<br><b>7"</b>   |
| Longitudinal: <b>#4</b>  | Transverse: <b>#5</b>       |  |                             |
| Location on bridge:<br> |                             | Bar location inside core:<br> |                             |

Notes:

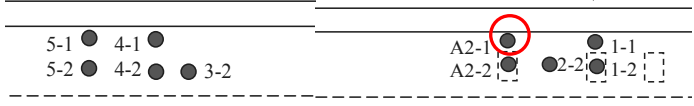

- Cracks at the bar level (possible delamination)
- The chain drag survey indicated no signs of delamination at this location
- Half cell potential readings indicated a low probability of corrosion activity at this location
- Bar shows evidence of corrosion

Bridge: 27815

Core: A2-1



Bridge: 27815  
Core: A21

|  |                            |  |                             |
|--|----------------------------|--|-----------------------------|
| Cracks:<br><b>Observed</b>   | Corroded Bar:<br><b>No</b> | Delamination:<br><b>Yes</b>  | Core diameter:<br><b>4"</b> |
| <b>Bar Size</b>  |                            | Cover to rebar face:<br><b>4½"</b>   | Core length:<br><b>5"</b>   |
| Longitudinal: <b>#4</b>  | Transverse: <b>#5</b>      |  |                             |
| Location on bridge:<br> |                            | Bar location inside core:<br> |                             |

Notes:

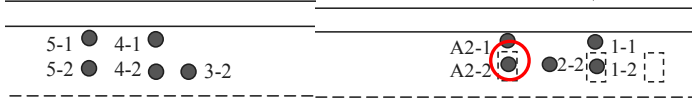
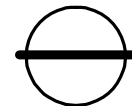
- Delamination crack at bar level
- The chain drag survey indicated no signs of delamination at this location
- Half cell potential readings was not measured at this location
- Bar shows no evidence of corrosion

Bridge: 27815

Core: A2-2



Bridge: 27815  
Core: A22

|  |                            |  |                             |
|--|----------------------------|--|-----------------------------|
| Cracks:<br><b>None observed</b>  | Corroded Bar:<br><b>No</b> | Delamination:<br><b>None</b>   | Core diameter:<br><b>4"</b> |
| <b>Bar Size</b>  |                            | Cover to rebar face:<br><b>5"</b>  | Core length:<br><b>6½"</b>  |
| Longitudinal: <b>#4</b>  | Transverse: <b>#5</b>      |  |                             |
| Location on bridge:<br> |                            | Bar location inside core:<br> |                             |

Notes:

- The chain drag survey indicated delamination area close to this location
- Half cell potential readings was not measured at this location
- Bar shows no evidence of corrosion

**APPENDIX B:  
DIFFUSION COEFFICIENT CALCULATION**

## Determination of Diffusion Coefficient

When concrete is permanently surrounded by a salt solution, at a given time  $t$ , the concentration  $C$  of chloride in concrete at depth  $x$  can be calculated by this estimation model of simple diffusion under steady regime.

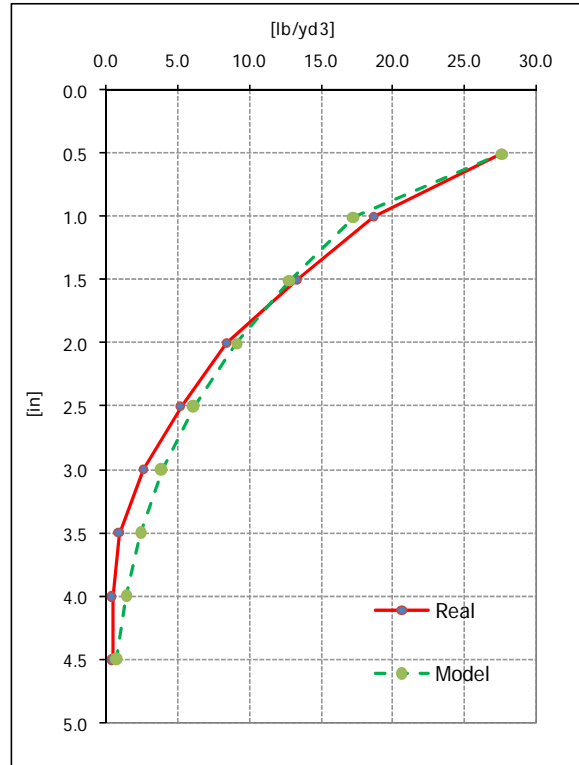
$$\frac{\partial C}{\partial t} = D \frac{\partial^2 C}{\partial x^2} \quad (B.1)$$

Where

|   |   |
|---|---|
| C | = Chloride concentration (lb/yd <sup>3</sup> )            |
| t | = Time in years   |
| D | = Effective diffusion coefficient (in <sup>2</sup> /year) |
| x | = Depth in inches   |

This common model of chloride ingress into concrete is called Fick's law. The limitations of this technique are that Fick's Law assumes that the diffusion is constant with time and that the surface concentration of chloride ions is also constant over time. Neither of these assumed factors is present in long-term concrete studies. However, the effective diffusion coefficients and surface concentrations estimated in the bibliography reviewed corroborate the use of this technique. Fick's second law can be used to determine the length of time it takes chloride ions to migrate through the concrete in a bridge deck and reach the top mat of reinforcing steel. The lower the diffusion coefficient, lower the chloride intrusion in the concrete will be. In particular, the results determined from this reported data provide useful and realistic information for material performance.

To obtain the effective diffusion coefficients, least-squares curve fitting technique was used to calculate first the saltwater-exposed surface chloride concentration and then iterate to calculate the best fit of Fick's law. The measured chloride concentrations at the tested depths were used along with least-square fitting techniques to determine  $D_{\text{eff}}$  and  $C_s$ . Figure D.1 shows the measured and predicted chloride ingress curves. The data are relatively well fitted by the diffusion curves for all non-delaminated cores, however, in core with delamination observed was not possible to use this technique due to the presence of cracks and saltwater-exposed from different surfaces.



**Figure D.1** Measured and Predicted Chloride Ingress Curves

This technique was conducted using a common spreadsheet program, which includes minimization and solver function. All calculations were performed assuming Fick’s law of diffusion according to the following equation.

$$C(x) = C_s \left[ 1 - \operatorname{erf} \left( \frac{x}{2\sqrt{tD_{\text{eff}}}} \right) \right] \quad (B.2)$$

Where

- x = Depth in inches
- t = Time in years
- C<sub>s</sub> = Chloride surface concentration (lb/yd<sup>3</sup>)
- D<sub>eff</sub> = Effective diffusion coefficient (in<sup>2</sup>/year)
- erf() = Gaussian error function,  $\operatorname{erf}(z) = \frac{2}{\sqrt{\pi}} \int_0^z e^{-t^2} dt$

It is acknowledged that the effectiveness of the epoxy -as a barrier- it is impacted by the presence of coating damage or defect in the form of holidays, mashed areas, and bare areas. The defects in the coating are normally generated during application of the coating, storage and handling, transportation to site, assembly of mats, placement in forms, and placement of the concrete. Corrosion on epoxy-coated rebars initiates at defects in the form of crevice corrosion and can spread by undercutting the coating. Therefore, the model used allows corrosion initiation on epoxy-coated rebars in the finite elements that have suffered epoxy coating damage.

The use of the more refined model, taking into account the chloride binding by concrete, allows increasing the reliability of the determined diffusion coefficients. For tested cement concretes with water/cement ratios of 0.6 and 0.5, the chloride apparent diffusion coefficient decreases from 0.300 to 0.010 in<sup>2</sup>/yr.